Effects of 405nm HINS-Light on Mammalian Cells and Potential Disinfection Applications

Richard McDonald

In partial fulfillment of the requirements

for the degree of Doctor of Engineering

2012

University of Strathclyde

Bioengineering Unit:

Doctoral Training Centre in Medical Devices

and

Department of Electronic and Electrical Engineering:

Robertson Trust Laboratories for Electron Sterilisation Technologies

DECLERATION OF AUTHORS RIGHTS

This thesis is the result of the author's original research. It has been composed by the author and has not been previously submitted for examination which has led to the award of a degree.

ACKNOWLEDGMENTS

The author would like to thank his supervisors Professor M. Helen Grant and Professor Scott J. MacGregor for their continuous guidance, support and encouragement throughout the course of this study.

Special thanks are also due to Professor John G. Anderson and Dr Michelle Maclean for their invaluable input and advice provided throughout the research.

Thanks are also due to Mrs Catherine Henderson for limitless and patient advice in the cell lab, Mrs Elizabeth Goldie for vital assistance with microscopy, and Mr Dave Currie for invaluable support in the ROLEST lab. I am also grateful to Dr Tim Ashton of Vascutek Ltd for supplying materials used in the course of this research.

It would have been impossible to complete this thesis without the encouragement and support from family and friends, for which I am eternally grateful.

This research has been funded by the Engineering and Physical Sciences Research Council.

ABSTRACT

Hospital acquired infection affects approximately 10% of patients admitted to hospital, and is responsible for over 5000 deaths in the UK annually. The cost to the NHS has been estimated at around £1 bn per year. Infections acquired during invasive procedures have particularly high mortality rates, and the majority of these infections are thought to be caused by airborne bacteria present during procedures. High-intensity narrow-spectrum (HINS) light is a novel light-based disinfection system which may be able to aid in the continuous battle against bacteria.

HINS-light has been shown to have bactericidal properties, causing near complete inactivation of a number of medically relevant bacteria. The purpose of this study was to investigate potential patient-based applications of HINS-light, to establish if HINS-light could be used during invasive procedures where exposure of tissue to HINS-light would occur.

The effect of HINS-light on wound healing was investigated with a fibroblast populated collagen lattice (FPCL) wound model. High intensities of HINS-light (15 $mWcm^{-2}$: 1 hour exposure) were found to delay FPCL contraction, inhibit α-smooth muscle actin expression and reduce cell viability. Exposure to intensities at and below 5 $mWcm^{-2}$ for 1 hour had no significant inhibitory effects on any measured aspect of fibroblast function.

Infection is a significant risk in orthopaedic joint replacement procedures. To establish if HINS-light could be employed to reduce the number of bacteria present during these procedures without damaging exposed bone tissue, osteoblast cells were exposed to HINS-light. Cell viability was assessed via alkaline phosphatase assay, osteoblast collagen production, osteocalcin expression, and microscopy techniques. Exposure to 15 $mWcm^{-2}$ HINS-light for 1 hour was found to have inhibitory effects, while exposure to 5 $mWcm^{-2}$ and below for 1 hour had no significant effects.

Having established that 5 $mWcm^{-2}$ HINS-light could be applied to mammalian cells for 1 hour without significant detrimental effects, this dose was applied to polyester prosthetic vascular graft materials. This dose of HINS-light had no significant effects on the mechanical properties of the tested materials, and caused no visible damage. Extracts produced after treatment of the materials with HINS-light did not cause cytotoxicity to human aortic smooth muscle cells.

The bactericidal effects of 5 $mWcm^{-2}$ HINS-light were investigated on various clinically relevant bacterial species with variable success. Significant reductions in populations of *Staphylococcus epidermidis*, *Staphylococcus aureus* and Methicillin resistant *Staph. aureus* could be achieved when exposed to HINS-light in liquid suspension, with lesser inactivation of *Acinetobacter baumannii* and *Pseudomonas aeruginosa*, and no effect on populations of *Escherichia coli*. However, reduced inactivation rates for all bacteria were observed when exposing the bacteria on agar surfaces, a situation which closer resembles the wound environment.

Despite showing that a bactericidal level HINS-light exposure could be established that would not be detrimental to living tissue, the bactericidal benefits of this dose may not be sufficiently beneficial for medical use in practice. Reduced bacterial inactivation by HINS-light in nutritious environments such as a wound bed, combined with the limited penetration into tissue, suggest that the ability of HINS-light to reduce the number of bacteria in a wound would be limited. It is suggested that medical uses of HINS-light should focus on environmental disinfection, and decontamination of medical devices, rather than direct disinfection of wounds.

CONTENTS PAGE

LIST OF FIGURES

LIST OF TABLES

LIST OF ABBREVIATIONS

5-ALA	5-amino laevulinic acid
ALP	Alkaline phosphatase
AO	Acridine orange
APS	Ammonium persulphate
BA	Bacteriological agar
BSA	Bovine serum albumin
CFU	Colony forming units
CoNS	Coagulase-negative stapylococci
dH2O	Distilled water
DMEM	Dulbecco's Modified Eagle's Medium
DMSO	Dimethyl sulfoxide
DNA	Deoxyribonucleic acid
Eap	Extracellular adherence protein
ECM	Extracellular matrix
EDTA	Ethylene diamine tetraacetic acid
EPS	Extracellular polymeric substance
EtO	Ethylene oxide
EtOH	Ethanol
FPCL	Fibroblast populated collagen lattice
GAG	Glycosaminoglycans
GI	Gastrointestinal
HAI	Hospital acquired infection
hASMC	Human aortic smooth muscle cells
HINS	High-intensity narrow-spectrum
ICAM-1	Intercellular adhesion molecule 1
LED	Light emitting diode
LLLT	Low level laser therapy
LOOH	Lipid hydroperoxides
MSCRAMMs	Microbial surface components recognising adhesive matrix molecules

MRSA	Methicillin-resistant *Staphylococcus aureus*
MTT	3-(4,5-Dimethylthiazol-2-yl)-2,5-diphenyltetrazolium bromide
NaPi	Sodium phosphate
NSAID	Non-steroidal anti inflammatory drug
NHS	National Health Service
NR	Neutral red
OD	Optical density
OC	Osteocalcin
PBS	Phosphate buffered saline
PDT	Photodynamic therapy
PET	Polyethylene terephthalate
PGE2	Prostaglandin E2
PGDF	Platelet derived growth factor
PI	Propidium iodide
pNPP	p-Nitrophenyl phosphate
PVDF	Polyvinylidene fluoride
ROLEST	Robertson Trust Laboratories for Electronic Sterilisation Technologies
ROS	Reactive oxygen species
SDS-PAGE	Sodium dodecyl sulfate polyacrylamide gel electrophoresis
SEM	Scanning electron microscopy
SMA	Smooth muscle actin
Spp	Species (of bacteria)
SSI	Surgical site infection
TEMED	N,N,N,N- tetramethylethylenediamine
TGF-β	Transforming growth factor beta
TMB	$3,3^1,5,5^1$-tetramethyl benzidine
TNF	Tumor necrosis factor
TSA	Tryptone soya agar
TSB	Tryptone soya broth
TTBS	Tween tris buffered saline

UHMWPE	Ultra high molecular weight polyethylene
UTI	Urinary tract infection
UV	Ultraviolet

Chapter 1

INTRODUCTION

1.1 Hospital acquired infection

Hospital acquired infections (HAI), defined as infections which are not present at the time the patient enters hospital, are an ever increasing problem in modern healthcare affecting approximately 1 in 10 patients admitted to UK hospitals. Current attempts to resolve the problem involve campaigns to improve hygiene in the hospital, particularly hand washing (figure 1.1). Yet despite these campaigns, HAI still cause significant patient mortality. It is clear that a novel approach to bacterial inactivation is required to reduce the prevalence of HAI.

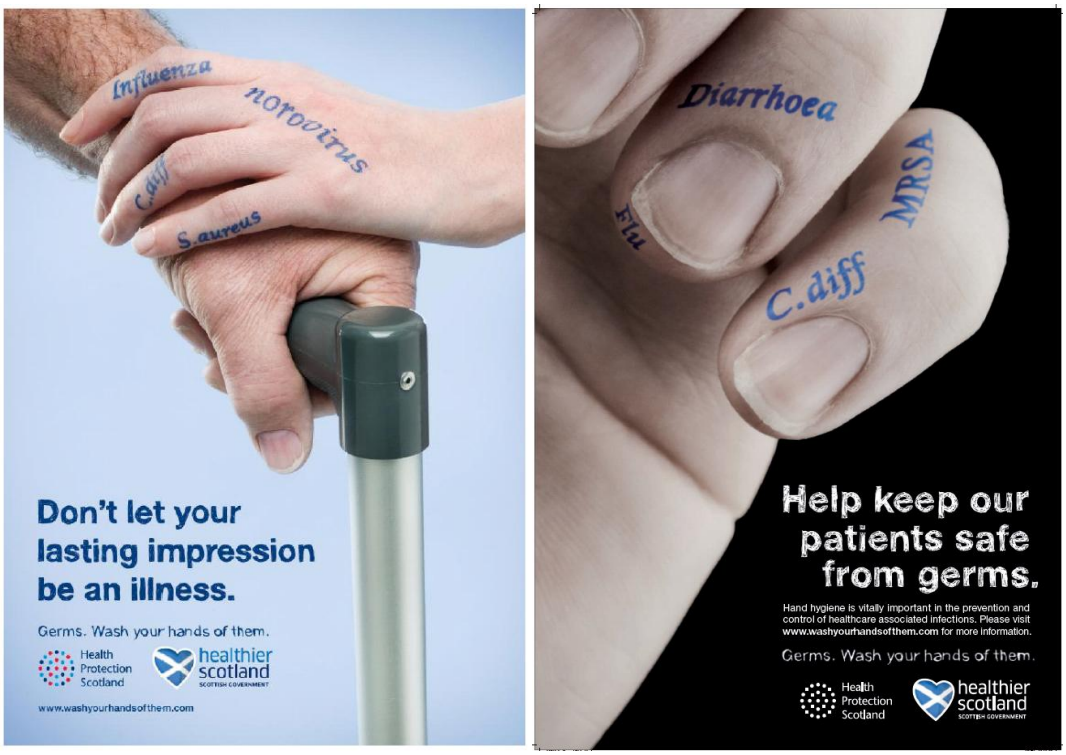

FIGURE 1.1 *Posters from the Health Protection Scotland and Healthier Scotland "Wash your hands of them" campaign, 2010.*

1.1.1 Prevalence

The most recent large scale survey of HAI in the UK was performed by Health Protection Scotland on 13754 inpatients in Scottish acute and non-acute hospitals between October 2005 and October 2006. They discovered an overall prevalence of 9.5% in acute hospitals and 7.3% in non-acute hospitals (Reilly et al., 2007). Higher rates have been reported in intensive care units, where 20.6% of 10038 patients from 1417 Intensive Care Units across Western Europe were reported to have acquired an infection (Vincent et al., 1995). The study by Reilly and co-workers found that the prevalence of HAI increased with patient age, with a sharp increase in patients over 60. The distribution between male and female patients is fairly even, with significant differences only being observed in the 25-44 year old age group, where prevalence was found to be increased in males. This study also investigated the distribution of HAI over specialities, with surgical and geriatric wards having the highest prevalence (table 1.1). Similar trends were reported in non-acute hospitals.

TABLE 1.1 Prevalence of HAI by speciality in Scottish NHS acute hospitals *(Reilly et al., 2007)*

Speciality	Number of in-patients with HAI	HAI prevalence %
Care of the Elderly	199	11.9
Dentistry	2	12.5
Gynaecology	10	4.8
Haematology	8	6.7
Medicine	491	9.6
Obstetrics	4	0.9
Oncology	12	8.8
Orthopaedics	105	9.2
Other	0	0
Psychiatry	9	3.5
Surgery	247	11.2
Urology	16	6.3
Total	**1103**	**9.5**

1.1.2 Morbidity and mortality

HAIs have a significant effect on the patient. A study of approximately 4000 patients admitted to an English district general hospital found the average duration of hospital stay for patients who had contracted an HAI was increased from 8 to 22 days, and the period before the patient could return to work was increased from 23 to 29 days (Plowman et al., 2001). Similar results were found in another study by Erbaydar and co-workers performed between 1992 and 1994 at Istanbul University Hospital. This study used one-to-one matching of patients, such that variables such as age, pre-operative stay, presence of malignancy or diabetes and use of in-dwelling medical devices were accounted for. In a sample size of 151 patients who had acquired an HAI and were able to be matched to an uninfected comparison patient, the hospital stay was found to be increased by 10.6 days (Erbaydar et al., 1995).

Inconvenience and discomfort are not the biggest concern though. The Plowman study reports an 11% increase in mortality rates in patients who acquire an infection during their hospital stay. The mortality rates of in-patients with an HAI which presented during their hospital stay was 13%, compared with 2% for those who did not present with an HAI in hospital (Plowman, 2000). A report published by the House of Commons in 2004 found that HAIs are responsible for over 5000 deaths in the UK each year, and are a contributing factor in over 1500 deaths (Improving Patient Care by Reducing the Risk of Hospital Acquired Infection: A Progress Report, National Audit Office 2004). In the US, deaths associated with HAIs in hospitals exceeded the number attributable to several of the top ten leading causes of death. A survey performed in 2002 found 1.7 million patients with an HAI, of which 155,668 died. 98,987 were deemed to be caused by or associated with the HAI (Klevens et al., 2007).

The greatest risk factor for HAI is prolonged hospital stay (Tess et al., 1993), which is of course necessary for those already in a poor state of health. HAI therefore are most commonly seen in elderly patients, or patients with underlying medical conditions. Patients with compromised immune systems are particularly at risk.

This could take the form of a medical condition such as autoimmune diseases, or patients in which the primary barrier to infection, the skin, is compromised by surgical procedures or for example placement of catheters (Kollef et al., 2008).

1.1.3 Financial burden of HAI

The economic burden of HAI is also considerable, and is closely linked to the increased duration of patient hospital stay. The study by Plowman et al (2001) found the mean cost of treating a patient with HAI to be £4782, an increase of £3153 over an un-infected patient. The cost of resolving the infection itself does not contribute a great deal to the increased cost. Microbiological tests and investigations, antimicrobials, antibiotics and other drug costs represented around 10% of the increase. The largest contributing source to the increase in cost was found to be nursing costs at 42% followed by hospital overheads associated with the extended stay at 33%. Many studies include nursing costs as part of the cost of extended stays, giving contributions towards total cost of infection of the extended stay as high as 95% (Coello et al., 1993). Extending these findings to a national scale gives estimates of costs to the NHS of around £1bn each year. The estimates made in the Plowman study were considerably higher than a previous study performed in 1995 by the Department of Health and the Public Health Laboratory, and the Plowman report has received some criticism for the sampling method. The study was performed in only one location, making extrapolation of the data to a national scale difficult due to variations in infection control practices across different hospitals. They also investigated the cost associated with all types of HAI, and although the study number of approximately 4000 patients was relatively large, some infections such as bloodstream infections had a sample size of only four, giving large confidence intervals for associated costs for certain infections. However, a review of studies shows that the added cost per HAI calculated in the Plowman study is comparable to other findings (Wilcox & Dave, 2000). The findings of this review are summarised in table 1.2, where the cost per case has been converted to pounds sterling and standardised to 1995/1996 valuations.

TABLE 1.2 *Studies on effect of HAI on length of stay and associated costs. Adapted from (Wilcox & Dave, 2000)*

Study	Country	Infection (sample size)	Increase in length of stay	Cost per case (£)
Haley et al. (1981)	USA	All (177)	1	891
Girard et al.(1983)	France	Neonatal (61)	6.7	1118
Mugford et al.(1989)	UK	Caesarean (41)	2.1	1011
Kappstein et al. (1992)	Germany	Pneumonia (34)	10.1	5533
Coello et al. (1993)	UK	UTI (35)	3.6	498
Coello et al. (1993)	UK	Wound (12)	10.2	1553
Wilcox et al. (1996)	UK	C. Diff	21	4107
Zoutman et al. (1998)	Canada	Wound (108)	10.2	1780
Plowman (2000)	UK	All (309)	11	3000
Reilly (2007)	UK	All (1103)	6.6	2548

The Reilly study is the most recent study to have been performed in Scotland. Of the 11608 patients surveyed in all 45 acute hospitals in Scotland, HAIs were found in 1103 patients. HAIs were found to increase the length of stay by 6.6 days, from 10.2 to 16.8 days. The cost of additional days in hospital was calculated at £319 per day. Extrapolating these data to a national level gives an extra 575200 bed days due to HAI, at a cost of £183 million (Reilly 2007).

1.2 Types of infection

Hospital acquired infections take many forms. The most common infection type reported in the Scottish National HAI Prevalence Survey was found to be urinary tract infection (UTI), accounting for 17.9% of cases, while the Plowman study reported a greater figure of 35% (table 1.3). The major risk factor for UTI is the use

of indwelling catheters, with risk increasing with increasing length of catheterisation period. The bacteria most commonly associated with UTI are the endogenous intestinal flora such as *Escherichia coli*, *Enterobacter*, *Klebsiella*, *Enterococci*, and *Proteus spp*. However, more general skin flora such as the *staphylococcus* species and *corynbacterium* are also found, and it is thought that inadequately decontaminated equipment and hands of healthcare workers may introduce environmental and common skin bacteria during insertion or maintenance of the urinary catheter (Maki & Tambyah, 2001). The use of indwelling or implanted medical devices such as orthopaedic implants and vascular grafts is increasing with technological advancements, and so the incidence of device-associated infection is increasing (von Eiff et al., 2005). Surgical site infections (SSI) are the next most common, accounting for around 16% (Andersen et al., 2009; Reilly et al., 2008). The pathogen responsible for SSI varies according to surgical site. *Escherichia coli, Enterococcus spp., Streptococcus spp., Pseudomonas aeruginosa* and *Staphylococcus aureus* were found to be responsible for the majority of infection in abdominal surgery (Munez et al., 2011), while *Staphylococcus aureus* and coagulase-negative *Staphylococcus* such as *Staph. epidermidis* were more prevalent in orthopaedic, vascular and trauma surgery (Misteli et al., 2011; Owens & Stoessel, 2008).

To take infection acquired during hip replacement surgery as a specific example of HAI, studies have shown incidence rates from 1 – 5%, increasing considerably for revision procedures (Hamilton & Jamieson, 2008; Ridgeway et al., 2005; Wilson et al., 2008). Of these, *Staph aureus* is found to be the causative organism in the majority of cases. In the English mandatory surveillance system data set, covering 22160 procedures performed in English hospitals between April 2004 and March 2005, Staph aureus was identified in 64% of infections, 67% of which were Methicillin resistant strains (Wilson et al., 2008). *Staph epidermidis* has also been identified in a large number of cases (Hamilton & Jamieson, 2008). Phage-typing has been used to attempt to identify the source of the organism, showing that 31% of organisms found to cause wound sepsis were also found on the operating staff (Lidwell et al., 1984).

TABLE 1.3 *Prevalence of types of infection from the Scottish National HAI Prevalence Survey, 2006 (Reilly et al., 2008)*

HAI type	No.	%
Urinary tract	222	17.9
Surgical site	197	15.9
Gastrointestinal	191	15.4
Eye, ear, nose, throat or mouth	155	12.5
Lower respiratory tract (other than pneumonia)	139	11.2
Skin and soft tissue	137	11
Pneumonia	109	8.8
Blood stream	55	4.4
Reproductive	17	1.4
Cardiovascular system	11	0.9
Bone and joint	6	0.5
Central nervous system	2	0.2
Systemic	2	0.2

1.3 Source of infection

The human body is home to many types of bacteria, summarised in table 1.4, which are not normally harmful to healthy individuals. In fact, most bacteria have a symbiotic relationship with the host. Commensal bacteria found on the skin provide protection against colonisation and infection from pathogenic microbes, and stimulation of the development of the host immune system (Chiller et al., 2001). For example *Staphylococcus epidermidis*, the most common microbe found on the skin, has been shown to influence the immune response of keratinocytes by Toll-like receptor signalling (Cogen et al., 2008). Bacteria in the gut ferment undigested carbohydrates, prevent colonisation by potential pathogens, and help develop the immune system. In return, the surfaces of the human body provide a stable environment for bacteria to survive on, with constant supply of nutrients.

There are six main routes of transmission through which bacteria can contaminate and infect a susceptible host. Contact transmission is the most common mode of contamination. It is normally divided into two sub-categories, direct and indirect. Direct contact involves transmission through direct body to body contact, with physical transfer of bacteria from the source to the patient. This can occur during routine healthcare procedures, in which the medical professional is a carrier of the pathogen, or from other patients or visitors to the patient. Indirect contact transmission involves an intermediary step, such as the contamination and insufficient cleaning of medical equipment which is shared between patients. Common vehicle transmission and vector borne transmission are less commonly found to be the cause of HAI in western healthcare environments. Common vehicle transmission involves contamination of water supplies or food sources, and vector transmission is where the microorganism is spread through vectors such as mosquitoes, rats or flies. Droplet transmission can occur from an infected source during coughing, sneezing and talking. An infecting microorganism can become suspended in the warm, moist droplet and can travel a few metres, increasing the risk of infection for those around the source. Airborne transmission can also occur from coughing and sneezing, where particles of 5 μm or less can become aerosolised and remain suspended in the air where they can disperse over an entire room. Dust particles or skin fragments containing bacteria can also be spread by airborne transmission.

TABLE 1.4 *Bacteria commonly found on surfaces of the human body*, adapted from Todar's Online Textbook of Bacteriology. ++ = very common (nearly 100%), + = common (~25%), +/- = rare (<5%)

BACTERIUM	Skin	Conjunctiva	Nose	Pharynx	Mouth	Lower GI	Ant. Urethra	Vagina
Staphylococcus epidermidis	++	+	++	++	++	+	++	++
Staphylococcus aureus	+	+/-	+	+	+	++	+/-	+
Streptococcus mitis				+	++	+/-	+	+
Streptococcus salivarius				++	++			
Streptococcus mutans				+	++			
Enterococcus faecalis				+/-	+	++	+	+
Streptococcus pneumoniae		+/-	+/-	+	+			+/-
Streptococcus pyogenes	+/-	+/-		+	+	+/-		+/-
Neisseria spp		+	+	++	+		+	+
Neisseria meningitidis			+	++	+			+
Enterobacteriaceae (Escherichia coli)		+/-	+/-	+/-	+	++	+	+
Proteus spp.		+/-	+	+	+	+	+	+
Pseudomonas aeruginosa				+/-	+/-	+	+/-	
Haemophilus influenzae		+/-	+	+	+			
Bacteroides spp.						++	+	+/-
Bifidobacterium bifidum						++		
Lactobacillus spp.				+	++	++		++
Clostridium spp.					+/-	++		
Clostridium tetani						+/-		
Corynebacteria	++	+	++	+	+	+	+	+
Mycobacteria	+		+/-	+/-		+	+	
Actinomycetes				+	+			
Spirochetes				+	++	++		
Mycoplasmas				+	+	+	+/-	+

1.3.1 Airborne transmission

High concentrations of airborne contaminants are known to be a source of infection during surgical procedures. The number of infections following orthopaedic implant surgery has been shown to correlate with the number of airborne bacteria measured within a 30cm area around the wound (Lidwell et al., 1983). 98% of the microorganisms found in the wound were shown to originate from airborne transmission, and comparison of the airborne bacterial concentrations with the number of bacteria washed out during surgery suggest that 35% of these bacteria were thought to have fallen directly on the wound, with the remainder having fallen on surgical instruments or the gloves of the surgeon, leading to an indirect contamination of the surgical site (Whyte et al., 1982). Despite modern laminar airflow operating theatres, contaminants can remain in the air following surgical procedure. It is common practice to try and schedule "dirty" cases, that is cases where there is known infection such as removing an infected implant, to be undertaken after "clean" procedures. However, examples where this schedule cannot be maintained do occur and it has been shown that there is a small but increased risk of the following patients becoming infected with the known microorganism of the preceding "dirty" cases (Namdari et al., 2011). This was found to be the case despite normal cleaning procedures with broad-spectrum disinfectants between patients. The number and activity of staff in the operating theatre has been shown to greatly contribute to the airborne bacterial levels. It is not only staff who have direct contact with the patient during surgery that pose a risk of infection. An investigation carried out following three cases of post-operative *Staphylococcus aureus* wound infection in the same ward identified a surgical orderly as the probably source of infection. Bacteriological investigations identified the strain of *Staph aureus* to be unusual, in that it was resistant to novobiocin and tetracycline, and sensitive to penicillin. This particular strain was isolated in large numbers from the hair and skin of the orderly, who suffered from eczema. The orderly had no contact with the patient, but it was concluded that their presence during surgery had contributed to the infection. Strains of the bacteria were also isolated from air samples taken from ward areas in which the orderly had visited (Ayliffe & Collins, 1967). The operating theatre in this example did not have a mechanical air flow device; laminar flow ventilation was

pioneered in the 1960s and 70s, and only widely adopted in orthopaedic surgical theatres in the 1980s. In laminar flow operating theatres, a continuous flow of highly filtered 'bacteria-free' air is recirculated under positive pressure into the operating field and air contaminants generated during surgery are removed from the site (figure 1.2). This has been shown to significantly reduce airborne bacterial levels, with studies during the introduction of this technique showing 95% reductions in the number of airborne bacteria, measured by slit-sampling (Alexakis et al., 1976). However, even with modern laminar flow ventilation, unacceptably high numbers of isolates are still reported during arthroplasty surgery (Owers et al., 2004). In this supposedly ultra clean environment, bacterial concentrations as high as 236 CFU/m^3 have been reported during cardiological operations, around 70% of which were Gram-positive *Staphylococci* (Pastuszka et al., 2005). Qudiesat and co-workers found the numbers of airborne bacteria in fully vented operating theatres during cardiac surgery to be around 100 CFU/m^3, with surface swabs giving counts of around 45 CFU (Qudiesat et al., 2009). A limit of 180 CFU/m^3 for an average 5 min period has been set in the UK for conventionally vented operating theatres. With the use of ultra-clean air and total body exhaust gowns, the limit is <1 CFU/m^3 sampled within 30cm of the wound (UK Department of Health document, Health Technical Memorandum 2025).

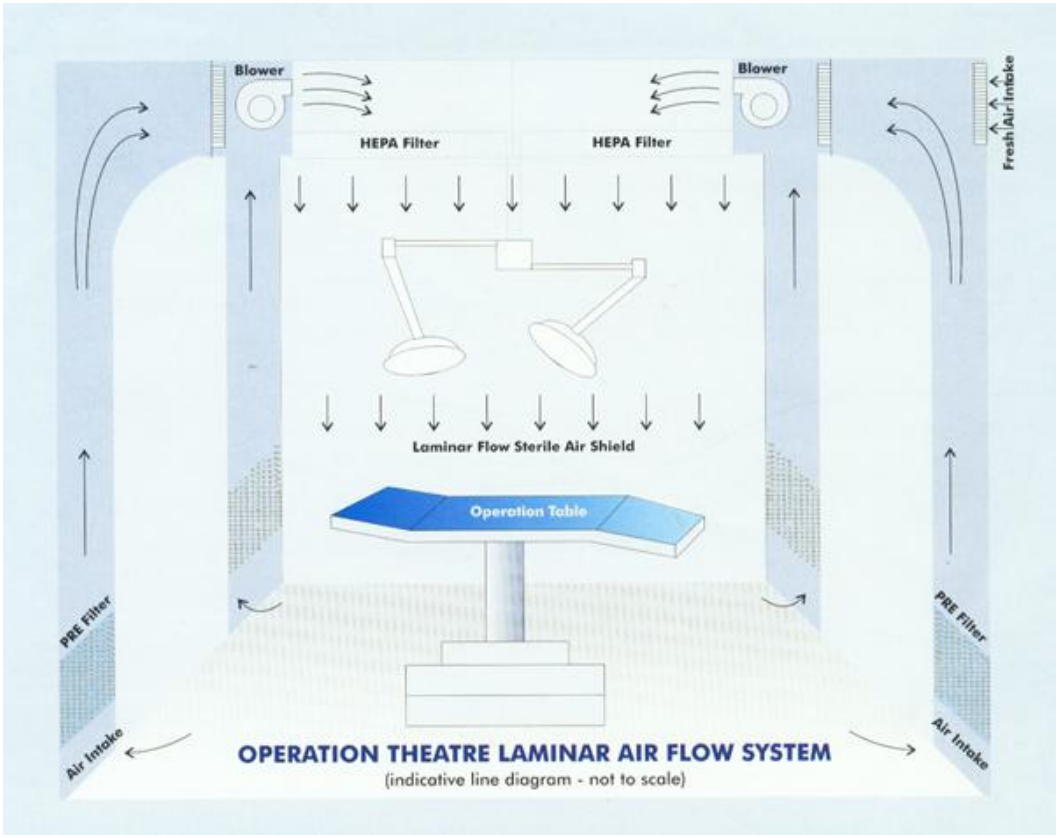

FIGURE 1.2 *Line diagram of air flow in vertical laminar flow operating theatre (http://www.microfilt.com/operation_theatre.html)*

Bacterial shedding from staff in the operating theatre is thought to be the source of the majority of airborne contaminants. It has been shown that the difference in temperature between the human body and ambient air creates a convective air current which carries particles away from the body. As many as 10^7 bacteria carrying skin fragments can be released from the body in a 24 hour period (Clark & de Calcina-Goff, 2009), detached mainly by the abrasive action of fabrics upon the skin (Benediktsdottir & Hambraeus, 1982). Traditional surgical wear has also been shown to act as bellows which pump shed fragments into the air, with Schlieren images (images which can show optical inhomogeneities invisible to the human eye caused by variation in optical path lengths) showing dispersal of fragments from around the edges of a surgical gown and from the cuffs of surgical scrubs (Clark & de Calcina-Goff, 2009) . Mechanical cleaning methods and movement of people have also been shown to significantly contribute to the number of airborne particles, as settled particles are disturbed and resuspended in the air (Clark et al., 1985).

1.3.2 Bacterial survival

As well as surviving and thriving on the human body, bacteria have been shown to survive on inanimate surfaces for extended periods of time. Table 1.5 summarises the findings of a review carried out in 2005 on all literature concerned with bacterial survival on dry inanimate surfaces, including steel, plastic and fabrics (Kramer et al., 2006). Both Gram-positive and –negative bacteria that are responsible for a variety of HAI were found to survive for several months on these surfaces.

This ability to survive on surfaces for extended periods allows transfer of bacteria from patient to surface, then to other patients, contributing to the spread of HAI around the hospital environment. There are specific examples of this leading to infection outbreaks. Embil and co-workers (2001) report a case of MRSA outbreak in 12 patients in a plastic surgery and burns unit. The outbreak also spread to a community hospital to which a patient from the burns unit had been transferred. All the strains were shown to be identical by pulsed-field gel electrophoresis. The source of the outbreak was traced to a single contaminated stretcher and hand held shower unit from the burns unit, and the outbreak was terminated by replacement of these pieces of equipment (Embil et al., 2001). Similarly, a contaminated shared electronic ear-probe thermometer was found to be responsible for an outbreak of vancomycin-resistant *Enterococcus* infection among seven patients on a general medical-surgical ward (Porwancher et al., 1997).

TABLE 1.5 *Survival of bacteria on dry inanimate surfaces, adapted from Kramer and co-workers (2006).*

Type of bacterium	**Duration of persistence (range)**
Acinetobacter spp.	3 days to 5 months
Bordetella pertussis	3 – 5 days
Campylobacter jejuni	up to 6 days
Clostridium difficile **(spores)**	5 months
Chlamydia pneumoniae, C. trachomatis	≤ 30 hours
Chlamydia psittaci	15 days
Corynebacterium diphtheriae	7 days – 6 months
Corynebacterium pseudotuberculosis	1–8 days
Escherichia coli	1.5 hours – 16 months
Enterococcus spp. including VRE and VSE	5 days – 4 months
Haemophilus influenzae	12 days
Helicobacter pylori	≤ 90 minutes
Klebsiella spp.	2 hours to > 30 months
Listeria spp.	1 day – months
Mycobacterium bovis	> 2 months
Mycobacterium tuberculosis	1 day – 4 months
Neisseria gonorrhoeae	1 – 3 days
Proteus vulgaris	1 – 2 days
Pseudomonas aeruginosa	6 hours – 16 months; on dry floor: 5 weeks
Salmonella typhi	6 hours – 4 weeks
Salmonella typhimurium	10 days – 4.2 years
Salmonella spp.	1 day
Serratia marcescens	3 days – 2 months; on dry floor: 5 weeks
Shigella spp.	2 days – 5 months
Staphylococcus aureus**, including MRSA**	7 days – 7 months
Streptococcus pneumoniae	1 – 20 days
Streptococcus pyogenes	3 days – 6.5 months
Vibrio cholerae	1 – 7 days

1.4 Bacterial levels required to cause infection

Traditionally, a bacterial count around 10^5 to 10^6 CFU is associated with an increased incidence of infection and inhibited wound healing in otherwise healthy samples (Landis, 2008). For example, Murphy and co-workers demonstrated that successful closure of wounds in goats with pedicled flaps would not proceed successfully when the wound was contaminated with more than 10^5 CFU per gram of tissue (Murphy et al., 1986). Similarly, Bendy and co-workers found that decubitis ulcers would not heal until bacterial levels were below 10^6 CFU/ml of wound fluid (Bendy et al., 1964), and Krizek and Davis found that visceral cultures with bacterial counts greater than 10^6 CFU/g of tissue resulted in fatal sepsis (Krizek & Davis, 1966). During the Vietnam war the US Army carried out research into burn wound sepsis with similar results (Lindberg et al., 1965; Teplitz et al., 1964).

The introduction of indwelling medical devices significantly decreases the numbers of bacteria required to cause infection. Elek (1956) found that $7.5x10^6$ CFU of *Staphylococcus pyogenes* was the minimum dose required to cause pus formation, swelling and redness when injected under the skin of human volunteers. However, they also soaked silk suture material in a *Staphylococcus aureus* suspension and allowed it to dry. The number of bacteria on the material was enumerated and the suture pulled through the skin of volunteers and tied in place. Evidence of infection around the stitch was visible with doses as low as 100 CFU (Elek, 1956). It has been estimated that infection following total hip replacement surgery can be caused by as few as 10 CFU (Charnley & Eftekhar, 1969), and experiments on the use of ultraclean air and whole-body exhaust-ventilated suits show that even when the airborne bacterial count is as low as 1 CFU/m^3 of air sampled, sepsis following total hip or knee replacement surgery can still occur (Lidwell et al., 1982).

1.4.1 Biofilms

A contributing factor to the ability of such low numbers of bacteria to cause deep infection is their ability to form biofilms (McCann et al., 2008). A biofilm is an aggregate of bacteria which is attached to a surface and embeds itself in a matrix of extracellular polymeric substance (EPS) known as “slime” (Mack et al., 2006). The

process of biofilm formation can be separated into four distinct phases; conditioning film deposition, microbial attachment, colonisation and final formation. Despite technological advancements in material surface characteristics, upon contact with the body a device will obtain a conditioning film consisting of various proteins and electrolytes dependent on where the material is implanted (Tenke et al., 2004). Bacteria which in vitro would not be able to adhere to the device surface can now attach to the conditioning film. The process by which bacteria can adhere to the surface is not fully understood but may involve microbial surface components recognizing adhesive matrix molecules (MSCRAMMs) (Fitzpatrick et al., 2005). Bacteria then begin to colonise the surface, and produce the polysaccharide slime which helps to anchor the organisms to the surface. The slime surroundings make the bacteria significantly less susceptible to the host response and traditional antimicrobial treatment (von Eiff et al., 2005). It is also thought that the biofilm provides a buffer to changing environmental conditions and easier access to nutrients via mass transfer (Habash & Reid, 1999).

1.5 UV inactivation

UV-light in the operating theatre has been shown to be more effective than laminar flow ventilation at reducing the number of airborne bacteria. A study by Berg and co-workers in 1991 found the mean count of colony forming units per m^3 to be 7.67 with laminar flow ventilation, reduced to 2.96 CFU/m^3 with 254nm UV-C radiation replacing the ventilation system (Berg et al., 1991). Similarly, Lowell and co-workers reported a reduction in infection rates following total hip replacement of 3.06 to 0.53% by the installation of UV lamps (Lowell et al., 1980). A large study performed over 19 years on 5980 joint replacement procedures found that UV radiation decreased the risk of post-operative infection from 1.77 to 0.57% (Ritter et al., 2007). The use of UV radiation is, however, associated with a number of problems for both the patient and staff. They developed conjunctivitis and erythema of the skin, protected against by the introduction of eye protection and fully covering protective clothing. Sun screen was used to protect any exposed areas. Despite claims that intensities as high as 300 μWcm^{-2} do not cause any untoward effects, safety considerations have meant that an intensity limit of 30 μWcm^{-2} was introduced

(Lidwell, 1994). However, despite the impressive reductions in airborne bacterial counts and infection rates, UV radiation has not been widely adopted in the UK. The protective clothing required by operating staff is deemed to be too hot, thick and uncomfortable for routine use (Gosden et al., 1998; Taylor et al., 1995). The use of UV lighting during procedures is more commonly used in operating theatres in the US and Sweden.

1.6 Light inactivation of bacteria

As has been shown in the previous section, UV radiation can successfully be employed to reduce the number of bacteria in the hospital environment. It has also been shown that visible light is capable of inactivating bacteria (Maclean et al., 2009). The mechanism through which this occurs is explained here.

1.6.1 The electromagnetic spectrum

Sunlight is composed of electromagnetic waves of wavelength 100 to 10^6 nm (1mm). Only a small portion of this is visible to the human eye, from roughly 380 nm to 780nm. Wavelengths below 380nm are classified as ultraviolet (UV), which is further split into three categories; UV-A, UV-B and UV-C depending on wavelength. Wavelengths of radiation longer than visible light are known as infra-red (IR), also spilt into A,B and C sub-categories. This is a relatively small portion of the full electromagnetic spectrum, which also consists of very short wavelength gamma and X-rays, which have well understood medical applications, and longer wavelength radiation radio waves (Figure 1.3).

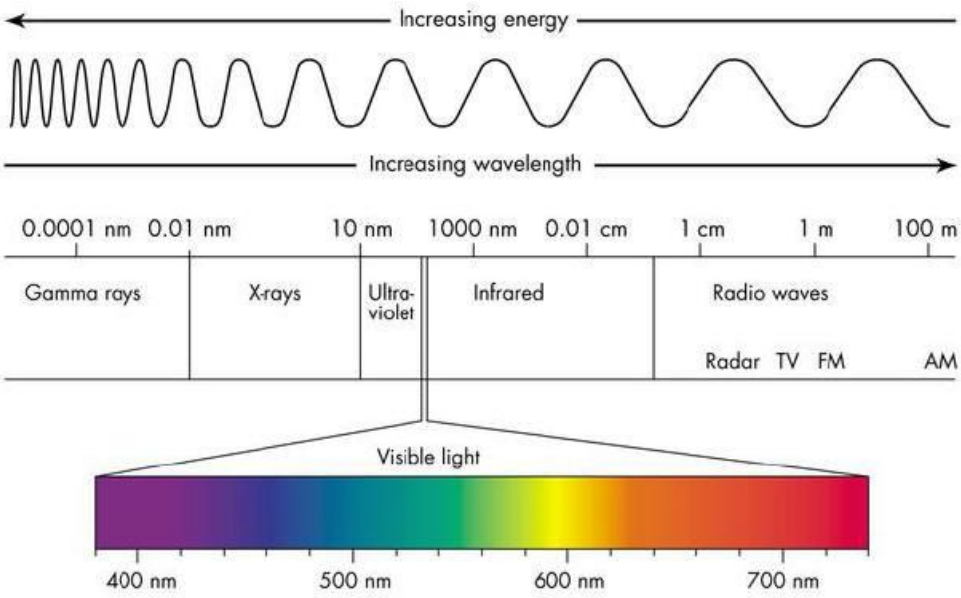

FIGURE 1.3 *The electromagnetic spectrum.*

Electromagnetic radiation produced by the sun has long been known to have biological effects, probably the most common of which is sunburn caused by over exposure of skin to UV-B radiation which damages the DNA of epidermal cells. Visible light also has a variety of established biological applications, and is the main treatment method for neonatal jaundice (Maisels & Watchko, 2003), through the isomerisation of bilirubin by high intensity green-blue light. It is also commonly used in the treatment of acne, where combinations of blue and red light have been shown to have antibacterial and anti-inflammatory properties (Kawada et al., 2002; Papageorgiou et al., 2000), and depressive disorders such as seasonal affective disorder where it is thought to alter melatonin levels that affect mood (Terman & Terman, 2005; Winton et al., 1989). Light has also been used in the treatment of cancer, known as photodynamic therapy, where targeted light is applied in conjunction with a photosensitising agent to destroy the cancerous cells. An explanation of the mechanism through which this occurs is useful to help understand the bactericidal properties of blue light.

1.6.2 Photodynamic therapy

Photodynamic therapy (PDT) involves the administration and subsequent illumination of a photosensitive molecule by visible light of an appropriate wavelength, dependent on the particular photosensitiser used. Illumination causes excitation of the photosensitising molecule and starts a series of reactions which results in the production of reactive oxygen species (ROS). The production of these ROS can lead to cell death through oxidative reaction with the surrounding biomolecules within the cell (Hamblin & Hasan, 2003). This is not a particularly new therapeutic approach; the ancient Egyptians used vegetable and plant extracts as a photosensitiser in combination with exposure to sunlight to treat skin conditions such as vitiligo. The basis of this therapy is still used (Mahmoud et al., 2008). As well as cancer therapy, PDT is also licensed for the treatment of age-related macular degeneration, arthritis, psoriasis, Barrett's oesophagus, atherosclerosis and restenosis in veins and arteries (Hamblin & Hasan, 2003).

The most commonly used photosensitising molecule used in cancer therapy is hematoporphyrin derivative, a complex mixture of porphyrins which have been particularly effective as they are retained by tumour tissues (Cao et al., 2009; Kessel, 1982). Upon illumination of the porphyrin by the appropriate wavelength of light (a description of porphyrins and their wavelength sensitivity will follow), the porphyrin undergoes excitation from the stable ground state to a singlet excited state. This refers to a state where all of the electrons in the molecule are spin-paired, a quantised measure of the angular momentum of a particle. From this excited state the porphyrin can either decay back to the ground state, releasing energy in the form of a photon of light with wavelength around 600 nm, or undergo intersystem crossing to a lower energy but longer lived state known as the triplet state. The second pathway is a "forbidden" process as it requires spin inversion, which should make it less likely to occur than the "allowed" process of fluorescence, however, the very high occurrence of the "forbidden" intersystem crossing pathway in porphyrins is why they make such successful photosensitisers. Only around 5% of excited molecules are thought to decay through fluorescence, with the rest undergoing intersystem crossing to the triplet state (Perun et al., 2008). There are two possible pathways

from the triplet state, known as type I and II reactions (figure 1.4). In type I reactions the excited triplet photosensitiser interacts directly with the substrate molecule, either by hydrogen atom abstraction or by electron transfer to produce a reactive radical species, mainly hydrogen peroxide and superoxide. The substrate molecule could be amino acids within the cell or the cell membrane. In type II reactions the triplet state reacts with the ground state triplet oxygen producing the excited singlet oxygen ($^1O_2$) which is highly reactive (Wijesekera & Dolphin, 1985). It is thought that the singlet oxygen reacts with unsaturated lipids in the cell membrane forming lipid hydroperoxides (LOOH). These hydroperoxides react with ferrous iron initiating free radical chain reactions producing ROS, aldehydes and other toxic products that disrupt the cell membrane leading to cell death (Schafer & Buettner, 1999; Thomas & Girotti, 1989)

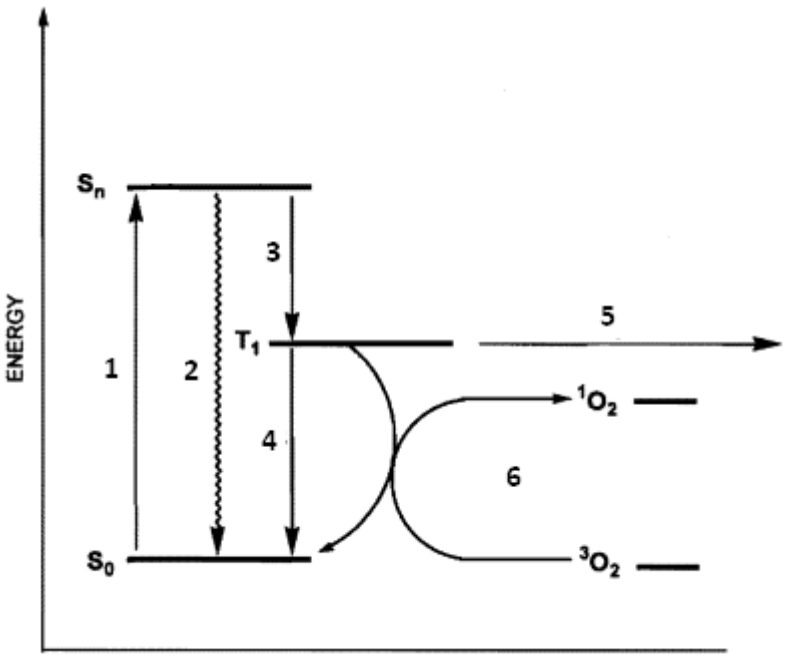

FIGURE 1.4 *Jabionski diagram of photosensitiser excitation and subsequent pathways, modified from Sternberg (1998). Key: 1 = absorption of light, 2 = fluorescence, 3 = Intersystem crossing, 4 = phosphorescence, 5 = type I photoreaction, 6 = type II photoreaction (Sternberg & Dolphin, 1998).*

The majority of damage caused by PDT is thought to occur through the type II pathway. Singlet oxygen is a highly reactive oxidising species that can react with a

variety of biomolecules (Fuchs & Thiele, 1998). It is thought that the damage caused by PDT to cells is through reactions between singlet oxygen and the cell membrane. Malik and Lugaci (1987) incubated Friend erythroleukaemia cells with 5-amino levulinic acid (ALA), which stimulates endogenous porphyrin content of the cells. Cells were exposed to 380 nm light for 2 min, with the effects after a number of days incubation assessed by scanning electron microscopy (SEM) and flow cytometry. After exposure and 2 days incubation with the 5-ALA, outer deformations and irregularities were observed in the cell membrane. By day 5, PDT was observed to form holes and cause severe damage to the membrane. However, SEM did not reveal significant damage to the nucleus. Flow cytometry showed a rapid increase in cell volume, associated with damage to the membrane and sudden influx of water into the damaged cell (Malik & Lugaci, 1987). Similarly, Ahn and co-workers (2004) employed scanning and transmission electron microscopy to examine the effect of PDT with a hematoporphyrin derivative photosensitiser on CaSki human cervical squamous cell carcinoma cells. One hour exposure to 630 nm light was found to cause plasma membrane disruption, cell shrinkage and cytoplasm leakage. There was no evidence of damage to the nuclear membranes. The plasma membrane was observed to have completely disintegrated by 6 hours later (Ahn et al., 2004).

1.7 Porphyrins

Porphyrins are a class of naturally occurring molecules that are found everywhere in nature. They are involved in a wide range of biological processes including photosynthesis, pigmentation changes, catalysis and oxygen transport (Goldoni, 2002). The basic structure which is common to all of the porphyrin molecules consists of four pyrrolic subunits which form a substituted aromatic macrocyclic ring. The pyrrole ring consists of four carbon atoms and one nitrogen atom, each with a hydrogen atom bound to it. The pyrrole subunits are linked together by four methine bridges, unsaturated $-CH=$ groups (figure 1.5).

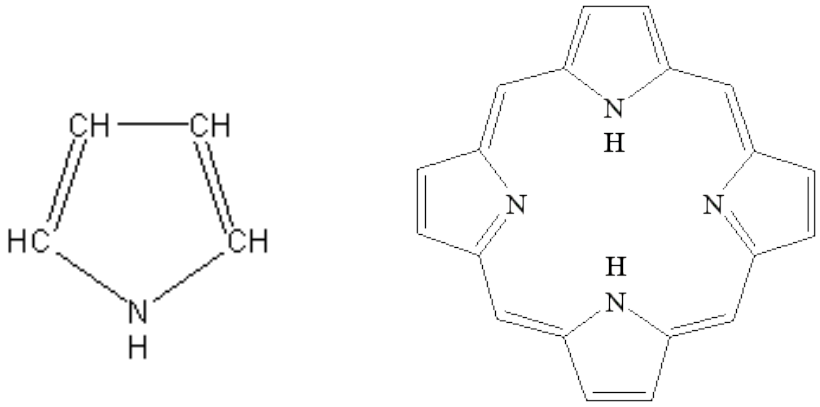

FIGURE 1.5 *The pyrrole ring (left), four of which are joined by methine bridges to form the basic tetrapyrrole porphyrin molecule (right).*

The structure of the tetrapyrrole molecule provides a vacant site at its centre which is ideally suited for metal incorporation, forming metalloporphyrins. The metal ion which is incorporated, and the addition of any side chains, determine the function of the porphyrin. For example, the addition of magnesium creates chlorophyll, while an iron atom produces haem. Metalloporphyrins are not useful in photodynamic inactivation, however, as the metal rapidly quenches the ROS (Krasnovskii et al., 1982). Free-base porphyrins are present in organisms as the precursors to metalloporphyrins (Wijesekera & Dolphin, 1985), and these are required for photodynamic inactivation to be effective (Evensen, 1995).

The absorption spectrum of a typical porphyrin (figure 1.6) shows intense absorption around 405 nm, known as the Soret band. This would suggest that blue light should be the most effective at exciting porphyrins to generate the ROS required to kill bacteria. The absorption peaks of the different porphyrin molecules have been shown to vary slightly, but all are around 405 nm (table 1.7).

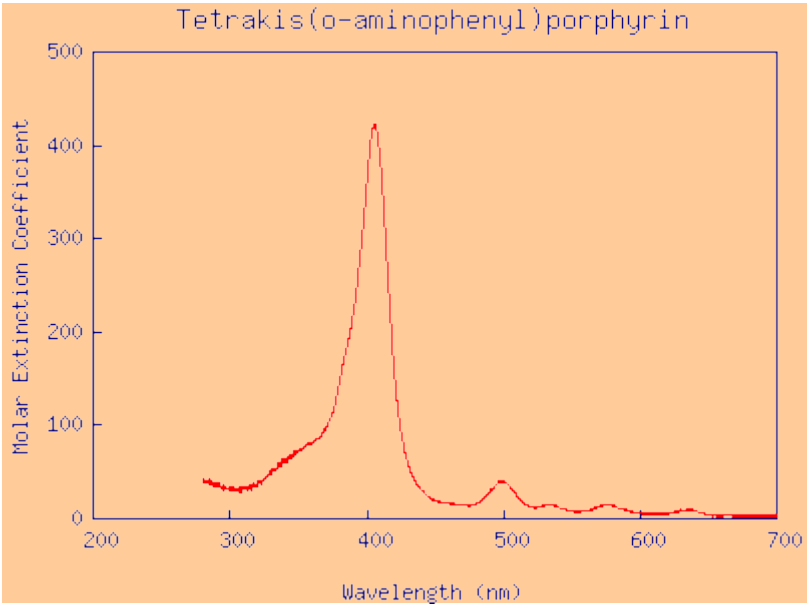

FIGURE 1.6 *Typical absorption spectrum of porphyrins, (Du et al., 1998).*

TABLE 1.7 *Absorption peaks of various porphyrin molecules. Adapted from (Rimington, 1960)*

Porphyrin	**Absorption max (nm)**
Uroporphyrin III octamethyl ester (syn.)	405-6
Uroporphyrin I octamethyl ester (nat.)	406
Coproporphyrin III tetramethyl ester	399.5
Aetioporphyrin I	399.5
Deuteroporphyrin dimethyl ester	399
Haematoporphyrin dimethyl ester	402
Porphin	396-5
Phylloerythrin methyl ester	415
Protoporphyrin dimethyl ester	407.5

There are several smaller absorption peaks from 450 to 700 nm, known as Q-bands and light in this region has previously been used for inactivation of bacteria (Nussbaum et al., 2003; Wilson, 2004). Red light is generally used in PDT for cancer treatment as it is able to penetrate further into tissue (figure 1.7), and the use

of exogenous photosensitising agents can amplify the photodynamic effect to the required level. For bacterial inactivation by endogenous porphyrins, the intensity of red light required would be considerably higher than blue light.

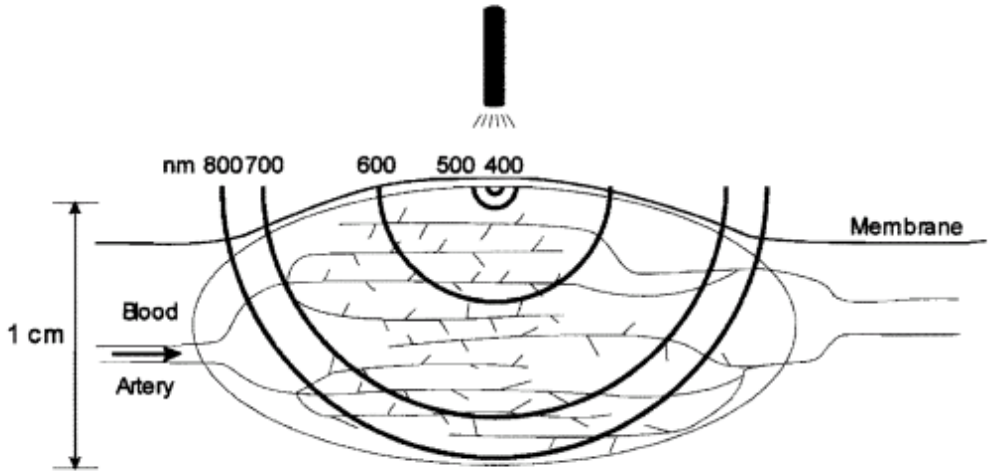

FIGURE 1.7 *Wavelength dependence on depth of penetration of light into tissue (Sternberg & Dolphin, 1998).*

1.7.1 Inactivation of bacteria and mammalian cells by endogenous porphyrins activated by blue light.

The use of photosensitising agents such as the hematoporphyrins or 5-ALA is not necessary to achieve cell damage in bacteria after exposure to light. Many strains of bacteria naturally produce high levels of porphyrin, and these porphyrins can be excited and generate singlet oxygen formation in the same way as exogenously applied sensitisers. Ashkenazi and co-workers have demonstrated this with the *P. acnes* bacterium. Exposing the bacteria to 75 Jcm^{-2} blue light with no photosensitising agent causes a decrease in cell viability of 2 orders of magnitude. Increasing the dose further decreased the viability of the cells to a greater extent (Ashkenazi et al., 2003). Photodynamic inactivation by excitation of endogenous porphyrins with blue light has since been shown to be possible on a wide range of bacteria, summarised in table 1.6.

TABLE 1.6 *Organisms shown to be susceptible to damage by blue light irradiation without the use of exogenous photosensitisers*

Organism	Wavelength (nm)	Dose (Jcm^{-2})	log_{10} reduction	Dose/log_{10} reduction	Reference
Acinetobacter baumannii	405 (± 5)	108	4.2	25.7	Maclean et al. (2009)
Clostridium perfringens	405 (± 5)	45	4.4	10.2	Maclean et al. (2009)
Enterococcus faecalis	405 (± 5)	216	2.6	96	Maclean et al. (2009)
Escherichia coli	407 - 420	75	2	37.5	Ashkenazi et al. (2003)
Fusobacterium nucleatum	450 - 480	94	6	15.7	Feuerstein et al. (2005)
Helicobacter pylori	405 (± 2)	32	5	6.4	Ganz et al. (2005)
Klebsiella pneumaniae	405 (± 5)	180	4.2	42.8	Maclean et al. (2009)
MRSA	405 (± 5)	45	5	9	Maclean et al. (2009)
Porphyromanas gingivalis	450 - 480	62	6	10.3	Feuerstein et al. (2005)
Prevotella spp.	488 – 514	80	4	20	Henry et al. (1996)
Proteus vulgaris	405 (± 5)	144	4.7	30.6	Maclean et al. (2009)
Pseudomonas aeruginosa	405 (± 5)	180	3.9	46.2	Maclean et al. (2009)
Staphylococcus aureus	405 (± 5)	36	5	7.2	Maclean et al. (2009)
Staphylococcus epidermidis	405 (± 5)	42	4.6	9.1	Maclean et al. (2009)
Streptococcus pyogenes	405 (± 5)	54	5	10.8	Maclean et al. (2009)

The intensity of light required for complete inactivation varies for different strains of bacteria, and this is thought to be due to the different concentrations of porphyrins present in different cell types (Lipovsky et al., 2009). The experiments of Lipovsky et al exposed two clinical isolates of *S. aureus* to broadband visible light with wavelengths from 400 to 800nm at an intensity of 300 $mWcm^{-2}$. A 10 min exposure, giving a dose of 180 Jcm^{-2}, resulted in a 99.8% reduction in viability of a methicillin sensitive strain of *Staph aureus*, while the same dose only caused a 55.5% reduction in viability of a Methicillin-resistant strain. Maclean and co-workers achieved a complete 5-$\log_{10}$ reduction in population of *S. aureus* with a 630 Jcm^{-2} dose (350 $mWcm^{-2}$ for 30 min) of broadband visible light. They used narrow band-pass filters to identify the causative wavelength to within 10nm, finding that the largest $\log_{10}$ reductions were caused in the 405 ± 5 nm region (Maclean et al., 2008).

In further experiments at the 405 nm wavelength, Maclean and co-workers established that a variety of bacterial species were susceptible to blue light inactivation. *S. aureus* was shown to be the most susceptible, followed by MRSA and *S. epidermidis* (Maclean et al., 2009). It appears that visible-light inactivation is generally more efficient for gram-positive bacteria, which could be due to the higher production of coporphyrin relative to gram-negative species as identified by Nitzan and co-workers (2004). They measured six times higher concentrations of coporphyrin in *S.aureus* and *S.epidermidis* bacteria than in gram-negative species, which were shown not to produce a predominant porphyrin, instead producing roughly equal concentrations of a variety of porphyrins including protoporphyrin, uroporphyrin, coporphyrin, 5- and 7- carboxy porphyrin.

With each porphyrin having a slightly different peak absorption band, it is possible that the lack of a predominant porphyrin is why Gram-negative bacteria appear to require a higher dose of blue light exposure to achieve useful levels of inactivation. These Gram-negative bacteria that prove more resistant to inactivation by blue light include *Klebsiella pneumaniae* and *Pseudomonas aeruginosa*. These are bacteria that are frequently isolated from infected patients. *P. aeruginosa* for example is found to be the infecting bacteria in over 50% of burn wound infections (Al-

Akayleh, 1999), while *Klebsiella* species are a common cause of hospital acquired urinary tract infection and pneumonia (Podschun & Ullmann, 1998). *E. coli*, a common cause of gastrointestinal infection and outbreaks which are well documented in the media, has also been shown to be particularly resistant to visible light inactivation (Maclean et al., 2009).

The dose of blue light radiation required to cause complete inactivation of the least susceptible species is very large, and the effect on mammalian cells of this level of radiation is unknown. Mammalian cells have previously been shown to be susceptible to visible light induced damage. Epithelial cells (Godley et al., 2005), gingivial fibroblasts (Taoufik et al., 2008), hepatocytes (Malik & Lugaci, 1987) and keratinocytes (Pflaum et al., 1998) have all been shown to be affected in some way by exposure to blue light. However, mammalian cells have various protective mechanisms that bacteria lack that theoretically should allow them to survive higher levels of oxidative insult (Bouillaguet et al., 2008). Various antioxidant enzymes have been shown to scavenge ROS before they can cause cell necrosis. Wang and co-workers identified phospholipid hydroperoxide glutathione peroxidase as being able to reduce the effectiveness of PDT. The singlet oxygen generated by stimulation of a porphyrin based photosensitiser reacts with unsaturated lipids in the membrane to form lipid hydroperoxides (LOOH), which are what disrupt the cell membrane. Phospholipid hydroperoxide glutathione peroxidase removes the LOOH before membrane damage can occur (Wang et al., 2001). Other studies have also shown this to be an important protective mechanism against $^1O_2$-induced cytotoxicity (Bickers & Athar, 2006; Thomas & Girotti, 1989). Enzymes and antioxidants such as superoxide dismutase, lactoperoxidases, peroxiredoxins, ascorbic acid and α-tocopherol can act in combination with β-carotene (Bohm et al., 2001; Marin-Garcia, 2005; Pflaum et al., 1998).

1.8 Summary

It is clear that despite modern sterilisation and cleaning techniques, hospital acquired infection is still a significant and costly problem. It would appear that airborne

contamination by bacteria is a common cause of HAI. High intensity blue light has been shown to have significant bactericidal action on various strains of bacteria which are known to cause these infections. The aim of this research is to investigate potential applications of HINS blue light in the medical environment. It is clear from the bacterial inactivation results that HINS-light could decrease the bacterial burden in operating theatres and ward areas, potentially decreasing the prevalence of HAI, particularly types of infection like surgical site infection and post implant infection where airborne bacteria is thought to be the main source of infection. However, the effects that blue light exposure may have on the mammalian tissues that would also receive exposure have not been established. Bacterial inactivation and decreased risk of HAI is obviously desirable, however, if the intensity of blue light required to achieve this is such that significant damage is also caused to other exposed tissues the potential applications of HINS-light inactivation would be limited to situations where human exposure would be minimised.

The aim of this research is to investigate if blue light has a detrimental effect on the function of tissues that receive exposure, and if so to establish a level of radiation which is not harmful.

1.9 Research objectives

A potential application of HINS-light is to maintain the sterility of wounds. Wounds present a point of entry for bacteria through which any airborne bacteria could take hold during dressing changes. To this end, an in-vitro model of wound healing, the fibroblast populated collagen lattice, will be used to establish if exposure of an open wound to HINS-light may have any inhibitory effect on wound healing.

- The effect of a range of intensities of HINS-light on contraction of the fibroblast populated collagen lattice wound model will be established.
- The effect of HINS-light on expression of alpha- smooth muscle actin, a protein marker of fibroblast contractile activity will be investigated.
- The MTT assay will be used to quantify the number of metabolically active fibroblasts present in the wound model following exposure to HINS-light.

- Live/dead staining of cells on the wound model following HINS-light exposure will be performed.
- The possibility that HINS-light induced inhibition of prostaglandin E2 is responsible for any effects measured will be investigated.
- A maximum dose at which no detrimental effects are observed will be established.

As described above, surgical site infection during implant of medical devices is a common mode of HAI. Use of HINS-light during implant procedures may provide a method of reducing numbers of bacteria in the operating field, thus minimising the risk of an infection developing. The effect of HINS-light on the mammalian cells which would receive irradiation will be investigated, specifically the effect on osteoblasts, the cells responsible for bone formation. These cells would receive exposure during the implantantion of hip replacement components, one of the most common procedures resulting in infection. Detrimental affects on osteoblast function would severely impede implant integration into the hip joint, and the subsequent stability of the hip replacement.

- The effect of HINS-light on osteoblast synthesis of alkaline phosphatase (ALP), an established marker of bone formation function, will be evaluated.
- Collagen is a major component of new bone. The effect of HINS-light exposure on collagen synthesis will be established.
- Osteoblast expression of osteocalcin following exposure to HINS-light will be measured.
- Any damage to the cell membrane caused by exposure to HINS-light will be visualised by scanning electron microscopy.
- A maximum dose at which no detrimental effects are observed will be established.

As mammalian tissue will receive exposure, so too will the materials that are being implanted. As an example of these materials, the effect of HINS-light exposure on the materials used in vascular repair procedures will be investigated. Infection of prosthetic vascular grafts is a serious problem and reducing the bacterial bioburden with the use of HINS-light could prove beneficial. The effect of the maximum safe dose, established in the mammalian cell experiments, on prosthetic graft materials will be investigated.

- SEM will be used to visualise any defects induced by HINS-light exposure on the surface of the materials.
- The mechanical strength of the materials will be measured before and after HINS-light exposure.
- Extracts of HINS-light exposed materials will be tested with human aortic smooth muscle cells to establish if HINS-light induces any cytotoxic leachable degradation of the materials.
- All experiments will be performed immediately following exposure and after a period of 2 to 3 months in storage, to establish if HINS-light causes any long-term oxidative damage.

Finally, having established a safe level of exposure for mammalian tissue to HINS-light, the photoinactivation properties of this safe maximum dose will be investigated on various relevant bacterial species.

- Gram-positive species
    - *Staphylococcus epiderimis*
    - *Staphylococcus aureus*
    - Methicillin resistant *Staphylococcus aureus*
- Gram-negative species
    - *Acinetobacter baumannii*
    - *Escherichia coli*
    - *Pseudomonas aergunosa*
- The ability of HINS-light, at the maximum safe dose, to inactivate *Staphylococcus epidermidis* on prosthetic vascular graft materials was also investigated.

- Scanning electron microscopy was used to visualise any morphological damage to *Staphylococcus epidermidis* following exposure to HINS-light.

From these results, the potential of HINS-light as a patient based decontamination device will be assessed, and potential applications in the healthcare environment discussed.

Chapter 2

MATERIALS AND METHODS: GENERAL

This chapter details the materials and methods which are common throughout this research. Any minor modifications to the general method are detailed in the appropriate chapter. Methods specific to each chapter are detailed in the methods section of the appropriate chapter.

2.1 High intensity narrow spectrum (HINS) light

2.1.1 HINS-light setup

The HINS-light system (Figure 2.1) delivered high intensity light in the blue region of the visible spectrum. The system consisted of an array of nine narrow-band light emitting diodes (LEDs) purchased from GE Illumination (product code Vio GE-VHD-1A-3D8). As delivered, the LEDs emit a warm white light via hemispherical phosphor coated caps which were carefully removed to expose three 405 nm diodes. The uncapped LEDs were arranged in a 3x3 grid pattern (6cm x 6cm) (Figure 2.1 (C)) attached to a heat sink supported by two pillars above a molded base which fixed the position of the treatment dish. This was manufactured in the Electronic and Electrical Engineering department of the University of Strathclyde. The distance from the sample plate to the LEDs was 8 cm. The heat sink ensured the operating temperatures of the LEDs remained constant for the duration of light treatments, and that no heating of the samples occurred. Sample temperature remained constant at 22°C for the duration of experiments. Three inter-changeable bases were required to accommodate different sample types, which consisted of a 50 mm Petri dish, 90 mm Petri dish and a rectangular multiwell plate base (Figure 2.2 (B)). The LED units were powered by a Rapid Electronics Switching Mode Power Supply (model number 85-1901, UK).

The 3x3 array of uncapped LEDs had a peak output at 405 nm and a 14 nm bandwidth at full-width half-maximum, measured on the combined output of the 3x3 LED array by spectrometer (model HR2000, Ocean Optics) (Figure 2.2). Four light units were available for use, and there was no variation between the intensity profiles of the individual units.

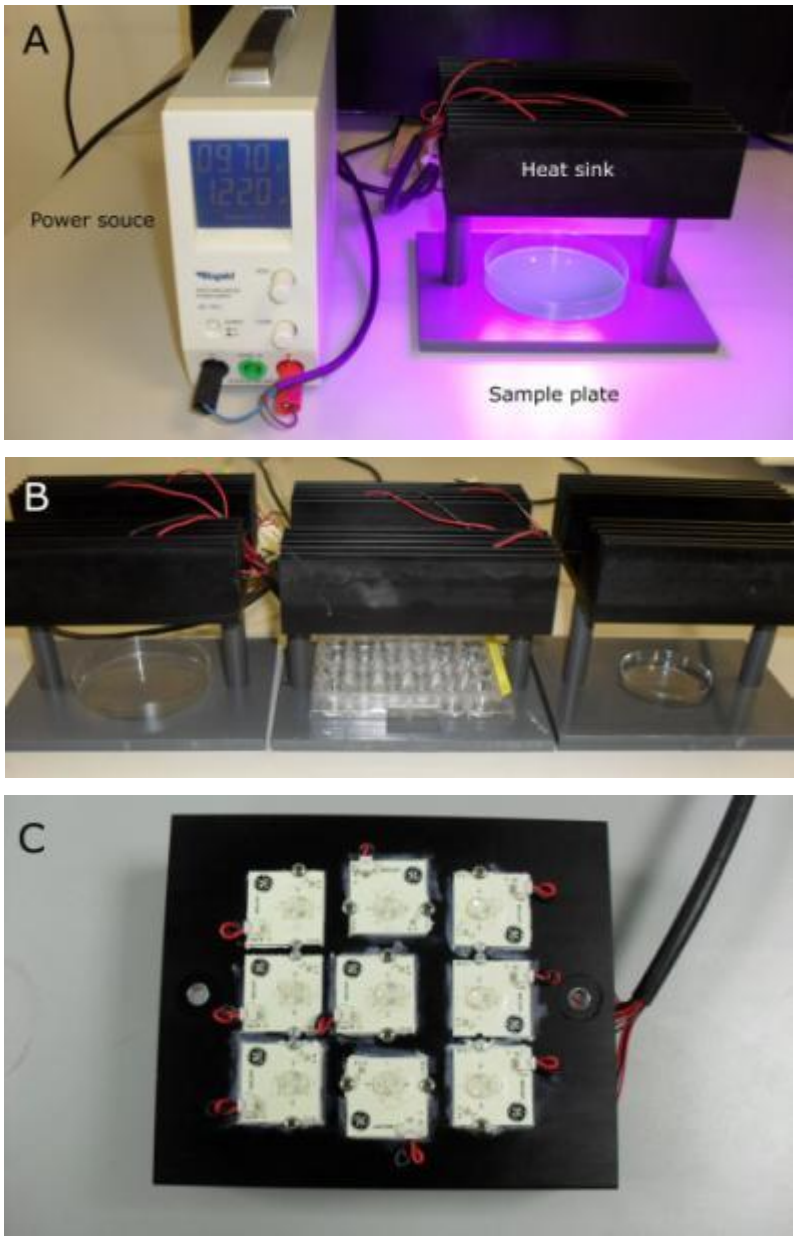

FIGURE 2.1 *HINS-light setup. Image (A) shows the treatment setup, image (B) shows the different base plates used depending on type of sample, and image (C) shows the 3x3 array of LED fixed to the underside of the heat sink.*

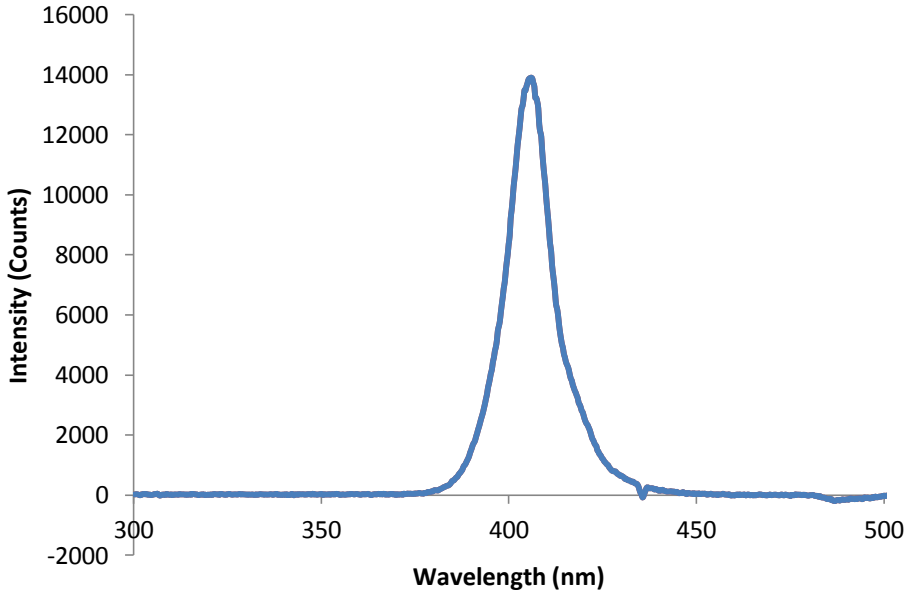

FIGURE 2.2 *Emission spectrum of 3x3 array of LEDs*

2.1.2 Intensity distribution

Treatments were performed at a range of intensities from 0.8 to 15 $mWcm^{-2}$ for 1 hour, giving a total dose range of 2.9 to 54 Jcm^{-2}. To achieve a wide range of dose responses, initial experiments were performed at an intensity of 0.5, 1.8 and 15 $mWcm^{-2}$, for which the intensity distributions across the base plate are shown in figure 2.3. Light intensity was measured at 0.5 cm intervals in both axes using a radiant power meter (model 70260, Oriel Instruments) and photodiode detector (model 1Z02413, Ophir) calibrated at 405 nm, and the mean intensity plotted as a function of radial position.

Due to the non-uniform intensity distribution, only the central wells of multiwell plates were used during exposure experiments, as indicated in figure 2.4. The maximum distance from the central point to the furthest edge of the selected wells is approximately 2.2 cm.

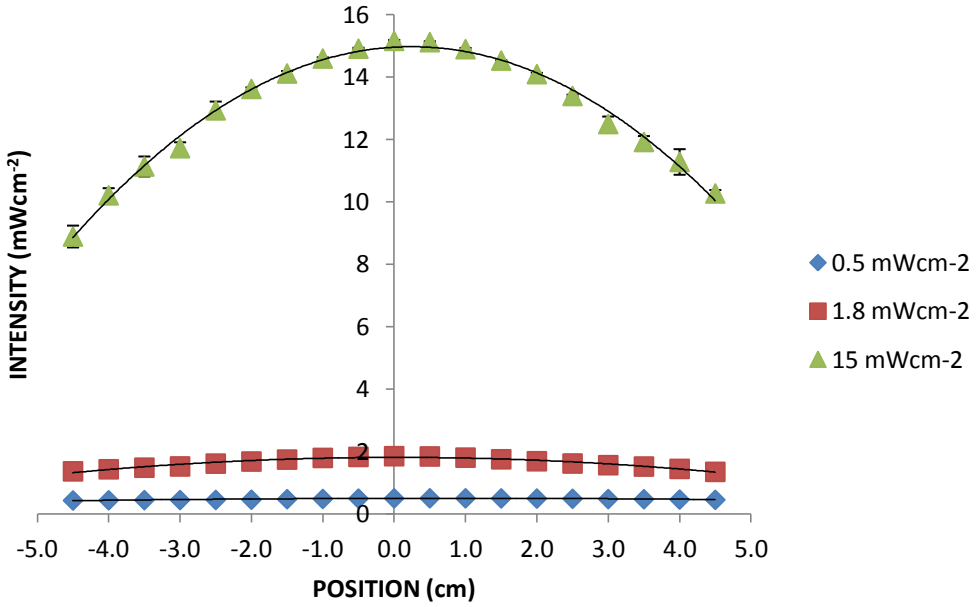

FIGURE 2.3 *Intensity profile of 405 nm LED array.*

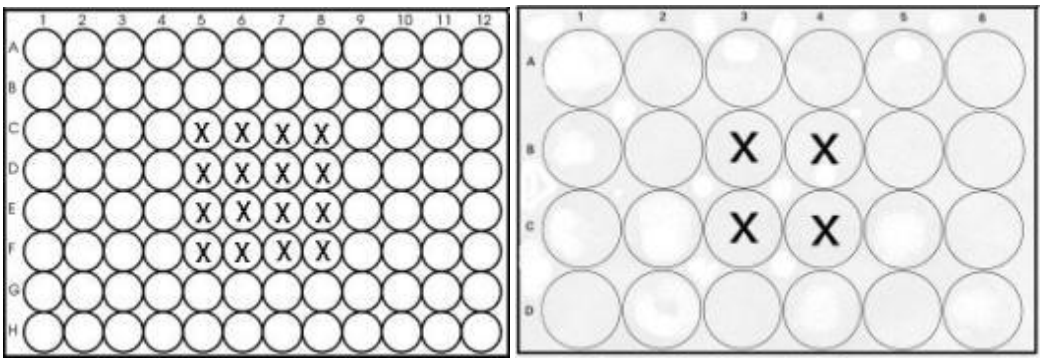

FIGURE 2.4 *Wells used for HINS-light sample exposure indicated with "X".*

2.1.3 Dose calculations

To calculate the dose applied to samples, the following formula was used:

$$E = Pt$$

Where E is the energy, or dose, applied, measured in Joules per unit area (Jcm^{-2}), P is the power (intensity) of light per unit area (Wcm^{-2}), and t is the duration of exposure in seconds.

2.2 Mammalian cell culture

This section details the cell lines used in this research and how they were maintained. The methods used for measuring the effect of HINS-light exposure on cell viability and function are detailed in the appropriate chapters.

2.2.1 Cell lines

The following cell lines were used throughout this research:

- Immortalised mouse fibroblast (3T3) cells, established from NIH Swiss mouse embryo (Todaro & Green, 1963)
- Immortalised rat osteoblast (FFC) cells (McKay et al., 1996)
- Primary human aortic smooth muscle cells (hASMCs), Lonza (Slough, UK)

2.2.2 Maintaining a cell line

All cells were cultured in Dulbecco's Modified Eagle's Medium (DMEM) (Lonza, catalogue number BE12-604F) supplemented with 10 % (v/v) foetal calf serum (PAA Laboratories, catalogue number A15-101), 1% (v/v) non-essential amino acids, penicillin (50 units/ml) and streptomycin (50 μg/ml). Cells were cultured as monolayers in 75 cm^2 tissue culture flasks in a humidified atmosphere of 5 % CO_2 in air at 37 °C. Cells were spilt every 3-4 days by decanting the growth medium and washing adherent cells twice in versene (0.02 % w/v), a chelating agent that prevents the cells from clumping when detached. Cells were detached from the flask by the addition of 2 ml 0.05 % trypsin in versene (w/v) for approximately 3 min. Complete DMEM was added to halt the action of trypsin and any cell clumps broken up by rapidly pipetting the solution up and down. Cells were split at a ratio of 1:15. Immortalised cell lines were continually passaged and taken for experimental use as required. Primary hASMCs cells were used between passage 2 and 4.

For experimental use, cells were removed from culture as for routine splitting and cell numbers estimated by haemocytometer. The required cell concentration was prepared in complete DMEM and seeded onto the surface in an appropriate volume; 0.2 ml, 1 ml and 3 ml, for 96 well plates, 24 well plates and 50 mm Petri dishes respectively. The seeding density used was either $5x10^3$ cells/cm^2 or $2.5x10^4$ cells/cm^2 depending on the test being performed (density used is specified in appropriate sections).

After seeding, cells were incubated for a minimum of 4 hr to allow attachment before HINS-light exposure. Culture medium was replaced with phosphate buffered saline (PBS) for the duration of HINS-light exposure due to possible generation of ROS in the culture medium. Cell viability has been shown to be significantly reduced by exposure to visible and near-UV radiation when exposed in culture medium compared to PBS (Smith, 2009; Stoien & Wang, 1974). The main component of culture medium responsible for ROS generation has been shown to be riboflavin, with tryptophan, tyrosine, pyridoxine and folic acid all enhancing the effect (Grzelak et al., 2001). After exposure, cells were incubated in fresh media until required, with media being refreshed every 2-3 days for the duration of the experiment.

2.3 Microbiological techniques

This section details the microorganisms and culture methods used in this research.

2.3.1 Bacterial strains used

The bacterial strains used throughout this research are listed in table 2.1. All bacteria were obtained from the National Collection of Type Cultures (NCTC), Collindale, UK, with the exception of methicillin-resistant *Staphylococcus aureus* 16A which was isolated from an infected wound at the Glasgow Royal Infirmary.

TABLE 2.1 *Bacterial strains used in this research*

MICROORGANISM	SOURCE	COLLECTION NUMBER
Staphylococcus epidermidis	NCTC	11964
Staphylococcus aureus	NCTC	4135
Methicillin-resistant *Staphylococcus aureus*	Glasgow Royal Infirmary	16A
Acinetobacter baumannii	NCTC	12156
Escherichia coli	NCTC	9001
Pseudomonas aeruginosa	NCTC	9009

2.3.2 Bacterial culture

Bacteria were obtained from the culture collection and reconstituted by inoculation into an appropriate broth before being stored on Microbank beads (ProLab Diagnostics) at -70 °C. For regular use, bacteria were cultured on tryptone soya agar (TSA) slopes, by streaking a TSA plate with the bead, incubating for 24 hr at 37 °C and sub-culturing from this onto a TSA slope. Slopes were stored at 4 °C and used as the source of inoculum for experimental use. To ensure consistency of bacterial strains fresh slopes were re-streaked every 4-5 weeks.

For routine experimental use, cultures were prepared in tryptone soya broth by aseptically extracting a streak of bacteria from the slope using a sterilised loop and transferring this into a conical flask of 100 ml broth. This was incubated at 37 °C for 18 – 24 hr under rotary conditions (120 rpm). The inoculated broth was centrifuged at 4300 rpm for 10 min to produce a pellet which was resuspended in 100 ml PBS to give a population density of approximately 10^9 colony-forming units per millilitre (CFU/ml). Serial dilutions were used to obtain the required bacterial density for experimental use.

2.3.3 Serial dilutions

Serial dilutions were performed by adding 1 ml of undiluted bacterial suspension to 9 ml PBS, giving a 10^{-1} dilution. This new supension was mixed in a vortex mixer (FisherBrand) to ensure uniform distribution and 1 ml of the new suspension added to a further 9 ml PBS to give a 10^{-2} dilution. This process was repeated until the required dilution was achieved.

2.3.4 Media and diluents

Culture media were prepared by dissolving the appropriate weight in distilled H_2O (dH_2O). Sterilisation was achieved by autoclaving at 121 °C for 15 min (110 °C for PBS). Table 2.2 details the media used during this research. Blood agar was prepared by adding 35 ml defibrinated horse blood (Oxoid, UK) to the blood agar base (500 ml) after sterilisation, giving a 7% v/v blood concentration. For preparation of agar plates and slopes, sterilised molten agar was allowed to cool to 48 °C and maintained at this temperature in a water bath. Approximately 20 ml of molten agar was poured into 90 mm Petri dishes or 10 ml into Universal tubes which, once set, were stored in the incubator overnight to dry before use.

TABLE 2.2 *Media and diluents used in bacterial culture*.

MEDIA	SUPPLIER	WEIGHT
Tryptone soya broth	Oxoid	13 g/L
Trytone soya agar	Oxoid	40 g/L
Agar bacteriological	Oxoid	15 g/L
Blood agar	Oxoid	40 g/L
PBS	Oxoid	1 tablet/100 ml

2.3.5 Bacterial enumeration

To calculate the decrease in population during inactivation experiments, the number of bacteria was counted before and after treatment. The count is recorded as colony-forming units per millilitre (CFU/ml). Samples were plated onto the appropriate agar

plate and incubated for 24 hr at 37 °C before enumeration. The plating and counting methods used depended on the expected population, and the various methods are described here.

2.3.5.1 Manual spread plating

Manual spread plating consisted of pipetting the required volume of bacterial suspension onto the agar plate surface and distributing evenly around the surface with an L-shaped spreader bar. The required volume depended on the expected population, and serial dilutions were used prior to spreading to ensure it was feasible to count the number of returned colonies. After incubation, a colony count of the entire plate was obtained and multiplied by the dilution factor to give the number of CFU/ml of the original sample.

2.3.5.2 Spiral plating

Spiral plating was carried out using a WASP 2 automatic plater (Don Whitley Scientific, UK), shown in figure 2.5. This can be used in two different modes:

a) As a simple alternative to manual spreading whereby 100 µl of bacterial suspension is spread onto plates in a uniform spiral distribution. In this case, after incubation, a colony count of the entire plate is obtained and multiplied by the dilution factor to give the number of CFU/ml of the original sample.

b) As a method that enables enumeration of a high concentration of bacteria on a single plate. In this case the WASP 2 automatic spreader creates spiral plates by dispensing 50 µl of bacterial suspension onto the agar surface in a logarithmic distribution. This creates a 1000 fold dilution from the centre of the plate to the outermost edge. Bacterial enumeration is achieved by centring a counting grid over the plate, with segments of the grid corresponding to known volumes of sample. The number of colonies per segment is converted to CFU/ml by reference to supplied charts or automatically using a PC and the ACOLYTE (Synbiosis, USA) software package. Again, if expected populations were anticipated to be too large to count, dilutions were performed prior to spreading and the returned count multiplied by the

dilution factor to give actual CFU/ml. An example of a spiral plate with uniform distribution and a spiral plate with logarithmic distribution is shown in figure 2.6.

FIGURE 2.5 Don Whitley Automatic Spiral plater (WASP 2)

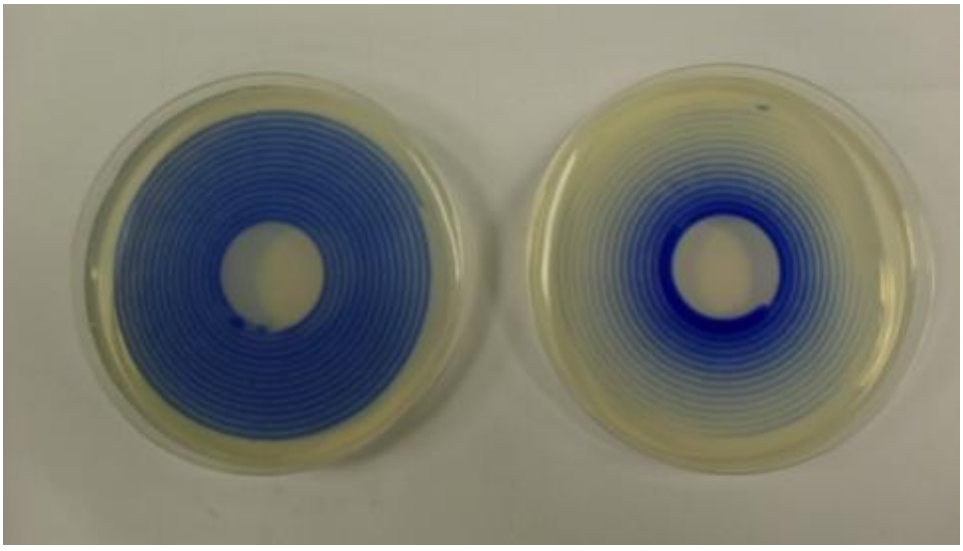

***FIGURE 2.6** Spread plate with uniform distribution on left, spiral plate with logarithmic distribution on right.*

Chapter 3

EFFECTS OF HINS-LIGHT ON WOUND HEALING

3.1 Introduction

The aim of the experiments described in this chapter was to investigate the use of 405 nm HINS-light as a potential wound disinfection technique, with a view to exploiting the difference in repair mechanism between mammalian cells and bacteria such that disinfection could be achieved without damaging the wound healing cells (Croteau & Bohr, 1997; Roehlecke et al., 2009). Traditional disinfection technologies are inappropriate for wound disinfection due to the damage they cause to mammalian tissue. UV radiation, for example, is known to cause skin cancer and damage to the eye (Norval et al., 2007). The fibroblast populated collagen lattice (FPCL) wound healing model (Bell et al., 1978) was used to investigate the effects of a range of doses of HINS-light on the contractile activity of fibroblasts. The effects were assessed in terms of cell motility and morphology, contraction of the lattice, and expression of the contractile protein α-smooth muscle actin (α-SMA). The involvement of prostaglandins in mediating the observed effects of HINS-light was also explored, as this has previously been shown to be a possible mechanism of gamma radiation induced inhibition of FPCL contraction (Carnevali et al., 2003).

3.1.1 Normal wound healing

The processes involved in normal wound healing are well understood and the description that follows has used Baum and Arpey (2005), Martin (1997) and Velnar et al.(2009) as key sources of information.

The normal wound healing process can be divided into four distinct but overlapping phases:

1/ Haemostasis: This begins immediately following tissue injury, where the first requirement is to stop bleeding. It occurs via vasoconstriction of damaged vessels

and initiation of the coagulation cascade, leading to clot formation. Platelets adhere to the damaged tissue helping to form the initial clot, and release various growth factors and vasoactive amines (including platelet derived growth factor (PDGF), insulin-like growth factor 1, epidermal growth factor, transforming growth factor-β (TGF-β), platelet factor-IV, serotonin, prostaglandins, and histamine). The coagulation cascade consists of two pathways, the tissue factor pathway and contact activation pathway, which both join a final common pathway that ultimately converts fibrinogen to fibrin, the main component of the haemostatic plug (Wolberg, 2007). The clot, comprising of fibronectin, vitronectin, von Willibrand factor and thrombospondin, forms a matrix allowing migration of cells. After haemostasis has been established (approx. 5-10min) active vasodilation and increased capillary permeability allows protein rich serum to enter the extravascular space.

2/ Inflammatory phase: Within one to two hours of injury, activation of the classical and alternative pathways of the complement cascade leads to inflammation. Polymorphonuclear leukocytes (PMN) are attracted to the wound area via chemotaxis and begin to phagocytose bacteria and remove devitalised tissue fragments and other debris, by release of oxygen free radicals and lysomal enzymes. Following removal of bacteria (around two to three days) excess PMNs are removed by macrophages or extrusion to the wound surface and do not contribute further to uncomplicated wound healing. The macrophages have differentiated from monocytes also attracted to the wound site, and by around day 3 are the most predominant cell type in the leukocyte population. Macrophages appear to have an important regulatory role, and are responsible for chemotaxis and proliferation of fibroblasts, production and debridement of collagen by these fibroblasts, proliferation of smooth muscle cells, and angiogenesis by proliferation of endothelial cells. Also occurring in this early inflammatory phase, epithelial cells at the wound edge begin to migrate over the wound surface and deposit components of the new basement membrane. By the late inflammatory phase (day 3) this will have developed into a full, thickened epidermal layer.

3/ Proliferation phase: This begins around day three and continues for approximately three weeks after injury. Fibroblasts are attracted to the wound site by PDGF, TGF-β, tumor necrosis factor (TNF) and interleukins, and within 7 days are the dominant cells in the wound. They adhere to and migrate upon the early extracellular matrix which consists mainly of fibronectin and hyaluronan. Fibroblasts produce further fibronectin and hyaluronan, and add collagen and proteoglycans to the matrix. The new extracellular matrix is an important regulator of proliferation and differentiation of cells within it. It consists of fibrous proteins (collagen, fibronectin, laminin and elastin) which provide structural support to the cells within, and allow for migration around, the matrix, and a glycosaminoglycan (GAG) ground substance (proteoglycans – heparin sulphate, chondroitin sulphate, keratan sulphate, and hyaluronic acid). Fibroblasts begin secreting collagen two to three days after wounding with production peaking around the second week. As fibroblasts are laying down collagen, collagenases are continually degrading it. In the proliferative phase synthesis exceeds degradation. Once haemostasis is achieved the number of fibroblasts decreases via apoptosis, signalling the start of the maturation/remodelling phase.

These processes require oxygen and therefore angiogenesis occurs in this proliferative phase. Angiogenesis is triggered by several growth factors (vascular endothelial growth factor, PDGF, TGF-β and basic fibroblast growth factor) which attract endothelial cells towards the "capillary sprout" of undamaged tissue. The endothelial cells proliferate, mature and organise themselves into new capillary tubes to oxygenate the developing fibroblast population. As the end of the proliferative phase approaches the demand for oxygen decreases and the unnecessary blood vessels are removed by apoptosis.

Contraction of the wound begins to occur in the proliferative phase around one week after injury. Fibroblasts differentiate into myofibroblasts, developing bundles of contractile microfilaments, cell-to-matrix attachment sites and intercellular adherence and gap junctions. The transition of fibroblasts to myofibroblasts appears to result from the combined action of mechanical tension, TGF-β and the splice

variant ED-A of cellular fibronectin (Gabbiani, 2003). Myofibroblasts are responsible for the largest proportion of wound contraction, peaking at 5 – 15 days following injury when contraction can be occurring at around 0.75mm per day. Contraction can reduce the area of the wound by up to 80%, at which point the myofibroblasts stop contracting and undergo apoptosis.

4/ Maturation phase: Around three weeks after injury, collagen synthesis and collagenase activity reach an equilibrium state. After this point, synthesis and breakdown continue but there is no increase in collagen content in the wound. Collagen fibrils are reorganised into thicker bundles and take on a more organised lattice structure. The new tissue gains strength by cross-linking and the majority of type III collagens are replaced with type I until they reach the 4:1 ratio of normal skin. The wound will regain around 80% of the strength of normal tissue. The extracellular matrix is degraded until the concentration of GAGs and other components is that of normal tissue.

3.1.2 Fibroblast populated collagen lattice wound model

While using a collagen substrate as a more in vivo-like environment for studying fibroblast behaviour, it was noted that "the activity of motile cells within a lattice makes a disturbance, causing a gradual collapse of the lattice to a dense, opaque body less than one-tenth of the original size" (Elsdale & Bard, 1972). This phenomenon was utilised by Bell et al when experimenting on a dermal component of a skin substitute for use in repair of skin wounds or burns (Bell et al., 1978). Despite initial promise this was unsuccessful as a skin graft, but their fibroblast populated collagen lattice (FPCL) has subsequently become established as an in vitro model for wound contraction.

Three mechanisms have been proposed for the contraction of fibroblast seeded collagen lattices; cell contraction, cell locomotion and cell elongation. Contraction in all three mechanisms is caused by elimination of water from between the fibrils which causes them to become more compacted. The mechanism of contraction is dependent on the method of manufacture of the collagen lattice. In the original

manufacture method, as introduced by Bell et al, the FPCLs are classed as free floating, in that they are cast in a Petri dish and released to contract immediately once set.

Cell contraction

This method of cell contraction is normally associated with myofibroblasts. Cells, which are attached to collagen fibrils and are under tension, can contract their bodies via ATPase activity which causes the sliding of actin-myosin filaments which in turn causes cell contraction (Ehrlich & Rajaratnam, 1990).

Cell locomotion

This method of contraction is associated with free floating FPCLs. Fibroblasts attach to collagen fibrils via integrins, and these integrin-fibril complexes are attached to the cytoplasmic microfilaments of the cell. Rapid myosin ATPase activity, which is associated with generating cell locomotion, causes the complexes to contract, pulling the fibrils over the cell membrane and bundling them into compacted collagen fibres.

Cell elongation

This occurs in the initial stages of FPCL preparation, as cells are transforming from the spherical form they take during culture to the stretched form they take when attached to the collagen matrix. As the cells elongate the collagen fibrils bundle together, expelling the water from between them and causing compaction. This mechanism only occurs in FPCLs which are seeded at a high density. In lower density FPCLs the force is not large enough for contraction to occur.

The FPCL has been used in many investigations since its development, but how accurately can it model the healing wound? It has some obvious limitations; granulation tissue in the healing wound consists of many cell types compared to the FPCL which consists of just one, and the FPCL is limited to 2-dimensional movement. An investigation into the FPCL as a model for chronic wound healing found that the contraction of collagen lattices populated with fibroblast cultures from wound biopsies did not have a correlation with the degree of wound closure in the

patients from whom the fibroblasts were cultured (Kuhn et al., 2000). The findings of this group also suggest that the age, source and type of fibroblasts used in the model have a large effect on model behavior. These variations were also noted by Finesmith et al, who seeded FPCLs with fibroblasts cultured from granulation tissue of various ages and found that the contractile ability varied significantly. Their results also noted that the time at which FPCL contractile activity was at its maximum did not coincide with the time at which a full-thickness wound would normally be experiencing maximum contraction (Finesmith et al., 1990). On the other hand, a review of FPCLs in 2003 examined the data from hundreds of original articles which utilised the FPCL, and showed a number of similarities between the FPCL model with respect to granulation and scar tissue (Carlson & Longaker, 2004). The gross and cellular morphology was found to be comparable, and it was found that the collagen matrix of FPCLs evolves to show similarities to the extra cellular matrix of granulation tissue. Biologically, FPCLs and scar/granulation tissue are comparable with respect to cell proliferation, survival, apoptosis and protein synthesis. Limitations in the model or lack of evidence pointing to model suitability are noted with respect to matrix metalloproteinases and cytokine secretion. The response of the FPCL model to various exogenous factors, such as corticosteroids, interferons and TNF-α, were noted to be analogous to granulation tissue. Carlson's review concludes that although the FPCL is not a perfect replica of the healing wound, with consideration taken of the known limitations, it has been an "adequate" model for the majority of investigations.

3.1.3 Wound infection

Wound infection presents a significant complication to the normal process of wound healing (Edwards & Harding, 2004). When the integrity of skin is compromised, such as by a wound, pathogenic microbes can contaminate the underlying tissue. The source of the bacteria can be environmental, from surrounding skin or from endogenous sources. Contamination by bacteria does not necessarily cause infection; normal wound healing can progress if bacterial levels are below 10^5 to 10^6 CFU/g of tissue (Landis, 2008). Compromised host immune response, or the presence of necrotic tissue, creates ideal growth conditions for bacteria which can allow bacteria

to proliferate to a level where infection is established and wound healing is delayed or halted. In the case of *Staphylococcus aureus* wound infection, extracellular adherence protein (Eap) of the bacteria has been identified as a cause of impaired wound healing. Eap has been shown to interfere with recruitment of inflammatory cells through direct interactions with adhesive proteins of the host cells, particularly intercellular adhesion molecule 1 (ICAM-1) (Chavakis et al., 2002; Haggar et al., 2004), and also to block angiogenesis in the proliferative phase (Athanasopoulos et al., 2006). Traditional management of infected wounds involves identification of the infecting organism, oral antibiotic treatment of the infection, debridement of necrotic tissue and application of appropriate dressings depending on the type of wound (Collier, 2004; Thomas, 1997).

3.1.4 Blue light and fibroblasts

There has not been a great deal of research directed towards the use of blue light to maintain the sterility of living tissue, however, there has been some research into more active wound healing applications of blue light. The use of low level laser therapy (LLLT) to enhance wound healing is well documented (Mester et al., 1985; Ribeiro et al., 2004), however, more recently the use of blue LED light has also been found to have similar properties. Using 10 minute exposures of 50 $mWcm^{-2}$ 470 nm LED light, Adamskaya et al demonstrated a significant decrease in wound size and enhanced epithelialisation relative to untreated controls in rat excision wound models (Adamskaya et al., 2010). Similarly, the findings of Wataha et al. that low doses of blue light (400-500 nm) shortened the population doubling time of fibroblasts led them to the conclusion that blue light could be used therapeutically to enhance activity of slowly dividing cells during healing (Wataha et al., 2004). Conversely, there has also been some interest in applications of blue light to slow down wound healing. Recently, Oplander et al carried out an investigation into the anti-proliferative properties of blue light on dermal fibroblasts as a novel treatment for hypertrophic scarring, fibrotic skin disease and keloid formation (Opländer et al., 2011).

3.2 Methods and materials

3.2.1 Cell culture

Immortalised 3T3 mouse fibroblast cells were cultured as described in section 2.2

3.2.2 Isolation of acid-soluble collagen

Type-1 collagen was isolated from rat tail tendons. The rat tails were rinsed with 70% v/v ethanol before dissection. Tails were cut in half with a sterilised scalpel and the skin removed by incising along the length of the section and peeling it away. Each tail had six tendon bundles which were removed with sterile forceps. Tendons were collected in sterile dH_20 until sufficient tails had been processed, at which point excess water was removed by filtering through gauze (Type 13 light, Clini Supplies Ltd). Approximately 8 tails worth of tendon was dissolved in 500 ml 0.5 M acetic acid for 48 hr. After this time any un-dissolved matter was removed by filtering through sterile gauze and the solubilised tendon solution transferred to 50 cm lengths of dialysis tubing. Prior to use the dialysis tubing had been boiled for 1 hr in 50 % (v/v) ethanol, followed by 2x 1 hr in 10 mM $NaHCO_3$/1 mM ethylenediaminetetraacetic acid (EDTA), and 2x 1 hr in dH_20, in that order. Tubing was stored at 4 °C in dH_2O until required. The solubilised tendon solution was dialysed twice against 0.1x DMEM for 24 hr at 4 °C. Following this, the collagen solution was removed from dialysis tubing and sterilised by centrifugation at 10000 rpm for 2 hr at 6 °C. The supernatant was transferred into sterile bottles and the concentration of collagen solution in each bottle calculated by weighing 1 ml of the dried sample. The concentration was taken as the average mg/ml of three samples. Sterility of the collagen solution was verified by incubating a 1 ml sample from each bottle in Sabouraud's medium and brain heart infusion for 3 days.

3.2.3 Preparation of collagen lattices

Collagen gels 0.3 % (w/v) were formed by mixing collagen solution with 1 ml of 10x DMEM / 0.4 M NaOH (2:1) and making up to 10 ml with 1/1000 (v/v) acetic acid. The required volume of collagen solution was calculated from the concentration of the extracted stock. Typically, collagen at around 3.57 mg/ml was used, giving 8.4

ml collagen solution for a 0.3 % (w/v) collagen gel. The pH was adjusted to 8 – 8.5 by drop wise addition of 1 M NaOH, judging the pH by the point at which the solution changed colour from yellow to pink/purple. 5 ml of this gel forming solution was pipetted into 60 mm Petri dishes and allowed to set for a minimum of 4 hours at room temperature in a laminar-air-flow cabinet before use.

3.2.4 Seeding of collagen gels with 3T3 cells

Prior to seeding, gels were washed twice in complete DMEM, by incubation for at least 15min. Gels were seeded at $2.5x10^4$ cells/cm^2. Cells were counted using a haemocytometer and the required cell number was prepared in 3 ml complete DMEM which was pipetted onto the gel surface. Cells were allowed to attach for 24 hours in an incubator. The area of the gel was calculated from the internal diameter of the Petri dish as 19.2 cm^2. After 24 hours the medium was removed and a sterile spatula was used to detach the FPCL from the walls of the 60 mm Petri dish. The FPCL was then transferred to a 90 mm dish to prevent sticking of the gel to the walls of the dish, and floated in 13 ml complete DMEM. 5 ml of growth medium was removed every second day and replaced with fresh DMEM.

3.2.5 FPCL contraction

The size of collagen gels was measured daily by placing the Petri dish containing the FPCL on a piece of standard graph paper illuminated from below by a light box. Images of the FPCL were captured on a Nikon D300 digital camera fixed in position above the light box. The surface area was calculated using ImageJ image processing software. The number of pixels that the FPCL occupied was measured by outlining the gel circumference and comparison with the pixel number of a 1 cm^2 square of graph paper gave the FPCL area. A matlab programme was used to automate this process by automatic selection of the FPCL area by colour subtractions and adjustment of the contrast threshold such that only the FPCL contributed to the pixel count. This significantly quickened the image processing procedure and comparison of the different techniques did not show any difference in area calculations. Six separate measurements of the same FPCL by the ImageJ method gave a mean area of 19.4 ± 0.9 cm^2, while the matlab programme gave 19.3 ± 0.3cm^2. The contraction

pattern of a free-floating FPCL is shown in figure 3.1. FPCL contraction can be split into three distinct phases (Nishiyama et al., 1988). There is an initial lag phase during which little contraction occurs, due to insufficient number of cells. The duration of this depends on the seeding density and proliferative rate of the cells, and was found to last less than 24 hours with the density of 3T3 cells used throughout all FPCL experiments. Following the lag phase there is a period of rapid contraction, termed the log phase. This begins once cell numbers reach a critical level, continues until approaching maximum contraction, and is identified as from days 1 to 5. Slow contraction continues from this point onwards.

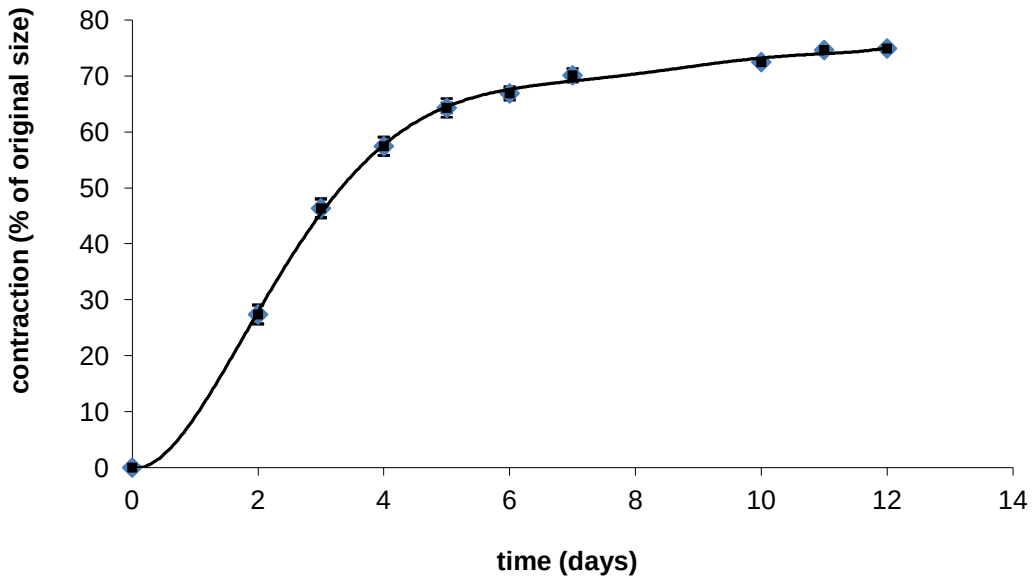

FIGURE 3.1 *Contraction of free floating FPCL (n=4 ± SEM).*

3.2.6 Measurment of fibroblast function/viability

FPCLs were exposed to HINS light on one of the three key points; either lag, log or slow contraction phases, which when taking the point when FPCLs were transferred to the large Petri dish as day 0 of contraction, were established to be day 1, 3 and 5 respectively. The tests described below were used to establish the effect of HINS-light exposure on fibroblast function or viability.

3.2.6.1 Fibroblast contractile function

The effect of HINS-light on the ability to contract the FPCL was assessed by daily measurements of the surface area of FPCL as described in section 3.2.5..

3.2.6.2 MTT-collagenase assay

The MTT assay was used to quantify cell viability following HINS-light treatment. MTT (3-(4,5-Dimethylthiazol-2-yl)-2,5-diphenyltetrazolium bromide) enters the cell and is reduced to a purple formazan product by intracellular reductase enzymes. At the appropriate time points, cell culture medium was removed from the dish and the FPCL returned to a 60 mm Petri dish. 3 ml MTT (10 mM) was pipetted onto the surface of the collagen gel and incubated for 4 hr at 37 °C. MTT was removed and the cells released from the FPCL by the addition of 3 ml collagenase (0.5% (w/v), type II from Gibco) to the FPCL surface for up to 1 hour, or until the cells had visibly detached from the gel. Cells were collected, centrifuged at 2000rpm, the supernatant discarded and the cells resuspended in 2 ml dimethyl sulfoxide (DMSO) to solubilise the product. Samples were diluted 1:10 and the absorbance measured at 540 nm using a two-channel spectrophotometer (Shimazdu, model UV-2101PC). This method was adapted from that developed and validated by Ho et al (2009).

3.2.6.3 α-smooth muscle actin expression

Immunoblotting was used to establish the effect of HINS-light on the expression of α-SMA in fibroblasts. Samples were taken at 48 and 144 hours after treatment. Cells were detached from the collagen as for the MTT assay, but then centrifuged at 800 rpm for five minutes and washed twice in 1 ml PBS. Cells were then homogenised in 1 ml 0.1M sodium phosphate (NaPi) buffer (pH 7.4) using 7 strokes of a motorised Potter-Elvehjem homogeniser, consisting of a cylindrical PTFE pestle rotating in a close fitting glass sample tube which subjects the cells to shearing forces. The homogenised cell solution was immediately divided into 50 µl aliquots and stored at -80°C until analysis. Protein concentration (mg/ml) was established via Lowry assay (described in section 4.2.3.4) and the homogenized samples were

prepared in Laemmli buffer (appendix A) to give a final loading concentration of 10 µg/well. Samples were boiled in stop-lock Eppendorf tubes for 2 minutes. Immunoblotting was carried out in two stages:

1. Sodium dodecyl sulfate polyacrylamide gel electrophoresis (SDS-PAGE) was used to separate the proteins according to molecular weight. The resolving and stacking gels were prepared as shown in table 3.1. Samples were loaded into wells and run at 50 mA for 15 minutes to stack the samples and then at 150 V until the dye front approached the bottom of the gel.

TABLE 3.1 *Preparation of gels for western blotting*

Solution	10% Resolving gel	Stacking gel
Acrylamide/bis acrylamide (40% (w/v) solution)	5.625 ml	0.5 ml
Stacking gel buffer	-	1.25 ml
Resolving gel buffer	5.625 ml	-
1.5% Ammonium persulfate	1.125 ml	0.25 ml
Distilled water	10.125 ml	3 ml
Tetramethylethylenediamine (TEMED)	17 µl	5 µl

2. Immunoblotting

After electrophoresis the proteins were transferred onto a polyvinylidene fluoride (PVDF) membrane using the arrangement shown in figure 3.2.

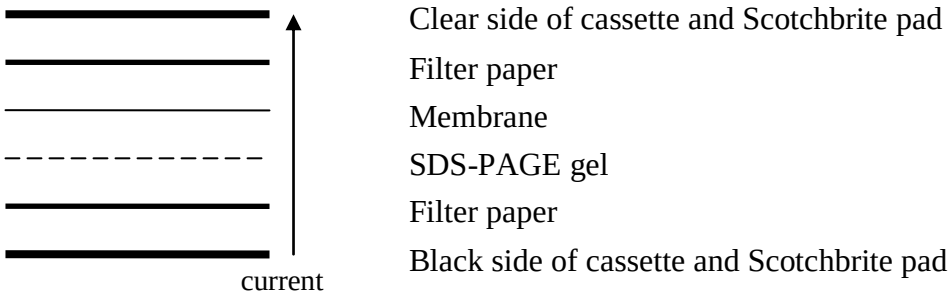

FIGURE 3.2 *Cassette configuration for blot transfer.*

The Scotchbrite pads, filter paper, membrane and gel were soaked in Towbin's transfer buffer (composition in Appendix) for 15 minutes prior to transfer. The transfer was carried out at 200 mA overnight.

After transfer the PVDF membrane was placed in 3% (w/v) gelatin in Tween Tris Buffered Saline (TTBS; composition in Appendix) for 1 hour at 37 ℃, then incubated on an orbital shaker for 30 min at room temperature in the same buffer. The membrane was then washed in TTBS for 5 min with agitation, before the primary rabbit polyclonal antibody (ab1694, AbCam, Cambridge UK) was added. The antibody was supplied at 0.2 mg/ml and diluted to 1 µg/ml in 1% (w/v) gelatin in TTBS. It was added for 1 hour at 37 ℃, followed by 30 minutes at room temperature with agitation. The antibody was removed, and the membrane washed three times in TTBS for 5 minutes at room temperature. The secondary anti-rabbit IgG antibody (Sigma-Aldrich) was diluted 1:10000 in 1% (w/v) gelatin in TTBS and added for 1 hour at 37 ℃, and then shaken for 30 min at room temperature. The membranes were then washed twice in TTBS for 5 min and once in Tris buffered saline (TBS) for 5 min. Membranes were developed using an alkaline phosphatase detection system (Bio-Rad, California), for approximately 15 minutes until the colour developed. They were then scanned on a Canon (CanoScan, N670U) scanner and relative optical density of the bands analysed using NIH ImageJ.

3.2.6.4 Live/dead staining

Live/dead staining was performed with propidium iodide and acridine orange at 24, 48 and 120 hours following HINS-light exposure. 2 ml (1:1) propidium iodide (20 μg/ml in PBS) and acridine orange (100 μg/ml in PBS) was used to stain FPCLs. The stains were added for 1 min in dark conditions before rinsing with PBS. Samples were then fixed with approximately 10 ml formalin (40%) until analysis was performed. The fixed FPCLs were stored at 4 °C wrapped in parafilm to prevent evaporation of the fixative.

Propidium iodide binds to the DNA of cells with compromised membranes, thus staining dead or dying cells. It fluoresces at 617 nm (orange/red). Acridine orange is a cell permeable, nucleic acid selective dye with an emission maximum at 525 nm. The nuclei of viable cells therefore appear green . Analysis was performed using a Zeiss AxioImager ZI microscope with 20x water lens by Mrs Elizabeth Goldie. Samples were stored for a maximum of two weeks prior to analysis. Acridine orange and propodium iodide have been shown to be stable stains over this period of time (Bank, 1987; Mascotti et al., 2000).

3.2.7 Prostaglandin E2 inhibition

An increased cellular production of prostaglandin E2 (PGE2) induced by radiation insult has been shown to inhibit fibroblast proliferation, migration, chemotaxis and FPCL contraction (Kohyama et al., 2001). To investigate whether the inhibitory effect of HINS-light on the fibroblast mediated contraction of the collagen gel was also due to increased PGE2 production by the cells, the non-steroidal anti-inflammatory drug (NSAID) indomethacin was used to inhibit PGE2 production (Delamere et al., 1994) by the fibroblasts prior to HINS light treatment.

A stock solution of 10 mM indomethacin (Sigma, product code I7378) was prepared by dissolving 3.58 mg in 1 ml dimethyyl sulfoxide (DMSO) solvent. From the stock solution, a 3 μM solution was prepared by diluting with DMEM. Gels were seeded with fibroblasts as before but in 2 ml DMEM, and the cells allowed to attach for

three hours before the addition of 1 ml of the 3 µM indomethacin solution to give a final culture concentration of 1 µM. Experiments were conducted to ensure that indomethacin itself, or the DMSO that it was dissolved in, had no toxic effect on the cells (Figure 3.3). The DMSO alone was diluted to 10^{-4} in DMEM to give the same volume as that used to dilute the stock solution of indomethacin to 1 µM. 3T3 cells incubated with DMEM provided the control. Cell viability was assessed by MTT assay as described in 3.2.5.2 at 2 and 6 days incubation. Culture medium was changed every 2 days.

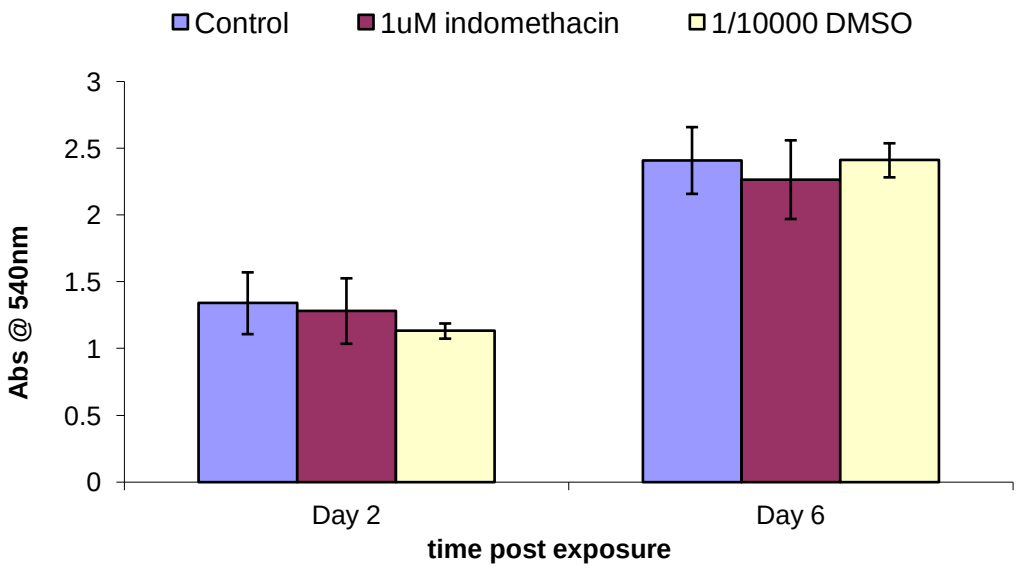

FIGURE 3.3 *Toxicity of 1 µM indomethacin and a 1/10000 dilution of DMSO. n=3 ± SEM. No significant effects found (P > 0.05).*

Contraction was measured in the presence and absence of HINS-light exposure. Following treatment with HINS-light, contraction was measured daily (as described in section 3.2.5) and MTT-collagenase assay performed (as described in section 3.2.5.2) at various time points. Indomethacin was present throughout the contraction time, with medium changes performed every 2-3 days.

3.2.8 Statistical analysis

Where appropriate, results are expressed as mean ± standard error of the mean (SEM). Significance has been established by one-way ANOVA followed by either Dunnett's comparison test, which compares the means of each group against the mean of the reference group, or Fisher's test which compares the means of different groups against each other.

3.3 Results

3.3.1 FPCL contraction

FPCLs were exposed to 1 hr durations of HINS-light at 0.5, 1.8 and 15 $mWcm^{-2}$. Contraction curves of FPCLs following exposure are shown in figure 3.4. HINS-light treatment during lag phase (at day 0) at 0.5 and 1.8 $mWcm^{-2}$ did not cause any significant delay in FPCL contraction. Treatment at 15 $mWcm^{-2}$ caused an immediate and extended halt in FPCL contraction (figure 3.4(A)). A similar trend is observed when exposing cells during the active phase (at day 3) of contraction (figure 3.4(B)); FPCLs exposed to 0.5 and 1.8 $mWcm^{-2}$ continue contracting with no significant deviation, while FPCLs exposed to 15 $mWcm^{-2}$ HINS-light stop contracting. Exposure on day 5 after FPCLs had reached maximum contraction (figure 3.5(C)) had no significant effect on FPCL area during the following four days, with FPCLs exposed to 15 $mWcm^{-2}$ HINS-light maintaining ~72% contracted size.

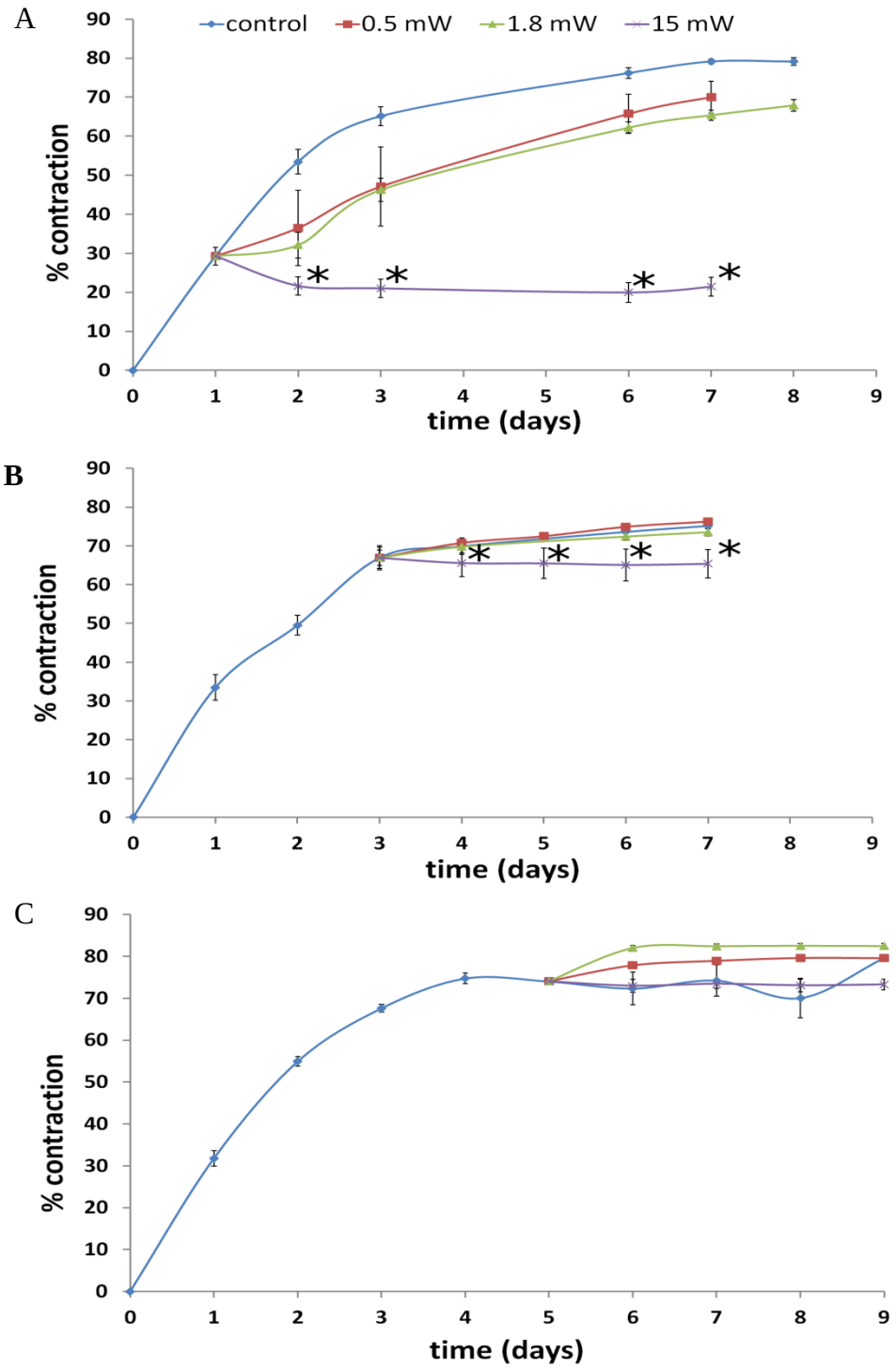

FIGURE 3.4 *Contraction of FPCLs exposed to 0.5, 1.8 and 15 mWcm^{-2} HINS-light for 1 hr, on day 0 (A), 3 (B) and 5 (C) of contraction. n = 3 ± SEM, *indicates significant difference from control at each time point (P < 0.05, ANOVA followed by Dunnett's comparison)*

3.3.2 MTT assay

The MTT assay results show that exposure at the start of the contraction period at 0.5 and 1.8 $mWcm^{-2}$ did not cause a significant difference in cell number up to 120 hours post-treatment (Figure 3.5(A)). Exposure to 0.5 and 1.8 $mWcm^{-2}$ on days 3 and 5 of contraction also did not cause a significant change in cell number over the remainder of contraction; 72 or 24 hours respectively (figure 3.5(B) and (C)). Treatment at 15 $mWcm^{-2}$ for 1 h during the lag phase caused an 80 % (± 3%) decrease in cell number after 24 h. By 120 h post treatment, cells in FPCLs treated at 15 $mWcm^{-2}$ did not show significant recovery with a reduction of 73 ± 6% compared to the untreated control. Exposure to 15 $mWcm^{-2}$ HINS-light during the active phase of contraction also caused a significant decrease in cell number which remained at 72 hr post exposure (39 ± 5 % at 24 hr, 23 ± 5 % at 72 hr post exposure). 15 $mWcm^{-2}$ exposure after the majority of the contraction had occurred caused a significant 84 ± 3 % decrease in viable cell number.

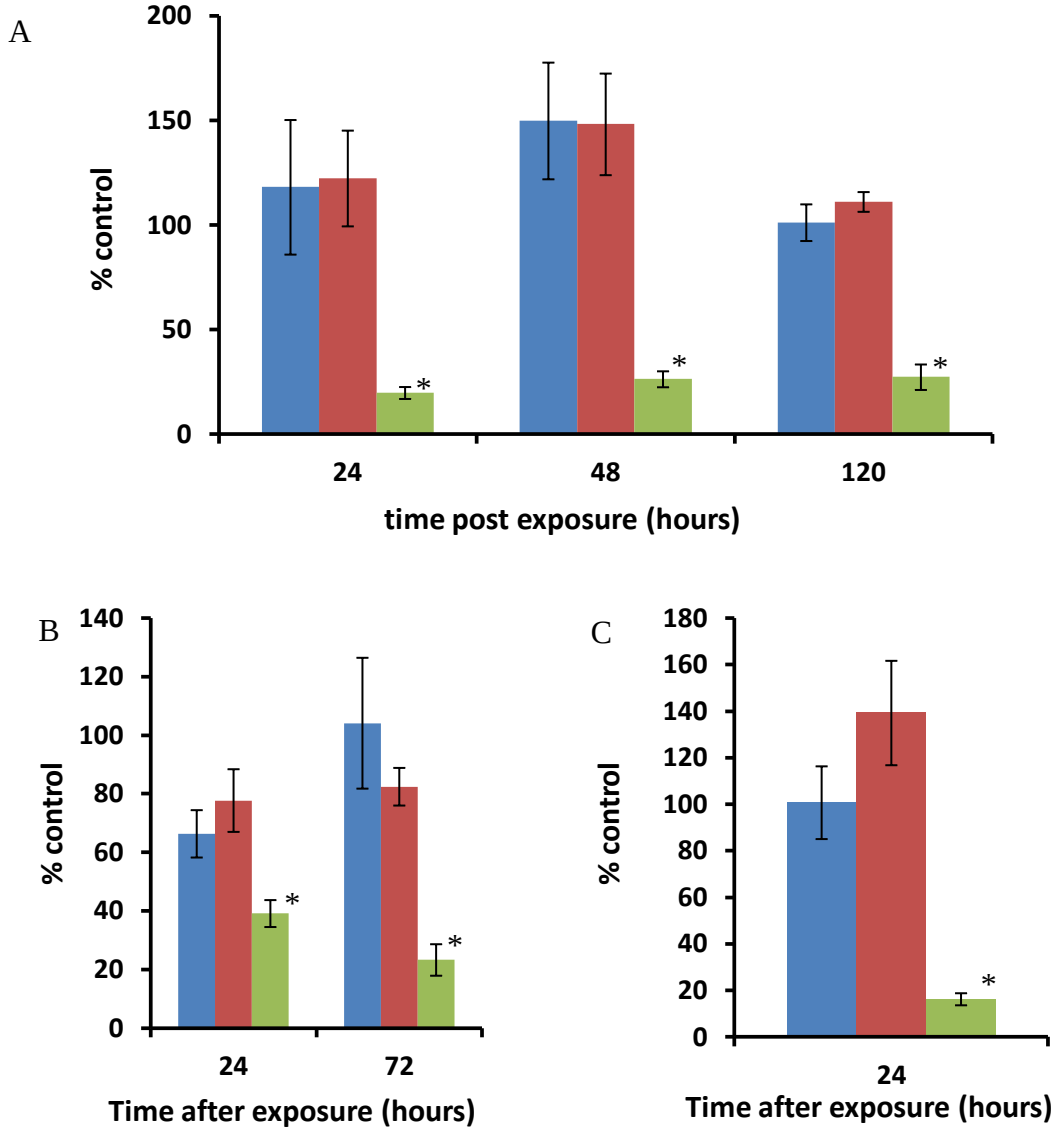

FIGURE 3.5 *MTT assay results for FPCLs exposed to HINS-light at 0.5 (blue), 1.8 (red) and 15 mWcm^{-2} (green) during lag(day 0) (A), log (day 3) (B) and slow contraction phases (Day 5) (C) phase of contraction. Treatment at 15 mWcm^{-2} at any time point caused a significant reduction in cell number which did not recover over the contraction period. n=3, *P<0.05, (ANOVA followed by Dunett's comparison)*

The MTT assay was also used to establish the intensity at which the effects of HINS-light became significantly inhibitory (Figure 3.6). This was found to be at intensities above 5 $mWcm^{-2}$, at which point cell number dropped significantly to 90 ± 5 % of the untreated control.

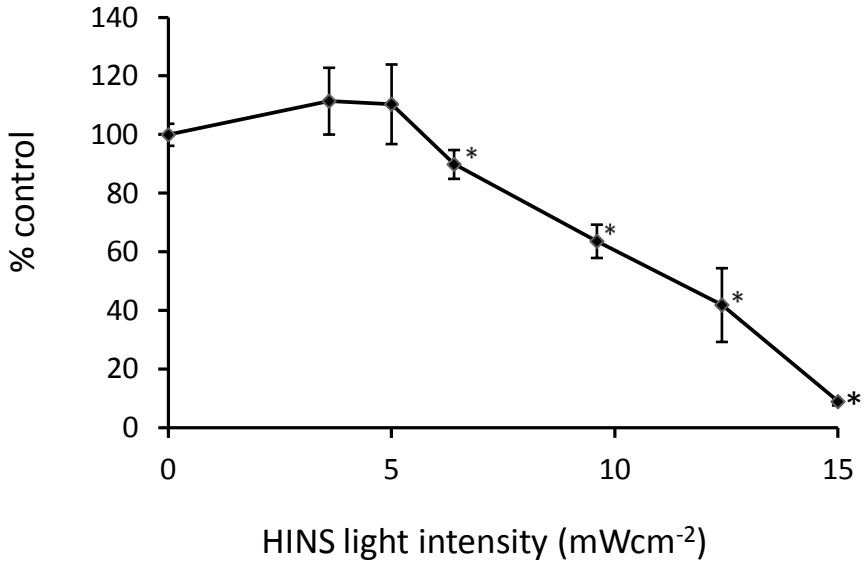

FIGURE 3.6 *MTT assay of FPCLs 24 hr post exposure. * indicates significant decrease in cell number as compared to exposure at 5 $mWcm^{-2}$ ($P < 0.05$, ANOVA followed by Dunnett's comparison, $n = 4 \pm SEM$)*

3.3.3 Propidium iodide and acridine orange staining

Staining with propidium iodide and acridine orange showed no discernable visual difference in morphology between control FPCLs and those treated at 0.5 and 1.8 $mWcm^{-2}$ during the lag phase of contraction (Figure 3.7). In contrast, FPCLs treated at 15 $mWcm^{-2}$ did not appear to proliferate at the same rate as control FPCLs, and the cells lost the normal elongated morphology of fibroblasts. By 120 hours post exposure to 15 mWcm-2 HINS-light, cells appeared to show some signs of recovery, regaining the stretched morphology associated with healthy fibroblasts.

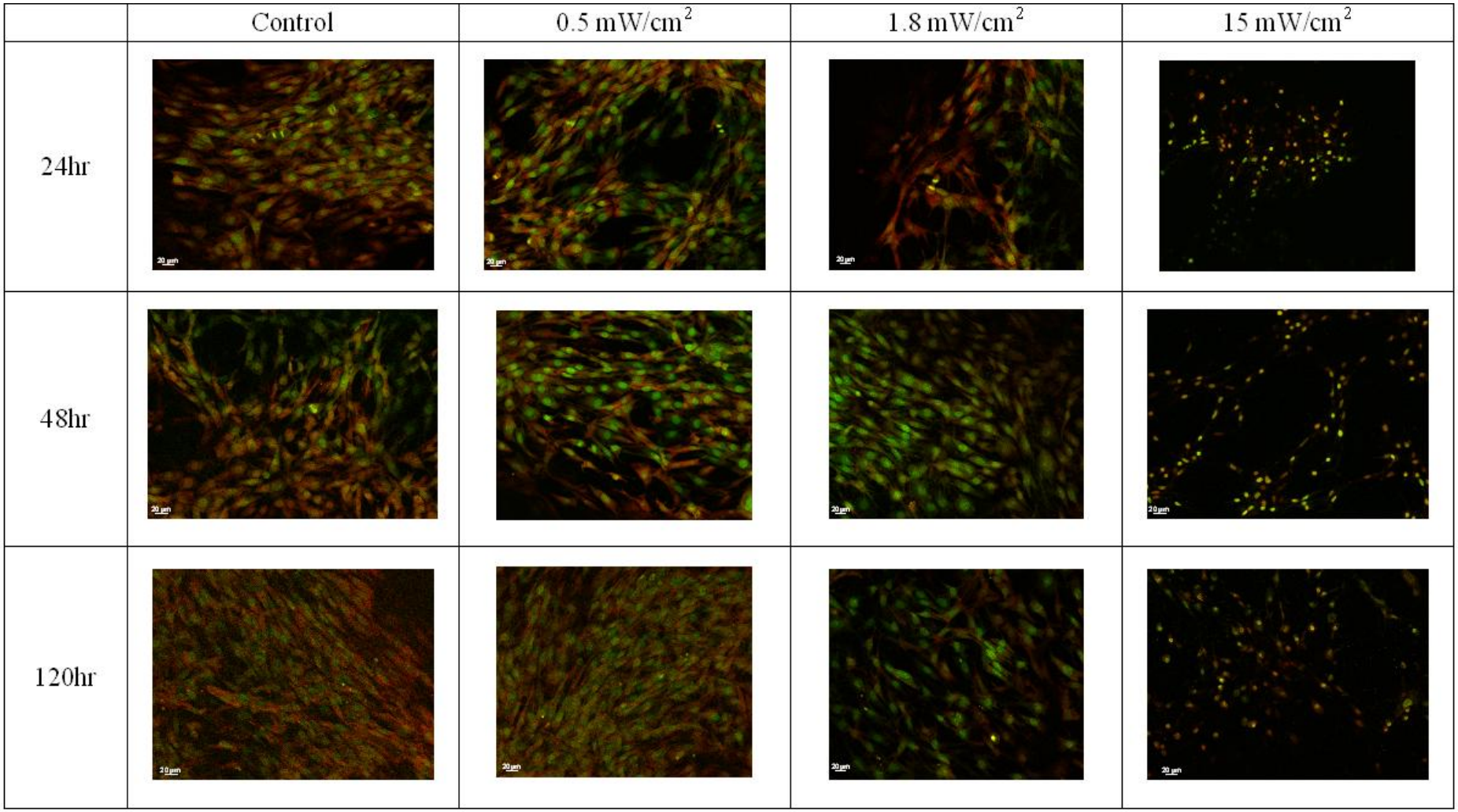

FIGURE 3.7 *Fluorescene microscopy of propidium iodide and acridine orange stained FPCLs. Scale bars are 20µm.*

3.3.4 α-SMA immunoblotting

An example of the bands produced by immunoblotting are shown in Figure 3.8(A). There was insufficient protein content in cells collected from FPCLs exposed to 15 $mWcm^{-2}$ HINS-light taken at 48 hours post treatment to perform SDS-PAGE, therefore there are no results for this combination.

Analysis of optical density of bands is shown in Figure 3.8(B). Exposure to 0.5 and 1.8 $mWcm^{-2}$ HINS-light appeared to cause a slight but non-significant reduction in α-SMA expression at 48 hours post exposure. FPCLs exposed to 0.5 $mWcm^{-2}$ HINS-light had 75 ± 10% the expression of controls, while those exposed to 1.8 $mWcm^{-2}$ was 54 ± 21%. By 144 hours post exposure, FPCLs exposed to 0.5 $mWcm^{-2}$ appeared to have completely recovered (95 ± 5%), while the reduction in α-SMA expression in FPCLs exposed to 1.8 $mWcm^{-2}$ persisted (76 ± 6%). FPCL exposure to 15 $mWcm^{-2}$ HINS-light caused almost complete inhibition in α-SMA expression 48 hours following exposure. By 144 hours post exposure α-SMA expression had only partially recovered to 11 ± 4% of the untreated control.

A

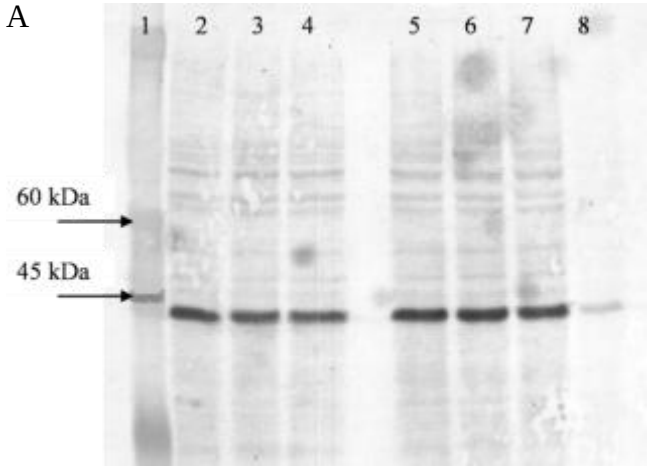

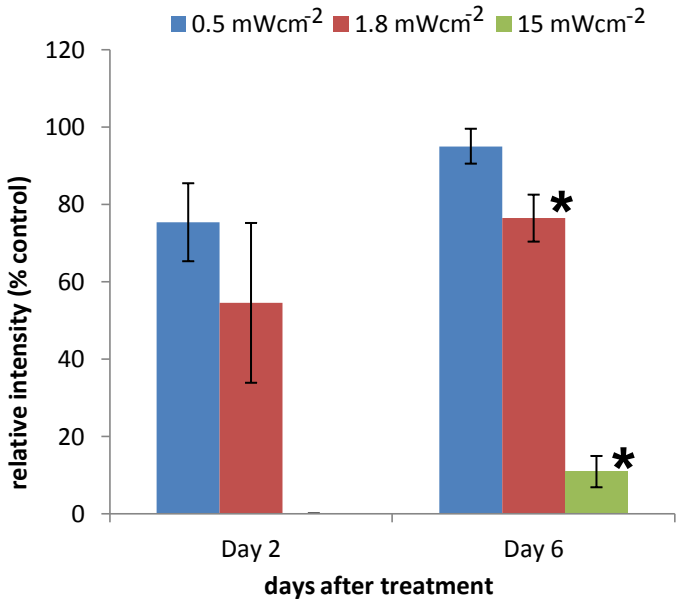

B

FIGURE 3.8 *(A) Western blot of α-SMA in FPCLs exposed to 1 hour of HINS-light at intensities of 0.5 mWcm^{-2}, 1.8 mWcm^{-2} and 15 mWcm^{-2}. Bands are: (1) molecular marker, (2) control after 48 hours, (3) 0.5 mWcm^{-2} after 48 hours, (4) 1.8 mWcm^{-2} after 48 hours, (5) control after 144 hours, (6) 0.5 mWcm^{-2} after 144 hours, (7) 1.8 mW cm^{-2} after 144 hours, and (8) 15 mWcm^{-2} after 144 hours. Molecular weight of α-SMA is 42 kDa. Figure 4 (B). Optical density analysis of α-SMA protein bands in western blot. *P < 0.05 using ANOVA followed by Dunnett's comparison. n = 3 ± SEM*

3.3.5 Involvement of prostaglandins in the inhibition of contraction by HINS-light

Treatment of fibroblasts with 1 μM indomethacin had no significant effect on inhibition of FPCL contraction either in the presence or absence of 15 $mWcm^{-2}$ HINS-light (Figure 3.9). Indomethacin alone was shown to have no significant inhibitory effect on FPCL contraction ($P > 0.05$).

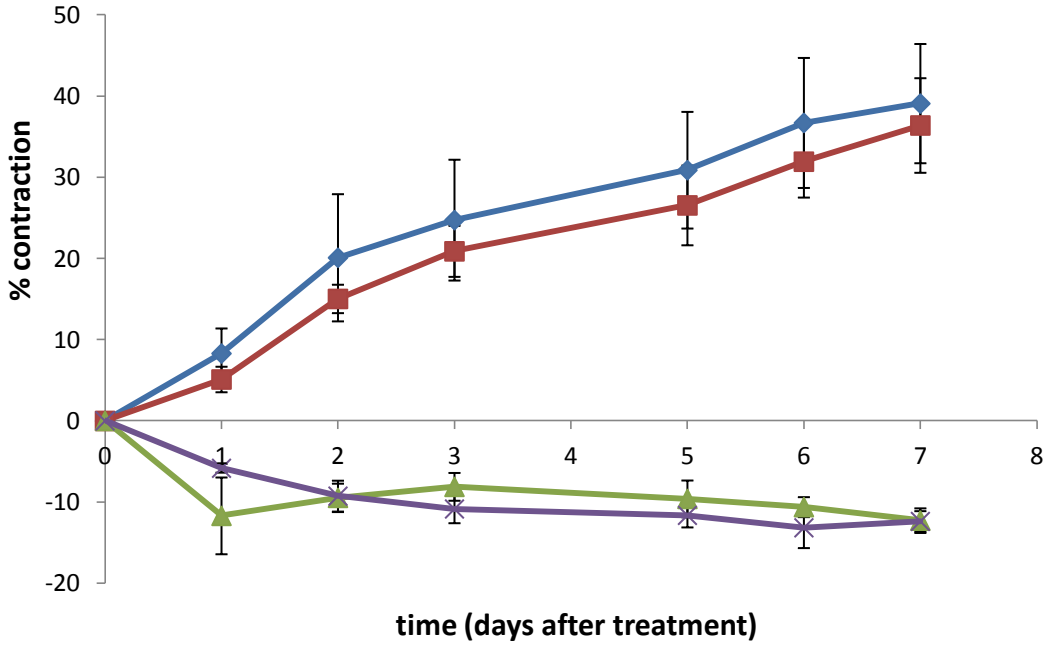

FIGURE 3.9 *Effect of 1 μM indomethacin on HINS-light induced inhibition of FPCL contraction. FPCLs exposed to 15 $mWcm^{-2}$ HINS-light for 1 hour and treated with indomethacin are indicated in purple, no treatment in green. FPCLs not exposed to HINS-light are indicated by; (red) indomethacin treatment, and (blue) no indomethacin. Indomethacin does not significantly reduce the inhibitory effect of HINS-light on contraction of FPCLs treated at 15 $mWcm^{2}$ for 1 hour (n = 3 ± SEM, $P > 0.05$ using ANOVA followed by Dunnett's comparison).*

MTT assay results confirm that the addition of indomethacin had no significant effect on cell viability when exposing cells to HINS-light at 15 $mWcm^{-2}$. At 24 hours after exposure, cell number on indomethacin treated FPCLs was 101 ± 24 % of

non-indomethacin treated FPCLs (n=3 ± SEM, $P > 0.05$ using ANOVA followed by Dunnett's comparison).

3.4 Discussion

The results show that HINS-light exposure has an intensity dependent inhibitory effect on fibroblast function. One hour exposures to low intensities of HINS-light (0.5 and 1.8 $mWcm^{-2}$) have no significant inhibitory effect on FPCL contraction. There is also no significant decrease in cell number as measured by the MTT assay, and no noticeable changes in cell morphology in samples stained with propidium iodide and acridine orange. Furthermore, expression of the α-smooth muscle actin protein, a well established marker of fibroblast contractile activity (Hinz et al., 2001) was unaffected. These findings suggest that at these doses, HINS-light has little or no inhibitory effect on fibroblast viability or function. At higher doses of 54 Jcm^{-2}, delivered over 1 hour at an intensity of 15 $mWcm^{-2}$, the results show that HINS-light does have a noticeable effect on fibroblast function. Contraction of FPCLs halts within 24 hours of exposure, and the cells do not appear to recover contractile function significantly within 140 hours of the exposure. Investigation of the number of cells present on the FPCL following exposure shows that within 24 hours there is an approximate 80% reduction in cell number, and there is no significant recovery within 120 hours. Imaging of the FPCL visually confirms this, and also shows that the cells lose their classic elongated fibroblast morphology (Ehrlich & Rajaratnam, 1990).

Following exposure to 15 $mWcm^{-2}$ HINS-light, FPCLs stopped contracting. The stage of contraction at which FPCLs were exposed had no effect on the inhibition of gel contraction; both FPCLs exposed during the lag phase (day 0) and the active phase (day 3) halted contraction and did not recover any contractile activity in the remaining experimental time. FPCLs exposed during the slow contraction phase (day 5) had already achieved maximum contraction and no effect on FPCL area was recorded in the following few days. The use of FPCL contraction to assess the effects of external factors is relatively common, although there are no reports of the

effects of blue light radiation for comparison with these results. Strong et al seeded collagen lattices with fibroblasts cultured with the photosensitiser Sn(IV) chlorin e6 before being exposed to 630 nm Argon ion laser with doses between 10 and 100 Jcm^{-2}. They found that a dose of 80 Jcm^{-2} completely halted fibroblast contraction, and found a direct correlation between contraction rates and cell viability (Strong et al., 1997). Another study using red laser light by Ho et al found that a dose of 3 Jcm^{-2} of 5 mW 632.8 nm He-Ne laser caused a significant decrease in contraction of FPCLs. There was no evidence of reduced cell viability accompanying this reduced contraction; instead this was partly attributed to a rearrangement of the collagen fibers in the matrix and distribution of the cellular actin filaments (Ho et al., 2009). Although useful as evidence of light induced effects on FPCL contraction, the wavelength and source of the light, and the manner in which it is applied is sufficiently different from HINS-light that these studies are not particularly useful as evidence to support our findings.

There is significantly more evidence on the use of the MTT assay to assess cell viability following blue light exposure. The MTT assay is used to assess viability of cells based on their ability to reduce a tetrazolium salt to a purple coloured formazan end product which can be measured colorimetrically (Mosmann, 1983). The reduction occurs in the mitochondria and cytosol of living cells, hence it can be interpreted as a measure of viability, however, the reduction is dependent on the activity of intracellular reductase enzymes and so variation in tetrazolium reduction may be due to changes in metabolic activity as well as cell death (Sieuwerts et al., 1995). Smith and co-workers exposed 3T3 fibroblasts to a blue LED light source similar to the HINS-light used in this work (Smith et al., 2009). Exposure was performed under comparable conditions at intensities of 0.1, 1 and 10 $mWcm^{-2}$ for 1, 8 and 24 hours. They demonstrated that 1 hr exposure to 0.1 and 1 $mWcm^{-2}$ light had no significant inhibitory effect on viability as assessed by MTT and Neutral Red assay. Membrane integrity was also assessed by lactate dehydrogenase (LDH) leakage into the culture medium and response to oxidative stress assessed by intracellular reduced glutathione levels. Both were found to be unaffected by exposure to low intensities of blue light.

The MTT-collagenase assay results suggest that exposure to 1.8 $mWcm^{-2}$ HINS-light for 1 hour may increase cell metabolism. There is a significant increase in MTT absorbance at 48 hours post treatment, indicating an increase in metabolic activity of the cell or an increase in cell number. This is likely to be caused by an adaptive stress response of the fibroblasts, also reported by Wataha and co-workers after exposing human gingival fibroblasts to 400 – 500 nm laser light of 5 Jcm^{-2} over 10 seconds (Wataha et al., 2004). Further examples of increases in viability measurements following low doses of blue light irradiation are found by Oplander et al (2011), who found a significant increase in cell number (assessed by neutral red) following exposure to 30 Jcm^{-2} 480 nm light.

Significant decreases were observed in the formazan production of fibroblasts exposed to 15 $mWcm^{-2}$ HINS-light. This decrease was not dependent on the phase of contraction during which the fibroblasts were exposed, and the decrease remained for up to 120 hours following the exposure. These findings are supported by those of Smith et al who also found that exposure to higher doses of HINS-light caused a significant decrease in cell viability. This was apparent after treatment duration was increased to 8 and 24 hr for 0.1 and 1 $mWcm^{-2}$ exposures, and for all durations of exposure to 10 $mWcm^{-2}$ HINS-light. This is consistent with the findings of Godley and co-workers who demonstrated a significant decrease in cell viability via MTT assay after a 6 hour exposure to 2.8 $mWcm^{-2}$ 390 – 550 nm light (a dose of 60 Jcm^{-2}) (Godley et al., 2005).

Other examples of blue light induced toxicity come from Lockwood and co-workers who demonstrated a significant increase in ROS generation in epithelial cells exposed to 30 Jcm^{-2} blue light (Lockwood et al., 2005). In addition, Wataha and co-workers, using a modified version of the MTT assay to measure succinnic dehydrogenase (SDH) activity, found significant decreases in the mitochondrial activity of fibroblasts exposed to 60 Jcm^{-2} blue light (Wataha et al., 2004), and Hwang and co-workers also demonstrated decreased SDH activity and decreased proliferation of human gingival fibroblast cells exposed to over 12 Jcm^{-2} blue light (Hwang et al., 2008).

There is little in the way of evidence to support the findings of this study that high intensities of blue light decrease fibroblast expression of α-SMA, however, a correlation has been shown between the expression of α-SMA and the ability of fibroblasts to contract collagen lattices (Hinz et al., 2001). Although the results show a decrease in α-SMA expression at 24 hours following exposure to 0.5 and 1.8 $mWcm^{-2}$ HINS-light, due to a large variation in samples this was not statistically significant. However, by 144 hours following exposure a significant decrease was measured in the cells exposed to 1.8 $mWcm^{-2}$. A significant and substantial decrease was also recorded in cells exposed to 15 $mWcm^{-2}$ HINS-light at 144 hours, although this showed some recovery from the 24 hour sample where there was insufficient protein content to run a sample. The decrease in α-SMA expression at lower intensities without an associated reduction in FPCL contraction is surprising given that a direct correlation has been shown between FPCL contraction and α-SMA expression (Verjee et al.) However, the conditions of contraction examined in their study are very specific, investigating Dupuytren's myofibroblasts in tensioned FPCLs, and it may well be the case that in the more general case of free floating FPCLs that α-SMA is a more sensitive measure of fibroblast damage that FPCL contraction.

Microscopic analysis of the propidium iodide and acridine orange stained FPCLs suggests that a significant reduction in cell number occurs following high intensity HINS-light exposure. Fibroblasts exposed to the lower doses of HINS-light appear to have a normal morphology of elongated bodies with distinct extensions. They also appear to assume some form of alignment, with extensions generally stretching out parallel to their neighbours. Cells that have been exposed to 15 $mWcm^{-2}$ HINS-light appear to have lost this elongated morphology by 24 hours following exposure. There also appears to be a slight increase in the number of red stained nuclei, marking non viable cells, and a reduction in cell number suggesting that the high intensity HINS-light has resulted in cell death and subsequent detachment from the FPCL. This implies that the halt in contraction of FPCLs, and the decreases in MTT reduction and α-SMA expression can be at least partly attributed to the decrease in cell number.

Indomethacin is a member of the nonsteroidal anti-inflammatory drug (NSAID) family. It is used clinically for relief of mild to moderately severe pain accompanied by inflammation, and in the treatment of conditions such as osteoarthritis, rheumatoid arthritis and gout. It is a cyclooxygenase (COX) inhibitor, and is relatively selective for COX 1 (Kato et al., 2001). COX 1 is an enzyme responsible for the formation of prostanoids, including prostaglandins. Prostaglandins are a group of lipid compounds derived enzymatically from arachidonic acid, an essential fatty acid. Arachidonic acid is oxidised by COX enzymes to form the endoperoxides PGG2 and PGH2, which are rapidly converted through various enzymes to the more stable active prostaglandin compounds, including prostaglandin E2 (PGE2). Prostaglandin E2 plays a role in wound healing, regulating inflammation, the fibrotic response (Futagami et al., 2002) and collagen expression (Huang et al., 2007). It has been shown to inhibit fibroblast proliferation (Huang et al., 2007), migration, chemotaxis (Kohyama et al., 2001) and FPCL contraction (Aron et al., 2007; Vlad et al., 2006).

There are many examples in the literature of prostaglandin inhibition by NSAIDs, and specifically indomethacin. In 1971, three papers were published concerning the inhibition of prostaglandins. Ferreira et al. demonstrated the inhibition of prostaglandin release by indomethacin from dog spleen (Ferreira et al., 1971), and Smith and Willis inhibited prostaglandin release from human platelets with aspirin (Smith & Willis, 1971). J.R. Vane's experiments in 1971 showed that indomethacin inhibits the synthesis of prostaglandins in isolated stomach strips and colon from the rat, and reduced the level of prostaglandin-like activity in guinea-pig lung homogenates, leading to the hypothesis that the mechanism of action of asprin-like drugs, including indomethacin, is through prostaglandin synthesis inhibition. Following this Nobel Prize winning work, intense research in the area confirmed their hypothesis, and identified the role of cyclooxygenase enzymes. Indomethacin has been shown to have inhibitory effects on PGE2 levels in many cell and tissue types (Bhattacherjee & Eakins, 1974; Flower, 1974; Ford-Hutchinson et al., 1976; Vane, 1996). It can be used to investigate the effect of prostaglandins on fibroblast activity. An investigation into the effects of epidermolysis bullosa on PGE2

synthesis used FPCL to measure fibroblast function. Fibroblasts treated with 10 μg/ml (27.8 μM) indomethacin prior to seeding in a FPCL had no effect on collagen gel contraction after 48 hours compared to a non-treated control, but did reduce PGE2 accumulation in the media (Ehrlich & White, 1983). In an experiment investigating inhibition of collagen lattice contraction by granulomas, which increase the concentration of PGE2 in the media and halt collagen lattice contraction, indomethacin at 5 μg/ml (13.9 μM) was shown to abrogate the effects of the granulomas on lattice contraction and again to decrease the concentration of PGE2 (Ehrlich & Wyler, 1983). A study into the effects of gamma radiation on wound healing by Carnevali et al., also used indomethacin to inhibit PGE2 synthesis/release in FPCLs. Gamma radiation was found to decrease the ability of fibroblasts to contract a collagen lattice, possibly due to the increase in PGE2 concentration in the supernatant media that was recorded. Treatment of fibroblasts with 1 μM indomethacin prior to seeding in the collagen gel inhibited the production of PGE2 by 99% and partly reversed the inhibitory effect of the radiation on collagen lattice contraction (Carnevali et al., 2003).

Inhibition of fibroblast prostaglandin E2 synthesis by indomethacin had no effect on FPCL contraction following exposure to HINS-light, suggesting that prostaglandins do not mediate the HINS-light induced inhibition of fibroblast function contrary to the case with gamma radiation (Carnevali et al., 2003).

The cells used in this research are 3T3 fibroblasts, a cell line derived from embryonic mouse fibroblasts (Todaro & Green, 1963). They were used in this research because, unlike primary cells, they have unlimited number of divisions allowing for more reproducible results. They also have well defined characteristics that do not alter with repeated passaging and are one of the cell lines recommended in International Standard 10993-5, "Biological evaluation of medical devices – Tests for in vitro cytotoxicity". However, some differences have been noted in the properties of 3T3 cells in comparison to primary human dermal fibroblasts and keratinocytes. They have been shown to more effectively contract collagen gels than primary human foreskin fibroblasts (Montesano & Orci, 1988), and have been shown to have

different responses to various stimulants compared with their primary counterparts (Gal et al., 2009; Gold et al., 2006). Steinberg et al investigated the capability of different fibroblast cell lines to contract collagen gels, using the cell number required to reduce the gel size by 50 % in 24 hr as their measure of contraction ability. They found that established cell lines, including three 3T3 strains and two rat fibroblast cell lines, needed approximately 10 times more cells (an increase from $6x10^3$ to $6x10^4$ cells) than primary cells to halve the gel size, and this was attributed to a decrease in the number of actin cables in established cell types (Steinberg et al., 1980). However, they also showed that culture conditions (temperature and serum concentration) have at least as much of an effect on contractile ability as cell type does. The source of primary fibroblasts and the age of subject from whom they are sourced has also been shown to have a large effect on contractile ability in FPCL wound models (Finesmith et al., 1990). In vitro testing of the effect of HINS-light on fibroblasts cultured from human wound biopsies, using the method described by Brem et al (Brem et al., 2008), would be a progression on the method used here, however, taking into consideration the variation described above, careful attention would need to be paid to culture conditions and seeding density to achieve a more realistic wound model than that provided by 3T3 fibroblasts.

There are further complications that the use of primary cell cultures would not help to clarify. The more complex situation of actual wounds involving many cell types and interactions with wound exudates and blood products would not be modelled, and this would need to be investigated to confirm the non-damaging properties of HINS-light on the wound healing process. It is known that the photodynamic inactivation of bacteria is affected by the presence of blood products (Lambrechts et al., 2005b; Spesia et al., 2010), specifically albumin which has been shown to have ROS scavenging properties (Iglesias et al., 1999). It is as yet unknown what effect these blood products would have on the response of mammalian cells to HINS-light, however, as low intensities of HINS-light did not induce significant damage in fibroblasts, and assuming that any damage caused is through the generation of ROS, it could be assumed that the presence of ROS scavengers would not exacerbate any damage that did occur. Furthermore, the scavenging effects of serum albumin could

allow for a higher maximum non-inhibitory dose of HINS-light. However, the complexity of the situation is illustrated by the findings of Grzelak et al, who showed that exposure of cell culture medium to white light caused cytotoxic effects when the medium was subsequently used to culture cells. This was attributed to the generation of ROS by light exposed riboflavin, with tryptophan, tyrosine, pyridoxine and folic acid contributing to the effect (Grzelak et al., 2001). This is one of the reasons why the exposures described in this chapter were performed in PBS. The inhibitory effects of blue light are not therefore restricted to intracellular production of ROS. The effects of production of ROS in the wound bed further limits the usefulness of in vitro assessment of blue light effects on wound healing. In vivo testing would be the next step required in the development of HINS-light for clinical applications.

Some examples of in vivo testing are available in the literature; Adamskaya et al investigated the effect of 50 min exposures of blue (470 nm) and red (629 nm) LED irradiation for 5 consecutive days at 10 $mWcm^{-2}$ on full-thickness excision wounds on rats (Adamskaya et al., 2010). Blue light was found to significantly decrease wound area by 50% relative to unexposed and red light exposed rats at 7 days post wounding. On day 7 post operation, rats were euthanized and the entire wound area harvested for histological assessment. No difference was found in depth of granulation tissue in either red or blue light exposed wounds, but a significant increase in re-epithelialisation was found in wounds exposed to blue light. Keratin-17, part of the epithelial cytoskeleton involved in regulation of wound healing, was found to be down-regulated in blue light exposed samples relative to red light samples, suggesting that wound healing was more complete. Other examples of animal models of wound healing have been used but concentrate on red or near infra-red laser or LED exposures. Whelan et al found that 880 nm LED exposure caused a significant reduction in size of wounds created by punch biopsies in the dorsum of Sprague-Dawley rats (Whelan et al., 2001). These rats were exposed to a dose of 4 Jcm^{-2} (50 $mWcm^{-2}$ delivered for 80 s) on 14 consecutive days, with wound size measured daily and found to be 20% smaller than control wounds at 7 days post operation, associated with an increase in fibroblast growth factor (FGF-2) as determined by ELISA. This study also looks at the effect of 670, 720 and 880 nm

combined LED arrays on lacerations received by crew members of U.S. Navy submarines. Healing time was found to be reduced from 14 days to 7 days by exposure of the wounds to a 4 Jcm^{-2} dose. Nassbaum et al provide a further example of in vivo studies (Nussbaum et al., 2009). They exposed $1cm^2$ full-thickness wounds created in the lower back of Sprague-Dawley rats to fibre coupled lasers operating at 808 or 635 nm three times per week following wounding. The laser beam was passed through a beam expander to cover the entire wound area at an intensity of 0.028 Wcm^{-2} with duration of exposure varied to give a dose of 1 or 20 Jcm^{-2}. At 3 days after wounding, wavelengths of 808 nm (1 and 20 Jcm^{-2}) and 635 nm (20 Jcm^{-2}) were found to increase the maximum area of the wound by 29 %, and by day 19 wounds exposed to 635 nm at 20 Jcm^{-2} remained 10.2% larger than control wounds. Histological examination of the wounds exposed to 635 nm light showed that a dose of 1 Jcm^{-2} caused greater evidence of the late stages of wound healing; less stromal odema, evidence of re-epithelialisation, more activated fibroblasts and evidence of angiogenesis. In contrast, those exposed to 20 Jcm^{-2} still exhibited evidence of early wound healing, and in particular no re-epithelialisation or collagen deposition. Further evidence of the effects of light on wound healing come from Klebanov et al., who showed that exposure to 630 nm LED stimulated the transition of healing wounds from the inflammatory to the proliferative phase, and subsequent accelerated decrease in wound area (Klebanov et al., 2005). Vidinsky et al who exposed sutured wounds in rats to 660 nm LED daily and found accelerated wound healing caused by earlier regression of inflammatory phase, faster completion of re-epithelialisation and acceleration in maturation phase (Vidinsky et al., 2005).

There are a great deal more examples of the effect of red light than blue light on wound healing. Although the results in this chapter show that exposure of 3T3 fibroblast cells to 1 hour of HINS-light intensities of 5 $mWcm^{-2}$ and below do not have an inhibitory effect on fibroblast function, in vivo studies such as those described above would need to be conducted to further develop this technology. Nevertheless, the results demonstrate that HINS-light treatment merits further investigation as a potential tool to help maintain the sterility of a wound or as a technique that could be used to aid wound disinfection.

Chapter 4

EFFECT OF HINS-LIGHT ON OSTEOBLAST FUNCTION

4.1 Introduction

4.1.1 Aims

A potential application of HINS-light is as a tool to be used during surgical procedures to maintain environmental and surface sterility. Hospital acquired infections are an ever increasing problem in the healthcare environment. A significant portion of medical devices fail due to acquired infection, and infection rates following arthroplasty surgery are as high as 4%, with considerably higher rates after revision surgery (Hamilton & Jamieson, 2008). Its well documented bactericidal properties suggest that HINS-light may be a useful aid to help reduce the incidence of infection, and associated costs with treatment of infection and revision surgery. This chapter investigates the effect of HINS-light on osteoblast cells, the cell type responsible for bone formation. If HINS light were to be implemented as a disinfection method during arthroplasty surgery, bone would potentially be exposed to HINS-light, and any inhibitory effects on osteoblast function may impede the osseointegration of the implant and limit the applications of HINS-light during surgical procedures of this nature.

4.1.2 Bone cell function

Bone is constantly undergoing a remodelling process, with osteoclasts absorbing old bone and osteoblasts replacing it. In adults, approximately 10% of the skeleton is replaced annually, and this is regulated by various systemic hormones such as vitamin D and parathyroid hormone. An imbalance of osteogenesis causes clinical conditions such as osteoporosis (increase in osteoclast activity) and osteosclerosis (increased bone formation). Ageing and changes to mobility will also affect the balance of bone turnover, resulting in changes to bone structure, mass and strength.

Osteoblasts are mononucleate cells that are responsible for bone formation. They differentiate from osteoprogenitor cells found in bone marrow and periosteum, and this process is induced by transcription and growth factors which can be either tissue specific (e.g bone morphogenic protein, Cbfa1) or non-tissue specific (e.g. c-fos, egr). Osteoblasts then go through a period of proliferation, encouraged by several growth factors such as bone morphogenic proteins, transforming growth factor-β and insulin like growth factors. The bone differentiation marker alkaline phosphatase (ALP) is expressed at this point. Osteoblasts produce a matrix of a protein mixture known as osteoid, which mainly consists of type 1 collagen and a ground substance made up of compounds including osteocalcin (OC) and chondroitin sulphates. This matrix is what mineralises to form bone. The process of mineralisation is not fully understood, but ALP vesicles released by the osteoblast are thought to play a part. After around ninety days the osteoid will become fully mineralised and the job of the osteoblasts is done (Langton & Njeh, 2003). Then approximately 60% of osteoblasts will undergo programmed apoptosis (Jilka et al., 1998), with the remainder either eventually becoming trapped by their own matrix, at which point they become osteocytes, or forming a layer of lining cells. Lining cells form an inactive osteoblast cell layer covering bone surfaces that are neither undergoing bone formation or resorption. They are thought to be capable of activating bone remodelling, and can return to active osteoblast activity. The cells may have a role in regulation of the movement of calcium and phosphate ions into and out of the bone (Gallagher et al., 1996).

Osteoclasts are large mutli-nucleate cells responsible for bone resorption. They are derived from hematopoietic stem cells. Bone resorption is required during many skeletal processes, and plays a role both in the maintenance of blood calcium levels, and in the continuous physiological remodelling of bone that occurs in the adult skeleton (Vaananen et al., 2000). When an osteoclast becomes active it migrates to a resorption site and forms a seal with the bone via a special area of the cell membrane known as the sealing zone. Once attached the cell membrane underneath the sealing zone takes on a ruffled appearance, with internal membranes being transferred to the area and fusing with acidic intracellular vesicles to create long finger-like extensions

that penetrate the bone. The hard mineral based exterior of the bone is dissolved by the targeted excretion of HCl from the ruffled border into the resorption lacunae. The organic bone matrix is degraded by proteolytic enzymes, probably lysosomal cysteine proteinases and matrix metalloproteinases. The degradation products are subsequently removed from the resorption lacunae by transcytotic vesicules, which transport these products from the ruffled border to the secretory domain of the membrane from which they are released into the extracellular space (Miyamoto & Suda, 2003; Nesbitt & Horton, 1997; Vaananen et al., 2000).

Osteocytes are the most abundant cell found in compact bone. They are found in lucanae, the small cavity formed in the matrix that the cell has produced and are connected to other osteocytes and osteoblasts by long cytoplasmic extensions that run through canaliculi allowing communication and exchange of nutrients and waste products. They are less active than osteoblasts, but perform important functions in control of bone turnover. Osteocytes sense mechanical strain on bones and translate that into biochemical signals which control the extent and location of bone production and resorption. More recent research has shown that osteocytes might have a more active role than originally thought. They have been shown to modify their enclosing bone environment in response to stimuli, and are capable of both matrix formation and resorption to alter the mechanical properties and fluid shear stress of bone (Bonewald, 2006).

4.1.3 Arthroplasty surgery

To ascertain if any alteration in osteoblast function caused by HINS-light would have an effect on the success of arthroplasty procedures, it is useful to understand the surgical process involved. Concentrating on total hip replacement surgery (figure 4.1), there are a variety of approaches used to gain access to the bone, but all result in the tissues around the hip being parted to allow access to the joint. The femoral head is dislocated from the socket and the surface of the acetabulum reamed away to allow placement of a prosthetic cup. This is normally metal, ceramic or polyethylene, and is fixed in place by either polymethylmethacrylate cement, screw, press-fit or porous in-growth methods.

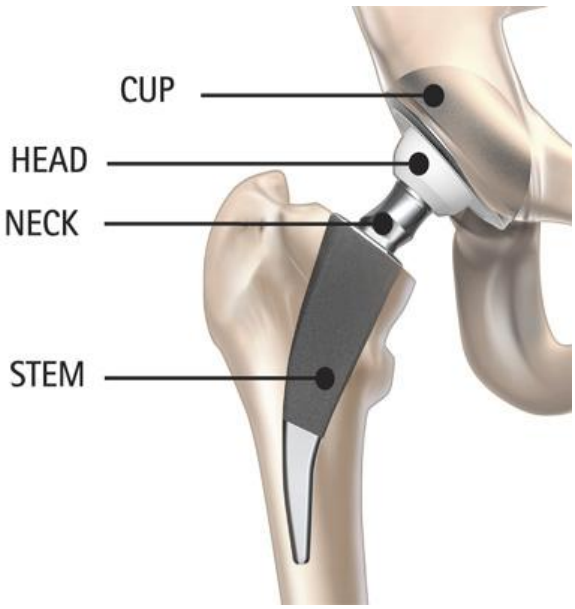

FIGURE 4.1 *Schematic diagram of AESCULAP Implant System (http://www.soactivesofast.com/default.aspx?pageid=1528)*

In total hip replacement, the femoral head is removed and replaced with either an ultra high molecular weight polyethylene (UHMWPE) or alloy component. The latter is more common, with titanium, stainless steel and cobalt-chromium alloys being used at present, with ongoing research into improving materials. The femoral component consists of a ball section which fits into the cup and a stem section which is fixed into the femur. This can be fixed initially with or without cement during surgery, and is followed by a secondary fixation process which occurs during the healing process. Secondary fixation can be split into an initial phase in which surrounding bone is destroyed, followed by a repair phase where bone formation integrates the implant with the bone. This is followed by a stabilisation phase during which the bone is remodelled in response to the new mechanical loading experienced (Dhert et al., 1998).

Good fit of the components is crucial to reduce degradation and corrosion of the implants, and to reduce patient pain following surgery (Willert & Buchhorn, 1999). Secondary fixation of the components obviously relies on appropriate bone cell function. Studies have been performed to ensure that low level laser irradiation, an emerging area of interest for acceleration of bone healing, does not have any adverse

effects on osseointegration of implants. One such study performed by Dörtbudak et al investigated the effects of a 100 mW, 690 nm low energy laser on osteoclast function. Holes were drilled in the iliac crest of baboons, and the surface exposed to 1 min of laser irradiation before and after inserting titanium implants. Wounds were closed and baboons sacrificed five days post operation to assess viability of osteocytes and resorbed bone area. Laser irradiation was found to have significantly increased the viability of osteocytes although there was no difference in the total number of cells per unit area. The authors also found no difference in the eroded surface area of exposed bone. They suggest that the increased number of viable osteocytes implies the presence of more vital bone tissue in irradiated areas, resulting in accelerated osseointegration of the implants (Dörtbudak et al., 2002). The effect of infra-red laser irradiation on attachment of titanium implants to shin bones of mice was also assessed by Maluf and co workers (2010). The area around the implant was exposed to six doses of 8 Jcm^{-2} 795nm laser irradiation every two days starting immediately after the implants were inserted into holes drilled in the bone. The torque required to dislodge the implant was measured at 14 days post operation, and was found to be significantly higher in the laser irradiated group relative to the control group. Ionizing x-ray radiation has been shown to inhibit the proliferation of osteoblasts and decrease their viability, leading to the conclusion that high dose x-ray should not be used to assess osseointegration of dental implants (Dare et al., 1997). It is therefore not inconceivable that high intensity blue light may also have some effect, either stimulatory or inhibitory, on osteoblasts that would be exposed to HINS-light if it was used as a tool to help maintain sterility during operations.

Four markers of osteoblast function or viability have been used to establish what effect HINS-light may have; alkaline phosphatase activity (ALP), collagen synthesis, osteocalcin (OC) expression, and proliferation. ALP and OC are used clinically to measure bone turnover. ALP is an enzyme that plays an important role in osteoid formation and mineralisation, and is commonly used to measure osteoblast activity *in vitro*. OC is a protein synthesised only by osteoblasts, ondontoblasts and hypertrophic chondrocytes and is a well accepted marker of osteoblast function (Price et al., 1980; Thomas et al., 1990). Picric Sirius red staining was used to

quantify and visualise osteoblast production of collagen, and growth rate in terms of protein content was assessed by Lowry assay. Scanning electron microscopy was employed to establish if HINS-light had any visible effect on cell morphology.

4.2 Methods

4.2.1 Cell culture

Immortalised rat osteoblast cells were used in these experiments. The cell line was produced by transfecting neonatal rat osteoblasts at passage 4 with pUK42, a plasmid (10.9 kb) containing the complete sequence of SV40, except for a 6bp deletion at the origin of replication. This plasmid also contains the RSVneo gene which provides Geneticin resistance, and selection of positively transfected cells was by resistance to the antibiotic Geneticin. (G418, Gibco). They were maintained as described in section 2.2.2.

4.2.2 HINS-light

Cells were exposed to HINS-light in the central wells of multiwell plates, to achieve a uniform distribution of intensity over the wells as described in section 2.1.2. The HINS-light setup was as described in section 2.1.

4.2.3 Markers of osteoblast function

4.2.3.1 Alkaline phosphatase

The ALP assay was performed at 24 and 72 hours following HINS-light exposure. Cells were seeded at $2x10^4$ cells/cm^2 in the central wells of 96 well plates. When the desired duration of incubation following exposure had passed, DMEM was removed and wells washed with PBS. 200 µl p-nitrophenyl phosphate (pNPP) in glycine buffer (1 mg/ml) (composition given in appendix) was then added to each well. pNPP is dephosphorlysed to p-nitrophenol and phosphate in the presence of ALP. The absorbance of p-nitrophenol was measured at 405 nm immediately and at 15 min after addition. ALP activity, measured in IU/l, was given by:

$$ALP\ activity = \frac{(OD_{15} - OD_0)\ \times 1000}{t \times \varepsilon}$$

Where OD_{15} and OD_0 are the optical densities measured at 15 and 0 min, 1000 is a conversion factor to convert ml to l, t is the incubation time, and ε is the extinction coefficient of p-nitrophenol (18.75 mM/cm) (Bowers & McComb, 1966).

4.2.3.2 Collagen synthesis

Collagen production by osteoblasts was measured using a modification of the colorimetric assay described by (Walsh et al., 1992). Cells were seeded at $2x10^4$ cells/cm^2 in the central 16 wells of 96 well plates. At 24 or 72 hr following exposure, cells were fixed with Bouin's solution (appendix 1) before 200 µl picric Sirius red stain (appendix 1) was added to each well for 1 hour with gentle shaking. Wells were washed with 0.01 M HCl and the cell layer dissolved in 200 µl NaOH (0.25 M). Absorption at 550 nm was measured against a 0.01 M NaOH blank (Tullberg-Reinert & Jundt, 1999). Picric Sirius red staining was also used to visualise the effect of HINS light exposure. The procedure was performed as above except that cells were cultured on thin circular glass slides in 24 well plates. Instead of dissolving the cell layer and measuring absorption, the cells were visualised with bright field microscopy techniques on a Zeiss Axioimager microscope.

Known volumes of collagen from rat tail extraction, performed as described in section 3.2.2, were used to generate a standard curve from which the collagen concentration of samples was calculated (figure 4.2).

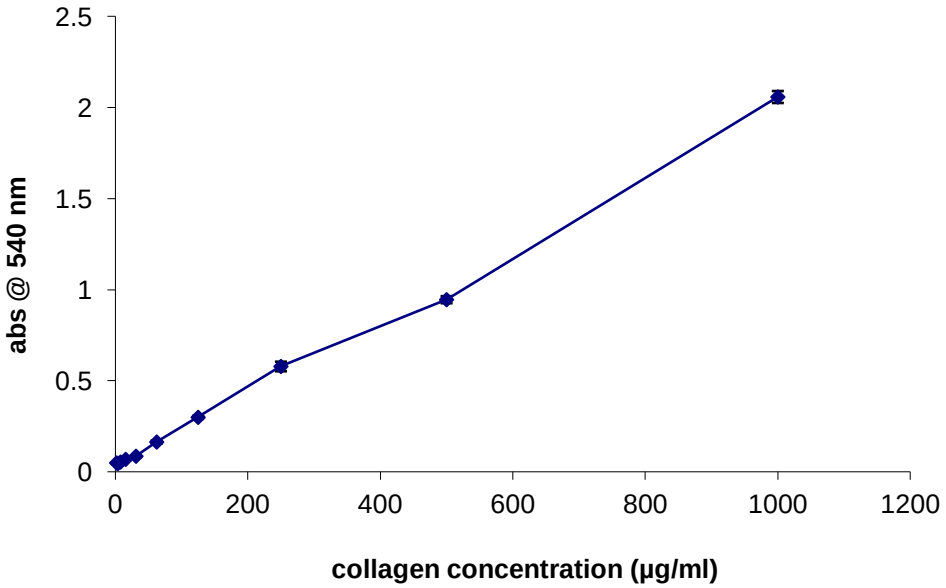

FIGURE 4.2 *Collagen standard curve (mean +/- SEM, n = 6). Where the error bars cannot be seen there are so small that they are incorporated into the symbol.*

4.2.3.3 Osteocalcin

Osteocalcin in cell culture media was measured via an ELISA kit (BT-490, Biomedical Technologies Inc, Stoughton, USA) on days 3, 6 and 10 following exposure. Cells were seeded at $2x10^4$ cells/cm^2 and incubated in 1,25 dihydroxy Vitamin D_3 ($(OH)_2D_3$) at a concentration of 10^{-8} M to stimulate osteocalcin expression (Martinez et al., 2001a). Cells were exposed to HINS-light in PBS at 1.8, 5 and 15 $mWcm^{-2}$ intensities for 1 hr. 48 hours prior to sample collection, complete DMEM was removed and replaced with serum free DMEM, still containing 10^{-8} M vitamin D_3. At the appropriate time, medium was collected and frozen at -80°C. In accordance with the instructions supplied by Biomedical Technologies, 50 µl of sample buffer were added to 25 µl of samples and standards and incubated overnight at 4°C. Standards were prepared at 0.33, 1, 2.5, 5, 10 and 20 ng/ml. Wells were washed with PBS before 100 µl of osteocalcin antiserum was added to each well at 37°C for 1 hr. Wells were washed as before and 100 µl donkey anti-goat IgG peroxidise added to each well and incubated at room temperature for 1 hr. After another wash step, 100 µl of a 1:1 mix of peroxidase substrate TMB ($3,3^1,5,5^1$-

tetramethyl benzidine) and hydrogen peroxide were added for 30 min at room temperature in the dark. 100 µl of stop solution were added before absorbance at 450 nm was measured.

Values available in the literature on the concentration of Vitamin D3 required for stimulation of osteocalcin production varied from 10^{-7} to 10^{-9} M (Kassem et al., 1994; Martinez et al., 2001b). The optimum concentration for the cell line used in this work was assessed by osteocalcin production of control osteoblasts seeded at $2x10^4$ cells/cm^2 and cultured for three days prior to assay. 10^{-8} M was found to provide the maximum osteocalcin levels (figure 4.3).

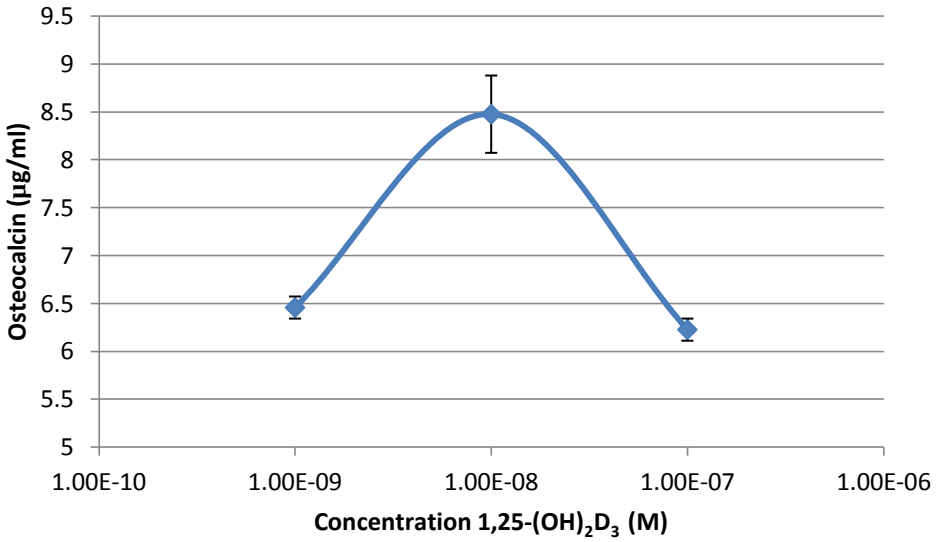

FIGURE 4.3 *Concentration of 1,25 dihydroxy vitamin D_3 found to provide maximum osteocalcin levels was 10^{-8} M (n = 2 ± range)*

4.2.3.4 Proliferation

Cell protein content was measured via Lowry assay (Lowry et al., 1951). Osteoblasts were seeded at $5x10^3$/cm^2 in 24 well plates. At each time point after exposure, medium was removed from the required wells and cells washed twice with 1 ml PBS. Incubation was continued with the dried cell layers remaining in the wells until all time points have passed, at which point all the cell samples were then solubilised overnight in 200 µl 0.5 M NaOH. Bovine serum albumin (BSA) protein

standards at 200, 150, 100, 50, 25 and 0 µg/ml were used to generate a standard curve. 5 ml of a solution A (1ml $CuSO_4$ (1% w/v) + 1 ml NaK tartrate (2 % w/v) + 98 ml Na_2CO_3 (2 % w/v)) were added to both standards and samples, mixed, and incubated at room temperature for 10 min. 0.5 ml solution B (1:4 dilution of Folin and Ciocalteu's Phenol Reagent in dH_2O) were then added, mixed immediately and left for 30 – 90 min at room temperature. Absorbance of samples was measured at 725 nm against dH_2O, and the concentration in the samples calculated from the BSA standards.

4.2.4 Scanning electron microscopy (SEM)

SEM was performed at the Integrated Microscopy Unit at Glasgow University, with the assistance of Dr Laurence Tetley and Mrs. Margaret Mullin. Cells were seeded at $2x10^4$ cells/cm^2 into 24 well plates with 10 mm glass coverslips placed in the bottom of required wells. The wells and coverslips were coated in poly-l-lysine (Sigma P4707) for 5 min and allowed to dry overnight prior to cell seeding. Cells were allowed to attach for 4 hours before being exposed to HINS-light. Post exposure, cells were fixed with 2.5% Glutaraldehyde solution (composition in appendix) for 1 hr at 4 °C. Cell layers were rinsed with 0.1 M NaPi buffer (Appendix) (pH 7.4) with 2% (w/v) sucrose and stored in this buffer overnight. Cells were transported to Glasgow University the following morning and rinsed a further three times for 5 min in 0.1M PO_4 buffer. Cells then underwent secondary fixation in 1% osmium tetroxide for 1 hr, followed by three 10 min washes with dH_2O. Cells were negatively stained with 0.5% aqueous uranyl acetate for 1 hr in the dark, and washed twice with dH_2O. Cells were then dehydrated in ethanol consisting of 2x 5 min steps of 30, 50, 70 and 90% ethanol, followed by 4x 5 min Absolute and dried Absolute ethanol steps. The coverslips were then removed from the wells and dried with hexamethyldisilazane (HMDS) for 2x 5min. Samples were fixed onto aluminium tabs with carbon tape, sputter coated with a gold/palladium mixture and viewed at magnifications ranging from 250x to 30000x at 10 kV.

The surface area of cells was calculated from SEM images using a similar method to that described for FPCL area measurements (section 3.2.6.1). The number of pixels

that the cell occupied was compared to the number of pixels in a known area defined by the scale bar in the images to give the surface area.

4.3 Results

4.3.1 ALP activity

A 1 hr exposure to intensities of HINS-light at or below 5 mWcm^{-2} (18 Jcm^{-2}) was shown not to cause a significant reduction in expression of ALP enzyme at 24 hr post exposure. Intensities above 5 mWcm^{-2} caused a statistically significant decrease in expression of ALP. By 72 hours post exposure, osteoblasts treated at 15 mWcm^{-2} showed minimal signs of recovery. Cells exposed to 5 mWcm^{-2} HINS- light and below did not show a significant decrease in ALP expression compared with the control at 72 hr post exposure (figure 4.4).

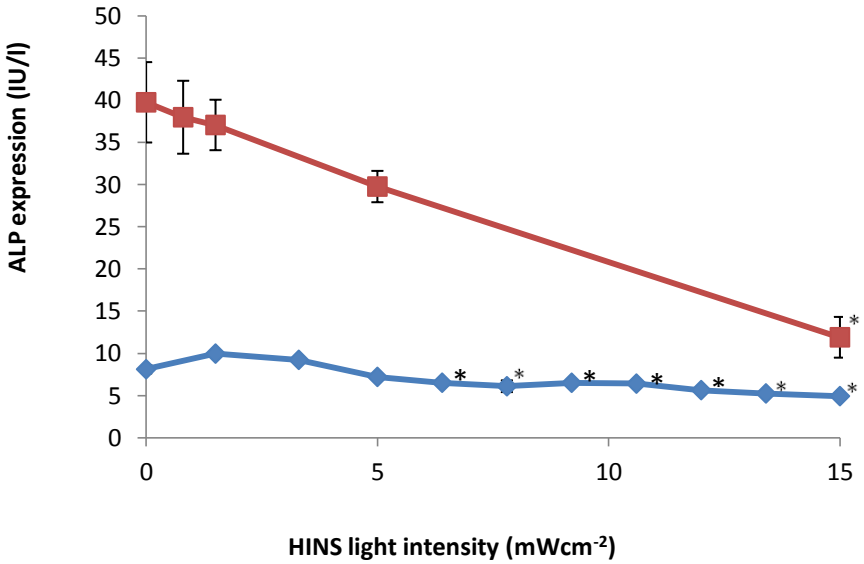

FIGURE 4.4 *ALP expression at 24 (♦) and 72 (■) hours post exposure of osteoblasts treated at between 0.5 and 15 mWcm^{-2}.* ******* *indicates significant difference from control (P < 0.05, ANOVA followed by Dunnett's comparison, n=3 ± SEM)*

4.3.2 Collagen synthesis

Collagen synthesis was not affected by exposure to up to 5 mWcm^{-2} HINS-light, at either 24 or 72 hr post exposure. A significant decrease in synthesis was shown in osteoblasts exposed to 15 mWcm^{-2} HINS light at 24 hr post exposure, and this significant decrease persisted at 72 hr post exposure (figure 4.5).

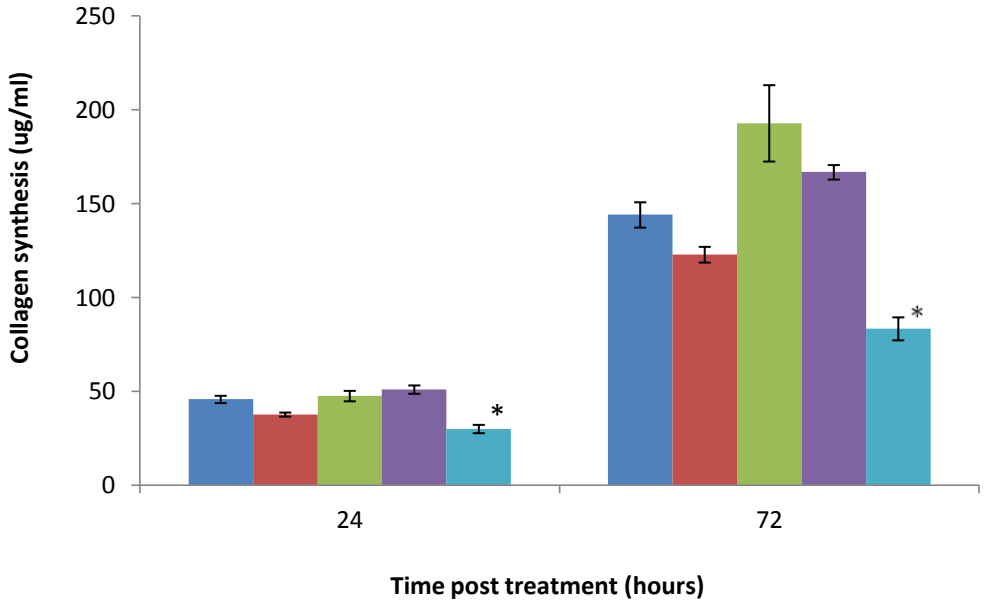

FIGURE 4.5 *Collagen synthesis by osteoblasts exposed to HINS-light . Cells were exposed to (from left to right at each time point); control, 0.5 mWcm^{-2}, 1.8 mWcm^{-2}, 5 mWcm^{-2} and 15 mWcm^{-2} for 1 hour.* ******* *indicates significant difference from control (P<0.05, ANOVA followed by Dunnett's comparison, n=3 ± SEM)*

Differential interference contrast (DIC) microscopy images of control cells and cells exposed to 1 hr of 15 mWcm^{-2} HINS light are shown in figure 4.6 (A) and (B) respectively. Microscopy was performed at 48 hours following exposure. Red areas in the image show deposition of collagen, and there did not appear to be any obvious visual difference between control and 15 mWcm^{-2} exposed cells. Osteoblasts exposed to 15 mWcm^{-2} also retained the elongated shape of healthy osteoblasts and no obviously damaged cells were present in the sample. Images obtained at 5 days following exposure had such high collagen content that individual cells were indistinguisable, however, there appeared to be no obvious difference in colour

density of those exposed to 15 mWcm^{-2} HINS-light (figure 4.6 (D)) and the control sample (figure 4.6(C)).

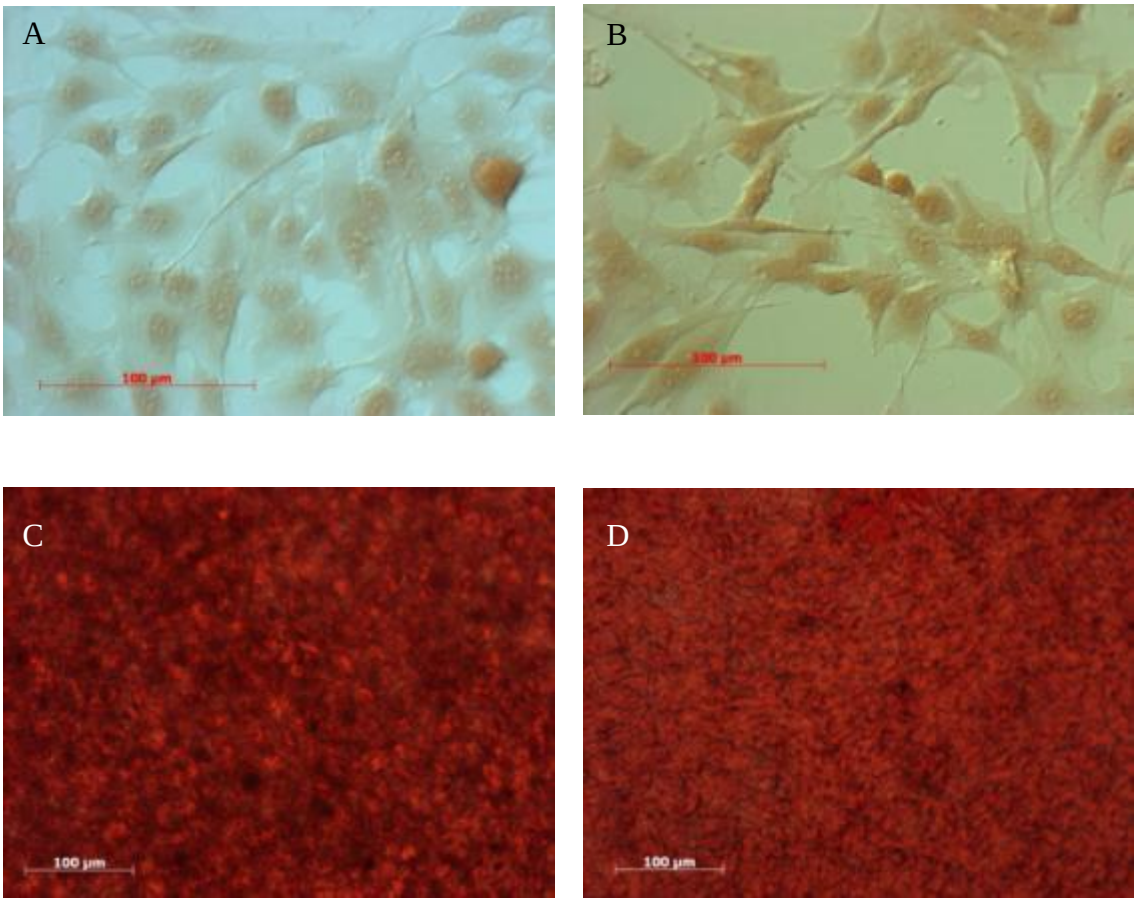

FIGURE 4.6 *DIC microscopy images of osteoblasts stained with picric Sirius red.* Image (A) and (B) show control cells and those exposed to 15 mWcm^{-2} HINS-light for 1 hour, at 48 hr post exposure. (C) and (D) show control and 15 mWcm^{-2} at 120 hr post exposure. Scale bars are 100 µm.

4.3.3 Osteocalcin expression

No decrease was observed in osteocalcin expression by osteoblasts exposed to 5 mWcm^{-2} or lower HINS-light for 1 hour at up to 10 days post exposure. OC expression was significantly suppressed in osteoblasts exposed to HINS-light intensities of 15 mWcm^{-2} for 1 hr at 3 and 6 days post exposure (figure 4.7). By 10 days post exposure, expression of osteocalcin in cells exposed to 1 hr of 15 mWcm^{-2} was not significantly different to the control.

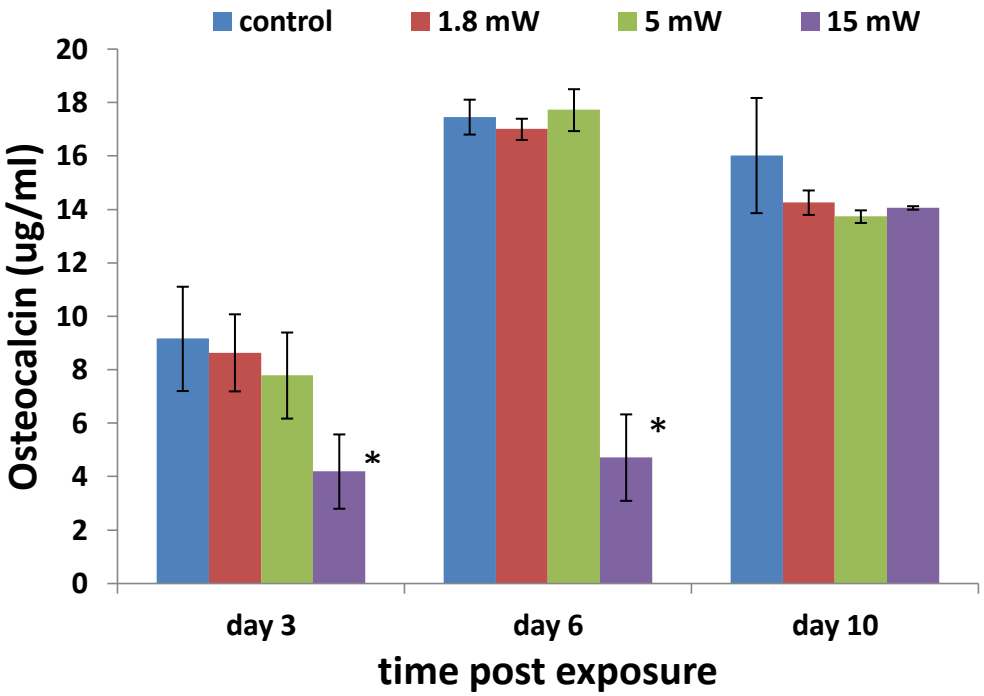

FIGURE 4.7 *Osteocalcin expression following 1 hour HINS-light exposure. From left to right at each timepoint; control, 1.8 mWcm^{-2}, 5 mWcm^{-2}, 15 mWcm^{-2}.* ******* *indicates significant difference from control ($P < 0.05$, ANOVA followed by Dunnett's comparison, $n=3 \pm SEM$, except for control and 15 mWcm^{-2} samples on days 3 and 6 where $n = 6$)*

4.3.4 Proliferation

The proliferation of osteoblasts following HINS-light exposure was assessed by measuring total protein content of the cells via Lowry assay up to 4 days post exposure (figure 4.8). Although there were no significant differences observed in protein content of osteoblasts exposed to up to 15 mWcm^{-2} HINS-light, it would appear that there was a slight reduction in protein concentration, and thus the proliferation rate, of osteoblasts exposed to the maximum intensity.

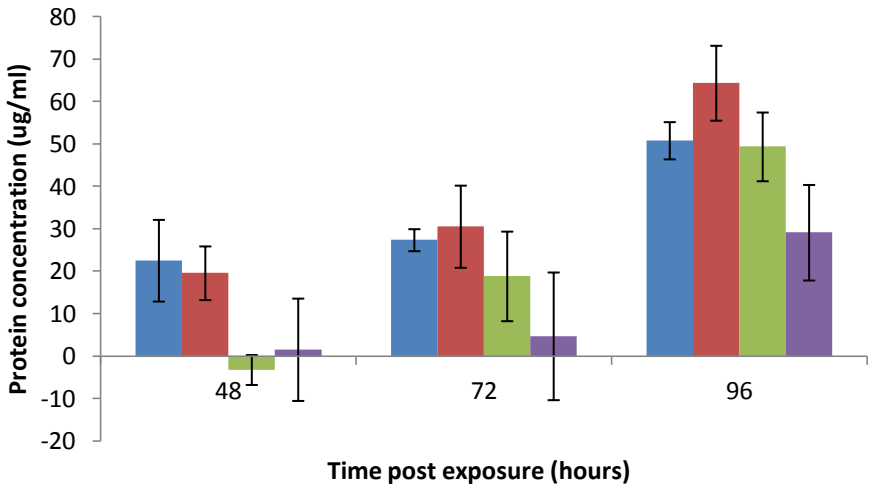

FIGURE 4.8 *Proliferation of osteoblasts following exposure to (left to right); control, 0.5 mWcm^{-2}, 1.8 mWcm^{-2} and 15 mWcm^{-2} HINS-light by Lowry assay. 15 mWcm^{-2} HINS light appeared to cause a reduction in protein content of osteoblasts although no significant differences were found (P>0.05, ANOVA followed by Dunnett's comparison, n=3 ± SEM)*

4.3.5 SEM

Scanning electron microscopy was performed on cells immediately following a 1 hr exposure to 5 and 15 mWcm^{-2} HINS-light. Cells that had not been exposed to HINS-light had a classic osteoblast morphology (figure 4.9 A). They appear well stuck down and stretched out, with some cells still visibly in the process of sticking down. High magnification images of individual cells (figure 4.9 B) showed no remarkable surface features.

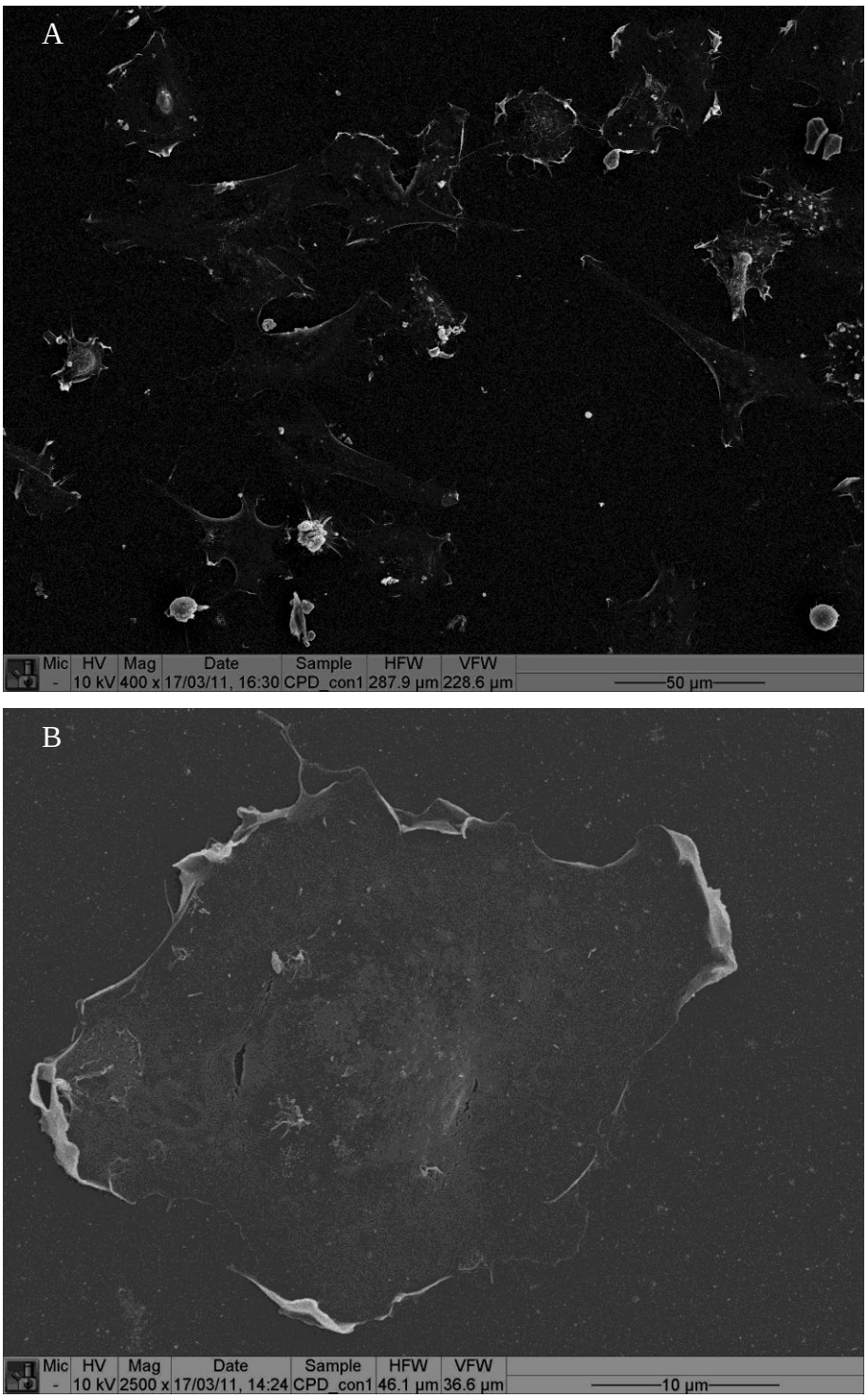

FIGURE 4.9 *SEM of control sample, showing (A) general morphology of sample, and (B) 2500x magnification of single cell.*

Samples exposed to 5 mWcm^{-2} HINS-light are shown in figure 4.10 (A) and (B). High magnification images of the cell surface did not show any obvious defects.

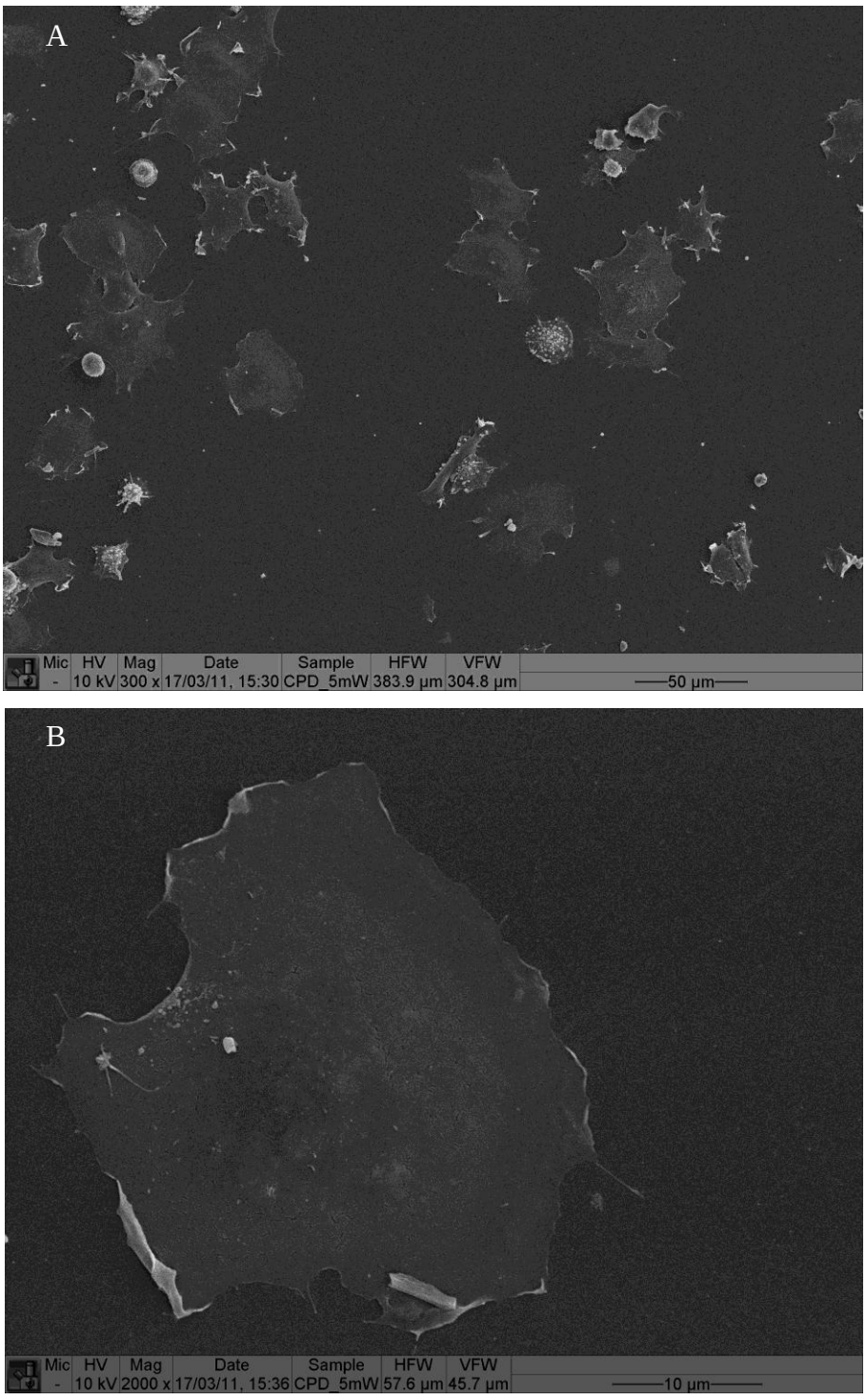

FIGURE 4.10 *SEM of osteoblasts exposed to 5 mWcm^{-2} HINS-light for 1 hour, at (A) 300x magnification, and (B) 2000x magnification.*

Osteoblasts exposed to 1 hour of 15 $mWcm^{-2}$ had a noticeably different appearance to control cells (figure 4.11). Although the cell density appeared similar, the proportion of cells that were stuck down and stretched out was less. Higher magnification images of the cell surface showed lots of small imperfections, like cuts or folds in the membrane. There was also evidence of blebbing on the surface of some cells (figure 4.11 (B)).

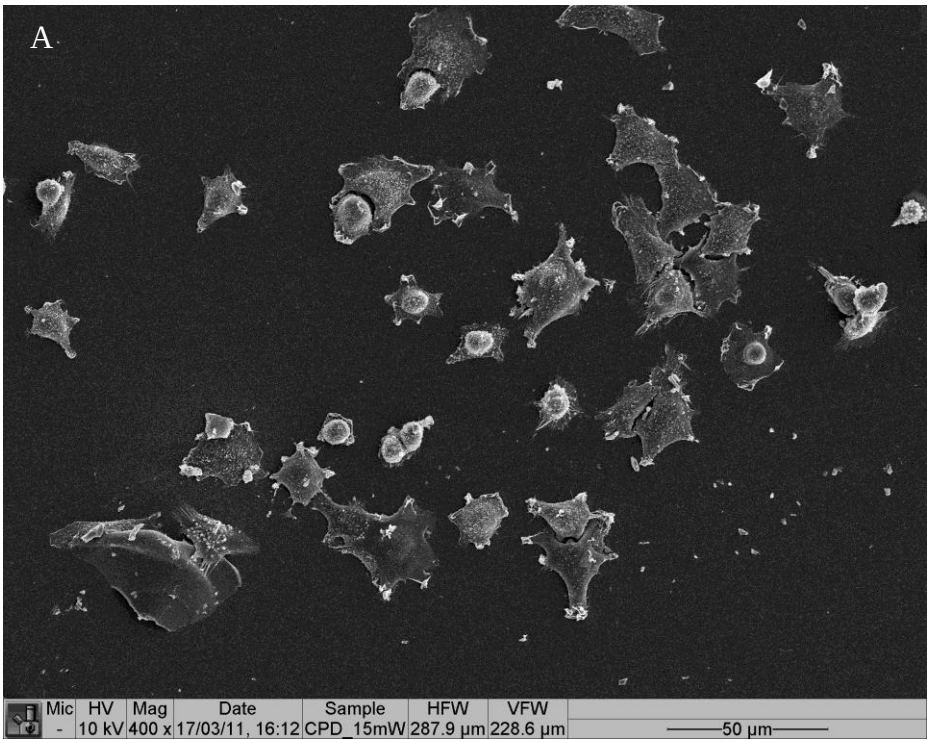

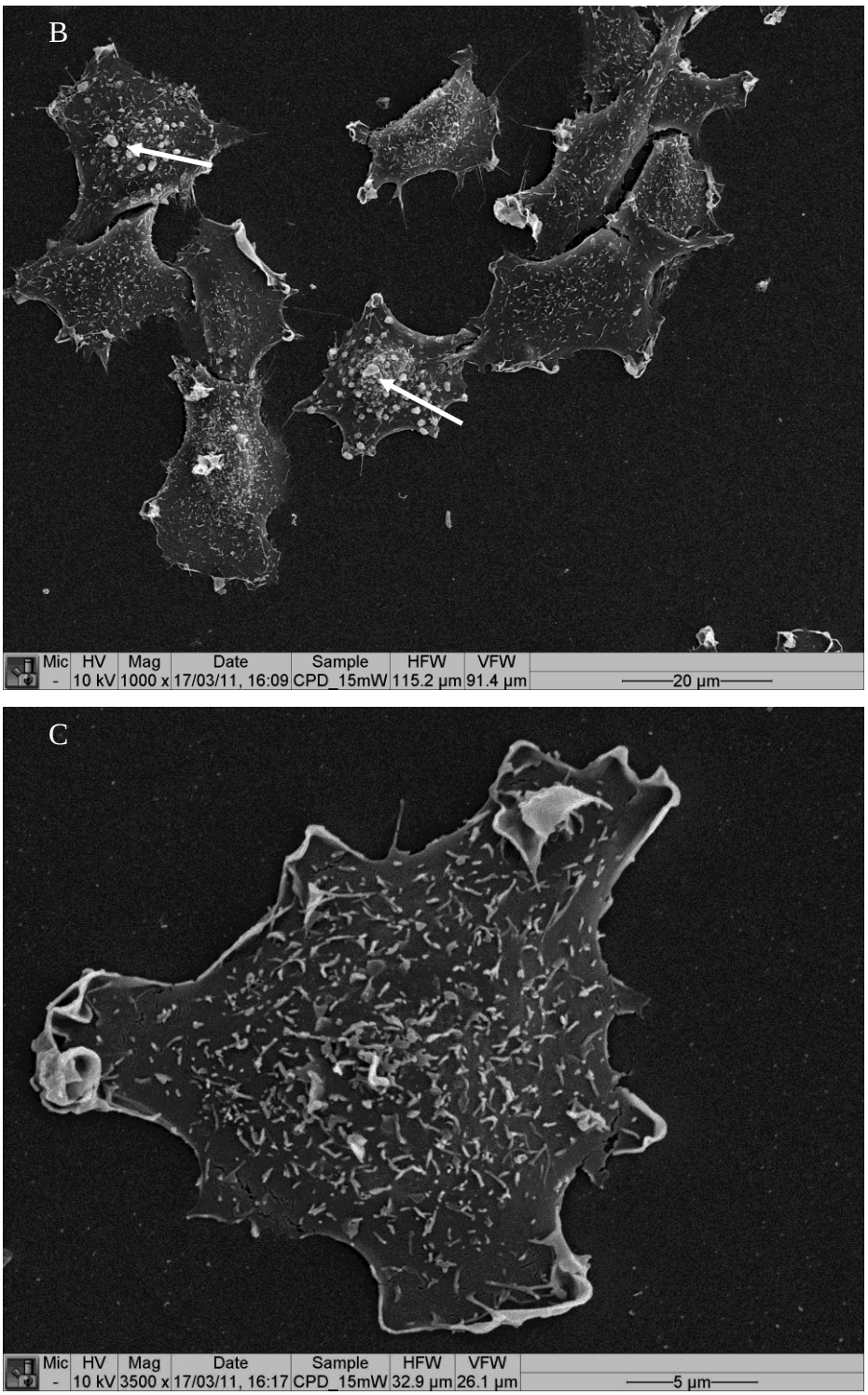

FIGURE 4.11 *Osteoblasts exposed to 1 hr of 15 mWcm^{-2} HINS-light, at (A)400x, (B)1000x, and (C) 3000x magnification. Examples of suspected bleb formation marked with arrows.*

Analysis of the proportion of viable cells and the mean surface area of the individual cells, calculated from a range of sample images, is presented in table 4.1.

TABLE 4.1 *Analysis of osteoblast SEM images. $n \geq 6$, where each sample contained at least 15 cells. * signifies significant difference from control ($P < 0.05$, ANOVA followed by Dunnett's comparison)..*

	% viable cells (± SEM)	Surface area (μm^2 ± SEM)
Control	81 ± 0.1	84.7 ± 12.9
5 mWcm^{-2}	77 ± 2.6	53.0 ± 13.2
15 mWcm^{-2}	66 ± 3.7 *	31.5 ± 8.5 *

4.4 Discussion

These results show that intensities of HINS-light of 5 mWcm^{-2} and below, applied over 1 hour, do not have a significant inhibitory effect on osteoblast function. Exposure to intensities above this have been shown to have a significant effect on the normal function of osteoblasts.

ALP is an enzyme responsible for dephosphorylation of various molecules, including nucleotides, proteins and alkaloids. Clinically, ALP levels can be used to help diagnose bone disorders such as Paget's disease, a condition involving imbalanced bone resorption and formation resulting in enlarged or deformed bones. In vitro, it is well established as a measure of osteoblast ability to synthesis bone (Hoemann et al., 2009). It is therefore encouraging to see that 1 hour exposures to 5 mWcm^{-2} HINS-light had no inhibitory effect on ALP activity. No significant difference compared with control cells was measured at either 24 or 72 hours following exposure. Increasingly large decreases relative to control were, however, seen at 24 hr post exposure as the intensity was increased from 5 to 15 mWcm^{-2}. This significant decrease was still in effect at 72 hours post exposure, where an 88% decrease in ALP expression was observed following exposure to 15 mWcm^{-2}. This implies that 1 hr exposure to intensities above 5 mWcm^{-2} is detrimental to osteoblast function. No examples of the effect of blue light on ALP activity have been published for

comparison, but there are some papers that investigate the effects of red and near infra-red laser light. One group investigated the effects of low doses (1.5 – 3 Jcm^{-2}) of 830 nm light on human osteoblast cells with a view to using the laser to modulate the activity of cells surrounding implants during surgery. They found that these low doses had no effect on ALP synthesis (Khadra et al., 2005). Stein et al (2008) measured ALP levels at up to 72 hr hours following exposure of human osteoblasts to a 400 mW diode laser with 670 nm wavelength. The duration of exposure was 2.5 or 5 s giving a dose of 1 or 2 Jcm^{-2} respectively. They found a slight increase in ALP activity over the observation period following exposure to 1 Jcm^{-2}, but increasing the dose to 2 Jcm^{-2} resulted in decreased ALP activity and viability.

With collagen being the major component of extracellular matrix, the ability of osteoblasts to produce collagen is an important function in the bone formation process. As such it is a useful measure of osteoblast function. Picric Sirius red staining showed that 1 hr exposures to HINS-light at intensities at or below 5 $mWcm^{-2}$ did not have an inhibitory effect on the ability of the osteoblasts to synthesise collagen. No significant change relative to control cells was observed at either 24 or 72 hours following exposure. Collagen synthesis was shown to be significantly reduced by exposure to 15 $mWcm^{-2}$ HINS-light at both 24 and 72 hours following exposure. Similar conclusions can be drawn as for the effect on ALP activity; that exposure to intensities at or below 5 $mWcm^{-2}$ for up to 1 hour have no significant effect on the ability of osteoblasts to synthesise collagen, while exposure to the higher intensities of HINS-light significantly reduces this function. Collagen synthesis has been shown to be both stimulated (Saracino et al., 2009; Stein et al., 2005) and inhibited (Marques et al., 2004) by laser irradiation, although no studies have been performed using an equivalent wavelength or irradiance of light comparable to those used in the present study.

Microscopic examination of cells stained for collagen production with picric Sirius red are a little unexpected in that they do not show the obvious decrease in collagen content that would be expected from the colorimetric assay results. This could simply be due to the relatively small change in colour caused by variation in collagen

content being imperceptible to the eye. The images from 48 hours post exposure suggest that individual cells express similar levels of collagen, implying that the decrease in collagen synthesis observed is due to a decrease in cell number rather than a decrease in collagen producing function of the cells. There is no visible evidence of any dead cells, however, any apoptopic cells or cell debris may have been removed during the many washing steps.

Similar results to ALP activity and collagen synthesis were found when investigating the effect of HINS-light on OC expression. OC is the most abundant non-collagenous protein produced by osteoblasts, and studies on OC knock-out mice suggest that it has osteogenic regulatory functions (Ducy et al., 1996). In certain clinical situations, it is thought that OC is a more sensitive measure of osteoblast damage than ALP (Boiskin et al., 1989). The BTI ELISA kit used in these experiments measures the concentration of OC that has been secreted into the culture medium, shown to be an effective and reliable method of determining osteogenic potential (Nakamura et al., 2009). Performing the assay at 72 hours (3 days) following exposure showed that exposure of up to 5 $mWcm^{-2}$ did not significantly effect the OC expression, while exposure to 15 $mWcm^{-2}$ caused a significant reduction. The same pattern was found at 6 days post exposure. However, by 10 days following exposure the osteoblasts exposed to 15 $mWcm^{-2}$ HINS-light appeared to have recovered and the concentrations of OC found in the cell culture media were in the same range as in the cells that had been exposed to 1.8 and 5 $mWcm^{-2}$ intensities.

As has previously been shown to be the case, osteoblasts did not secrete measurable volumes of OC prior to stimulation with the hormone 1,25 dihydroxy vitamin D_3 (Carpenter et al., 1998). The active form of vitamin D_3 has been shown to play a role in osteoblast differentiation by increased bone-specific ALP activity, synthesis of growth factors and matrix proteins (Kurihara et al., 1986; Majeska & Rodan, 1982; Spiess et al., 1986).

There are various studies on the effect of laser irradiation on OC expression. Khadra et al (2005) found that exposure to 1.5 and 3 Jcm^{-2} near-UV laser irradiation did not have inhibitory effects on OC levels of irradiated human osteoblasts. In fact, they found that 3 Jcm^{-2} had a stimulatory effect on OC production. Similarly, Saracino et al (2009) exposed human osteoblasts to daily doses of superpulsed laser light at 904 – 910 nm wavelength, with minimum peak power of 45W and total energy of 60J, for 5 min. This had no significant effect on mRNA content of OC until the tenth day where a significant increase was observed (Saracino et al., 2009). These are the closest comparisons available to the effects of blue light irradiation, and due to the difference in wavelengths are not particularly useful. Both of these sources also report an increase in other measures of osteoblast function, such as ALP activity and collagen synthesis, and it is logical to conclude that these should go hand in hand. It is not surprising therefore that the higher doses of HINS-light causes a decrease in OC levels. This correlates well with the decreases seen in ALP and collagen at the same doses.

The pattern of OC expression is consistent with that observed in other rat studies, which show lower levels of OC expression during the growth phase of the cells, and maximum expression once cells have reached confluence and extracellular matrix deposition is at its peak (Owen et al., 1991). Studies on human osteoblasts appear to show some differences in cell development to rat cells. Unlike rat osteoblasts, the increase in OC does not appear to be dependent on proliferative phase (Siggelkow et al., 1999b), however, similarities were noted in the production of collagen and ALP activity between the two species (Siggelkow et al., 1999a).

The Lowry assay was used to measure the proliferation of the cells following exposure to HINS-light. The total protein concentration of the cells was measured at 48, 72 and 96 hours following exposure, and showed that exposure to 15 $mWcm^{-2}$ HINS-light appeared to inhibit proliferation up to 96 hours following the exposure. However, contrary to the previous results where no damaging effects have been caused by the lower intensities of HINS-light, 1.8 $mWcm^{-2}$ exposures also appeared to cause a decrease in protein concentration, suggesting a decrease in cell number.

This is probably due to the large error associated with these results, and therefore should not cause undue concern over the safety of HINS-light. The results of the more accurate ALP, OC and collagen synthesis assays show that 1.8 $mWcm^{-2}$ HINS-light does not appear to reduce osteoblast function in any significant way.

SEM analysis helps to confirm the results of the osteoblast function assays. Exposure to 5 $mWcm^{-2}$ does not cause any visual difference to the cell morphology, and the density of cells in the sample was not significantly reduced. The appearance of membrane features on osteoblasts exposed to 1 hour of 15 $mWcm^{-2}$ HINS-light is interesting. The resolution of the images is not sufficient to positively identify the features, but there is undoubtedly some disturbance caused to the membrane of the cells. One possibility is that these features are the initial stages of formation of blebs; bulges in the membrane which appear soon after exposure to lethal stimulation (Barros et al., 2003). Fully formed blebs are apparent in many cells which had been exposed to 15 $mWcm^{-2}$ HINS-light. Small tears are visible at the periphery of the cells, especially apparent at filopodial extensions. These are present in all samples, and this is not an effect of the HINS-light exposure. It is caused by shrinking and subsequent tearing of the cell during the dehydration process.

Quantitative analysis of the images shows significant reductions in cell viability and cell surface area following exposure to 15 $mWcm^{-2}$ HINS-light for 1 hour. The viability of a cell was not always obvious from the micrographs, and so a cell was considered to be healthy if it was well stuck down and there was no obvious blebs or blisters on the cell surface. Conversely, cells with a spherical appearance or with damaged membranes were counted as dead. There is obviously a degree of subjectivity to the distinction which limits the conclusions that can be drawn from these data, however, it does confirm the general trend observed throughout these results. Cell surface areas were calculated from a random sample of cells from all images. The decrease in surface area observed following exposure to 15 $mWcm^{-2}$ light partly confirms the reduction in viability, as a lesser percentage of sampled cells in this group had the stretched morphology and associated large surface area of viable cells.

These results demonstrate that HINS-light has a dose dependent inhibitory effect on osteoblast function. The implication of the results is that intensities of 5 $mWcm^{-2}$ and below, delivered over an hour, should not cause damaging effects to osteoblasts exposed during procedures such as hip replacement which result in exposure of bone surfaces to the external environment. However, the cell line used was a rat cell type, and as mentioned above, some studies have noted differences in the behaviour of rat and human osteoblasts To extend these studies further, the experiments should be repeated using a primary human osteoblast cell type. The source and age of these cells would require careful selection to best replicate the in vivo situation. Another option would be to use animal models, commonly used to measure the effects of red and infra-red laser on bone healing (Tajali et al., 2010). These studies generally involve the exposure of surgically created defects in rat bones to various doses of laser irradiation, followed by histological examination of the exposed area to assess bone formation. The use of an animal model would provide a more accurate maximum value at which HINS-light would have no inhibitory effects on bone formation. Despite 15 $mWcm^{-2}$ HINS-light having significant inhibitory effects on osteoblast function in vitro, this may well have no effect on bone formation or osseointegration of implants in an animal model. Light of 405 nm wavelength will not penetrate deeply into bone; much less than the same intensity of red light would. Porcine studies have shown that a 4.3 $mWcm^{-2}$, 635 nm laser penetrates 0.16 ± 0.04 cm into trabecular bone (Bisland & Burch, 2006). As penetration of the visible light spectrum increases with wavelength, it would be expected that blue light would penetrate less than this. For comparison, 50% of 800 nm red light photons will penetrate 2 cm into soft tissue, compared to 80 µm for 255 nm photons (Macrene, 2006). Any damage to osteoblasts would therefore only occur on the bone surface, the effect of high intensities of HINS-light on overall bone turnover would not be as significant as the results in this chapter suggest.

The lack of penetration of blue light into tissue will limit any effects that HINS-light may have on osseointegration of an implant. Osseointegration is not a surface process. Taking total hip replacement surgery as an example, osseointegration of the femoral stem will occur deep within the cavity of the bone, where exposure to HINS-

light during the procedure will be minimal. To fully establish what, if any, effects HINS-light had on osseointegration of implants, the use of an animal model will be required. Methods to assess osseointegration of titanium implants in a sheep model have been described (Cunha et al., 2007). Sheep are an appropriate model for orthopaedic research due to similarities with humans with respect to weight, size, bone and joint structure, and bone remodelling process (Martini et al., 2001; Potes et al., 2008).

Considering that osseointegration and bone formation occurs throughout the full depth of the bone, and that penetration of HINS-light into bone tissue would be very limited, it is unlikely that HINS-light could cause any significant delay in osseointegration at the intensities and duration of exposure found to be non-damaging in the in vitro experiments described in this chapter. The limitation in depth of penetration which makes significant damage to bone function unlikely may also limit how effective HINS-light could be as a tool for disinfection. Inactivation of any bacteria that is not directly on the surface will be unlikely to occur. However, as discussed in the introduction, the source of most infections is airborne bacteria either from the patient or from the operating staff, that falls upon the surgical site directly or is indirectly transferred into the surgical site (Charnley & Eftekhar, 1969; Hussein et al., 2001). Therefore, if HINS-light is capable of inactivating bacteria with a dose that is proven to be non-harmful to living-tissue, it could be used to decrease the incidence of infection acquired during joint replacement procedures.

The results in this chapter suggest that HINS-light could be applied to bone tissue without significant undesirable effects on bone formation following exposure. Further refinement of the maximum dose at which no effect is caused is required. One aspect of the use of HINS-light exposure during implantation procedures that has not been discussed here is the effect of HINS-light on the material itself. Bacteria on the surface of an implant material is known to be a cause of infection (Vinh & Embil, 2005), and reducing numbers of surface bacteria would have obvious benefits. However, the effects of HINS-light on biomaterials are as yet unknown. This will be investigated in the following chapter.

Chapter 5

EFFECTS OF HINS-LIGHT ON PROSTHETIC VASCULAR GRAFT MATERIALS

5.1 Introduction

If HINS-light was to be applied during surgical procedures to maintain sterility, mammalian tissue would not be the only surface that was exposed to irradiation. This chapter investigates the effect(s) HINS-light may have on implant biomaterials which could receive significant exposure during surgery should HINS-light be employed during implantation procedures. The aim of this chapter was to investigate the effect of HINS-light on polyester vascular graft materials. During surgical procedures involving the placement of vascular graft materials, the surface of the material would be exposed to irradiation by HINS-light if it was being employed to maintain sterility within the operating theatre. Any detrimental effects that HINS-light may have on the properties of the material itself would limit the potential of HINS-light to be used as a tool to maintain the sterility of operating theatres during surgery.

5.1.1 Hylamer polymer failure

Although it seems unlikely that blue light, something that we are exposed to daily, could have damaging effects on a materials mechanical properties, it would not be the first time that a sterilisation technology resulted in the unexpected failure of a material. The most recent high profile case was that of "Hylamer" ultra high molecular weight polyethylene (UHMWPE), a modified polyethylene introduced by DePuy International in the early 1990s as a component of total joint replacement. The polymer had been altered by high pressure and high temperature manufacturing techniques to alter the crystalline structure of the polymer and increase the polymer chain length, thought to give the material better wear resistance. This material was considered to be a significant advancement in implant technology; it had been shown to provide increased fatigue resistance, tensile strength, compressive strength and

density, and had been shown to provide lower rates of wear than conventional materials (Li & Burstein, 1994). Based on this evidence, it was widely selected for use in younger patients where increased activity and movement was anticipated. It was used in replacement of hip and shoulder joints, in DePuy's "Duraloc Acetabular liners", "Ogee Acetabular cups" and "Global Glenoid shoulder" products.

There was no sign of any trouble in the short term, however, within around three to five years post implant surgery, unusually high failure rates were noticed, particularly with total hip replacements using the Duraloc acetabular liner. These implants were failing through increased wear, with evidence of periacetabular and femoral osteolysis and premature loosening of the hip implant (Graeter & Nevins, 1998; Livingston et al., 1997). Failure rates of the implants were found to be as high as 67.6% at five years post operation (Norton et al., 2002). Other reviews of the Duraloc Hylamer liner found survivorship rates of 86% at four years, with survivorship referring to the implant rather than the patients (Chmell et al., 1996). Fifty % of patients who received Hylamer implants required revision surgery due to periprosthetic osteolysis and severe eccentricity of the metal head at 10 year follow up (Visentin et al., 2005).

The surprising large failure rate has been attributed to the sterilisation method used. All the above cases involved hip implants which had been gamma radiation sterilised in the presence of oxygen. It has since been established that gamma radiation causes breakage of C-C and C-H bonds in the polymer, resulting in the formation of radicals. The radicals react with oxygen to form carbonyl groups and further free radicals, which cause chain scissions and so reduce the molecular weight of the polymer. This results in increased density, stiffness and brittleness, and reduced fracture strength of the material. The case of Hylamer products was exacerbated by the storage conditions; they were packaged in air which allowed continued oxidation reactions with residual radicals during storage (Visentin et al., 2005). The wear rate of implants with a shelf life of greater than 10 months was found to be significantly higher than implants used before this point (Kiely et al., 2005). Gamma sterilisation in air was used from 1990 to 1993, and from 1993 to 1995 sterilisation in a nitrogen

environment and vacuum packing was employed. From 1995 onwards gas plasma sterilisation was used. Studies of implants that had been sterilised by the different methods confirms that gamma sterilisation in air was the cause of the Hylamer failures (Stea et al., 2006). In 2001 the Medical Devices Agency issued a safety warning concerning Hylamer implants and a voluntary recall was begun. In 2003 legal proceedings were issued against DePuy International by patient groups affected by Hylamer implants. The Hylamer troubles highlight the importance of in vitro testing of new materials, and of the effect that any new external factor may have on the material.

5.1.2 Poly(ethylene terephthalate) vascular grafts

The effect of HINS light on poly(ethylene terephthalate) (PET) vascular prostheses is investigated in this chapter. PET is a polymer with the repeating chemical structure shown in figure 5.1.

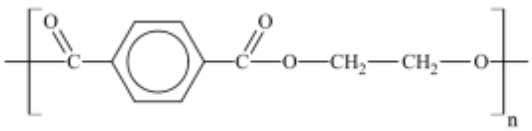

FIGURE 5.1 *Molecular structure of poly(ethylene terephthalate)*

It is used in the manufacture of plastic bottles and textiles where it is more commonly known as polyester. The materials used in this chapter are made by weaving or knitting polyester fibres into prosthetic vascular grafts. Vascular grafts are indicated in severe cases of vascular disease where the artery has become blocked and angioplasty has not proven successful. They can also be used to replace sections of weakened artery wall in cases such as abdominal aortic aneurysm where the wall of the artery has ballooned out. Success rates of vascular surgery are generally good, with failure rates being around 15% (Kakkos et al.); possible reasons for failure of vascular graft surgery include mechanical failure, graft occlusion and infection. Mechanical failure is normally caused by compliancy mismatch between the graft material and the host artery (Greenwald & Berry, 2000). Mechanical properties of the graft material are also thought to lead to intimal hyperplasia, a thickening of the

arterial wall, and this is the most common cause of failure in the long term (Dobrin et al., 1989). Occlusion can also be caused by thrombogenicity of the material (Rashid et al., 2004). Graft infection occurs in 1 – 5% of cases, depending on the site of the graft, and 1 year mortality rates following infection have been reported as high as 37% (Chambers, 2005). Methicillin resistant *Staphylococcus aureus* has been shown to be responsible for the majority of post operative infections (Taylor & Napolitano, 2004), with *Staphylococcus epidermidis* and other strains of *Staphylococcus aureus* also being present in a large number of cases (Bandyk et al., 1984; Zetrenne et al., 2007). The main cause of infection is thought to be from contamination of the graft during implantation (Kuehn et al., 2010).

Vascutek Ltd., Inchinnan, Glasgow provided polyester material samples that are either plain or gelatin sealed. Non-gelatin sealed materials require pre-clotting with the recipient's blood prior to implant to avoid excess blood loss immediately following implant. The sealing process utilised by Vascutek impregnates the material with gelatin such that it has zero porosity and so does not need pre-clotting prior to use. Prior to impregnation the gelatin is treated with the anhydride or chloride of a polycarboxylic acid to control the number of specific amino acid groups present in the gelatin. After vacuum impregnation of the material with gelatin, formaldehyde and/or glutaraldehyde is used to crosslink the remaining amino acids. The speed at which the gelatin is hydrolysed by the aqueous component of the recipient's blood is determined by the amount of crosslinks present in the gelatin. The gelatin sealed prostheses can also be loaded with antibiotics, commonly rifampicin, and heparin anticoagulant, which is slowly released as the gelatin dissolves (Drury et al., 1987; Strachan, 1993).

The surgical procedure varies greatly depending on location of the artery to be replaced and complexity of surgery required. It can be carried out endovascularly through incisions in the groin, or may require open surgery. Either way, it is conceivable that if HINS-light was being used in the operating theatre, that the graft material itself may receive a dose of irradiation. What effects could this have on the material? Photodegradation of PET is a known issue, and the mechanical

characteristics of PET are known to be affected by exposure to UV radiation (Fashandi et al., 2008). In a similar way as described above for gamma irradiation of UHMWPE, UV light is known to cause free radical formation and polymer chain scissions of PET (Fechine et al., 2004). Gamma radiation has also been shown to affect the cytotoxicity of materials. A 10 kGy dose of gamma irradiation to polyether-urethane was found to significantly increase the amount of cytotoxic compounds to levels that were harmful to fibroblasts (Haugen et al., 2007). If HINS-light was also to have these effects on PET vascular grafts, this would have undesirable effects on cellular integration of the graft. Re-epithelialisation of implanted grafts is desirable for long term patency of the graft in vivo. The mechanical properties of the graft are also important for success of the graft, and any weakening of the material or effects on elasticity by HINS-light could cause failure of the device (Stewart & Lyman, 2004; Van Damme et al., 2005).

In this chapter the materials have been exposed to the intensity of HINS-light that has been shown to not have any detrimental effect to mammalian cells over a 1 hour exposure. This is the maximum intensity at which it is anticipated HINS-light could be used in the hospital environment, and therefore represents the worst case exposure scenario. It is unlikely that materials would be exposed for periods of an hour, therefore the dose received would be lower than that applied here. The effects of HINS-light on the mechanical strength of the material have been investigated. Microscopic assessment of the topography and gelatin sealing was performed before and after exposure. The toxicity of the material was assessed by exposure of extracts to human aortic smooth muscle cells. These tests were performed immediately following exposure and after a period of three months in storage, to assess any longer term effects HINS-light may have on the materials.

5.2 Materials and methods

5.2.1 Materials

The materials used in this chapter were vascular prostheses materials provided by Vascutek Ltd, Inchinan, Glasgow. Four varieties of material were used:

- Knitted polyester
- Woven polyester
- Gelatin sealed knitted polyester
- Gelatin sealed woven polyester

SEM images of the various materials are shown in figure 5.2.

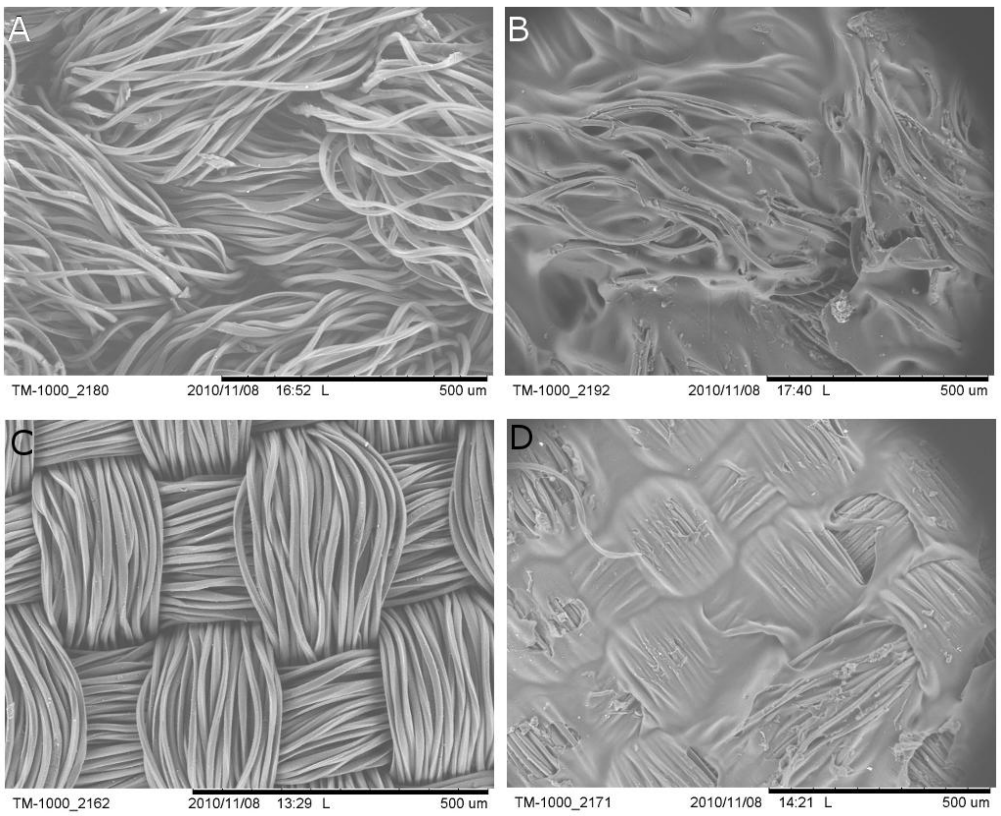

FIGURE 5.2 *SEM images of; (A) Knitted polyester, (B) Gelatin sealed knitted polyester, (C) Woven polyester, and (D) Gelatin sealed woven polyester. Scale bars are 500 µm.*

Materials were supplied uncrimped and unsterilised in tubular form. All materials were manufactured by Vascutek Ltd at their facility in Glasgow. All materials were

sterilised by submersion in 80% EtOH for 15 min and rinsed three times in dH_20 prior to use.

5.2.2 Mechanical testing

Mechanical tensile testing was performed with an Instron E10000 instrument fitted with a 25 kN dynamic load cell (figure 5.3). Materials were cut into 10cm x 2cm strips and exposed to HINS-light for 1 hr at 5 $mWcm^{-2}$ on both sides. At the required time point, strips of material were placed in the pneumatic grips of the Instron machine and pulled taut. Stretching was then applied at a constant rate of 30 mm/min until failure. Maximum load (N), tensile strength at maximum load (MPa), tensile strain at maximum load (%), load at break (N), stress at break (MPa), strain at break (%) and tensile stress at yield (MPa) was recorded by Instron Bluehill software. Testing was performed before, 24 hr after HINS treatment and at three months following exposure.

FIGURE 5.3 *INSTRON mechanical testing setup. Image B is a magnification of the area in the white box on image A.*

5.2.3 Scanning electron microscopy (SEM)

SEM of materials was performed before, immediately after, and at 3 months following 1 hr of 5 $mWcm^{-2}$ HINS-light exposure. SEM was performed on a HITACHI (Tokyo) TM-1000 table top SEM unit with up to 1200x magnification and 15 keV accelerating voltage. Samples were cut into 0.5cm^2 sections and affixed to aluminium tabs by double sided carbon tape. No coatings or gold spluttering was used. Images were examined for obvious defects to the fibres, such as strand breaks. The integrity of the gelatin sealing was visually compared.

5.2.4 Cytotoxicity testing

The neutral red (NR) assay was used to determine if HINS-light exposure resulted in an increase of leachables from the material which may have toxic effects on cells it subsequently came into contact with. Materials were exposed to HINS-light at 5 $mWcm^{-2}$ for 1 hr on each side before extraction was performed according to ISO 10993:12. The materials were cut into 1 cm^2 segments and submerged in serum-free DMEM at a ratio of 6cm^2/ml DMEM. Extraction was performed at 37 °C for 24 hours with agitation in sterile glass universal bottles.

Primary human aortic smooth muscle cells (hASMC) (Lonza, Slough, UK) were used to test effects of the extracted medium. Cells were aliquoted and stored in liquid nitrogen. Prior to use, cells were thawed and cultured in complete DMEM as described in section 2.2.2. Medium was replaced every two days until cells reached approximately 80% confluency when they were subcultured at $3.5x10^3$ cells/cm^2. Cells were used between passage two and four, at which point they were seeded in 96 well plates at a density of $2x10^4$ cells/cm^2. Cells were cultured for 48 hours before the addition of the extract solution.

Neutral red (NR) assay was performed in accordance with ISO 10993:5. NR solution was prepared at 0.05% w/v in PBS and allowed to dissolve for 24 hr at 37°C. Undissolved NR crystals were removed by filtration through a 0.2µm Millipore filter before use. Cells were incubated with undiluted control or exposed material medium extract for 48 hr. Cell culture medium was removed and cells incubated with 100 µl NR solution for 24 hr. NR solution was then removed and wells washed with 150 µl PBS before the addition of 100 µl NR destain (see appendix). Plates were agitated for 10 min until all NR was extracted from the cells and formed a homogenous solution. The absorption of the resulting coloured solution was measured at 540nm and the mean of the blanks subtracted to give the final value. Microplate configuration is shown in figure 5.4.

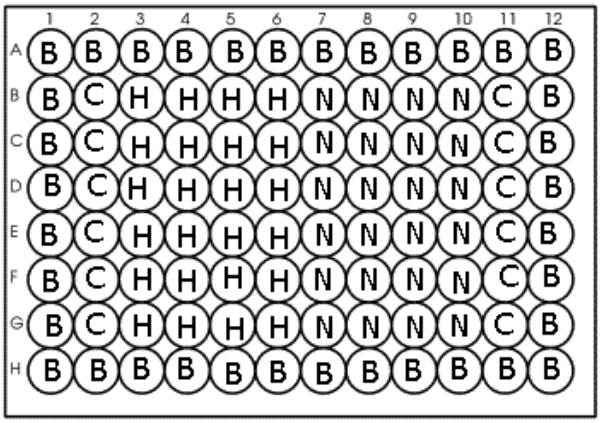

FIGURE 5.4 *Microplate configuration for Neutral Red cytotoxicity assay. B = Blank (no cells), C = Control (cells + culture medium), H = Extract medium from HINS-light exposed material, N = Extract medium from control material*

5.2.5 Storage conditions

After treatment and initial experiments, samples were stored for three months before experiments were repeated. Samples were stored in air in large Petri dishes at room temperature. Petri dishes were not sealed closed and samples were kept in darkened conditions.

5.3 Results

5.3.1 SEM

Figures 5.5 to 5.8 show SEM images of the materials immediately before and after exposure to 5 $mWcm^{-2}$ HINS-light for 1 hour. Figure 5.5 and 5.7 show non-gelatin sealed knitted and woven material. Exposure to HINS-light does not appear to cause any obvious defects to the fibres. There does not appear to be any changes to the general topology of the material and there are no obviously degraded strands. Higher magnification images of single fibres do not suggest that HINS-light exposure has caused any microscopic defects to the material. Figures 5.6 and 5.8 show gelatin sealed versions of the knitted and woven material. Exposure to HINS-light does not appear to have caused any increased degradation of the gelatin sealing. Immediately following exposure, gelatin coverage appears to be consistent with that of control groups.

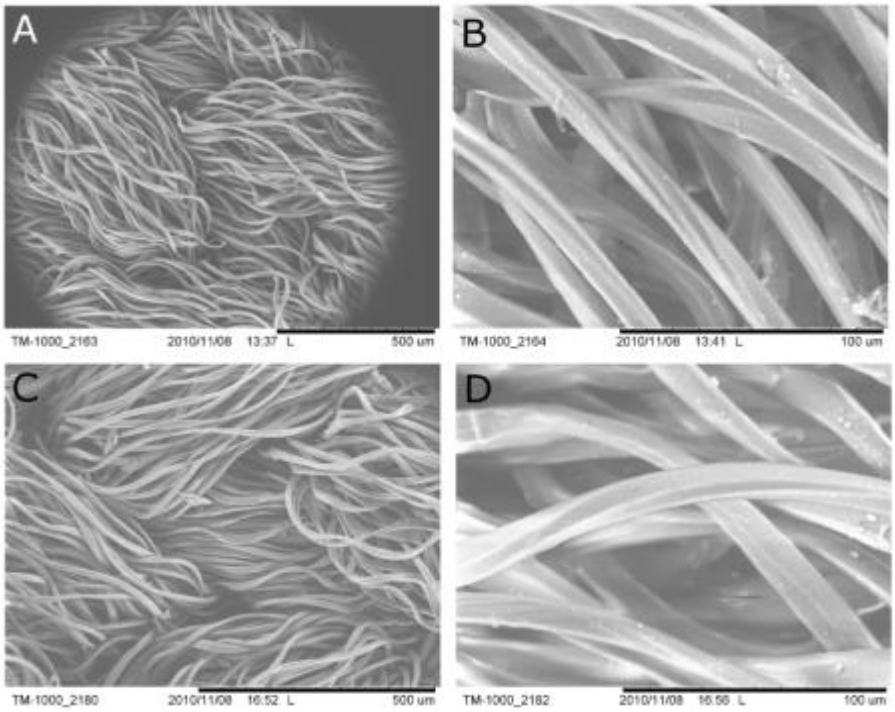

FIGURE 5.5 *Knitted PET before (A and B) and immediately following (C and D) exposure to 1 hr of 5 mWcm^{-2} HINS-light. Scale bars are; A,C – 500 µm, B,D – 100 µm.*

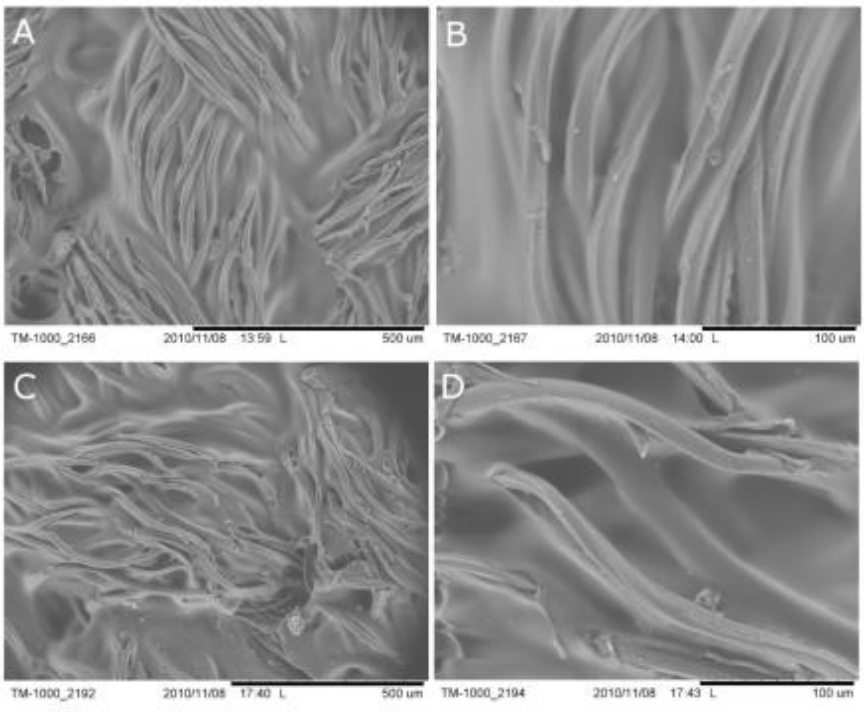

FIGURE 5.6 *Gelatin sealed knitted PET before (A and B) and after (C and D) exposure to 1 hr of 5 mWcm^{-2} HINS-light. Scale bars are; A,C – 500 µm, B,D – 100 µm.*

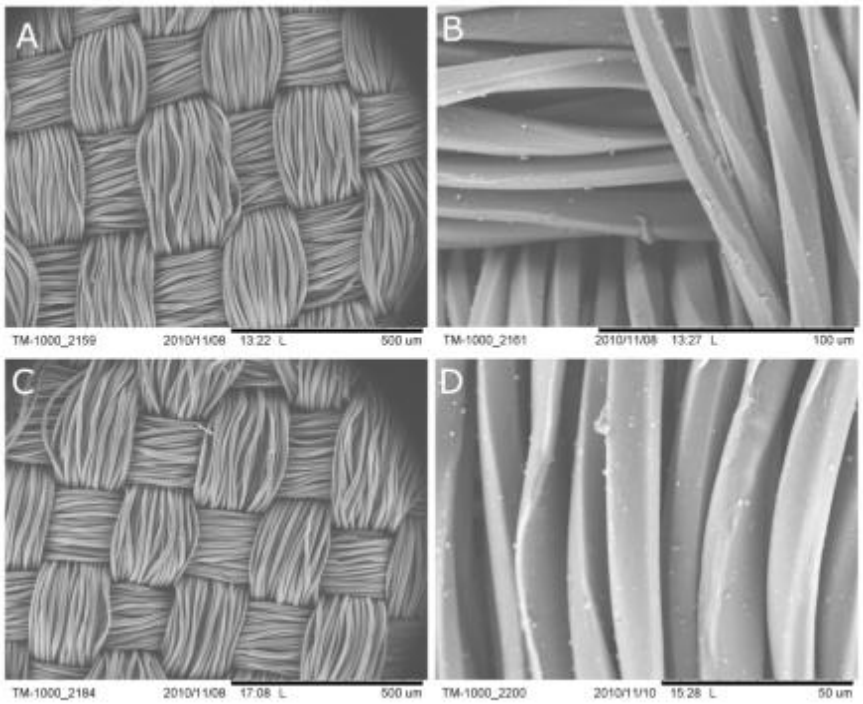

FIGURE 5.7 *Woven PET before (A and B) and immediately following (C and D) exposure to 1 hr of 5 mWcm^{-2} HINS-light. Scale bars are; A,C – 500 µm, B – 100 µm, D – 50 µm.*

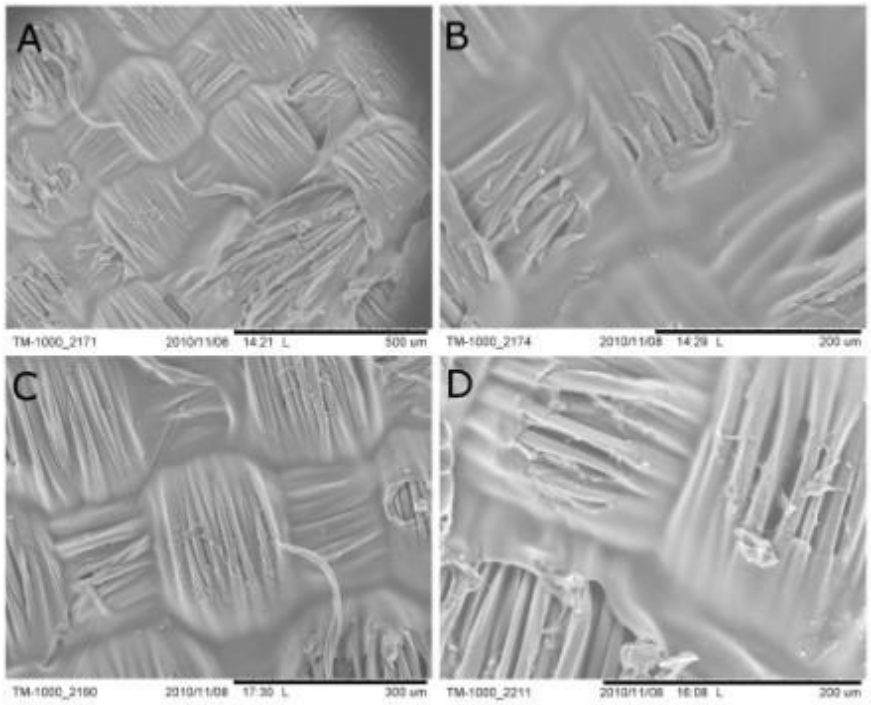

FIGURE 5.8 *Gelatin sealed woven PET; (A,B) before, and (C,D) after 1 hr, 5 mWcm^{-2} HINS-light exposure. Scale bars are; A – 500µm, B – 200µm, C – 300µm, D – 200µm.*

At three months following exposure, there remains no visible difference to control images (figures 5.9 – 5.12). The degree of gelatin resorption is comparable to that of control samples, and does not appear to have been accelerated by HINS-light exposure (figures 5.10 and 5.12).

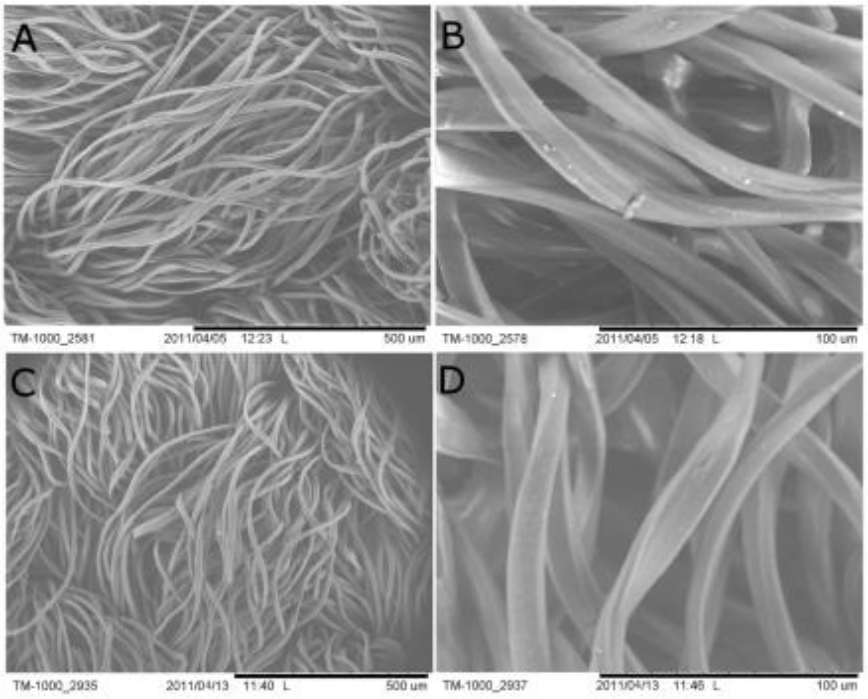

FIGURE 5.9 *SEM images of knitted PET material after three months in storage following exposure to 1 hr of 5 mWcm^{-2} HINS-light (C & D). Control in A & B. Scale bars shown in lower right corner of each image.*

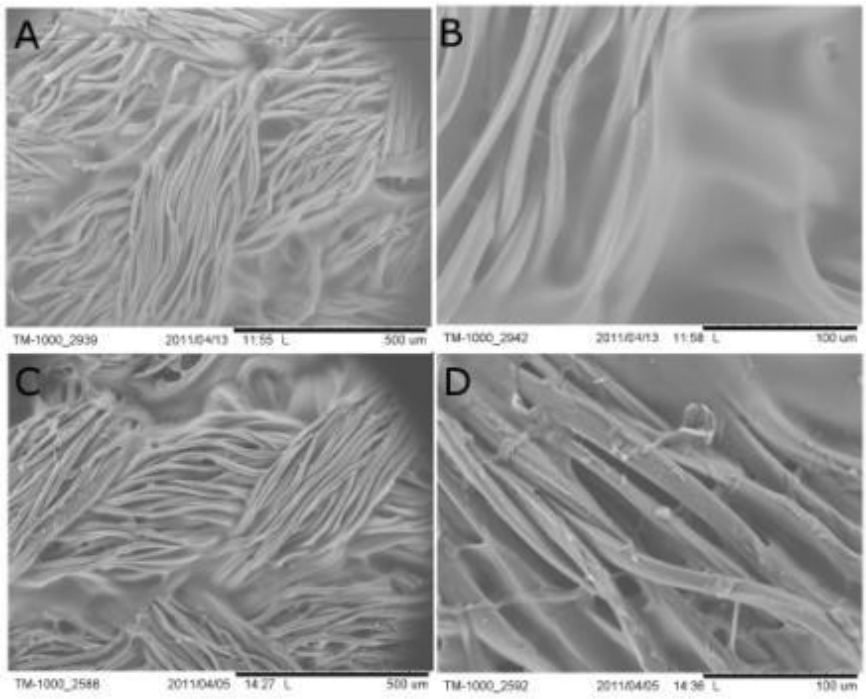

FIGURE 5.10 *SEM images of gelatin sealed knitted material after three months in storage following exposure to 1 hr of 5 mWcm^{-2} HINS-light (C & D). Control in A & B. Scale bars shown in lower right corner of each image.*

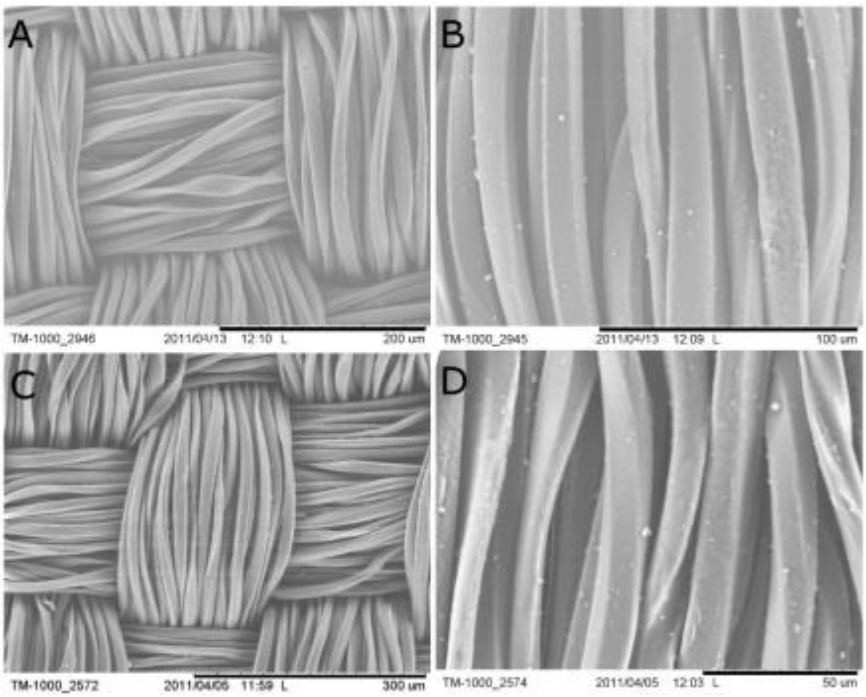

FIGURE 5.11 *SEM images of woven materials after three months in storage following exposure to 1 hr of 5 mWcm^{-2} HINS-light (C & D). Control in A & B. Scale bars shown in lower right corner of each image.*

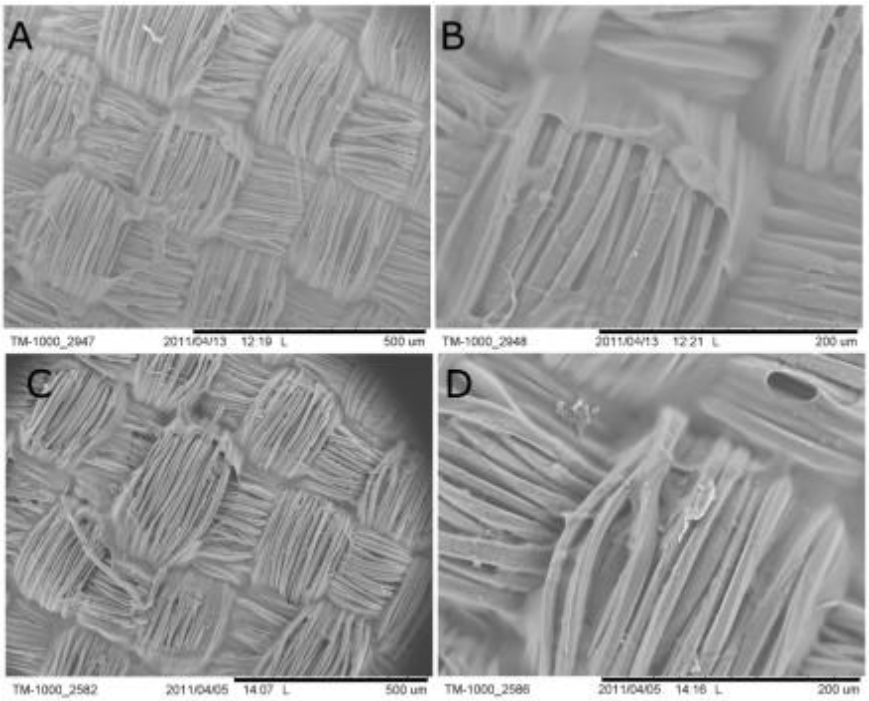

FIGURE 5.12 *SEM images of gelatin sealed woven material after three months in storage following exposure to 1 hr of 5 mWcm^{-2} HINS-light(C & D). Control in A & B. Scale bars shown in lower right corner of each image.*

5.3.2 Cytotoxicity testing of material extracts

The NR assay was used to test the viability of cells seeded with culture medium containing extracts from HINS-light exposed knitted and gelatin sealed knitted vascular grafts. The results of the NR assay are shown in figure 5.13 for knitted PET and 5.14 for the gelatin sealed version. No significant differences in cell viability were measured in hASMCs cultured with either the medium containing extracts from the control or the HINS-light exposed non-gelatin sealed material. For gelatin sealed knitted material, a significant decrease was observed in cell viability of hASMCs cultured with medium containing both the exposed and control material extract. There was no significant difference between the viability of cells cultured with the control extract and the extract medium from HINS-light exposed material ($P > 0.05$).

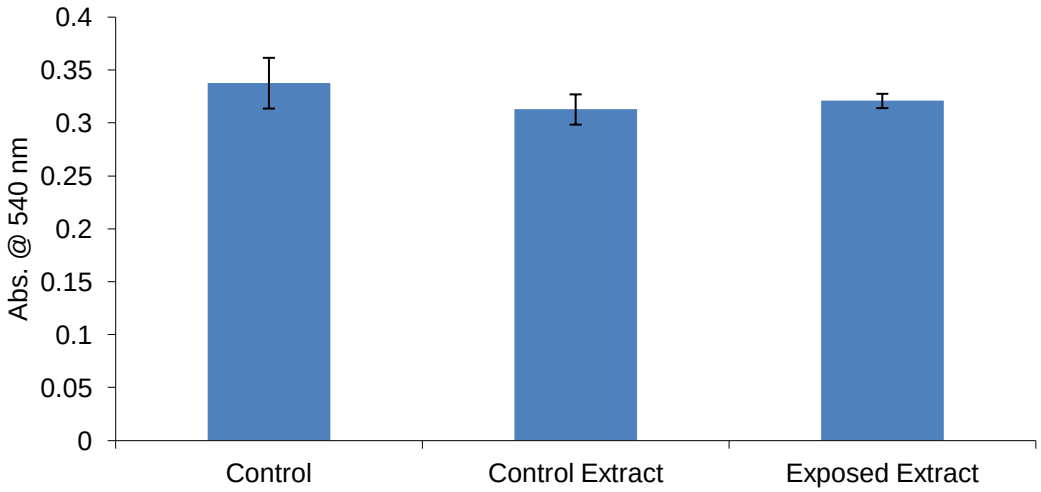

FIGURE 5.13 *Viability of hASMC cells cultured with control medium (left), medium containing extracts from non-exposed knitted materials (middle), and medium containing extracts from materials exposed to 1 hr, 5 mWcm^{-2} HINS-light. Assessed by NR assay. No significant difference (P > 0.05, n=3)*

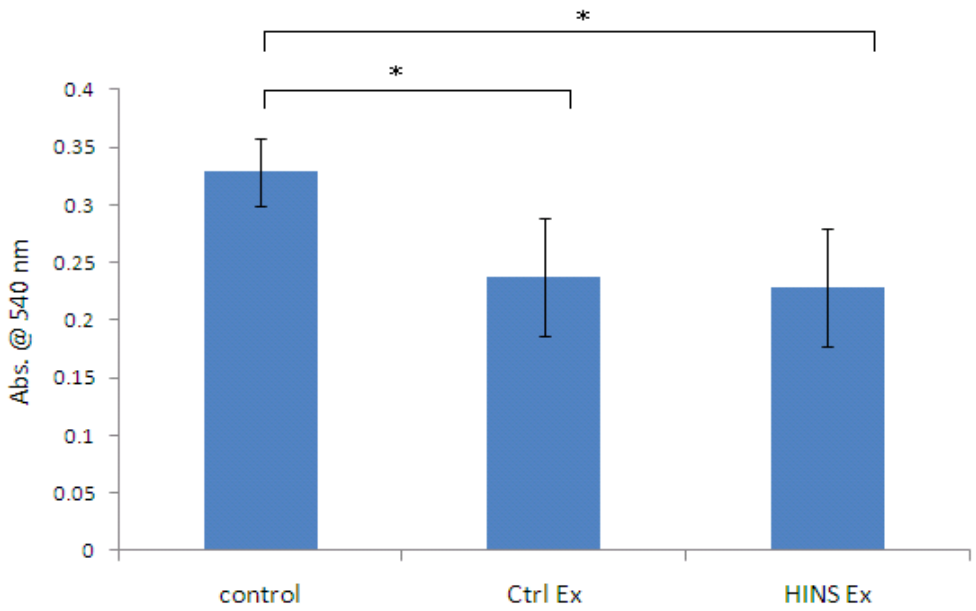

FIGURE 5.14 *Viability of hASMC cultured with control medium (left), medium containing extracts from non-exposed gelatin sealed knitted materials (middle), and medium containing extracts from materials exposed to 1 hr, 5 mWcm^{-2} HINS-light. * indicates significance (P < 0.05, ANOVA followed by Fisher's comparison, n=3).*

5.3.3 Mechanical testing

Figures 5.15 to 5.19 show extension/load charts for a selection of material samples from (A) control, (B) 24 hr, and (C) 3 month samples. The Instron Bluehill software limits the number of samples per chart to 4, with any additional samples being plotted separately. Tables 5.1 – 5.4 display quantitative results for each material at the same time points. Statistical analysis was performed by ANOVA followed by Dunnett's comparison, with a confidence level of $P = 0.05$. No statistically significant decreases in material properties were found between controls and HINS-light exposed samples.

Knitted PET

A

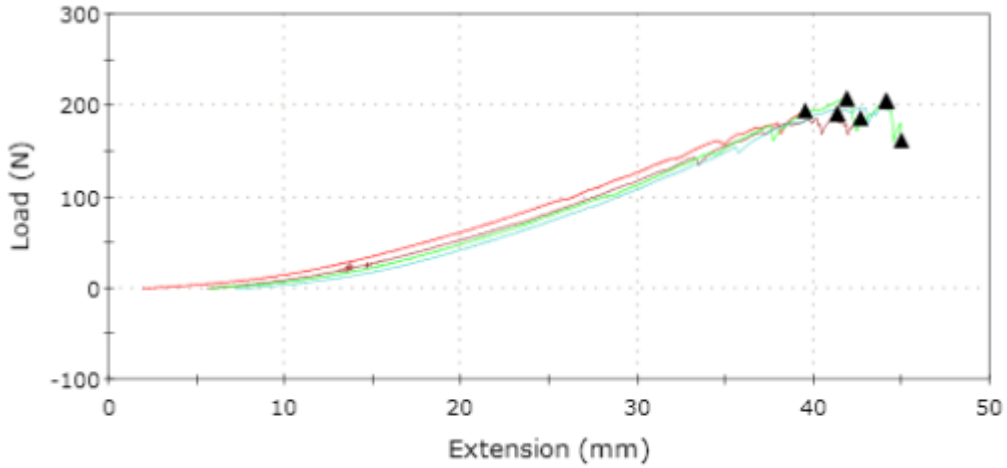

B

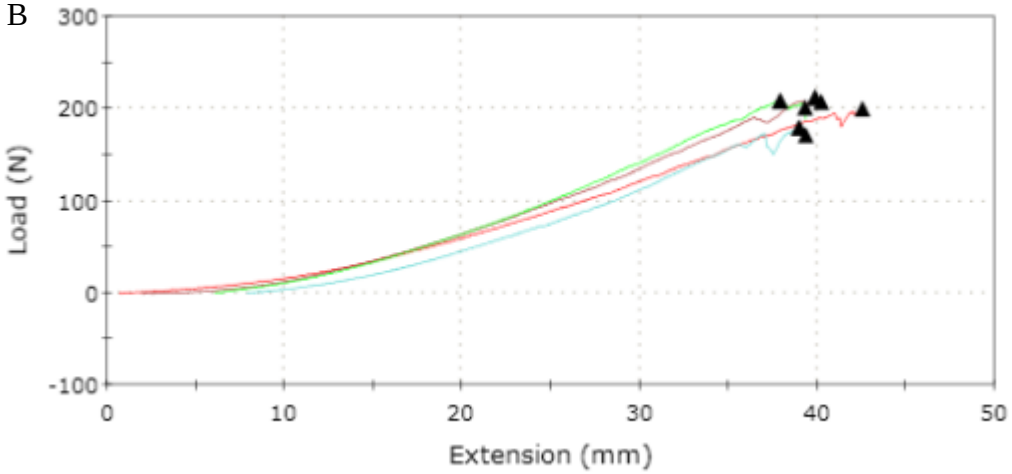

C

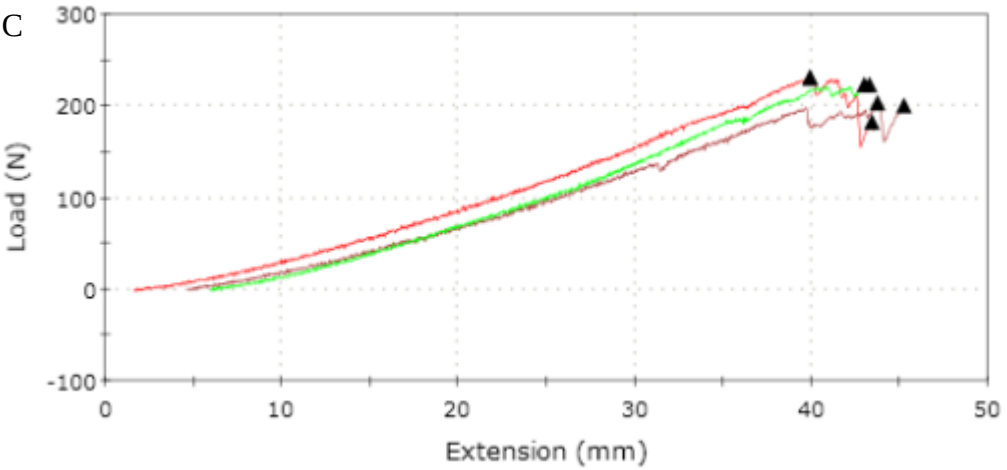

FIGURE 5.15 *Extension/load charts of knitted PET material. (A) control, and 1 hr, 5 mWcm^{-2} HINS-light exposed materials at (B) 24 hr post exposure, and (C) 3 months post exposure.*

TABLE 5.1 *Numerical results of mechanical testing of knitted PET. Results are mean ± SEM, (n=4).*

	Maximum Load (N)	Tensile stress at Maximum Load (MPa)	Tensile strain at Maximum Load (%)	Load at Break (Standard) (N)	Tensile stress at Break (Standard) (MPa)	Tensile strain at Break (Standard) (%)
Control	200 ± 7	10.0 ± 0.4	35.6 ± 2.5	194.8 ± 8.0	9.7 ±0.4	36.1 ± 2.4
24 hour post HINS	200 ± 4	10.0 ± 0.2	36.5 ± 0.4	186.8 ± 9.0	9.3 ± 0.4	37.6 ± 0.5
3 month post HINS	224 ± 6	11.2 ± 0.3	37.6 ± 0.4	200 ± 10.8	10.0 ± 0.5	39.6 ± 0.9

Gelatin sealed knitted PET

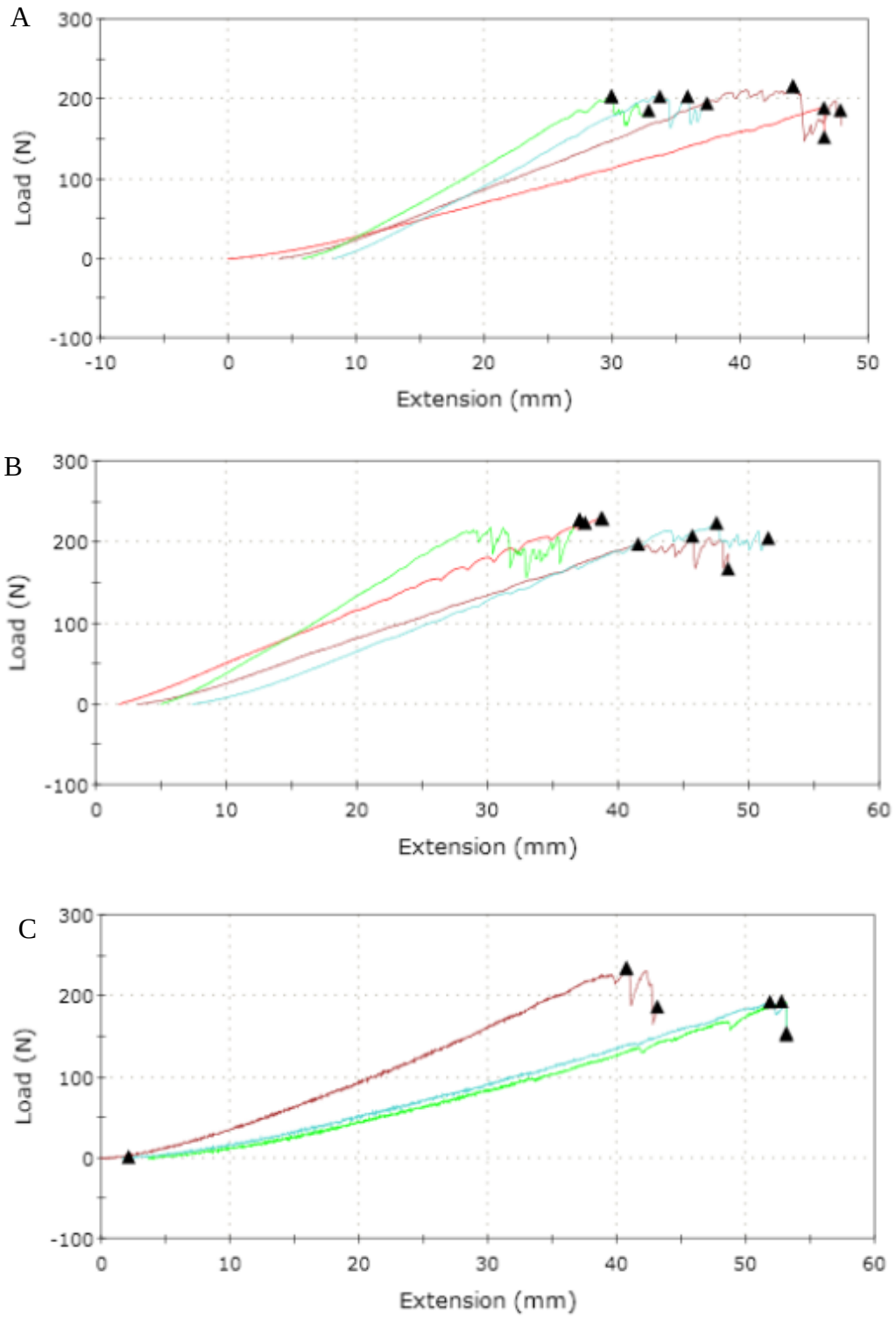

FIGURE 5.16 *Extension/load charts of gelatin sealed knitted PET material. (A) control, and 1 hr, 5 mWcm^{-2} HINS-light exposed materials at (B) 24 hr post exposure, and (C) 3 months post exposure.*

TABLE 5.2 *Mechanical testing of gelatin sealed knitted PET (n=4).*

	Maximum Load (N)	Tensile stress at Maximum Load (MPa)	Tensile strain at Maximum Load (%)	Load at Break (Standard) (N)	Tensile stress at Break (Standard) (MPa)	Tensile strain at Break (Standard) (%)
Control	203 ± 6	10.2 ± 0.3	34.5 ± 5.3	180.0 ± 9.3	9.0 ± 0.5	36.6 ± 5.0
24 hour post HINS	200 ± 4	10.0 ± 0.2	36.5 ± 0.4	186.8 ± 9.0	9.3 ± 0.5	37.6 ± 0.5
3 month post HINS	207 ± 14	10.4 ± 0.7	46.6 ± 3.0	164.7 ± 11.1	8.2 ± 0.6	48.0 ± 2.5

Woven PET

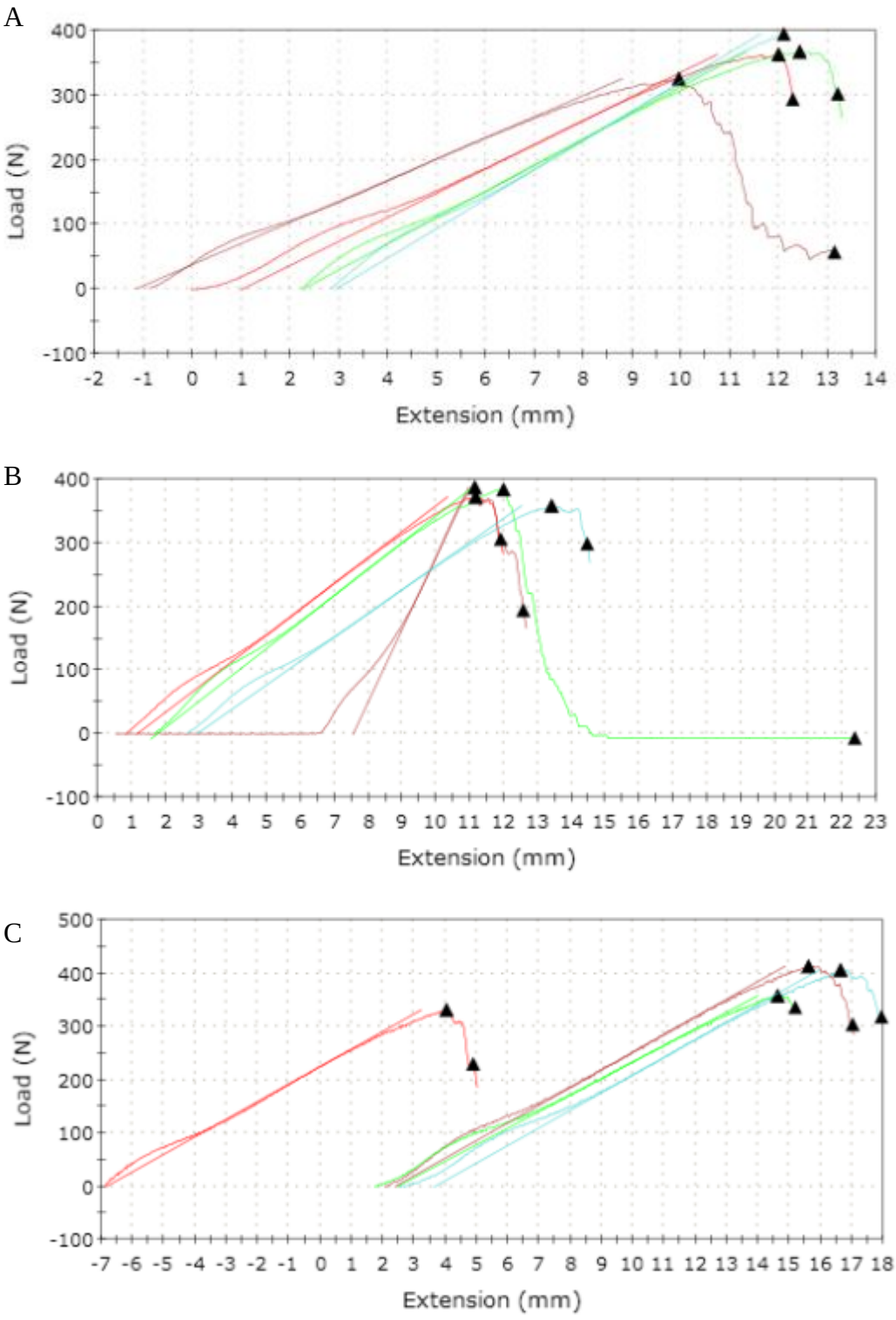

FIGURE 5.17 *Extension/load charts of woven PET material. (A) control, and 1 hr, 5 mWcm^{-2} HINS-light exposed materials at (B) 24 hr post exposure, and (C) 3 months post exposure.*

TABLE 5.3 *Numerical results of mechanical testing of woven PET. Results are mean ± SEM. (n=4)*

	Maximum Load (N)	Tensile stress at Maximum Load (MPa)	Tensile strain at Maximum Load (%)	Load at Break (Standard) (N)	Tensile stress at Break (Standard) (MPa)	Tensile strain at Break (Standard) (%)
Control	362 ± 14	18.1 ± 0.7	13.2 ± 0.7	262 ± 72	13.1 ± 3.6	14.5 ± 1.3
4 hour post HINS	375 ± 7	18.7 ± 0.3	13.1 ± 0.1	266 ± 36	13.3 ± 1.8	17.3 ± 2.8
3 month post HINS	375 ± 15	18.8 ± 0.8	13.1 ± 0.6	303 ± 19	15.1 ± 0.9	14.1 ± 0.7

Despite there appearing to be inconsistencies between the stress strain curves of control and exposed woven PET samples, examination of the scale on the charts shows this not to be the case. The plotting software does not allow exclusion of tests where something went wrong, and therefore chart B above includes a test where the break point was not recognised and extension continued beyond this point, while C includes the curve of a sample where extension was not calibrated prior to testing. Were the exclusion of these tests possible, and the inclusion of all repeats, the stress strain curves would not appear so different. Analysis of the numerical results, which only includes all successful sample tests, confirms that no statistically significant differences are caused by exposure to HINS-light.

Gelatin sealed woven material

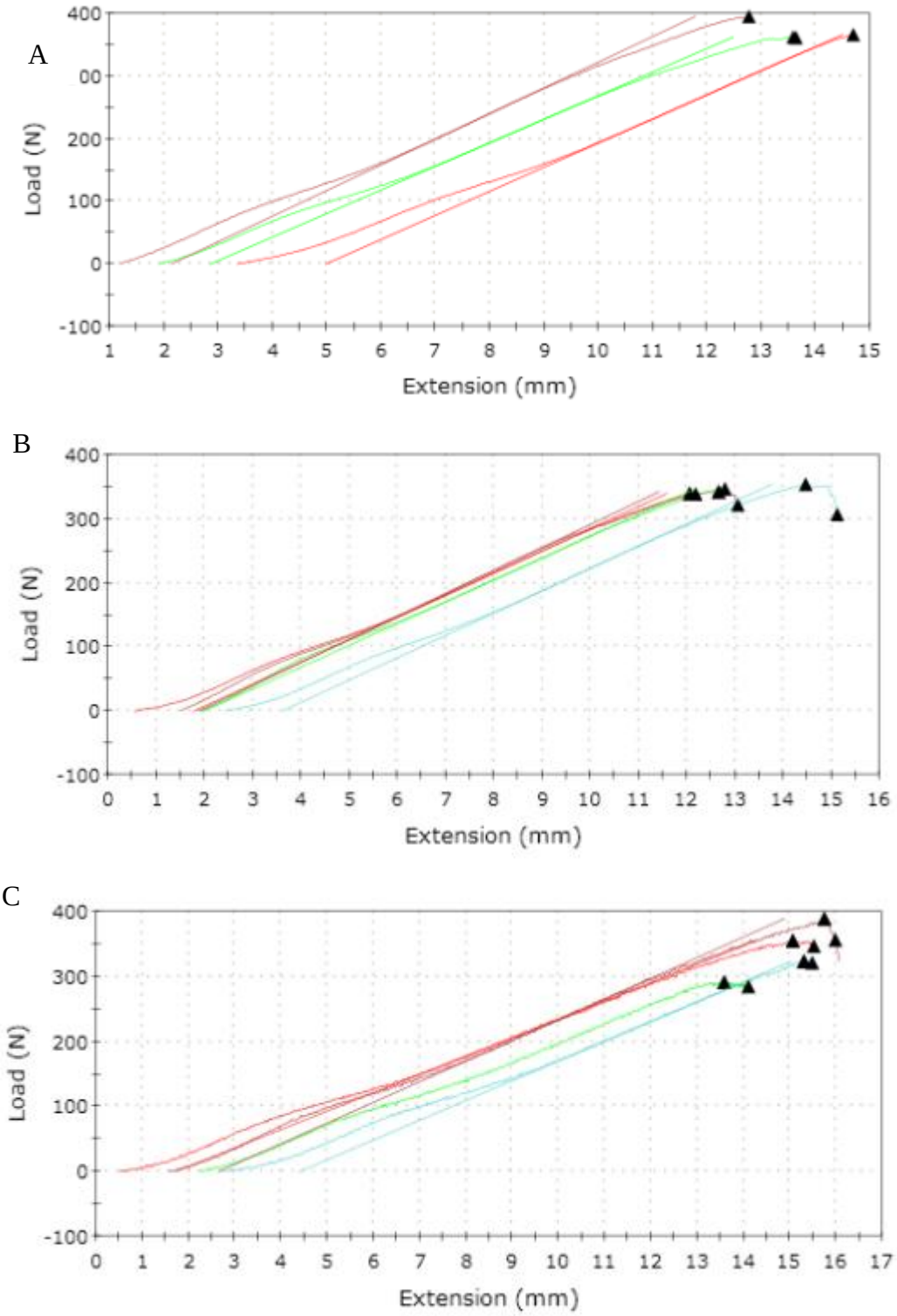

FIGURE 5.18 *Extension/load charts of gelatin sealed woven PET material. (A) control, and 1 hr, 5 mWcm^{-2} HINS-light exposed materials at (B) 24 hr post exposure, and (C) 3 months post exposure.*

TABLE 5.4 *Numerical results of mechanical testing of gelatin sealed woven PET. Results are mean ± SEM (n=4).*

	Maximum Load (N)	Tensile stress at Maximum Load (MPa)	Tensile strain at Maximum Load (%)	Load at Break (Standard) (N)	Tensile stress at Break (Standard) (MPa)	Tensile strain at Break (Standard) (%)
Control	374 ± 10	18.7 ± 0.5	14.4 ± 0.1	374 ± 11	18.7 ± 0.5	14.4 ± 0.1
24 hour post HINS	345 ± 3	17.3 ± 0.2	14.2 ± 0.3	328 ± 9	16.4 ± 0.4	14.6 ± 0.5
3 month post HINS	335 ± 17	16.7 ± 0.8	13.3 ± 0.6	321 ± 13	16.1 ± 0.7	13.6 ± 0.6

5.4 Discussion

These results have shown that HINS-light, at an intensity of 5 $mWcm^{-2}$ applied for 1 hour, does not have a significant detrimental effect on PET prosthetic vascular graft materials. This is the maximum intensity that has been shown not to be harmful to mammalian cell cultures, and so is the maximum intensity that these materials would be exposed to. As HINS-light does not damage materials at this intensity, HINS-light would therefore be safe to be used in hospital environments where these materials may receive exposure.

The effect of HINS-light on the prosthetic vascular grafts was assessed qualitatively via scanning electron microscopy. They show that HINS-light does not cause any visible damage to the fibres, such as strand breaks or fibre deformation. The general topography of the material is also unchanged by exposure. However, a lack of change to the appearance of the material does not necessarily indicate that the physical properties of the material will also remain unchanged. This has been shown to be the case with 25 kGy fast electron sterilisation of a polyester vascular prosthesis. Microscopic examination of the material did not reveal any visible damage to either the material or the copolymer coating, however, mechanical testing of the material before and after sterilisation showed a significant decrease in bursting strength following exposure (Niekraszewicz et al., 2010). This is not particularly surprising, given that it is known that, as with UHMWPE degradation by gamma radiation, the damage is at the molecular level. However, the images do confirm that exposure to HINS-light does not accelerate resorption of the gelatin coating on either sealed knitted or woven materials. Gelatin coverage does not noticeably differ in comparison to the control. The impregnated gelatin is designed such that it hydrolyses over a period of 14 days. The incomplete hydrolysis shown in images taken at three months post exposure is most likely due to the rinsing procedure used during sample preparation, allowing a degree of degradation of the gelatin sealant before the sample dried out.

These results also show that exposure to 5$mWcm^{-2}$ HINS-light for 1 hour does not increase the toxicity of the material itself. Human aortic smooth muscle cells,

cultured in medium containing extracts of the exposed material, did not show any signs of damage as assessed by NR assay. A decrease in cell viability was measured in cells cultured with extracts of both the HINS-light exposed and control gelatin sealed materials. There was a noticeable colour change in extract media of the gelatin sealed material compared to control media, indicating a change in pH of the cell culture medium. It is likely that the pH change has resulted in non-ideal conditions for the cells, leading to a decrease in cell viability. Alternatively, the gelatin sealing process involves the cross-linking of amino acids in the gelatin with both formaldehyde and glutaraldehyde, and it is possible that residues of these fixatives are responsible for the decrease in cell viability. This has been shown to be the case in the evaluation of a novel composite material intended for use as a bone substitute. The material combined tricalcium phosphate with formaldehyde cross-linked gelatin, and cytotoxicty of extracts of the material was assessed by Trypan Blue staining and counting of viable myoblast cells. The authors found a decrease in cell number caused by the extraction medium, and there was a correlation between the decrease in cell number and the concentration of formaldehyde used in the preparation of the material. Analysis of the extracts by gas chromatography confirmed that the extracts contained increasing amounts of uncross-linked formaldehyde with increasing initial concentration used in the preparation (Lin et al., 1998). However, another study using Vascutek supplied materials do not confirm the results found here. The toxicity of extracts of two knitted and one woven gelatin sealed PET prosthesis was tested on L929 mouse fibroblast cells. Supercritical fluid extraction with CO_2 was used, and the resultant extract diluted at a ratio of 1:1 with growth medium. Cells were incubated in the extract for 24 hr and the cytotoxic effect assessed via MTT assay. The results did not show a significant decrease in cell number for any of the three materials tested (Marois et al., 1996). Despite not recording a difference in cell number, direct contact assays did, however, suggest that one of the knitted materials was associated with cell death, with the appearance of rounded and lysed cells. They attributed this to uncontrolled topographical effects. The inconsistency between the extract assay results presented in this chapter and those of Marois and coworkers could possibly be attributed to the variation in the extraction method, or to the use of a less sensitive immortalised cell line relative to

the primary hASMC used in the results presented in this chapter. The MTT assay has also been shown to be not quite as sensitive as the NR uptake assay (Borenfreund et al., 1988), which may contribute to the discrepancies between the two studies.

Whatever the cause of the toxicity observed in the extract assay, it should be noted that it is present in extract medium from both the control material and the material exposed to 5 $mWcm^{-2}$ HINS-light for 1 hour prior to extraction. The cytotoxicity therefore, is not an effect of the HINS-light.

Mechanical testing of the materials helps to confirm that exposure to HINS-light does not damage the material or change its properties. The load/extension curves tell us about the strength and stiffness of the material, and are useful in determining the failure mode of the materials. Load and extension are directly related to stress and strain, and can be calculated from the dimensions of the sample material. Stress is defined as force per unit area, while strain is a measure of deformation of the material, calculated from the change in length of the sample. Comparison of the knitted materials before and after exposure to HINS-light show that the material deforms elastically until failure at around 200N load, by which point the sample has stretched by around 40 – 50 mm. There are no obvious changes in the profile of the curve caused by exposure to HINS-light. The woven fabrics are significantly stronger than the knitted material, requiring a load of around 350 N to cause failure. Woven fabrics have previously been shown to be stronger and more dilation resistant than knitted fabrics (Pourdeyhimi & Text, 1987; Van Damme et al., 2005). With this load, the materials had only extended by 10 – 15 mm. The profile of the curve suggests that after an initial elastic extension, the material yields with approximately 80 N load which is followed by plastic extension until failure. Again, the profiles of the load/extension curves are not affected by exposure of the material to HINS-light. Three months in storage conditions appear not to have affected the profiles of the load/extension curves for any of the materials.

Quantitative analysis of the results confirms that HINS-light exposure has not affected the mechanical properties of the materials. No significant change is seen in values of maximum load, stress and strain at maximum load, load at break, or stress and strain at break. The maximum load and load at break are different due to the elastic nature of the material and the definition of breaking point being a percentage of maximum load. Therefore, if the material fails by a gradual ripping and tearing process as is the case here, as opposed to a clean snap, the breaking load will be lower than the maximum load.

Examples of the effects of radiation on the physical properties of PET materials are available. It has been shown that exposure of PET fibres to gamma ray irradiation with a dose rate of 2.25 kGy/h at room temperature in air, decreases the tensile strength from 14.82 to 8.62 MPa and also decreases the elongation at break by 50% over non-irradiated samples (Haddad & Ebrahimi, 2006). The stress strain curves of UHMWPE material before and after irradiation were also compared by Haddad and Ebrahimi in the same publication. Stress strains curves between irradiated and control materials were visibly different, with irradiated materials displaying an increase in slope of the stress strain curve after material yield; an indication of near-ultimate hardening of the material. The effects of non-ionising radiation on PET fibres are also well known. Fashandi et al (2008) exposed two different yarns of PET fibre, differing in crystallinity and fibre orientation, to UV light from a xenon lamp with intensity of 140 W/m^2 over the 300 – 400 nm wavelength region. Exposure times varied from 75 to 300 hours. A 300 hr exposure gives a dose of 15.1 Jcm^{-2}, which although in a similar range to the dose applied in the HINS-light experiments, is applied over a much longer period at a greatly reduced intensity. The fibres were found to have a dose dependent response to exposure, and even the shortest exposure (75 hr) significantly decreased the tensile strength of the fibres. A 300 hr exposure reduced the strength of the materials from 35.5 to 16.7, and 18.8 to 6.1 cN/tex, a measure of breaking strength per fibre, where tex is a unit of measure for the linear mass density of fibres and is defined as the mass in grams per 1000 meters. Stress/strain curves show that after 300 hr exposure the extension at breaking point is significantly reduced for both yarns (Fashandi et al., 2008). The

effects are more pronounced in the less crystalline of the yarns, and this is attributed to the increased amount of oxygen available relative to the tightly packed highly crystalline yarn.

Photodegradation effects are most noticeable with UV wavelengths less than 355 nm (Holländer et al., 1996), and do not appear to be apparent following exposure to HINS-light. To understand why, it is useful to look at the mechanism of photodegradation of polymers. It is thought that photons of light are absorbed by impurities in the polymer, causing the creation of excited states which lead to scission through two pathways; Norrish type I and II reactions. In type I reactions, excited triplet states cleave the ester linkage of the polymer leading to the formation of radicals and termination of the polymer chain (Malanowski et al., 2009). Type II reactions involve intramolecular abstraction of a γ-hydrogen leading to pairs of saturated and unsaturated chain end groups. This leads to the production of volatile products such as COOH, CO and CO_2. (Day & Wiles, 1972; Hurley & Leggett, 2009; Rånby, 1989).

The energy of the striking photon must be equal to or higher than the chemical bond strength of the polymer for the photodegradation process to begin. The energy of a photon is given by the formula:

$$E = \frac{hc}{\lambda}$$

Where h is Planks constant, c is the photon speed, and λ is the wavelength. Therefore, the energy of the photon increases with decreasing wavelength. The energy of 300 nm UV photons is 399 kJ/mol, compared to 295 kJ/mol for 405 nm photons. The bond dissociation energies for C-C and C-H bonds are approximately 350 kJ/mol and 410 kJ/mol respectively (Cao & Yuan, 2003), therefore, it is easy to see why wavelengths of light in the visible region do not have the same effects as UV radiation (Suits & Hsuan, 2003).

The mechanical properties of the material are extremely important for long term patency of the implant. It has been shown that large variations in the material

response to loading between the graft and host artery can lead to intimal hyperplasia and failure of the graft (Salacinski et al., 2001). If HINS-light was to cause any variation to the mechanical properties of the graft material, its use during implant operations could be detrimental. Although the results show that there is no effect on tensile strength, other properties of the material are also important to the success of the material and testing to establish if HINS-light has any effect on these properties would be possible. As well as longitudinal strength, bursting strength or circumferential tensile strength could also be assessed, and the effect of HINS-light on the force required to pull a suture from the graft could be assessed. Porosity of the material, water permeability, leakage and water entry pressure would also all be valid tests of the effect of HINS-light on the material properties of the graft. However, these assessments are more aimed at the development of new materials. Given that HINS-light has had no effect on the physical properties assessed here, and that there has been no visible signs of accelerated degradation to the material via SEM, it would seem unnecessary to go through such an extensive range of tests.

The effect of HINS-light on other biomaterials would also need to be investigated. It has been shown that exposure of titanium prosthetics to UV radiation prior to implant can affect osseointegration of the implant (Ueno et al., 2010), and the surface chemical composition of cobalt chromium alloys has been shown to be altered by X-ray radiation (Marconnet et al., 2008). It did not prove possible to obtain samples of Co-Cr alloy prostheses materials from our industrial collaborators at the time of this investigation. However, the results presented in this chapter do not suggest that HINS-light, at the intensities that have been shown to be safe for mammalian tissue, could have a detrimental effect on the properties of polyester based biomaterials. The possibility that any damage may be caused to these vascular grafts by any exposure that may occur should HINS-light be utilised in the surgical theatre is very small.

Vascutek Ltd currently use ethylene oxide (EtO) to sterilise prosthetic vascular graft materials. EtO gas is an alkylating agent that disrupts the DNA of microorganisms and prevents them from reproducing. It is the most commonly used low temperature sterilisation method in use, due to its adequate bactericidal properties, high

penetration and compatibility with a wide range of materials (Mendes et al., 2007). However, if there is not a sufficient aeration period following sterilisation, EtO can produce toxic residues which can react with polymers in materials and give the material cytotoxic properties (Hastings et al., 1990). Could HINS-light be used in combination with existing sterilisation technologies, perhaps reducing the concentration of EtO required for complete sterilisation and so decreasing the risk of cytotoxic effects? In this situation the requirement for HINS-light to be non-harmful for human exposure would be lifted, allowing higher intensities and increased bactericidal activity. Further research would be required to establish that these higher intensities remained non-damaging to the material itself. However, the lack of penetration into materials would limit the potential bactericidal effects. The ability of HINS-light to inactivate various bacterial species, including on vascular graft material samples, is investigated in the following chapter.

Chapter 6

BACTERICIDAL EFFECTS OF HINS-LIGHT

6.1 Introduction

The previous chapters have investigated the effects of HINS-light on mammalian tissue and PET biomaterials, with a view to establishing a maximum safe dose that does not cause any undesirable effects on cell viability or material integrity. The aim of the experiments described in this chapter was to investigate what effect that maximum safe dose had on various strains of medically relevant bacteria. The effects of various exposure conditions were investigated, and the inactivation rates of bacteria on PET vascular graft materials were established.

6.1.2 Bacteria and infection

The bacteria used in this chapter are all medically relevant strains that are known to cause serious healthcare associated infection (HAI). *Staphylococcus epidermidis* is a Gram-positive, coagulase negative bacterium that is part of the normal human skin flora. As it is a potential pathogen that is commonly found on the skin and is easily transferred from person to person, it is a major cause of HAI (O'Gara & Humphreys, 2001). It is a common cause of wound infection (Bowler et al., 2001), and the main cause of infection associated with indwelling medical devices, such as the vascular implants investigated in the previous chapter (Broekhuizen et al., 2007). Part of the reason for their prevalence is their ability to form protective biofilms, which give the bacterial population increased protection from the host immune response and antibiotic treatment (Gotz, 2002; McCann et al., 2008; Rimondini et al., 2005).

Staphylococcus aureus, a Gram-positive bacterium, is also part of the natural flora and is carried in the nose and skin of approximately 20% of the population (Kluytmans et al., 1997), with evidence of ever increasing prevalence (Melville, 2011). *Staph. aureus* has been shown to be the most common bacterium responsible for orthopaedic implant infection (Khan et al., 2008), thought to account for around

22% of post operative infections in a study carried out on 165 patients who had received an orthopaedic implant which had subsequently required revision due to infection (Khosravi et al., 2009). The other bacteria species isolated from the infected tissues include *Pseudomonas aeruginosa* (16%), *E. coli* (15%), *Staph epidermidis* (9%) and *A. baumannii* (4%) amongst others. *Staph. aureus* is the most common cause of nosocomial infection. As with all infection, it is mostly found in patients who are immunocompromised in some way, which could be due to a physical break in the skin barrier, such as an open wound or indwelling catheter, or related to an underlying disease. Skin and soft tissue infections such as impetigo and cellulitis are the most common type of disease resulting from *Staph. aureus* infection, and they can normally be treated with topical antibiotics. Bacteraemia, endocarditis, osteomyelitis and pneumonia are more serious conditions that can develop if bacteria enter the bloodstream and spread to other organs, for which intravenous antibiotics may be required.

Antibiotic resistant strains of many bacteria are becoming problematic and this is thought to be due to the increased use of antibiotics in healthcare (Andersson & Hughes, 2011). Methicillin resistant *Staph. aureus* (MRSA) is the most well known of these. Within two years of the introduction of the antibiotic Methicillin in 1959, reports of resistant strains of *Staph. aureus* appeared (Jevons, 1961). With the continued use of antibiotics, it has become a common cause of HAI. The Scottish NHS carried out a prevalence survey in 2007 which found MRSA to be present in 17.2% of all HAI diagnosed in inpatients at acute hospitals (Reilly et al., 2007). It was second in incidence to *Clostridium difficile*. As with non-resistant strains, MRSA can be carried in the nose and skin of healthy people without any adverse effects on their health. MRSA infection is harder to treat due to its resistance to conventional antibiotics, and there is a constant battle to produce more effective antibiotics before further resistant strains of the bacteria emerge.

Pseudomonas aeruginosa is a Gram-negative rod shaped bacterium that is also a part of normal skin flora (Cogen et al., 2008). It is a relatively harmless bacterium, and as such serious infection is relatively rare, however, it is a frequent cause of infection

in immunocompromised patients (Japoni et al., 2009). Burn patients are particularly susceptible to *P. aeruginosa* infection, where extensive breaks in the skin barrier and the frequency of the bacteria in the hospital environment mean that over 50% of infected burns are found to be colonised by *Pseudomonas* (Al-Akayleh, 1999). A study on the source of infection found colonies to exist around sinks, on floors, on bed frames and on nurses hands (Chitkara & Feierabend, 1981). It is a very hardy bacterium due to its flexible metabolic requirements and innate resistance to harsh environmental conditions and so can establish itself on a wide variety of surfaces where it can exist for up to 16 months (Kramer et al., 2006). This means that it is also commonly associated with device-related infections, where transmission has occurred through contamination of a device surface.

Acinetobacter are Gram-negative rods found in soil, water and food. There are 33 different groups, of which *Acinetobacter baumannii* is the species most commonly associated with human disease. It is not commonly found in the skin flora of healthy humans (Karageorgopoulos & Falagas, 2008), although occasional and short duration colonisations have been found in moist areas such as hairline, groin and between the toes (Chu et al., 1999). It is problematic in the healthcare environment because it is capable of rapidly acquiring resistance to antibiotics. Significant increases in the prevalence of multi-drug resistant *A. baumannii* have been reported (Manchanda et al., 2010). Similarly to *P. aeruginosa*, it is also a very persistent bacterium that is able to exist for extended periods in non-ideal environments, with reports of bacteria surviving for up to 5 months on dry inanimate objects (Kramer et al., 2006). Outbreaks of infection occur with increasing frequency, with critically ill and trauma related patients most at risk of serious infection (El Shafie et al., 2004; Sebeny et al., 2008). Risk factors of infection include, but are not limited to; prolonged support by mechanical respiration, prolonged hospital stay, increased numbers of surgical interventions, and exposure to infected or colonised patients and staff (Simor et al., 2002). Pneumonia, bacteraemia, urinary tract infection, bone infection, secondary meningitis and soft tissue infection have all been associated with *A. baumannii*.

Escherichia coli is a Gram-negative rod shaped bacterium that is found as part of the normal gut flora, where along with many other bacterial species it has metabolic functions, fermenting indigestible residues, and providing protection for the host against exogenous microbes (Guarner & Malagelada, 2003). Contamination from *E. coli* is often caused by faecal-oral transmission and results in non-serious gastroenteritis. Contamination is often due to consumption of under cooked meat, drinking contaminated water supplies, poor hygiene and contamination of food during preparation (Ayçiçek et al., 2004). Pathogenic strains of *E. coli*, including O157:H7 which was responsible for the 1996 outbreak in central Scotland, are responsible for a number of deaths each year in the UK. The recent outbreak in Germany of a new strain of *E. coli* has so far resulted in 46 deaths worldwide (Shiga toxin-producing *E. coli* (STEC): Update on outbreak in the EU (27 July 2011, 11:00) from the European Centre for Disease Prevention and Control).

Environmental contamination is an important source of many of these bacterial infections. A study on the effectiveness of cleaning methods in a Glasgow hospital revealed surface colony counts of up to 33.8 CFU/cm^2 in ward areas (Dancer et al., 2009), and airborne contaminants in hospital wards have been shown to be as high as 254 CFU/m^3 (Hedin et al., 2010). Even operating theatres with full laminar flow ventilation have been shown to have measurable concentrations of airborne contaminants (Owers et al., 2004; Whyte et al., 1982). The ability of the bacteria to survive for extended periods on inanimate objects allows easy transmission and contamination throughout the hospital environment (Boyce, 2007). Any breakdown in infection control measures can lead to outbreaks resulting in closure of wards for extended periods. Current infection control procedures involve identification, isolation and appropriate treatment of the source, strict adherence to infection control guidelines on personal protective equipment and hand hygiene, and deep cleaning of the infected areas (Dancer, 2009; Karageorgopoulos & Falagas, 2008; Towner, 2009; Wenzel & Edmond, 1998).

Airborne contamination is thought to be the main cause of medical-device related infection (Gosden et al., 1998; Lidwell et al., 1983). The disastrous consequences of implant infection have been described in previous chapters. First line treatment of device-related infection is usually antibiotics, however, either due to the protective properties of biofilm formation or antibiotic resistance this is often unsuccessful. Removal of the device followed by aggressive debridement of infected tissue is often the only viable treatment method. Once the infected device is removed, antibiotic-loaded cement spacers may be inserted into the void, which in conjunction with antibiotics is used to remove any remaining traces of infection before a fresh implant is fitted (Hsieh et al., 2009). As well as the obvious risk and inconvenience to the patient, revision surgery is associated with a large cost increase to the NHS. Risk of repeat infection is also increased following revision surgery (Peersman et al., 2001).

With the known bactericidal properties of HINS-light, it could provide a potential method of reducing infection rates, through the inactivation of airborne bacteria and bacteria that land on the implant surface during surgery. It could also potentially be used to reduce levels of bacteria in ward areas, reducing the chance of infections spreading from patient to patient. The previous chapters have shown that a suitable combination of intensity and duration of HINS-light exposure can be achieved that is not harmful to mammalian tissue or certain biomaterials, which is an obvious requirement of any disinfection procedure used in areas where people will be present. To that end, the bactericidal properties of HINS-light at this safe limit were tested on the bacteria described here. The bactericidal efficiency was tested on bacteria suspended in solution and spread on various surfaces. Finally, bacteria exposed to HINS-light were examined by scanning electron microscopy to establish if HINS-light had any visible effects on bacteria, thereby possibly helping to elucidate the mechanism by which the bactericidal effect occurs.

6.2 Methods

6.2.1Bacterial inactivation experiments

The bacterial strains listed in section 2.3.1 were exposed to HINS-light with an intensity of 5 $mWcm^{-2}$ for 1 hour. The bacteria were exposed in two ways:

PBS suspension: The bacteria were prepared as described in section 2.3, and serially diluted to a population density of 10^3 CFU/ml. 1 ml of the bacterial suspension was pippetted into the central 4 wells of a 24 well plate which was exposed to HINS-light. The multiwell plate lid was removed for the duration of the exposure. Control samples were plated in an identical manner but shielded from HINS-light exposure. Following the hour of exposure, the remaining bacterial suspension was plated onto tryptone soya agar (TSA) plates, prepared as described in 2.3.4. The volume of bacterial suspension plated varied depending on the expected remaining population size, such that the number of colony forming units per plate did not exceed 100. This allowed more accurate bacterial enumeration. Plating methods used are described in section 2.3.5.

Surface exposure: The bacteria were prepared as above, but the bacterial suspension was plated onto agar plates prior to exposure. 100µl of bacterial suspension (approximately 100 CFU) was manually spread onto the agar surface. The suspension was allowed to dry into the agar surface for 15 min before the plates were exposed to HINS-light.

Following exposure, plates were incubated for 24 hr at 37 °C. Bacteria were enumerated as described in section 2.3.5.

6.2.2 Bacterial inactivation on PET materials

6.2.2.1 Material preparation

For exposure on PET biomaterial surface *Staphylococcus epidermidis* bacteria were prepared as described in section 2.3. Prior to use, the materials were cut into 2 cm^2 segments and sterilised in 80% EtOH for 15 min. Materials were then rinsed three times in dH_2O. 100 µl of bacteria suspension at 10^3 CFU/ml was pipetted onto the surface of the material, spread with an L-shaped spreader and allowed to soak into the material. The squares of material were exposed to HINS-light for 1 hour at 5 $mWcm^{-2}$.

6.2.2.2 Bacterial recovery from materials

Three methods of recovering any remaining viable bacteria from the material following exposure were trialled:

Contact plating: Squares of material were pressed onto a tryptone soya agar plate and removed. Plates were incubated for 24 hr at 37°C. Colony forming units were counted as described in 2.3.5.

Overlay: Following exposure in the centre of a 90mm Petri dish, TSA containing triphenyl tetrazolium chloride (TTC) was poured on top of the material. Plates were incubated for 24 hr at 37°C. Colonies are stained red by the TTC component of the agar (figure 6.1).

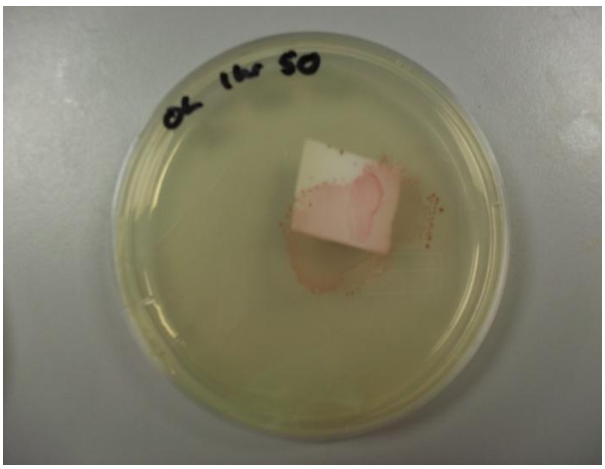

FIGURE 6.1 *Overlay method of bacterial enumeration on materials.*

Stomaching: Following exposure, squares of material were placed in stomaching bags containing 50 ml PBS. Bags were agitated in a MIX2 blender (DW Scientific, UK) for 1, 3 or 5 min and the resulting bacterial suspension passed through 0.45 µm membrane filter (Whatman, UK) by suction pump. The filter was then pressed onto a tryptone soya agar plate and incubated for 24 hr before enumeration, aided by a grid pattern printed on the membrane (Figure 6.2).

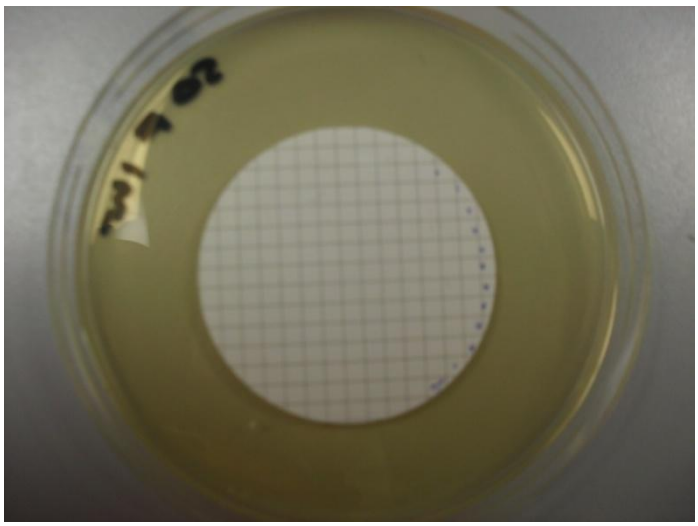

FIGURE 6.2 *Whatman membrane on TSA agar plate.*

The overlay and contact plating method proved ineffective for enumeration of remaining bacteria. Colonies merged together to give confluent growth so that individual colonies were not identifiable, thus it was not possible to quantify remaining populations. Stomaching of the material sample in PBS and filtering onto membrane provided distinct colony forming units that were easy to count, therefore this method was selected for use during inactivation experiments.

Table 6.1 shows the effect of stomaching time on bacterial recovery from non-gelatin sealed, knitted polyester relative to the same number of CFU plated directly on TSA plates as described in 2.3.5.1. Bacteria were left on the material for 1 hr before stomaching. As no significant differences were found between stomaching times, 3 min was used in all experiments.

TABLE 6.1 *Effect of stomaching time on bacteria recovery from non-gelatin sealed knitted polyester material. Results are mean % control ± SEM (n=3)*

Stomaching Time	Bacterial Recovery
1 min	90 ± 4%
3 min	86 ± 14%
5 min	81 ± 7%

Effect of gelatin sealing of the material on bacteria recovery was assessed in the same way and is presented in table 6.2. Comparisons were made immediately after allowing the bacteria to dry into the sample, and at 1 hr following that, to establish if bacteria adherence to the material increased over the duration of the experiments. No significant differences were observed between the types of material.

TABLE 6.2 *Effect of gelatin sealing and time on recovery of bacteria from materials. Results are mean % control ± SEM (n = 5).*

Material	0 min	60 min
Knitted PET	91 ± 5 %	113 ± 35 %
Gelatin-sealed knitted PET	109 ± 17 %	83 ± 12 %

6.2.3 SEM

SEM of HINS-light exposed *S. epidermidis* was performed at the Integrated Microscopy Unit at Glasgow University, with thanks to Dr Laurence Tetley and Mrs Margaret Mullin for their assistance. Bacteria were exposed to HINS-light in 1ml PBS suspension, in the central 4 wells of 96 well plates. Following exposure the bacterial suspension was collected and 3 ml centrifuged at 5030g for 5 min in two 1.5 ml eppendorf tubes. The supernatant was discarded and the pelleted bacteria resuspended in 1.5 ml 2.5% glutaraldehyde in 0.1M PO_4 buffer rinse solution for 45 min. After 45 min the suspension was centrifuged again at 5030g for 5 min, and resuspended in 0.1M PO_4 buffer with 2% sucrose. Samples were stored at 4°C overnight in this suspension and transported to Glasgow University immediately the following morning.

At Glasgow University the suspension was again centrifuged, resuspended and pipetted onto 10 mm poly-l-lysine coated coverslips. The coverslips were then prepared for microscopy as described for osteoblast cell culture in section 4.2.4.

To ensure sufficient bacteria numbers to visualise the bacteria, the bacterial density prior to HINS-light exposure had to be increased to 10^9 CFU/ml. To achieve similar bacterial inactivation rates as for 1 hr, 5 $mWcm^{-2}$ HINS-light exposure of 10^3 CFU/ml, the HINS-light intensity was increased to 15 $mWcm^{-2}$ for 3 hours (162 J/cm^{-2}). Bacterial kill achieved by exposure to 3 hr of 15 $mWcm^{-2}$ HINS-light was 99.9 ± 0.02 % (n=4).

6.3 Results

6.3.1 Inactivation of bacteria in PBS suspension

Table 6.3 shows the inactivation rates of various strains of bacteria following exposure in PBS suspension to 1 hr of 5 $mWcm^{-2}$ intensity HINS-light. *Staph. epidermidis* was found to be most susceptible, followed by *Staph. aureus*, methicillin resistant *Staph. aureus* and *P. aeruginosa*, for which significant reductions in bacterial populations were achieved. No statistically significant decrease was observed in populations of *A. baumannii* or *E. coli*.

TABLE 6.3 *Bacterial inactivation in PBS suspension, plated on TSA agar (n=3). * indicates significant difference from population of unexposed bacteria ($P < 0.05$).*

Bacterium	% kill (± SEM)
S. epidermidis	**99.0 (± 0.2) ***
S. aureus	**54.1 (± 14.5) ***
MRSA	**47.8 (± 14.6) ***
P. aeruginosa	**18.6 (± 3.1) ***
A. baumannii	**12.3 (± 2.3)**
E. coli	**3.9 (± 2.2)**

6.3.2 Inactivation of bacteria on agar surfaces

Table 6.4 shows inactivation rates of the same bacteria following exposure to 1 hr of 5 $mWcm^{-2}$ HINS-light on two different types of agar surface. Inactivation rates of bacteria exposed to HINS-light on TSA were generally reduced relative to exposure in PBS suspension. Significant reduction in bacterial populations were only achieved for *S. aureus* and *A. baumannii*. Inactivation rates on bacteriological agar were increased relative to exposure on TSA. MRSA and *P. aeruginosa* population suffered significant reductions in population

TABLE 6.4 *Inactivation of bacteria spread on tryptone soya agar (TSA) and bacteriological agar (BA) surface prior to HINS-light exposure (n=4). * indicates significant difference from population of unexposed bacteria (P < 0.05).*

Bacterium	**TSA (% kill ± SEM)**	**BA (% kill ± SEM)**
S. epidermidis	**7.9 (± 10.1)**	**40.0 (± 22.2)**
S. aureus	**20.6 (± 5.5) ***	**21.6 (± 3.2)**
MRSA	**17.8 (± 10.3)**	**82.8 (± 14.9) ***
P. aeruginosa	**8.7 (± 6.5)**	**76.2 (± 13.4) ***
A. baumannii	**19.0 (± 1.6) ***	**27.0 (± 8.0)**
E. coli	**1.5 (± 4.3)**	**1.7 (± 14.3)**

6.3.3 Inactivation of bacteria on PET biomaterials

Table 6.5 shows the inactivation of *Staph. epidermidis* on the four materials after a 1 hr exposure to 5 $mWcm^{-2}$ HINS-light. Results are % kill relative to unexposed controls that have undergone the same bacterial recovery and enumeration method as exposed samples. Inactivation rates are decreased relative to exposure in PBS suspension. The different materials do not appear to affect inactivation rates.

TABLE 6.5 *Inactivation of Staph. epidermidis on vascular biomaterials by 1 hr exposure to 5 mWcm^{-2} HINS-light.*

Material	% kill ± SEM	N
Knitted PET	63 ± 11	6
Gelatin-sealed knitted PET	66 ± 18	3
Woven PET	53 ± 4	3
Gelatin sealed woven PET	62 ± 7	3

6.3.4 SEM of HINS-light exposed bacteria

Figures 6.3(A & B) show control *Staph epidermidis* bacteria, while (C & D) show bacteria that have been exposed to 15 mWcm^{-2} HINS-light for 3 hours. Despite this dose causing almost complete inactivation, there is no obvious sign of damage to the bacteria when viewed by SEM. Bacteria remain round and form the grape-like clusters associated with *Staphylococcus* species.

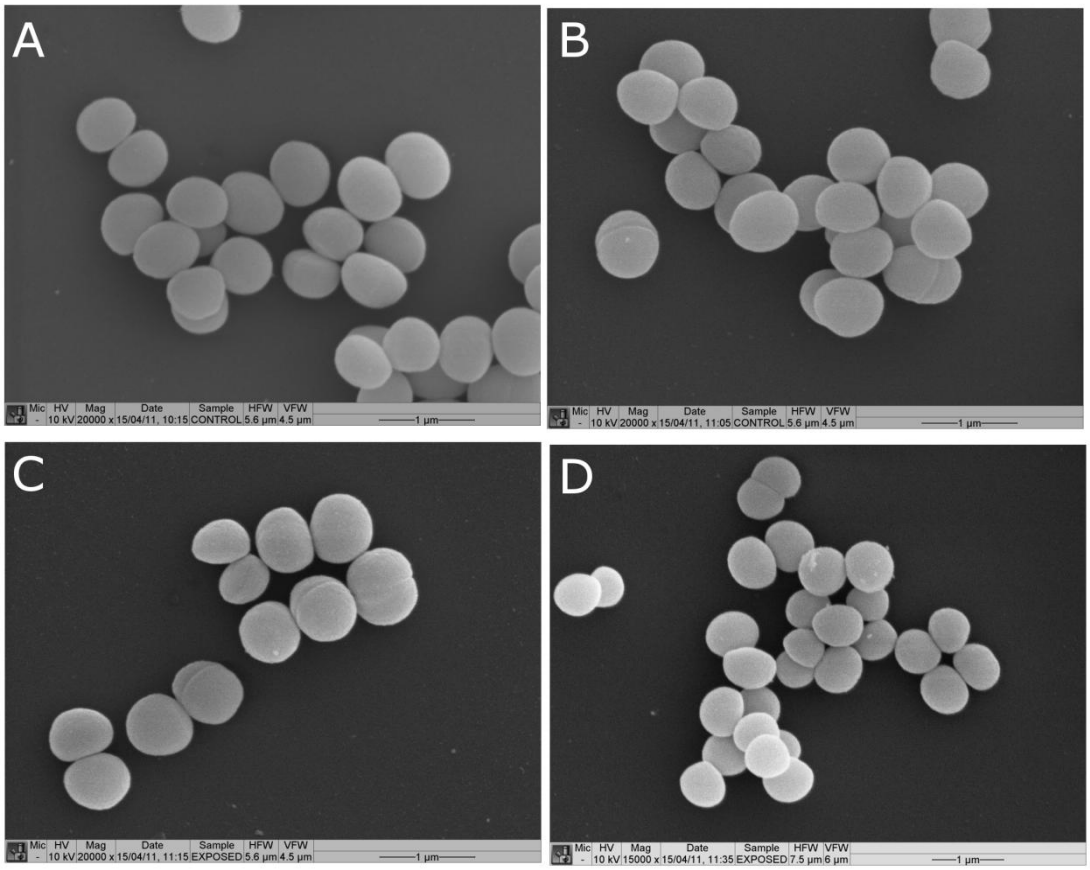

FIGURE 6.3 *SEM images of Staph. epidermidis exposed to 15 mWcm^{-2} HINS-light for 3 hours (C and D). Images A and B show control samples. Scale bars are 1µm.*

6.4 Discussion

The results in this chapter show that exposure of various strains of medically relevant bacteria to 5 mWcm^{-2} HINS-light for 1 hour causes a significant decrease in bacterial viability. This intensity and duration of HINS-light has been shown to not cause significant harm to mammalian cells or vascular prostheses biomaterials (sections 3.3, 4.3 and 5.3). HINS-light was also shown to effectively reduce the number of viable bacteria on infected PET biomaterials.

Staph. epidermidis was shown to be the most susceptible of the bacterial strains to HINS-light inactivation when exposed in PBS, with kill rates as high as 99%. The order of susceptibility to HINS-light induced inactivation in PBS suspension was

found to be: *S. epidermidis* > *S. aureus* > MRSA > *P. aeruginosa* > *A. baumannii* > *E. coli* as shown on table 6.3. The Gram positive bacteria, *S. epidermidis, S. aureus* and MRSA were more susceptible than the Gram negative bacteria tested. This confirms the findings of Maclean and co-workers, who, using a similar 405nm light setup as that described in this chapter, found that Gram-negative bacteria required a much larger dose of irradiation to achieve a similar level of inactivation as achieved with Gram-positive varieties. In the study by Maclean et al., 2009, *Staph. aureus* was found to be most susceptible, closely followed by MRSA and *Staph epidermidis*, which required a dose of 42 Jcm^{-2} to cause a 4.6 log_{10} reduction in the population. *E. coli* required a dose of 180 Jcm^{-2} to achieve a 3.1 log_{10} reduction. This increased resistance of Gram-negative bacteria to photoinactivation has also been reported following exposure of various Gram-negative bacteria to 407-420nm blue light (Nitzan et al., 2004).

The major difference between Gram-positive and negative bacteria is found in the membrane; Gram-positive bacteria possess a thick, porous peptidoglycan layer surrounding a cytoplasmic membrane, whereas the peptidoglycan layer of Gram-negative bacteria is thinner but is covered by an outer lipopolysaccharide membrane consisting of lipid A, core polysaccharide and O antigen. Gram-negative bacteria are generally more resistant to antiseptics and disinfectants, and it is thought that this is due to the greater protection offered by the outer membrane which acts as a barrier to limit the uptake of various antimicrobials (McDonnell & Russell, 1999). It has also been shown that Gram-negative bacteria can be less susceptible to photoinactivation than Gram-positive bacteria as the outer membrane acts as a barrier to certain photosensitisers, limiting uptake and reducing effectiveness of the applied light dose (Upadya & Kishen, 2009). The inactivation caused by HINS-light, however, does not require uptake of exogenous photosensitisers, and therefore this aspect of Gram-negative bacteria does not explain the reduced inactivation of Gram-negative bacteria as seen in these results. The findings of Skorb and coworkers do suggest that membrane differences may also be responsible for differences in non-sensitised photoinactivation of Gram-negative and positive bacteria. Exposure of *L. lactis* (Gram-positive) and *P. fluorescens* (Gram-negative) to 15 $mWcm^{-2}$ 310-400nm light

produced significantly different inactivation rates, attributed to variations in wall thickness and resistance to damage by ROS (Skorb et al., 2008).

Another possible explanation for the variation in efficiency of HINS-light induced bactericidal activity is variation in porphyrin production of the bacteria. It is known that different bacteria produce different levels and different types of porphyrin. Nitzan and co workers (2004) identified the porphyrins produced by a number of Gram-positive and –negative bacteria via HPLC analysis following incubation with δ-ALA. The photosensitiser δ-ALA is a naturally occurring metabolite produced during heme synthesis and acts to increase synthesis of the various porphyrins. They showed that Gram-positive *Staphylococcus* species such as *Staph. epidermidis* and *Staph. aureus* produced six times as much coporphyrin as the Gram-negative bacteria. Coporphyrin levels were significantly higher than the other porphyrin types in the Gram-positive *Staphylococcus* bacteria. Gram-negative bacteria did not produce a predominant porphyrin, with protoporphyrin, uroporphyrin, coporphyrin, 5- and 7- carboxy porphyrins all being present. Attempting to inactivate the bacteria with 407-420 nm blue light only proved successful for *Staph. aureus* and *Staph. epidermidis* bacteria, and it was concluded that this was due to the high level of coporhyrin present in these bacteria. They suggest that Gram-negative bacteria may not be inactivated so easily because the various porphyrins present in these bacteria exist in an aggregated state, which is known to alter the absorption profile of the porphyrins, or that the ROS radicals produced in Gram-negative bacteria are less efficient in attacking the essential molecules of the bacteria allowing it to survive (Ramberg et al., 2004). An alternative theory is that the various porphyrins have slightly different maximum absorption wavelengths, and that the very narrow band of the HINS-light setup used in the experiments described in this chapter only excites the coporphyrin compounds (Oliver & Rawlinson, 1955). HINS-light at the intensity and duration of exposure used in these experiments was found to have almost no effect at all on *E. coli* bacteria. This is consistent with the findings of Maclean and co-workers (2009), and also Murdoch and co-workers, who found *E. coli* required a dose of 288 Jcm^{-2} to obtain a 5 $\log_{10}$ reduction in CFU/ml (Murdoch et al., 2011). *E. coli* has been found to produce undetectable concentrations of most porphyrins, with

only protoporhyrin present at a trace value of less than 0.1 µmol/l (Kwon et al., 2003).

The difference in inactivation rates between the Gram-positive and –negative bacteria is less pronounced when exposing the bacteria on TSA surfaces, and in general are considerably lower than inactivation rates in PBS suspension. TSA is a relatively nutritious agar, and it is possible that access to nutrients during exposure may lessen the effect of HINS-light induced inactivation. To investigate this, inactivation was also attempted on bacteriological agar, a much less nutritious agar that has very low mineral levels. Therefore, if access to nutrients was responsible for the decrease in inactivation rates, exposure on bacteriological agar should be increased to similar levels as inactivation in PBS. This was seen to be the case for *Staph. epidermidis*, MRSA, *P. aeruginosa* and *A. baumannii*. No significant change was observed for *Staph. aureus* or *E coli*.

For HINS-light to be useful for maintaining sterility in device implant operations, high bacterial inactivation would be required on a variety of surfaces. The open wound would be a very nutritious area for any bacteria that fell upon it, particularly Gram-positive *staphylococci* that are known to be a common cause of wound infection (Cokebrook et al., 1960). The inactivation of bacteria in environments that more closely replicate the wound bed needs to be investigated. Lambrechts and co-workers have shown that the introduction of human blood plasma and human serum albumin reduces the sensitivity of a range of bacteria to photodynamic inactivation (PDI) with exogenous photosensitisers (Lambrechts et al., 2005b). Spesia and co-workers experienced a similar reduction in effectiveness of PDI when exposing *E. coli* in the presence of blood plasma (Spesia et al., 2010). These decreases could be attributed to a combination of the binding of exogenous porphyrins to albumin prior to absorption by the cell (Moan et al., 1985), and the ROS scavenging properties of albumin (Iglesias et al., 1999). The effect of protein absorption on bacterial inactivation by HINS-light is yet to be established.

Another potential complication is that of inactivation in the presence of mammalian cells. Smith (2009) found that exposing *S. epidermidis* to 10 $mWcm^{-2}$ HINS-light for 150 min caused a 99.9% decrease in bacteria population size. This intensity and duration of exposure was also shown to cause a 42% decrease in mammalian cell viability. Co-culture experiments were performed which involved exposing bacteria in a suspension which was on top of a monolayer of fibroblast cells. Following exposure the bacterial suspension was removed and enumerated in the usual way as described in this chapter, and the viability of fibroblasts assessed by MTT assay, similar to the method described in chapter 2 of this thesis. The results showed that exposure in the presence of mammalian cells reduced the inactivation rate of *S. epidermidis* to between 2 – 8%. Furthermore, the viability of the fibroblasts was reduced to 9 – 18% when exposed in the presence of bacteria (Smith, 2009). This was attributed to some unidentified factor that was released as a stress response by the mammalian cells, either due to oxidative stress caused by HINS-light exposure or due to the co-culture with bacteria. It seemed that the bacteria could utilise this factor to aid their survival, possibly through accelerated growth. Although it was thought that this effect could have been exaggerated due to the high numbers of bacteria relative to mammalian cells, this effect would require further investigation before HINS-light could be used in environments where bacteria and mammalian cells would be present together. The use of animal models could prove useful here. Zolfaghari and co-workers have demonstrated light-induced (665nm diode laser) significant 1.4 $\log_{10}$ CFU/wound inactivation of photosensitised MRSA that had been seeded onto open wounds in a mouse model (Zolfaghari et al., 2009). No necrotic effects were observed on the wound tissue. Similar results have been observed in infected burn models in mice, again using a photosensitiser and red laser exposure (Lambrechts et al., 2005a; Orenstein et al., 1997). As yet, no published studies have been performed on the bactericidal effects of high-intensity blue light in infected animal models. All in vivo studies have, however, reported significantly less inactivation that in vitro experiments using the same combinations of photosensitisers and light dose.

Photoinactivation of *Staph. epidermidis* on the various PET vascular prosthetic materials was found to be decreased relative to inactivation rates in PBS suspension. The most likely cause of this is that as the bacteria are absorbed into the material, the fibres of the material offer some protection from direct exposure to the HINS-light. Blue light does not have sufficient energy to penetrate through the material, so any bacteria that are not on the surface shall not receive the full dose of HINS-light. However, inactivation rates of around 60% were still achieved. An investigation into the inactivation of bacteria on other common implant materials would be useful to establish the full potential of HINS-light.

A possible criticism of these experiments is that the starting bacterial population is not sufficient to prove the inactivating properties of HINS-light. It is true that in sterilisation experiments starting populations are often as high 10^9 CFU/ml, and that bacterial counts greater than 10^5 CFU/ml are thought to be associated with an increased incidence of infection and inhibited wound healing (Bendy et al., 1964; Landis, 2008). However, the experiments in this chapter were designed to establish what effect HINS-light may have if it was used in hospital environments. These areas are cleaned regularly, and bacterial populations do not reach these high levels. Airborne contamination densities of hospital wards have been shown to be around 50 CFU/m^3, with *Staph epidermidis*, *Staph. aureus* and *E. coli* being the most commonly found contaminants (Ekhaise et al., 2008). Similar bacterial densities in air were found in wards in the University Hospital of Rennes, France (Gangneux et al., 2006). Contamination levels in hospitals in Sagar City, India were found to be an order of magnitude higher, at around $6x10^2$ CFU/m^3 (Bhatia & Vishwakarma, 2010). Contact plating of surfaces in isolation rooms of the Burns Unit at Glasgow Royal Infirmary gave total bacterial counts of 3.5 CFU/cm^2 (Maclean et al., 2010). Therefore, the starting population of 10^3 CFU/ml that was used in the experiments described in this chapter are considerably higher than the levels of bacteria that would be found in hospital environments. Coincidentally, a recent study by Reinis and co-workers found 10^3 CFU/ml to be the minimal infective dose of *S. epidermidis* on biomaterials implanted into rabbits (Reinis et al., 2010).

The SEM images do little to elucidate the mechanism of HINS-light induced inactivation. With bacterial killing thought to be caused by ROS damage to the bacterial membrane, it was hoped that SEM images may show signs of this damage. Various sterilisation technologies have been shown to visibly damage bacteria; pulsed electric field for example causes obvious disruption and rupturing of *E. coli* bacteria membranes (Dutreux et al., 2000), and visible-light induced inactivation of *E. coli* on palladium oxide and nitrogen-doped titanium oxide surfaces show obvious pits and holes on the bacteria surface (Wu et al., 2009). With a 99.9% inactivation rate, it is surprising that there are any healthy bacteria present at all, but there did not appear to be a significant change in bacteria density between the control and exposed samples. It is possible that with the bacteria being fixed in glutaraldehyde immediately following exposure that they have been fixed before any damage had the chance to occur.

6.5 Summary

HINS-light has been shown to have considerable bactericidal properties. Significant kill of three types of Gram-positive bacteria has been demonstrated, with lesser effects on the Gram-negative bacteria investigated, particularly *E. coli*. However, the Gram-positive *staphylococci* for which high levels of bacterial kill were achieved are one of the most common causes of hospital acquired infection, and therefore HINS-light could still prove a useful tool to decrease the risk of infection. HINS-light has also been shown to significantly decrease the numbers of bacteria on infected vascular implant material. With contamination of the material during implant thought to be the main cause of implant infection (Kuehn et al., 2010), and *Staph. epidermidis* being the most common bacteria found to be responsible for graft contamination (Zetrenne et al., 2007), HINS-light also has the potential to significantly reduce the incidence of infection during vascular graft surgery. Further work on the interaction between bacteria and mammalian tissue, and the effect that has on photoinactivation are required to establish the full potential that HINS-light has as a tool for reducing the risk of infection in hospital environments.

Chapter 7

SUMMARY AND FUTURE WORK

The aim of this study has been to establish if a safe level of exposure to HINS-light exists whereby no discernible detrimental effects to mammalian cells occur. The effect of this safe level on various common bacteria was established to investigate potential applications of HINS-light in the hospital environment.

7.1 Chapter summaries

7.1.1 HINS-light and fibroblast cells

This section of the work set out to determine whether HINS-light could be used to decontaminate the environment around open wounds without influencing the rate of wound healing. To this end, the effect of a range of intensities of HINS-light on fibroblast function and viability were assessed. Fibroblasts are responsible for wound healing, where their contractile activity draws the edges of wounds together to close the wound. Wound healing is a complex process, and increased numbers of bacteria in the wound can significantly inhibit wound closure (Edwards & Harding, 2004). Open wounds are a break in the skin natural defences against infection, and provide a location for airborne or carried bacteria in the hospital to gain access and establish colonies, resulting in HAI.

The effect of HINS-light on fibroblast function was assessed with the use of a fibroblast populated collagen lattice (FPCL). This is an accepted *in vitro* model of wound healing (Ehrlich et al., 2006). Fibroblasts were seeded on the surface of a collagen gel and exposed to HINS-light for 1 hour at a range of intensities. HINS-light was found to have an intensity dependent effect on fibroblast function. Intensities below 5 $mWcm^{-2}$, applied over an hour to provide a dose of 18 Jcm^{-2}, were found to cause no significant inhibition of fibroblast contractile activity. Intensities above 5 $mWcm^{-2}$ caused a significant delay in FPCL contraction, with the

highest intensities (15 $mWcm^{-2}$, providing a dose of 50 Jcm^{-2}) completely halting contraction.

The inhibition of FPCL contraction was found to correlate with the inhibition of α-SMA protein expression, a marker of fibroblast contractile activity. There was no observable decrease in intracellular α-SMA content in fibroblasts exposed to HINS-light intensities at or below 1.8 $mWcm^{-2}$ for 1 hour, while a significant decrease in α-SMA expression was observed in cells exposed to 15 $mWcm^{-2}$ intensities.

The metabolic activity of HINS-light exposed cells, assessed via the MTT assay, was altered in parallel with the α-SMA results. Fibroblasts exposed to 1.8 $mWcm^{-2}$ or less for 1 hour did not show a decrease in MTT reduction relative to unexposed controls, implying that there was no decrease in viable cell counts or in metabolic activity of the cells, while fibroblasts exposed to 15 $mWcm^{-2}$ light for 1 hour were shown to suffer a significant decrease in metabolic activity. This could have been associated with both a decrease in the total number of viable cells or in their metabolic activity. Microscopic examination of cells stained with propidium iodide and acridine orange provided visual confirmation that the highest intensity of HINS-light did cause a reduction in viable cell number, with a smaller proportion of cells displaying the elongated morphology of healthy fibroblasts.

The effects of HINS-light were not found to be caused by blue-light induced inhibition of prostaglandin E2 production, as has been shown to be the case for gamma radiation induced inhibition of fibroblast function (Carnevali et al., 2003).

7.1.2 Effect of HINS-light on osteoblast cells

The effect of HINS-light on osteoblast cells was investigated because infection acquired during joint replacement surgery is a relatively common, serious and expensive complication of arthroplasty procedures. HINS-light could be employed during arthroplasty surgery to reduce airborne and surface bacteria near the surgical site. This would result in exposure of bone tissue to HINS-light, with unknown effects.

Alkaline phosphatase (ALP) is an established marker of the ability of osteoblasts to synthesise bone. Osteoblasts were exposed to a range of HINS-light intensities from 1.8 to 15 $mWcm^{-2}$ for 1 hour, with ALP expression measured at 24 hours following exposure. A significant decrease in ALP expression occurred at intensities above 5 $mWcm^{-2}$, and this was still the case at 72 hours following exposure.

The elastic property of bone is largely attributable to collagen, therefore, the ability of osteoblasts to synthesise collagen following exposure to 1.8, 5 and 15 $mWcm^{-2}$ intensities of HINS-light for 1 hour was assessed. At 24 hours following exposure, only cells exposed to 15 $mWcm^{-2}$ showed a significant decrease in collagen levels. This decrease remained in place at 72 hours post exposure, while cells exposed to 5 $mWcm^{-2}$ and below did not differ significantly from unexposed controls.

Expression of osteocalcin was also shown to be inhibited by exposure to 15 $mWcm^{-2}$ HINS-light. At 3 and 6 days post exposure, there was a significant decrease in expression. However, by day 10 following exposure osteoblasts appeared to recover and osteocalcin expression was on a par with unexposed controls. Exposure to 1.8 and 5 $mWcm^{-2}$ HINS-light did not cause any deviation from control levels at any time point.

The Lowry protein content assay was used to quantify the number of viable cells following exposure. The results suggest that exposure to 15 $mWcm^{-2}$ HINS-light caused a sustained reduction in the number of viable cells, up to four days following exposure. However, this decrease in cell number was not statistically significant. No significant variation in cell number relative to unexposed control cells was measured in cells exposed to 0.5 or 1.8 $mWcm^{-2}$ HINS-light.

SEM of cell samples confirmed that there was a decrease in cell number, with a significantly higher proportion of apoptotic cells in samples exposed to 15 $mWcm^{-2}$ HINS-light. These cells appeared to not be attached to the surface as well as controls, and displayed a more spherical appearance and evidence of membrane blebbing. Exposure to the highest intensity of HINS-light also appeared to cause

some kind of disturbance to the membrane, with evidence of folds or nicks which were not present on control cells or on cells exposed to 5 $mWcm^{-2}$ HINS-light.

7.1.3 HINS-light and prosthetic vascular graft materials

Infection is a serious and often fatal complication of prosthetic vascular graft implant surgery, and it is a procedure in which a method of decreasing the bacterial burden has obvious benefits. However, it could prove disastrous if this decontamination method also had a detrimental effect on the properties of the implant materials. The effect of HINS-light on prosthetic vascular graft materials was investigated. A HINS-light intensity of 5 $mWcm^{-2}$ was applied to polyethylene terephthalate (PET) graft materials for 1 hour, having previously established that this dose does not have an effect on mammalian cells. Materials were provided by Vascutek, UK, and consisted of woven and knitted PET fabrics, and gelatin-sealed versions of the woven and knitted material.

SEM images of the material samples taken immediately before exposure, shortly following exposure and at 3 months following exposure did not show any visible difference to fibre structure or integrity. The gelatin sealing on the fabrics, which would hydrolyse over a period of 14 days *in vivo*, was found to not be affected by exposure to HINS-light over a period of 3 months in storage. No obvious degradation of the gelatin had occurred relative to unexposed gelatin-sealed fabric.

Mechanical testing of the materials was performed immediately following and at three months following exposure. Materials were stretched at constant load to failure, with maximum load, stress, strain and breaking load recorded. HINS-light exposure was shown to not significantly decrease any of these properties, at either time point.

Cytotoxicity testing was performed on extracts of HINS-light exposed vascular graft materials, using human aortic smooth muscle cells. The material samples were exposed to HINS-light, and extraction performed in cell culture medium. The viability of cells cultured with the extract media was assessed by Neutral Red assay.

The cytotoxicity of the materials was found to be unaffected by exposure to HINS-light. Although gelatin-sealed materials were found to have some cytotoxic effects, this was not increased by exposure to HINS-light.

7.1.4 Bactericidal properties of HINS-light

Finally, having established that 1 hour exposure to 5 $mWcm^{-2}$ HINS-light did not cause detrimental effects on mammalian cell function, and did not alter the properties of the biomaterials tested, the effects of this combination of intensity and duration on various relevant bacterial species was analysed.

On starting populations of 10^3 CFU/ml exposed to HINS-light in PBS suspension, exposure was found to cause a significant decrease in numbers of viable colony forming units of *Staphylococcus epidermidis*, *Staphylococcus aureus*, Methicillin resistant *Staphylococcus aureus* and *Pseudomonas aeruginosa*. *S. epidermidis* was found to be most susceptible (99.0% reduction in viable colonies), followed by *S. aureus (54.1%)*, MRSA (47.8%) then *P. aeruginosa (18.6%)*. No significant effect was observed on populations of *Acinetobacter baumannii (12.3%)* and *Escherichia coli (3.9%)*.

Exposure of bacteria to HINS-light was also performed on different agar surfaces to establish if bacterial access to nutrients affected the efficiency of inactivation. On highly nutritious Tryptone Soya Agar, only *S. aureus* and *A. baumannii* had significant inactivation (20.6 and 19.0% respectively), while *S. epidermidis (7.9%)*, MRSA (17.8%) and *P. aeruginosa (8.7%)* had small but statistically insignificant decreases in viable colony counts. On less nutritious Bacteriological Agar inactivation rates were generally higher, with MRSA (82.8%) and *P. aeruginosa (76.2%)* showing significant decreases in viable colonies. *S. epidermidis* (40%), *S. aureus* (21.6%) and *A. baumannii (27%)* did undergo some inactivation, and although statistically this was not significant, it was increased relative to inactivation tests on Trytone Soya Agar. The viability of *E. coli* populations was not affected by HINS-light exposure on either Trytone Soya Agar or Bacteriological Agar.

Inactivation rates of *S. epidermidis* seeded onto prosthetic vascular graft biomaterials were calculated, again following a 1 hour exposure to 5 $mWcm^{-2}$ HINS-light. Significant reductions in viable colony forming units were achieved, however, the material was found to provide a degree of protection towards to bacteria, likely by absorbing a proportion of the light before it could reach bacteria which were not on the material surface. Inactivation rates of around 60% were achieved on gelatin-sealed or plain, woven and knitted materials.

SEM was used to visualise *S. epidermidis* bacteria that had been exposed to HINS-light. Despite inactivation rates of 99.9%, no observable morphological difference was apparent between control and exposed bacteria. This was perhaps due to fixation being performed too soon following exposure to allow any oxidative membrane damaging effects to occur.

7.2 Limitations, future work and conclusions

7.2.1 Mammalian cell studies

A level of exposure has been established that does not affect two types of mammalian cell *in vitro*. However, more work is required before it could be claimed that HINS-light is completely safe for patient based applications. These findings suggest that a safe level of exposure *in vivo* could be established.

It should be noted that all experiments designed to assess the effect of HINS-light on mammalian tissue were performed on cell lines. The benefits of established cell lines are that they can undergo unlimited divisions without their characteristics altering, giving reproducible results. They are also much easier and cheaper to maintain than primary cells. However, cell lines do not always accurately replicate the properties of the cell type they were derived from, and it is accepted that they can have slightly different characteristics and can lose tissue-specific functions (Olschlager et al., 2009; Pan et al., 2009). The next stage in the development of patient-based applications would be to investigate the parameters assessed in this work with primary cell types. These may well prove more sensitive to insult by HINS-light irradiation. The response of different cell types would also need to be

evaluated. For example, there are many cells involved in wound healing, including leukocytes, keratinocytes endothelial cells and epithelial cells as well as the fibroblasts investigated in this work, and the sensitivity of all of these to IHNS-light should be established. An in vivo model would provide the most comprehensive understanding of how HINS-light exposure may affect mammalian cell processes.

The mouse model is the most common for wound studies, with a number of similarities to human skin that make mice particularly suitable for this purpose while also being relatively inexpensive and easy to maintain (Wong et al., 2011). Such models have previously been used to study the effects of low level laser therapy (Demidova-Rice et al., 2007) and LED exposure (Whelan et al., 2001) on wound healing. This would provide more compelling evidence than in vitro studies with primary cells on the effects of HINS-light on wound healing.

Similarly, sheep models have been used as in vivo models of osseointegration of implant materials (Chen et al., 2011; Likibi et al., 2004), and these could be employed to gain a more complete understanding on what effects HINS-light exposure may have on this process. Such an experiment could consist of the placement of titanium screws under different doses of HINS-light exposure, while the torque required to dislodge them provides a measure of osseointegration.

The bacterial inactivation results must be taken into account to decide if the considerable investment in time and resources that these in vivo experiments would require is worthwhile.

7.2.2 Bacterial work

The inactivation of *Staphylococcus epidermidis* is particularly impressive, with 99% reduction in viable colonies in PBS suspension. Although inactivation results on agar surfaces are not as impressive, the potential health benefits of such reductions are significant. *Staphylococcus aureus* and MRSA, and to a lesser extent *Acinetobacter baumannii* and *Pseudomonas aeruginosa*, have also been shown to be susceptible to HINS-light inactivation, and these bacteria are known to be a

considerable cause of hospital acquired infection. However, *Escherichia coli* bacteria were found not to be susceptible to HINS-light inactivation at the safe level of exposure. There are also many more bacteria than assessed in this study that are known to cause hospital acquired infection, and it would be useful to establish the effect of HINS-light at the intensities used in this work on a greater range of bacteria.. Literature review suggests that other relevant bacteria may be relativley resistant to photoinactivation (Ashkenazi et al., 2003; Henry et al., 1996; Maclean et al., 2009). The bacterial species used in these studies were, with the exception of MRSA, all obtained from the National Collection of Type Cultures (NCTC) which provides bacterial cultures with known properties and guaranteed provenance. However, as with the difference between primary and established cell lines, clinical isolates may respond differently from standardised cultures. The effect on fungi and viruses would also need to be assessed.

A significant finding of the bacterial exposure experiments was that the inactivation rates were reduced when exposing the bacteria on nutritious surfaces compared to those in either PBS suspension or on less nutritious agar surfaces. Burn wounds are known to provide a particularly protein rich environment in which bacteria can thrive (Church et al., 2006), while the loss of skin integrity following any surgical procedure will result in exposure of subcutaneous tissue which provides a moist, warm and nutritious environment that encourages microbial proliferation (Bowler et al., 2001). Therefore, inactivation experiments on surfaces that more closely replicate an open wound are required. Again, in vivo experiments could be used here, such as those described by Jawhara and Mordon (2004) involving the deliberate contamination of cutaneous wounds in rats with bioluminescent *E. coli* (Jawhara & Mordon, 2004*)*. Bioluminescent variations of *Staphylococcus* bacteria have also been developed that allow real time evaluation of bacterial colonisation (Kuklin et al., 2003), which could provide accurate, quantifiable results on the ability of HINS-light to halt the spread of infection.

As well as having ready access to a highly nutritious environment, bacteria in a wound will be in contact with mammalian cells. This provides a further

complication which may further reduce the bactericidal effects of HINS-light. Smith and co-workers found that separate exposure of 3T3 cells to 10 $mWcm^{-2}$ HINS-light for 150 minutes caused only a small decrease in cell viability, and that this dose resulted in almost complete inactivation of *Staph. epidermidis* bacteria. However, co-culture experiments had surprising results. When cells were exposed to HINS-light in the presence of bacteria, cell viability was found to be significantly reduced, while bacterial populations were now relatively unaffected by exposure. Through experiments involving refreshing of the bacterial suspension media between exposures to HINS-light, it was concluded that the mammalian cells released a factor into the suspending media, which the bacteria could use as a protective mechanism, but which resulted in increased mammalian cell death (Smith, 2009). A possible explanation of this is that infecting microbes have been shown to be capable of intercepting neurohormonal products of the stress response of the host cells, and can interpret these signals to initiate growth and the pathogenic process (Freestone et al., 2008). It is possible that the 3T3 cells may have released a chemical signal in response to the oxidative stress caused by HINS-light exposure, or by the presence of bacteria, or a combination of both, which resulted in increased bacterial survival.

It should be noted that the co-culture experiments performed by Smith were of a preliminary nature, and the number of mammalian cells relative to bacteria were not representative of early wound colonisation. However, the findings should introduce some caution into interpreting the bacterial inactivation results reported in this thesis with respect to inactivation on a wound surface. This effect of increased bacterial survival and decreased mammalian cell viability, in combination with the decreased bacterial inactivation rates when bacteria is exposed to HINS-light in highly nutritious environments such as a wound, may provide a significant limitation to the application of HINS-light to kill bacteria in an open wound.

Even disregarding the possible complications outlined above, the bacterial inactivation results are certainly not good enough to suggest that HINS-light could be utilised as an active patient-based disinfection technology. In chronic wounds or surgical sites which are already infected, the number of colony forming units will

almost certainly be too large for HINS-light to be beneficial at non-harmful intensities. In cases of chronic wound infection, a further limitation to the application of HINS-light is the limited depth of penetration of blue light into tissue. Blue light penetrates the least distance into human tissue of the visible light wavelengths. This is because both the absorption and scattering of light in tissue are much higher in the blue region. The high absorption of blue light by chromophores, and subsequent production of ROS as described in section 1.6.2, is why blue light is theoretically the most effective wavelength for photodynamic inactivation. However, this high attenuation of blue light also means it cannot normally be used for photodynamic therapy (McCaughan, 1999). Blue light photodynamic therapy is only applicable for surface conditions, and similarly bacterial inactivation by HINS-light will only occur on the skin surface. Blue light will not penetrate deeper than 2mm into human tissue (Moan et al., 1996), therefore the bactericidal applications of HINS-light will be limited to surface treatments.

7.2.3 Exposure conditions

All exposures in this work have been performed over 1 hour, with the intensity of the HINS-light varied to give different total doses. However, many procedures can last much longer than 1 hour which would result in doses greater than those used in this work. Further experiments to ensure the safety of prolonged exposures to HINS-light are required. It would also be interesting to establish if the effect of HINS-light is dose or intensity dependent. Would an exposure to twice the intensity for half as long result in the same effects as half the intensity for double the duration? This could provide more effective bacterial inactivation in procedures which are known to be of shorter duration.

7.2.4 Biomaterial compatibility

The effect of HINS-light on biomaterials has only been established on PET vascular graft materials. There are many more materials that could be adversely affected by exposure. It was impossible to source a reasonably priced sample of orthopaedic implant material for this work, but it would be essential to ensure that exposure to

HINS-light did not cause cytotoxic effects on these if it was going to be applied during orthopaedic implant procedures.

7.2.5 Device design

HINS-light is currently undergoing trials in the Burns Unit of the Glasgow Royal Infirmary as a general environmental disinfection system (HINS-EDS) (Maclean et al., 2010). The findings of the work reported in this thesis suggest that HINS-light could potentially be used as a more directed form of environmental disinfection. This could take the form of 405 nm LEDs incorporated into a lamp unit similar to the overhead lights used in operating theatres which can be manipulated such that the operating field and surrounding surfaces will be exposed. For localised exposure of a short duration, such as during high risk surgical procedures, HINS-light may be able to achieve a decrease in numbers of airborne and surface bacteria in the area immediately surrounding the surgical site without damaging the exposed mammalian tissues. To produce a light source which also provides practical illumination, the 405 nm LEDs could be combined with white light LEDs, resulting in a predominantly white illumination effect. This combination of 405 nm and white light LEDs is currently being trialled in ceiling mounted lights at the Glasgow Royal Infirmary (Maclean et al., 2010). The results reported by Maclean and co-workers are encouraging, with significant reductions in surface bacterial levels being achieved following extended exposures to low levels of HINS-light. The intensities of exposure used in the HINS-EDS system, up to a maximum intensity of 0.5 $mWcm^{-2}$, is well below the intensities found to inhibit mammalian cell function in this study, and therefore there is nothing in the findings of this study that should discourage the current work of utilising HINS-light as an environmental disinfection system.

HINS-light on its own is perhaps not the solution to infection acquired during invasive procedures. However, these results show that it has the potential to decrease the bacterial burden without inhibiting mammalian cell function, and that in combination with existing practices a significant reduction in environmental concentrations of certain bacterial populations could be achieved. For applications

such as exposure during high risk surgical procedures, the potential benefits of such a reduction are significant, and further development of HINS-light is encouraged.

PUBLICATIONS

McDonald R, MacGregor SJ, Anderson JG, Maclean M, and Grant MH (2011) Effect of 405-nm high-intensity narrow-spectrum light on fibroblast-populated collagen lattices: an in vitro model of wound healing, Journal of Biomedical Optics, Volume 16, Issue 4, pp. 048003-048003-4

McDonald R, Maclean M, Anderson JG, MacGregor SJ, and Grant MH (2011) Effect of 405nm High-Intensity Narrow-Spectrum Light on Osteoblast Function, eCM XII Implant Infection, Davos, European Cells and Materials Vol. 21. Suppl. 2, p 59

McDonald R, MacGregor SJ, Maclean M, Anderson JG, Grant MH (2010) The effect of high-intensity narrow spectrum light on osteoblast function. Proceedings of the 9th Annual Conference of the UK Society for Biomaterials (UKSB)

McDonald R, MacGregor SJ, Maclean M, Anderson JG, and Grant MH (2009) Effect of HINS light on the contraction of fibroblast populated collagen lattices. Tissue and Cell Engineering Conference, Glasgow, European Cells and Materials, 18 (Suppl.). p. 79

REFERENCES

Adamskaya, N., Dungel, P., Mittermayr, R., Hartinger, J., Feichtinger, G., Wassermann, K., et al. (2010). Light therapy by blue LED improves wound healing in an excision model in rats. *Injury, In Press, Corrected Proof*.

Ahn, W. S., Bae, S. M., Huh, S. W., Lee, J. M., Namkoong, S. E., Han, S. J., et al. (2004). Necrosis-like death with plasma membrane damage against cervical cancer cells by photodynamic therapy. *International Journal of Gynecological Cancer, 14*(3), 475-482.

Al-Akayleh, A. (1999). Invasive Burn Wound Infection. *Annals of Burns and Fire Disasters, 12*(4), 204-207.

Alexakis, P. G., Feldon, P. G., Wellisch, M., Richter, R. E., & Finegold, S. M. (1976). Airborne bacterial contamination of operative wounds. *The Western Journal of Medicine, 124*(5), 361-369.

Andersen, B. M., Rasch, M., Hochlin, K., Tollefsen, T., & Sandvik, L. (2009). Hospital-acquired infections before and after healthcare reorganization in a tertiary university hospital in Norway. *Journal of Public Health (Oxford), 31*(1), 98-104. Epub 2009 Jan 2018.

Andersson, D. I., & Hughes, D. (2011). Persistence of antibiotic resistance in bacterial populations. *FEMS Microbiology Reviews, 35*(5), 901-911.

Aron, P., Vlad, C. S., Audrey, S. L., Joseph, E. D., & Patricia, A. H. (2007). Differential regulation of free-floating collagen gel contraction by human fetal and adult dermal fibroblasts in response to prostaglandin E2 mediated by an EP2/cAMP-dependent mechanism. *Wound Repair and Regeneration, 15*(3), 390-398.

Ashkenazi, H., Malik, Z., Harth, Y., & Nitzan, Y. (2003). Eradication of Propionibacterium acnes by its endogenic porphyrins after illumination with high intensity blue light. *FEMS Immunology and Medical Microbiology, 35*(1), 17-24.

Athanasopoulos, A. N., Economopoulou, M., Orlova, V. V., Sobke, A., Schneider, D., Weber, H., et al. (2006). The extracellular adherence protein (Eap) of Staphylococcus aureus inhibits wound healing by interfering with host defense and repair mechanisms. *Blood, 107*(7), 2720-2727.

Ayçiçek, H., Aydogan, H., Küçükkaraaslan, A., Baysallar, M., & Basustaoglu, A. C. (2004). Assessment of the bacterial contamination on hands of hospital food handlers. *Food Control, 15*(4), 253-259.

Ayliffe, G. A. J., & Collins, B. J. (1967). Wound infections acquired from a disperser of an unusual strain of Staphylococcus aureus. *Journal of Clinical Pathology, 20*(2), 195-198.

Bandyk, D. F., Berni, G. A., Thiele, B. L., & Towne, J. B. (1984). Aortofemoral Graft Infection due to Staphylococcus epidermidis. *Archives of Surgery, 119*(1), 102-108.

Bank, H. L. (1987). Assessment of islet cell viability using fluorescent dyes. *Diabetologia., 30*(10), 812-816.

Barros, L. F., Kanaseki, T., Sabirov, R., Morishima, S., Castro, J., Bittner, C. X., et al. (2003). Apoptotic and necrotic blebs in epithelial cells display similar neck diameters but different kinase dependency. *Cell Death and Differentation, 10*(6), 687-697.

Baum, C. L., & Arpey, C. J. (2005). Normal Cutaneous Wound Healing: Clinical Correlation with Cellular and Molecular Events. *Dermatologic Surgery, 31*(6), 674-686.

Bell, E., Ivarsson, B., & Merrill, C. (1978). Production of a tissue-like structure by contraction of collagen lattices by human fibroblasts of different proliferative potential in vitro. *Proceedings of the National Acadamy of Sciences of the United States of America, 76*(3), 1274-1278.

Bendy, R. H., Jr., Nuccio, P. A., Wolfe, E., Collins, B., Tamburro, C., Glass, W., et al. (1964). Relationship of Quantitative Wound Bacterial Counts to Healing of Decubiti: Effect of Topical Gentamicin. *Antimicrobial Agents and Chemotherapy, 10*, 147-155.

Benediktsdottir, E., & Hambraeus, A. (1982). Dispersal of non-sporeforming anaerobic bacteria from the skin. *Journal of Hygiene (London). 88*(3), 487-500.

Berg, M., Bergman, B. R., & Hoborn, J. (1991). Ultraviolet radiation compared to an ultra-clean air enclosure. Comparison of air bacteria counts in operating rooms. *Journal of Bone and Joint Surgery (British volume), 73*(5), 811-815.

Bhatia, L., & Vishwakarma, R. (2010). Hospital Indoor Airborne Micoflora in Private and Government Owned Hospitals in Sagar City, India. *World Journal of Medical Sciences, 5*(3), 65-70.

Bhattacherjee, P., & Eakins, K. E. (1974). Inhibition of the prostaglandin synthetase systems in occular tissues by indomethican. *British Journal of Pharmacology, 50*(2), 227-230.

Bickers, D. R., & Athar, M. (2006). Oxidative Stress in the Pathogenesis of Skin Disease. *Journal of Investigative Dermatology, 126*(12), 2565-2575.

Bisland, S. K., & Burch, S. (2006). Photodynamic therapy of diseased bone. *Photodiagnosis and Photodynamic Therapy, 3*(3), 147-155.

Bohm, F., Edge, R., Foley, S., Lange, L., & Truscott, T. G. (2001). Antioxidant inhibition of porphyrin-induced cellular phototoxicity. *Journal of Photochemistry and Photobiology B: Biology, 65*(2-3), 177-183.

Boiskin, I., Epstein, S., Ismail, F., Thomas, S. B., & Raja, R. (1989). Serum osteocalcin and bone mineral metabolism following successful renal transplantation. *Clinical Nephrology, 31*(6), 316-322.

Bonewald, L. (2006). Osteocytes as multifunctional cells. *Journal of Musculoskeletal and Neuronal Interactions, 6*(4), 331-333.

Borenfreund, E., Babich, H., & Martin-Alguacil, N. (1988). Comparisons of two in vitro cytotoxicity assays--The neutral red (NR) and tetrazolium MTT tests. *Toxicology in Vitro, 2*(1), 1-6.

Bouillaguet, S., Owen, B., Wataha, J. C., Campo, M. A., Lange, N., & Schrenzel, J. (2008). Intracellular reactive oxygen species in monocytes generated by photosensitive chromophores activated with blue light. *Dental materials : official publication of the Academy of Dental Materials, 24*(8), 1070-1076.

Bowers, G. N., Jr., & McComb, R. B. (1966). A Continuous Spectrophotometric Method for Measuring the Activity of Serum Alkaline Phosphatase. *Clinical Chemistry, 12*(2), 70-89.

Bowler, P. G., Duerden, B. I., & Armstrong, D. G. (2001). Wound Microbiology and Associated Approaches to Wound Management. *Clinical Microbiology Reviews, 14*(2), 244-269.

Boyce, J. M. (2007). Environmental contamination makes an important contribution to hospital infection. *Journal of Hospital Infection, 65*(Supplement 2), 50-54.

Brem, H., Golinko, M., Stojadinovic, O., Kodra, A., Diegelmann, R., Vukelic, S., et al. (2008). Primary cultured fibroblasts derived from patients with chronic wounds: a methodology to produce human cell lines and test putative growth factor therapy such as GMCSF. *Journal of Translational Medicine, 6*(1), 75.

Broekhuizen, C. A., de Boer, L., Schipper, K., Jones, C. D., Quadir, S., Feldman, R. G., et al. (2007). Peri-implant tissue is an important niche for Staphylococcus epidermidis in experimental biomaterial-associated infection in mice. *Infection and Immunity, 75*(3), 1129-1136. Epub 2006 Dec 1111.

Cao, C., & Yuan, H. (2003). A New Approach of Evaluating Bond Dissociation Energy from Eigenvalue of Bonding Orbital-Connection Matrix for Câˆ’C and Câˆ’H Bonds in Alkane. *Journal of Chemical Information and Computer Sciences, 43*(2), 600-608.

Cao, L. Q., Xue, P., Lu, H. W., Zheng, Q., Wen, Z. L., & Shao, Z. J. (2009). Hematoporphyrin derivative-mediated photodynamic therapy inhibits tumor growth in human cholangiocarcinoma in vitro and in vivo. *Hepatology Research, 39*(12), 1190-1197. Epub 2009 Sep 1125.

Carlson, M., & Longaker, M. (2004). The fibroblast-populated collagen matrix as a model of wound healing: a review of the evidence. *Wound Repair and Regeneration, 12*(2), 134-147.

Carnevali, S., Mio, T., Adachi, Y., Spurzem, J. R., Striz, I., Romberger, D. J., et al. (2003). Gamma radiation inhibits fibroblast-mediated collagen gel retraction. *Tissue and Cell, 35*(6), 459-469.

Carpenter, T. O., Moltz, K. C., Ellis, B., Andreoli, M., McCarthy, T. L., Centrella, M., et al. (1998). Osteocalcin Production in Primary Osteoblast Cultures Derived from Normal and Hyp Mice. *Endocrinology, 139*(1), 35-43.

Chambers, S. T. (2005). Diagnosis and management of staphylococcal infections of vascular grafts and stents. *Internal Medicine Journal, 35*(Suppl 2), S72-78.

Charnley, J., & Eftekhar, N. (1969). Postoperative infection in total prosthetic replacement arthroplasty of the hip-joint with special reference to the bacterial content of the air of the operating room. *British Journal of Surgery, 56*(9), 641-649.

Chavakis, T., Hussain, M., Kanse, S. M., Peters, G., Bretzel, R. G., Flock, J. I., et al. (2002). Staphylococcus aureus extracellular adherence protein serves as anti-inflammatory factor by inhibiting the recruitment of host leukocytes. *Nature Medicine, 8*(7), 687-693. Epub 2002 Jun 2024.

Chen, D., Bertollo, N., Lau, A., Taki, N., Nishino, T., Mishima, H., et al. (2011). Osseointegration of porous titanium implants with and without an electrochemically deposited DCPD coating in an ovine model. *Journal of Orthopaedic Surgery and Research, 6*(1), 56.

Chiller, K., Selkin, B. A., & Murakawa, G. J. (2001). Skin Microflora and Bacterial Infections of the Skin. *Journal of Investigative Dermatology Symposium Proceedings, 6*(3), 170-174.

Chitkara, Y. K., & Feierabend, T. C. (1981). Endogenous and exogenous infection with Pseudomonas aeruginosa in a burns unit. *Int Surg., 66*(3), 237-240.

Chmell, M. J., Poss, R., Thomas, W. H., & Sledge, C. B. (1996). Early failure of hylamer acetabular inserts due to eccentric wear. *The Journal of arthroplasty, 11*(3), 351-353.

Chu, Y. W., Leung, C. M., Houang, E. T., Ng, K. C., Leung, C. B., Leung, H. Y., et al. (1999). Skin carriage of acinetobacters in Hong Kong. *Journal of Clinical Microbiology, 37*(9), 2962-2967.

Church, D., Elsayed, S., Reid, O., Winston, B., & Lindsay, R. (2006). Burn wound infections. *Clinical Microbiology Reviews, 19*(2), 403-434.

Clark, R. P., & de Calcina-Goff, M. L. (2009). Some aspects of the airborne transmission of infection. *Journal of The Royal Society Interface, 6*(Suppl 6), S767-S782.

Clark, R. P., Reed, P. J., Seal, D. V., & Stephenson, M. L. (1985). Ventilation conditions and air-borne bacteria and particles in operating theatres: proposed safe economies. *Journal of Hygiene (London). 95*(2), 325-335.

Coello, R., Glenister, H., Fereres, J., Bartlett, C., Leigh, D., Sedgwick, J., et al. (1993). The cost of infection in surgical patients: a case-control study. *Journal of Hospital Infection, 25*(4), 239-250.

Cogen, A. L., Nizet, V., & Gallo, R. L. (2008). Skin microbiota: a source of disease or defence? *British Journal of Dermatology, 158*(3), 442-455.

Cokebrook, L., Lowbury, E., & Hurst, L. (1960). The growth and death of wound bacteria in serum, exudate and slough. *Journal of Hygiene, 58*(4), 357-366.

Collier, M. (2004). Recognition and managment of wound infections [Electronic Version]. *World Wide Wounds*. Retrieved 9/11/11 from http://www.worldwidewounds.com/2004/january/Collier/Management-of-Wound-infections.html.

Croteau, D. L., & Bohr, V. A. (1997). Repair of Oxidative Damage to Nuclear and Mitochondrial DNA in Mammalian Cells. *Journal of Biological Chemistry, 272*(41), 25409-25412.

Cunha, A., Renz, R., Wantowski, G., Oliveira, R. d., Blando, E., & Hubler, R. (2007). A Surgical Procedure using Sheep as an Animal Model to Evaluate Osseointegartion. *Journal of Clinical Dental Research, 3*(1), 59-62.

Dancer, S. J. (2009). The role of environmental cleaning in the control of hospital-acquired infection. *Journal of Hospital Infection, 73*(4), 378-385.

Dancer, S. J., White, L. F., Lamb, J., Girvan, E. K., & Robertson, C. (2009). Measuring the effect of enhanced cleaning in a UK hospital: a prospective cross-over study. *BMC Medicine, 7*, 28.

Dare, A., Hachisu, R., Yamaguchi, A., Yokose, S., Yoshiki, S., & Okano, T. (1997). Effects of Ionizing Radiation on Proliferation and Differentiation of Osteoblast-like Cells. *Journal of Dental Research, 76*(2), 658-664.

Day, M., & Wiles, D. M. (1972). Photochemical degradation of poly(ethylene terephthalate). III. Determination of decomposition products and reaction mechanism. *Journal of Applied Polymer Science, 16*(1), 203-215.

Delamere, F., Holland, E., Patel, S., Bennett, J., Pavord, I., & Knox, A. (1994). Production of PGE2 by bovine cultured airway smooth muscle cells and its inhibition by cyclo-oxygenase inhibitors. *British Journal of Pharmacology, 111*(4), 983-988.

Demidova-Rice, T. N., Salomatina, E. V., Yaroslavsky, A. N., Herman, I. M., & Hamblin, M. R. (2007). Low-level light stimulates excisional wound healing in mice. *Lasers in Surgery and Medicine, 39*(9), 706-715.

Dhert, W. J. A., Thomsen, P., Blomgren, A. K., Esposito, M., Ericson, L. E., & Verbout, A. J. (1998). Integration of press-fit implants in cortical bone: A study on interface kinetics. *Journal of Biomedical Materials Research, 41*(4), 574-583.

Dobrin, P. B., Littooy, F. N., & Endean, E. D. (1989). Mechanical factors predisposing to intimal hyperplasia and medial thickening in autogenous vein grafts. *Surgery., 105*(3), 393-400.

Dörtbudak, O., Haas, R., & Mailath-Pokorny, G. (2002). Effect of low-power laser irradiation on bony implant sites. *Clinical Oral Implants Research, 13*(3), 288-292.

Drury, J. K., Ashton, T. R., Cunningham, J. D., Maini, R., & Pollock, J. G. (1987). Experimental and Clinical Experience with a Gelatin Impregnated Dacron Prosthesis. *Annals of Vascular Surgery, 1*(5), 542-547.

Du, H., Fuh, R.-C. A., Li, J., Corkan, L. A., & Lindsey, J. S. (1998). PhotochemCAD‡: A Computer-Aided Design and Research Tool in Photochemistry. *Photochemistry and Photobiology, 68*(2), 141-142.

Ducy, P., Desbois, C., Boyce, B., Pinero, G., Story, B., Dunstan, C., et al. (1996). Increased bone formation in osteocalcin-deficient mice. *Nature, 382*(6590), 448-452.

Dutreux, N., Notermans, S., Wijtzes, T., Góngora-Nieto, M. M., Barbosa-Cánovas, G. V., & Swanson, B. G. (2000). Pulsed electric fields inactivation of attached and free-living Escherichia coli and Listeria innocua under several conditions. *International Journal of Food Microbiology, 54*(1-2), 91-98.

Edwards, R., & Harding, K. G. (2004). Bacteria and wound healing. *Current Opinions in Infectious Diseases, 17*(2), 91-96.

Ehrlich, H. P., & Rajaratnam, J. B. M. (1990). Cell locomotion forces versus cell contraction forces for collagen lattice contraction: An in vitro model of wound contraction. *Tissue and Cell, 22*(4), 407-417.

Ehrlich, H. P., & White, M. E. (1983). Effects of Increased Concentrations of Prostaglandin E Levels With Epidermolysis Bullosa Dystrophica Recessive Fibroblasts Within a Populated Collagen Lattice. *Journal of Investigative Dermatology, 81*(6), 572-575.

Ehrlich, H. P., & Wyler, D. J. (1983). Fibroblast contraction of collagen lattices in vitro: Inhibition by chronic inflammatory cell mediators. *Journal of Cellular Physiology, 116*(3), 345-351.

Ehrlich, P., Bonnie, S., Koijan, K., & Fatuma, K. (2006). Elucidating the mechanism of wound contraction: Rapid versus sustained myosin ATPase activity in attached-delayed-released compared with free-floating fibroblast-populated collagen lattices. *Wound Repair and Regeneration, 14*(5), 625-632.

Ekhaise, F., Ighosewe, O., & Ajakovi, O. (2008). Hospital Indoor Airborne Microflora in Private and Government Owned Hospitals in Benin City, Nigeria. *World Journal of Medical Sciences, 3*(1), 19-23.

El Shafie, S. S., Alishaq, M., & Leni Garcia, M. (2004). Investigation of an outbreak of multidrug-resistant Acinetobacter baumannii in trauma intensive care unit. *Journal of Hospital Infection, 56*(2), 101-105.

Elek, S. D. (1956). Experimental Staphylococcal Infections in the Skin of Man. *Annals of the New York Academy of Sciences, 65*(3), 85-90.

Elsdale, T., & Bard, J. (1972). Collagen substrata for studies on cell behaviour. *Journal of Cell Biology, 54*(3), 626-637.

Embil, J. M., McLeod, J. A., Al-Barrak, A. M., Thompson, G. M., Aoki, F. Y., Witwicki, E. J., et al. (2001). An outbreak of methicillin resistant Staphylococcus aureus on a burn unit: potential role of contaminated hydrotherapy equipment. *Burns., 27*(7), 681-688.

Erbaydar, S., Akgün, A., Eksik, A., Erbaydar, T., Bilge, O., & Bulut, A. (1995). Estimation of increased hospital stay due to nosocomial infections in surgical patients: comparison of matched groups. *Journal of Hospital Infection, 30*(2), 149-154.

Evensen, J. F. (1995). The use of porphyrins and non-ionizing radiation for treatment of cancer. *Acta Oncologica, 34*(8), 1103-1110.

Fashandi, H., Zadhoush, A., & Haghighat, M. (2008). Effect of Orientation and Crystallinity on the Photodegredation of Poly(ethylene terephthalate) Fibers. *Polymer Engineering and Science, 48*(5), 949-956.

Fechine, G. J. M., Rabello, M. S., Souto Maior, R. M., & Catalani, L. H. (2004). Surface characterization of photodegraded poly(ethylene terephthalate). The effect of ultraviolet absorbers. *Polymer, 45*(7), 2303-2308.

Ferreira, S. H., Moncada, S., & Vane, J. R. (1971). Indomethacin and aspirin abolish prostaglandin release from the spleen. *Nature: New Biology, 231*(25), 237-239.

Feuerstein, O., Ginsburg, I., Dayan, E., Veler, D., & Weiss, E. I. (2005). Mechanism of Visible Light Phototoxicity on Porphyromonas gingivalis and Fusobacterium nucleatum. *Photochemistry and Photobiology, 81*(5), 1186-1189.

Finesmith, T., Broadley, K., & Davidson, J. (1990). Fibroblasts from wounds of different stages of repair vary in their ability to contract a collagen gel in response to growth factors. *Journal of Cellular Physiology, 144*(1), 99-107.

Fitzpatrick, F., Humphreys, H., & O'Gara, J. P. (2005). The genetics of staphylococcal biofilm formation—will a greater understanding of pathogenesis lead to better management of device-related infection? *Clinical Microbiology and Infection, 11*(12), 967-973.

Flower, R. J. (1974). Drugs Which Inhibit Prostaglandin Biosynthesis. *Pharmacological Reviews, 26*(1), 33-67.

Ford-Hutchinson, A. W., Smith, M. J. H., & Walker, J. R. (1976). Effects of indomethacin on prostaglandin levels and leucocyte migration in an inflammatory exudaye in vivo. *Proceedings of the British Psychological Society*.

Freestone, P. P. E., Sandrini, S. M., Haigh, R. D., & Lyte, M. (2008). Microbial endocrinology: how stress influences susceptibility to infection. *Trends in Microbiology, 16*(2), 55-64.

Fuchs, J. r., & Thiele, J. (1998). The Role of Oxygen in Cutaneous Photodynamic Therapy. *Free Radical Biology and Medicine, 24*(5), 835-847.

Futagami, A., Ishizaki, M., Fukuda, Y., Kawana, S., & Yamanaka, N. (2002). Wound Healing Involves Induction of Cyclooxygenase-2 Expression in Rat Skin. *Laboratory Investigations, 82*(11), 1503-1513.

Gabbiani, G. (2003). The myofibroblast in wound healing and fibrocontractive diseases. *The Journal of Pathology, 200*(4), 500-503.

Gal, P., Toporcer, T., Grendel, T., Vidova, Z., Smetana, K., Jr., Dvorankova, B., et al. (2009). Effect of Atropa belladonna L. on skin wound healing: biomechanical and histological study in rats and in vitro study in keratinocytes, 3T3 fibroblasts, and human umbilical vein endothelial cells. *Wound Repair and Regeneration, 17*(3), 378-386.

Gallagher, J. A., Gundle, R., & Beresford, J. N. (1996). Isolation and culture of bone-forming cells (osteoblasts) from human bone. *Methods in Molecular Medicine, 2*, 233-262.

Gangneux, J. P., Robert-Gangneux, F., Gicquel, G., Tanquerel, J. J., Chevrier, S., Poisson, M., et al. (2006). Bacterial and fungal counts in hospital air: comparative yields for 4 sieve impactor air samplers with 2 culture media. *Infect Control and Hospital Epidemiology, 27*(12), 1405-1408. Epub 2006 Nov 1422.

Ganz, R. A., Viveiros, J., Ahmad, A., Ahmadi, A., Khalil, A., Tolkoff, M. J., et al. (2005). Helicobacter pylori in patients can be killed by visible light. *Lasers in Surgery and Medicine, 36*(4), 260-265.

Girard, R., Fabry, J., Meynet, R., Lambert, D. C., & Sepetjan, M. (1983). Costs of nosocomial infection in a neonatal unit. *Journal of Hospital Infection, 4*(4), 361-366.

Godley, B. F., Shamsi, F. A., Liang, F.-Q., Jarrett, S. G., Davies, S., & Boulton, M. (2005). Blue Light Induces Mitochondrial DNA Damage and Free Radical Production in Epithelial Cells. *Journal of Biological Chemistry, 280*(22), 21061-21066.

Gold, L. I., Rahman, M., Blechman, K. M., Greives, M. R., Churgin, S., Michaels, J., et al. (2006). Overview of the Role for Calreticulin in the Enhancement of Wound Healing through Multiple Biological Effects. *Journal of Investigative Dermatology Symposium Proceedings, 11*(1), 57-65.

Goldoni, A. (2002). Porphyrins: fascinating molecules with biological significance. *ELETTRA Laboratory, Research Highlights 2001-2002: Atomic, Molecular and Supramolecular Studies*, 64-65.

Gosden, P. E., MacGowan, A. P., & Bannister, G. C. (1998). Importance of air quality and related factors in the prevention of infection in orthopaedic implant surgery. *Journal of Hospital Infection, 39*(3), 173-180.

Gotz, F. (2002). Staphylococcus and biofilms. *Molecular Microbiology, 43*(6), 1367-1378.

Graeter, J. H., & Nevins, R. (1998). Early osteolysis with hylamer acetabular liners. *The Journal of Arthroplasty, 13*(4), 464-466.

Greenwald, S. E., & Berry, C. L. (2000). Improving vascular grafts: the importance of mechanical and haemodynamic properties. *Journal of Pathology, 190*(3), 292-299.

Grzelak, A., Rychlik, B., & Bartosz, G. (2001). Light-dependent generation of reactive oxygen species in cell culture media. *Free Radical Biology and Medicine, 30*(12), 1418-1425.

Guarner, F., & Malagelada, J.-R. (2003). Gut flora in health and disease. *The Lancet, 361*(9356), 512-519.

Habash, M., & Reid, G. (1999). Microbial biofilms: their development and significance for medical device-related infections. *The Journal of Clinical Pharmacology, 39*(9), 887-898.

Haddad, M. B., & Ebrahimi, N. G. (2006). Effect of Radiation on the Properties of UHMWPE/PET Composite. *Iranian Polymer Journal, 15*(3), 195 -205.

Haggar, A., Ehrnfelt, C., Holgersson, J., & Flock, J. I. (2004). The extracellular adherence protein from Staphylococcus aureus inhibits neutrophil binding to endothelial cells. *Infection and Immunity, 72*(10), 6164-6167.

Haley, R. W., Schaberg, D. R., Crossley, K. B., Von Allmen, S. D., & McGowan Jr, J. E. (1981). Extra charges and prolongation of stay attributable to nosocomial infections: A prospective interhospital comparison. *The American Journal of Medicine, 70*(1), 51-58.

Hamblin, M., & Hasan, T. (2003). Photodynamic therapy: a new antimicrobial approach to infectious disease? *Photochemical and Photoboilogical Sciences, 3*, 436-450.

Hamilton, H., & Jamieson, J. (2008). Deep infection in total hip arthroplasty. *Canadian Journal of Surgery., 51*(2), 111-117.

Hastings, C. E., Martin, S. A., Heath Iii, J. R., Mark, D. E., Mansfield, J. L., & Hollinger, J. O. (1990). The effects of ethylene oxide sterilization on the in vitro cytotoxicity of a bone replacement material. *Toxicology in Vitro, 4*(6), 757-762.

Haugen, H. J., Brunner, M., Pellkofer, F., Aigner, J., Will, J., & Wintermantel, E. (2007). Effect of different gamma-irradiation doses on cytotoxicity and material properties of porous polyether-urethane polymer. *Journal of Biomedical Materials Research B: Applied Biomaterials, 80*(2), 415-423.

Hedin, G., Rynback, J., & Lore, B. (2010). Reduction of bacterial surface contamination in the hospital environment by application of a new product with persistent effect. *The Journal of hospital infection, 75*(2), 112-115.

Henry, C. A., Dyer, B., Wagner, M., Judy, M., & Matthews, J. L. (1996). Phototoxicity of argon laser irradiation on biofilms of Porphyromonas and Prevotella species. *Journal of Photochemisty and Photobiology B., 34*(2-3), 123-128.

Hinz, B., Celetta, G., Tomasek, J. J., Gabbiani, G., & Chaponnier, C. (2001). Alpha-Smooth Muscle Actin Expression Upregulates Fibroblast Contractile Activity. *Molecular Biology of the Cell, 12*(9), 2730-2741.

Ho, G., Barbenel, J., & Grant, M. H. (2009). Effect of low-level laser treatment of tissue-engineered skin substitutes: contraction of collagen lattices. *Journal of Biomedical Optics, 14*(3), 034002.

Hoemann, C. D., El-Gabalawy, H., & McKee, M. D. (2009). In vitro osteogenesis assays: Influence of the primary cell source on alkaline phosphatase activity and mineralization. *Pathologie Biologie, 57*(4), 318-323.

Holländer, A., Klemberg-Sapieha, J. E., & Wertheimer, M. R. (1996). The influence of vacuum-ultraviolet radiation on poly(ethylene terephthalate). *Journal of Polymer Science Part A: Polymer Chemistry, 34*(8), 1511-1516.

Hsieh, P.-H., Huang, K.-C., Lee, P.-C., & Lee, M. S. (2009). Two-stage revision of infected hip arthroplasty using an antibiotic-loaded spacer: retrospective comparison between short-term and prolonged antibiotic therapy. *Journal of Antimicrobial Chemotherapy, 64*(2), 392-397.

Huang, S., Wettlaufer, S. H., Hogaboam, C., Aronoff, D. M., & Peters-Golden, M. (2007). Prostaglandin E2 inhibits collagen expression and proliferation in patient-derived normal lung fibroblasts via E prostanoid 2 receptor and cAMP signaling. *American Journal of Physiology: Lung Cellular and Molecular Physiology, 292*(2), L405-413.

Hurley, C. R., & Leggett, G. J. (2009). Quantitative Investigation of the Photodegradation of Polyethylene Terephthalate Film by Friction Force Microscopy, Contact-Angle Goniometry, and X-ray Photoelectron Spectroscopy. *ACS Applied Materials & Interfaces, 1*(8), 1688-1697.

Hussein, J. R., Villar, R. N., Gray, A. J., & Farrington, M. (2001). Use of light handles in the laminar flow operating theatre--is it a cause of bacterial concern? *Annals of the Royal College of Surgeons of England, 83*(5), 353-354.

Hwang, I.-Y., Son, Y.-O., Kim, J.-H., Jeon, Y.-M., Kim, J.-G., Lee, C.-B., et al. (2008). Plasma-arc generated light inhibits proliferation and induces apoptosis of human gingival fibroblasts in a dose-dependent manner. *Dental materials : official publication of the Academy of Dental Materials, 24*(8), 1036-1042.

Iglesias, J., Abernethy, V. E., Wang, Z., Lieberthal, W., Koh, J. S., & Levine, J. S. (1999). Albumin is a major serum survival factor for renal tubular cells and macrophages through scavenging of ROS. *American Journal of Physiology - Renal Physiology, 277*(5), F711-722.

Japoni, A., Farshad, S., & Alborzi, A. (2009). Pseudomonas aeruginosa: Burn Infection, Treatment and Antibacterial Resistance. *Iranian Red Crescent Medical Journal, 11*(2), 244-253.

Jawhara, S., & Mordon, S. (2004). In vivo imaging of bioluminescent Escherichia coli in a cutaneous wound infection model for evaluation of an antibiotic therapy. *Antimicrobial Agents and Chemotherapy, 48*(9), 3436-3441.

Jevons, M. (1961). "Celbenin"-resistant Staphylococci. *British Medical Journal Letters, 1*, 124-125.

Jilka, R. L., Weinstein, R. S., Bellido, T., Parfitt, A. M., & Manolagas, S. C. (1998). Osteoblast programmed cell death (apoptosis) : Modulation by growth factors and cytokines. *Journal of bone and mineral research, 13*(5), 793-802.

Kakkos, S. K., Topalidis, D., Haddad, R., Haddad, G. K., & Shepard, A. D. Long-term complication and patency rates of Vectra and IMPRA Carboflo Vascular Access Grafts with aggressive monitoring, surveillance and endovascular management. *Vascular, 19*(1), 21-28.

Kappstein, I., Schulgen, G., Fraedrich, G., Schlosser, V., Schumacher, M., & Daschner, F. D. (1992). Added hospital stay due to wound infections following cardiac surgery. *Journal of Thoracic and Cardiovascular Surgery, 40*(3), 148-151.

Karageorgopoulos, D. E., & Falagas, M. E. (2008). Current control and treatment of multidrug-resistant Acinetobacter baumannii infections. *The Lancet Infectious Diseases, 8*(12), 751-762.

Kassem, M., Mosekilde, L., & Eriksen, E. (1994). Growth hormone stimulates proliferation of normal human bone marrow stromal. *Journal of Plant Growth Regulation, 4*(3), 131-135.

Kato, M., Nishida, S., Kitasato, H., Sakata, N., & Kawai, S. (2001). Cyclooxygenase-1 and cyclooxygenase-2 selectivity of non-steroidal anti-inflammatory drugs: investigation using human peripheral monocytes. *Journal of Pharmacy and Pharmacology, 53*, 1679-1685.

Kawada, A., Aragane, Y., Kameyama, H., Sangen, Y., & Tezuka, T. (2002). Acne phototherapy with a high-intensity, enhanced, narrow-band, blue light source: an open study and in vitro investigation. *Journal of Dermatological Science, 30*(2), 129-135.

Kessel, D. (1982). Components of Hematoporphyrin Derivatives and Their Tumor-localizing Capacity. *Cancer Research, 42*(5), 1703-1706.

Khadra, M., Lyngstadaas, S. P., Haanæs, H. R., & Mustafa, K. (2005). Effect of laser therapy on attachment, proliferation and differentiation of human osteoblast-like cells cultured on titanium implant material. *Biomaterials, 26*(17), 3503-3509.

Khan, M. S., ur Rehman, S., Ali, M. A., Sultan, B., & Sultan, S. (2008). Infection in orthopedic implant surgery, its risk factors and outcome. *Journal of Ayub Medical College Abbottabad, 20*(1), 23-25.

Khosravi, A., Ahmadi, F., Salmanzadeh, S., Dashtbozorg, A., & Montazeri, E. A. (2009). Study of Bacteria Isolated from Orthopedic Implant Infections and their Antimicrobial Susceptibility Pattern. *Research Journal of Microbiology, 4*(4), 158-163.

Kiely, P. D., Harty, J. A., & McElwain, J. P. (2005). Hylamer wear rates and shelf life: a clinical correlation. *Acta Orthopaedica Belgica, 71*(4), 429-434.

Klebanov, G. I., Shuraeva, N., Chichuk, T. V., Osipov, A. N., Rudenko, T. G., Shekhter, A. B., et al. (2005). A comparative study of the effects of laser and light-emitting diode irradiation on the wound healing and functional activity of wound exudate leukocytes. *Biofizika., 50*(6), 1137-1144.

Klevens, R. M., Edwards, J. R., Richards, C. L., Jr., Horan, T. C., Gaynes, R. P., Pollock, D. A., et al. (2007). Estimating health care-associated infections and deaths in U.S. hospitals, 2002. *Public Health Reports, 122*(2), 160-166.

Kluytmans, J., van Belkum, A., & Verbrugh, H. (1997). Nasal carriage of Staphylococcus aureus: epidemiology, underlying mechanisms, and associated risks. *Clinical Microbiology Reviews, 10*(3), 505-520.

Kohyama, T., Ertl, R. F., Valenti, V., Spurzem, J., Kawamoto, M., Nakamura, Y., et al. (2001). Prostaglandin E2 inhibits fibroblast chemotaxis. *American Journal of Physiology - Lung Cellular and Molecular Physiology, 281*(5), L1257-1263.

Kollef, M. H., Napolitano, L. M., Solomkin, J. S., Wunderink, R. G., Bae, I.-G., Fowler, V. G., et al. (2008). Health Care Associated Infection (HAI): A Critical Appraisal of the Emerging Threat, Proceedings of the HAI Summit. *Clinical Infectious Diseases, 47*(Supplement 2), S55-S99.

Kramer, A., Schwebke, I., & Kampf, G. (2006). How long do nosocomial pathogens persist on inanimate surfaces? A systematic review. *BMC Infectious Diseases, 6*(1), 130.

Krasnovskii, A. A., Jr., Venediktov, E. A., & Chernenko, O. M. (1982). Quenching of singlet oxygen with chlorophylls and porphyrins. *Biofizika., 27*(6), 966-972.

Krizek, T. J., & Davis, J. H. (1966). Endogenous Wound Infection. *The Journal of Trauma, 6*(2), 239-248.

Kuehn, C., Graf, K., Mashaqi, B., Pichlmaier, M., Heuer, W., Hilfiker, A., et al. (2010). Prevention of Early Vascular Graft Infection Using Regional Antibiotic Release. *Journal of Surgical Research, 164*(1), e185-e191.

Kuhn, M., Smith, P., Hill, D., Ko, F., Meltzer, D., Berg, J. V., et al. (2000). In vitro fibroblast populated collagen lattices are not good models of in vivo clinical wound healing. *Wound Repair and Regeneration, 8*(4), 270-276.

Kuklin, N. A., Pancari, G. D., Tobery, T. W., Cope, L., Jackson, J., Gill, C., et al. (2003). Real-Time Monitoring of Bacterial Infection In Vivo: Development of Bioluminescent Staphylococcal Foreign-Body and Deep-Thigh-Wound Mouse Infection Models. *Antimicrobial Agents and Chemotherapy, 47*(9), 2740-2748.

Kurihara, N., Ishizuka, S., Kiyoki, M., Haketa, Y., Ikeda, K., & Kumegawa, M. (1986). Effects of 1,25-dihydroxyvitamin D3 on osteoblastic MC3T3-E1 cells. *Endocrinology., 118*(3), 940-947.

Kwon, S. J., de Boer, A. L., Petri, R., & Schmidt-Dannert, C. (2003). High-level production of porphyrins in metabolically engineered Escherichia coli: systematic extension of a pathway assembled from overexpressed genes involved in heme biosynthesis. *Applied Environmental Microbiology, 69*(8), 4875-4883.

Lambrechts, S., Demidova, T., Aalders, M., Hasan, T., & Hamblin, M. (2005a). Photodynamic therapy for Staphylococcus aureus infected burn wounds in mice. *Photochemical & Photobiological Sciences, 4*, 503-509.

Lambrechts, S. A. G., Aalders, M. C. G., Verbraak, F. D., Lagerberg, J. W. M., Dankert, J. B., & Schuitmaker, J. J. (2005b). Effect of albumin on the photodynamic inactivation of microorganisms by a cationic porphyrin. *Journal of Photochemistry and Photobiology B: Biology, 79*(1), 51-57.

Landis, S. (2008). Chronic Wound Infection and Antimicrobial Use. *Advances of Skin & Wound Care, 21*(1), 531-540.

Langton, C. M., & Njeh, C. F. (2003). *The Physical Measurement of Bone (Medical physics & biomedical engineering)* (1 ed.): Taylor & Francis.

Li, S., & Burstein, A. H. (1994). Ultra-high molecular weight polyethylene. The material and its use in total joint implants. *Journal of Bone and Joint Surgery, 76*(7), 1080-1090.

Lidwell, O. M. (1994). Ultraviolet radiation and the control of airborne contamination in the operating room. *Journal of Hospital Infection, 28*(4), 245-248.

Lidwell, O. M., Lowbury, E. J., Whyte, W., Blowers, R., Stanley, S. J., & Lowe, D. (1982). Effect of ultraclean air in operating rooms on deep sepsis in the joint after total hip or knee replacement: a randomised study. *British Medical Journal (Clinical Research Ed.), 285*(6334), 10-14.

Lidwell, O. M., Lowbury, E. J., Whyte, W., Blowers, R., Stanley, S. J., & Lowe, D. (1984). Infection and sepsis after operations for total hip or knee-joint replacement: influence of ultraclean air, prophylactic antibiotics and other factors. *Journal of Hygiene (London), 93*(3), 505-529.

Lidwell, O. M., Lowbury, E. J. L., Whyte, W., Blowers, R., Stanley, S. J., & Lowe, D. (1983). Airborne contamination of wounds in joint replacement operations: the relationship to sepsis rates. *Journal of Hospital Infection, 4*(2), 111-131.

Likibi, F. l., Assad, M., Jarzem, P., Leroux, M. A., Coillard, C., Chabot, G., et al. (2004). Osseointegration study of porous nitinol versus titanium orthopaedic implants. *European Journal of Orthopaedic Surgery & Traumatology, 14*(4), 209-213.

Lin, F. H., Yao, C. H., Sun, J. S., Liu, H. C., & Huang, C. W. (1998). Biological effects and cytotoxicity of the composite composed by tricalcium phosphate and glutaraldehyde cross-linked gelatin. *Biomaterials., 19*(10), 905-917.

Lindberg, R. B., Moncrief, J. A., Switzer, W. E., Order, S. E., & Mills, W., Jr. (1965). The successful control of burn wound sepsis. *The Journal of Trauma, 5*(5), 601-616.

Lipovsky, A., Nitzan, Y., Friedmann, H., & Lubart, R. (2009). Sensitivity of Staphylococcus aureus Strains to Broadband Visible Light. *Photochemistry and Photobiology, 85*(1), 255-260.

Livingston, B. J., Chmell, M. J., Spector, M., & Poss, R. (1997). Complications of total hip arthroplasty associated with the use of an acetabular component with a Hylamer liner. *Journal of Bone and Joint Surgery, 79*(10), 1529-1538.

Lockwood, D. B., Wataha, J. C., Lewis, J. B., Tseng, W. Y., Messer, R. L. W., & Hsu, S. D. (2005). Blue light generates reactive oxygen species (ROS) differentially in tumor vs. normal epithelial cells. *Dental Materials, 21*(7), 683-688.

Lowell, J. D., Kundsin, R. B., Schwartz, C. M., & Pozin, D. (1980). Ultraviolet Radiation and Reduction of Deep Wound Infection Following Hip and Knee Arthroplasty. *Annals of the New York Academy of Sciences, 353*(1), 285-293.

Lowry, O. H., Rosebrough, N. J., Farr, A. L., & Randall, R. J. (1951). Protein measurment with the folin phenol reagent. *Journal of Biological Chemistry, 193*(1), 265-275.

Mack, D., Rohde, H., Harris, L. G., Davies, A. P., Horstkotte, M. A., & Knobloch, J. K. (2006). Biofilm formation in medical device-related infection. *The International Journal of Artificial Organs, 29*(4), 343-359.

Maclean, M., MacGregor, S. J., Anderson, J. G., & Woolsey, G. (2008). High-intensity narrow-spectrum light inactivation and wavelength sensitivity of Staphylococcus aureus. *FEMS Microbiology Letters, 285*(2), 227-232.

Maclean, M., MacGregor, S. J., Anderson, J. G., & Woolsey, G. (2009). Inactivation of Bacterial Pathogens following Exposure to Light from a 405-Nanometer Light-Emitting Diode Array. *Applied and Environmental Microbiology, 75*(7), 1932-1937.

Maclean, M., MacGregor, S. J., Anderson, J. G., Woolsey, G. A., Coia, J. E., Hamilton, K., et al. (2010). Environmental decontamination of a hospital isolation room using high-intensity narrow-spectrum light. *The Journal of hospital infection, 76*(3), 247-251.

Macrene, A.-A. (2006). Laser-mediated photodynamic therapy. *Clinics in Dermatology, 24*(1), 16-25.

Mahmoud, B. H., Hexsel, C. L., & Hamzavi, I. H. (2008). An update on new and emerging options for the treatment of vitiligo. *Skin Therapy Letter, 13*(2), 1-6.

Maisels, M. J., & Watchko, J. F. (2003). Treatment of jaundice in low birthweight infants. *Archives of Disease in Childhood - Fetal Neonatal Ed., 88*(6), F459-463.

Majeska, R. J., & Rodan, G. A. (1982). The effect of 1,25(OH)2D3 on alkaline phosphatase in osteoblastic osteosarcoma cells. *Journal of Biological Chemistry, 257*(7), 3362-3365.

Maki, D. G., & Tambyah, P. A. (2001). Engineering out the risk for infection with urinary catheters. *Emerging Infectious Diseases journal, 7*(2), 342-347.

Malanowski, P., Huijser, S., Scaltro, F., van Benthem, R. A. T. M., van der Ven, L. G. J., Laven, J., et al. (2009). Molecular mechanism of photolysis and photooxidation of poly(neopentyl isophthalate). *Polymer, 50*(6), 1358-1368.

Malik, Z., & Lugaci, H. (1987). Destruction of erythroleukaemic cells by photoactivation of endogenous porphyrins. *British Journal of Cancer, 56*(5), 589-595.

Maluf, A., Maluf, R., da Rocha Brito, C., França, F., & de Brito, R. (2010). Mechanical evaluation of the influence of low-level laser therapy in secondary stability of implants in mice shinbones. *Lasers in Medical Science, 25*(5), 693-698.

Manchanda, V., Sanchaita, S., & Singh, N. (2010). Multidrug resistant acinetobacter. *Journal of global infectious diseases, 2*(3), 291-304.

Marconnet, C., Wouters, Y., Miserque, F., Dagbert, C., Petit, J. P., Galerie, A., et al. (2008). Chemical composition and electronic structure of the passive layer formed on stainless steels in a glucose-oxidase solution. *Electrochimica Acta, 54*(1), 123-132.

Marin-Garcia, J. (2005). ROS Generation, Antioxidants, and Cell Death

Mitochondria and the Heart. In (Vol. 256, pp. 99-122): Springer US.

Marois, Y., Guidoin, R., Roy, R., Vidovsky, T., Jakubiec, B., Sigot-Luizard, M.-F., et al. (1996). Selecting valid in vitro biocompatibility tests that predict the in vivo healing response of synthetic vascular prostheses. *Biomaterials, 17*(19), 1835-1842.

Marques, M. M., Pereira, A. N., Fujihara, N. A., Nogueira, F. N., & Eduardo, C. P. (2004). Effect of low-power laser irradiation on protein synthesis and ultrastructure of human gingival fibroblasts. *Lasers in Surgery and Medicine, 34*(3), 260-265.

Martin, P. (1997). Wound healing--aiming for perfect skin regeneration. *Science., 276*(5309), 75-81.

Martinez, P, Moreno, I, De, M., F, et al. (2001a). *Changes in osteocalcin response to 1,25-dihydroxyvitamin D[3] stimulation and basal vitamin D receptor*

expression in human osteoblastic cells according to donor age and skeletal origin (Vol. 29). Amsterdam, PAYS-BAS: Elsevier.

Martinez, P., Moreno, I., De Miguel, F., Vila, V., Esbrit, P., & Martinez, M. (2001b). *Changes in osteocalcin response to 1,25-dihydroxyvitamin D[3] stimulation and basal vitamin D receptor expression in human osteoblastic cells according to donor age and skeletal origin* (Vol. 29). Amsterdam, PAYS-BAS: Elsevier.

Martini, L., Fini, M., Giavaresi, G., & Giardino, R. (2001). Sheep Model in Orthopedic Research: A Literature Review. *Comparative Medicine, 51*(4), 292-299.

Mascotti, K., McCullough, J., & Burger, S. R. (2000). HPC viability measurement: trypan blue versus acridine orange and propidium iodide. *Transfusion, 40*(6), 693-696.

McCann, M., Gilmore, B., & Gorman, S. (2008). Staphylococcus epidermidis device-related infections: pathogenesis and clinical managment. *Journal of Pharmacy and Pharmacology, 60*(12), 1551-1571.

McCaughan, J. S., Jr. (1999). Photodynamic therapy: a review. *Drugs & Aging., 15*(1), 49-68.

McDonnell, G., & Russell, A. D. (1999). Antiseptics and Disinfectants: Activity, Action, and Resistance. *Clinical Microbiology Reviews, 12*(1), 147-179.

McKay, G. C., Macnair, R., MacDonald, C., & Grant, M. H. (1996). Interactions of orthopaedic metals with an immortalized rat osteoblast cell line. *Biomaterials, 17*(13), 1339-1344.

Melville, N. (2011). Staphylococcus aureus USA300 Prevalence Tripled Since 2004. *21st European Congress of Clinical Microbiology and Infections Diseases*.

Mendes, G. C. C., BrandÃ£o, T. R. S., & Silva, C. L. M. (2007). Ethylene oxide sterilization of medical devices: A review. *American journal of infection control, 35*(9), 574-581.

Mester, E., Mester, A. F., & Mester, A. (1985). The biomedical effects of laser application. *Lasers in Surgery and Medicine, 5*(1), 31-39.

Misteli, H., Widmer, A. F., Rosenthal, R., Oertli, D., Marti, W. R., & Weber, W. P. (2011). Spectrum of pathogens in surgical site infections at a Swiss university hospital. *Swiss Medical Weekly, 140*, 13146.

Miyamoto, T., & Suda, T. (2003). Differentiation and function of osteoclasts. *The Keio Jounral of Medicine, 52*(1), 1-7.

Moan, J., Iani, V., & Ma, L. (1996). Choice of the proper wavelength for photochemotherapy. *Photochemotherapy: Photodynamic Therapy and Other Modalities, Proceedings 2625*, 544-549.

Moan, J., Rimington, C., & Western, A. (1985). The binding of dihematoporphyrin ether (photofrin II) to human serum albumin. *Clinica Chimica Acta, 145*(3), 227-236.

Montesano, R., & Orci, L. (1988). Transforming growth factor beta stimulates collagen-matrix contraction by fibroblasts: implications for wound healing. *Proceedings of the National Academy of Sciences of the United States of America, 85*(13), 4894-4897.

Mosmann, T. (1983). Rapid colorimetric assay for cellular growth and survival: Application to proliferation and cytotoxicity assays. *Journal of Immunological Methods, 65*(1-2), 55-63.

Mugford, M., Kingston, J., & Chalmers, I. (1989). Reducing the incidence of infection after caesarean section: implications of prophylaxis with antibiotics for hospital resources. *British Medical Journal, 299*(6706), 1003-1006.

Munez, E., Ramos, A., Espejo, T. A., Vaque, J., Sanchez-Paya, J., Pastor, V., et al. (2011). Microbiology of surgical site infections in abdominal tract surgery patients. *Cirugía Española, Epub ahead of print*.

Murdoch, L. E., Maclean, M., MacGregor, S. J., & Anderson, J. G. (2011). Inactivation of Campylobacter jejuni by exposure to high-intensity 405-nm visible light. *Foodborne Pathogens and Disease, 7*(10), 1211-1216.

Murphy, R. C., Robson, M. C., Heggers, J. P., & Kadowaki, M. (1986). The effect of microbial contamination on musculocutaneous and random flaps. *Journal of Surgical Research, 41*(1), 75-80.

Nakamura, A., Dohi, Y., Akahane, M., Ohgushi, H., Nakajima, H., Funaoka, H., et al. (2009). Osteocalcin secretion as an early marker of in vitro osteogenic differentiation of rat mesenchymal stem cells. *Tissue Engineering Part C: Methods, 15*(2), 169-180.

Namdari, S., Voleti, P. B., Baldwin, K. D., & Lee, G. C. (2011). Primary total joint arthroplasty performed in operating rooms following cases of known infection. *Orthopedics., 34*(9), 541-545.

Nesbitt, S. A., & Horton, M. A. (1997). Trafficking of Matrix Collagens Through Bone-Resorbing Osteoclasts. *Science, 276*(5310), 266-269.

Niekraszewicz, A., Kucharska, M., Wiśniewska-Wrona, M., & Kardas, I. (2010). Biological and Physicochemical Study of the Implantation of a Modified Polyester Vascular Prosthesis. *FIBRES & TEXTILES in Eastern Europe, 18*(6), 100- 105.

Nishiyama, T., Tominaga, N., Nakajima, K., & Hayashi, T. (1988). Quantitative evaluation of the factors affecting the process of fibroblast-mediated collagen gel contraction by separating the process into three phases. *Collagen and Related Research, 8*(3), 259-273.

Nitzan, Y., Salmon-Divon, M., Shporen, E., & Malik, Z. (2004). ALA induced photodynamic effects on Gram positive and negative bacteria. *Photochemical and Photobiological Sciences, 3*(5), 430-435.

Norton, M. R., Yarlagadda, R., & Anderson, G. H. (2002). Catastrophic failure of the Elite Plus total hip replacement, with a Hylamer acetabulum and Zirconia ceramic femoral head. *Journal of Bone and Joint Surgery 84-B*(5), 631-635.

Norval, M., Cullen, A. P., de Gruijl, F. R., Longstreth, J., Takizawa, Y., Lucas, R. M., et al. (2007). The effects on human health from stratospheric ozone depletion and its interactions with climate change. *Photochemical & Photobiological Sciences, 6*(3), 232-251.

Nussbaum, E. L., Lilge, L., & Mazzulli, T. (2003). Effects of low-level laser therapy (LLLT) of 810 nm upon in vitro growth of bacteria: relevance of irradiance and radiant exposure. *Journal of Clinical Laser Medicine and Surgery, 21*(5), 283-290.

Nussbaum, E. L., Mazzulli, T., Pritzker, K. P., Heras, F. L., Jing, F., & Lilge, L. (2009). Effects of low intensity laser irradiation during healing of skin lesions in the rat. *Lasers in Surgery and Medicine, 41*(5), 372-381.

O'Gara, J. P., & Humphreys, H. (2001). Staphylococcus epidermidis biofilms: importance and implications. *Journal of Medical Microbiology, 50*(7), 582-587.

Oliver, I. T., & Rawlinson, W. A. (1955). The absorption spectra of porphyrin alpha and derivatives. *Biochemical Journal, 61*(4), 641-646.

Olschlager, V., Schrader, A., & Hockertz, S. (2009). Comparison of primary human fibroblasts and keratinocytes with immortalized cell lines regarding their sensitivity to sodium dodecyl sulfate in a neutral red uptake cytotoxicity assay. *Arzneimittelforschung., 59*(3), 146-152.

Opländer, C., Hidding, S., Werners, F. B., Born, M., Pallua, N., & Suschek, C. V. (2011). Effects of blue light irradiation on human dermal fibroblasts. *Journal of Photochemistry and Photobiology B: Biology, 103*(2), 118-125.

Orenstein, A., Klein, D., Kopolovic, J., Winkler, E., Malik, Z., Keller, N., et al. (1997). The use of porphyrins for eradication of Staphylococcus aureus in burn wound infections. *FEMS Immunology & Medical Microbiology, 19*(4), 307-314.

Owen, T. A., Aronow, M. S., Barone, L. M., Bettencourt, B., Stein, G. S., & Lian, J. B. (1991). Pleiotropic Effects of Vitamin D on Osteoblast Gene Expression Are Related to the Proliferative and Differentiated State of the Bone Cell Phenotype: Dependency upon Basal Levels of Gene Expression, Duration of Exposure, and Bone Matrix Competency in Normal Rat Osteoblast Cultures. *Endocrinology, 128*(3), 1496-1504.

Owens, C. D., & Stoessel, K. (2008). Surgical site infections: epidemiology, microbiology and prevention. *Journal of Hospital Infection, 70, Supplement 2*(0), 3-10.

Owers, K. L., James, E., & Bannister, G. C. (2004). Source of bacterial shedding in laminar flow theatres. *Journal of Hospital Infection, 58*(3), 230-232.

Pan, C., Kumar, C., Bohl, S., Klingmueller, U., & Mann, M. (2009). Comparative Proteomic Phenotyping of Cell Lines and Primary Cells to Assess Preservation of Cell Type-specific Functions. *Molecular & Cellular Proteomics, 8*(3), 443-450.

Papageorgiou, P., Katsambas, A., & Chu, A. (2000). Phototherapy with blue (415 nm) and red (660 nm) light in the treatment of acne vulgaris. *British Journal of Dermatology, 142*(5), 973-978.

Pastuszka, J., Marchwinska-Wyrwal, E., & Wlazlo, A. (2005). Bacterial Aerosol in Silesian Hospitals: Preliminary Results. *Polish Journal of Environmental Studies, 14*(6), 883-890.

Peersman, G., Laskin, R., Davis, J., & Peterson, M. (2001). Infection in Total Knee Replacement: A Retrospective Review of 6489 Total Knee Replacements. *Clinical Orthopaedics and Related Research, 392*, 15-23.

Perun, S., Tatchen, J., & Marian, C. M. (2008). Singlet and triplet excited states and intersystem crossing in free-base porphyrin: TDDFT and DFT/MRCI study. *ChemPhysChem (A European Journal of Chemical Physics and Physical Chemistry), 9*(2), 282-292.

Pflaum, M., Kielbassa, C., Garmyn, M., & Epe, B. (1998). Oxidative DNA damage induced by visible light in mammalian cells: extent, inhibition by antioxidants and genotoxic effects. *Mutation Research/DNA Repair, 408*(2), 137-146.

Plowman, R. (2000). The socioeconomic burden of hospital acquired infection. *Eurosurveillance, 5*(4), 49-50.

Plowman, R., Graves, N., Griffin, M. A., Roberts, J. A., Swan, A. V., Cookson, B., et al. (2001). The rate and cost of hospital-acquired infections occurring in patients admitted to selected specialties of a district general hospital in England and the national burden imposed. *The Journal of Hospital Infection, 47*(3), 198-209.

Podschun, R., & Ullmann, U. (1998). Klebsiella spp. as Nosocomial Pathogens: Epidemiology, Taxonomy, Typing Methods, and Pathogenicity Factors. *Clinical Microbiology Reviews, 11*(4), 589-603.

Porwancher, R., Sheth, A., Remphrey, S., Taylor, E., Hinkle, C., & Zervos, M. (1997). Epidemiological study of hospital-acquired infection with vancomycin-resistant Enterococcus faecium: possible transmission by an electronic ear-probe thermometer. *Infection Control and Hospital Epidemiology 18*(11), 771-773.

Potes, J., Reis, J. d. C., Silva, F. e., Relvas, C., Cabrita, A., & Simoes, J. (2008). The Sheep as an Animal Model in Orthopaedic Research. *Experimental Pathology and Health Sciences, 2*(1), 29-32.

Pourdeyhimi, B., & Text, C. (1987). A Review of Structural and Material Properties of Vascular Grafts. *Journal of Biomaterials Applications, 2*(2), 163-204.

Price, P., Parthemore, J., & Deftos, L. (1980). New biochemical marker for bone metabolism. Measurement by radioimmunoassay of bone GLA protein in the plasma of normal subjects and patients with bone disease. *Journal of Clinical Investigation, 66*(5), 878-883.

Qudiesat, K., Abu-Elteen, K., Elkarmi, A., Hamad, M., & Abussaud, M. (2009). Assessment of airborne pathogens in healthcare settings. *African Journal of Microbiology Research, 3*(2), 66-76.

Ramberg, K., Melo, T. B., & Johnsson, A. (2004). In situ assessment of porphyrin photosensitizers in Propionibacterium acnes. *Zeitschrift fur Naturforschung Teil C Biochemie Biophysik Biologie Virologie, 59*(1-2), 93-98.

Rånby, B. (1989). Photodegradation and photo-oxidation of synthetic polymers. *Journal of Analytical and Applied Pyrolysis, 15*, 237-247.

Rashid, S. T., Salacinski, H. J., Fuller, B. J., Hamilton, G., & Seifalian, A. M. (2004). Engineering of bypass conduits to improve patency. *Cell Proliferation, 37*(5), 351-366.

Reilly, J., Stewart, S., Allardice, G., Noone, A., Robertson, C., Walker, A., et al. (2007). *NHS Scotland National HAI Prevalence Survey. Final Report 2007, Health Protection Scotland*.

Reilly, J., Stewart, S., Allardice, G., Noone, A., Robertson, C., Walker, A., et al. (2008). Results from the Scottish National HAI Prevalence Survey. *Journal of Hospital Infection, 69*(1), 62 - 68.

Reinis, A., Vetra, J., Stunda, A., Berzina-Cimdina, L., Kroica, J., Kuznecova, V., et al. (2010). In vitro and in vivo Examinations for Detection of Minimal Infective Dose for Biomaterials. In R. Magjarevic (Ed.), *6th World Congress of Biomechanics (WCB 2010). August 1-6, 2010 Singapore* (Vol. 31, pp. 1204-1207): Springer Berlin Heidelberg.

Ribeiro, M., Silva, D. F., Araújo, C. D., Oliveira, S. D., Pelegrini, C., Zorn, T., et al. (2004). Effects of low-intensity polarized visible laser radiation on skin

burns: a light microscopy study. *Journal of Clinical Laser Medicine and Surgery, 22*(1), 59-66.

Ridgeway, S., Wilson, J., Charlet, A., Kafatos, G., Pearson, A., & Coello, R. (2005). Infection of the surgical site after arthroplasty of the hip. *Journal of Bone and Joint Surgery (British Volume), 87*(6), 844-850.

Rimington, C. (1960). Spectral-absorption coefficients of some porphyrins in the Soret-band region. *Biochemical Journal, 75*(3), 620-623.

Rimondini, L., Fini, M., & Giardino, R. (2005). The microbial infection of biomaterials: A challenge for clinicans and researchers. A short review. *Journal of Applied Biomaterials & Biomechanics, 3*(1), 1-10.

Ritter, M. A., Olberding, E. M., & Malinzak, R. A. (2007). Ultraviolet lighting during orthopaedic surgery and the rate of infection. *Journal of Bone and Joint Surgery (American volume), 89*(9), 1935-1940.

Roehlecke, C., Schaller, A., Knels, L., & Funk, R. H. W. (2009). The influence of sublethal blue light exposure on human RPE cells. *Molecular Vision, 15*, 1929-1938.

Salacinski, H. J., Goldner, S., Giudiceandrea, A., Hamilton, G., Seifalian, A. M., Edwards, A., et al. (2001). The Mechanical Behavior of Vascular Grafts: A Review. *Journal of Biomaterials Applications, 15*(3), 241-278.

Saracino, S., Mozzati, M., Martinasso, G., Pol, R., Canuto, R. A., & Muzio, G. (2009). Superpulsed laser irradiation increases osteoblast activity via modulation of bone morphogenetic factors. *Lasers in Surgery and Medicine, 41*(4), 298-304.

Schafer, F. Q., & Buettner, G. R. (1999). Singlet Oxygen Toxicity Is Cell Line-dependent: A Study of Lipid Peroxidation in Nine Leukemia Cell Lines. *Photochemistry and Photobiology, 70*(6), 858-867.

Sebeny, P. J., Riddle, M. S., & Petersen, K. (2008). Acinetobacter baumannii Skin and Soft-Tissue Infection Associated with War Trauma. *Clinical Infectious Diseases, 47*(4), 444-449.

Sieuwerts, A. M., Klijn, J. G., Peters, H. A., & Foekens, J. A. (1995). The MTT tetrazolium salt assay scrutinized: how to use this assay reliably to measure metabolic activity of cell cultures in vitro for the assessment of growth characteristics, IC50-values and cell survival. *European Journal of Clinical Chemistry and Clinical Biochemistry, 33*(11), 813-823.

Siggelkow, H., Rebenstorff, K., Kurre, W., Niedhart, C., Engel, I., Schulz, H., et al. (1999a). Development of the osteoblast phenotype in primary human osteoblasts in culture: Comparison with rat calvarial cells in osteoblast differentiation. *Journal of Cellular Biochemistry, 75*(1), 22-35.

Siggelkow, H., Schulz, H., Kaesler, S., Benzler, K., Atkinson, M., & Hüfner, M. (1999b). 1,25 Dihydroxyvitamin-D₃ Attenuates the Confluence-Dependent Differences in the Osteoblast Characteristic Proteins Alkaline Phosphatase, Procollagen I Peptide, and Osteocalcin. *Calcified Tissue International, 64*(5), 414-421.

Simor, A., Lee, M., Vearncombe, M., JonesâPaul, L., Barry, C., Gomez, M., et al. (2002). An Outbreak Due to Multiresistant Acinetobacter baumannii in a Burn Unit: Risk Factors for Acquisition and Management. *Infection Control and Hospital Epidemiology, 23*(5), 261-267.

Skorb, E. V., Antonouskaya, L. I., Belyasova, N. A., Shchukin, D. G., Möhwald, H., & Sviridov, D. V. (2008). Antibacterial activity of thin-film photocatalysts based on metal-modified TiO2 and TiO2:In2O3 nanocomposite. *Applied Catalysis B: Environmental, 84*(1-2), 94-99.

Smith, J. B., & Willis, A. L. (1971). Aspirin selectively inhibits prostaglandin production in human platelets. *Nature: New Biology, 231*(25), 235-237.

Smith, S. (2009). *Effect of novel electronic sterilisation methods on the components of hybrid collagen-based biomaterials.* Glasgow, Scotland, University of Strathclyde.

Smith, S., Maclean, M., MacGregor, S. J., Anderson, J. G., & Grant, M. H. (2009). Exposure of 3T3 mouse Fibroblasts and Collagen to High Intensity Blue Light. In *13th International Conference on Biomedical Engineering* (pp. 1352-1355).

Spesia, M. B., Rovera, M., & Durantini, E. N. (2010). Photodynamic inactivation of Escherichia coli and Streptococcus mitis by cationic zinc(II) phthalocyanines in media with blood derivatives. *European Journal of Medicinal Chemistry, 45*(6), 2198-2205.

Spiess, Y. H., Price, P. A., Deftos, J. L., & Manolagas, S. C. (1986). Phenotype-Associated Changes in the Effects of 1,25-Dihydroxyvitamin D3 on Alkaline Phosphatase and Bone GLA-Protein of Rat Osteoblastic Cells. *Endocrinology, 118*(4), 1340-1346.

Stea, S., Antonietti, B., Baruffaldi, F., Visentin, M., Bordini, B., Sudanese, A., et al. (2006). Behavior of Hylamer polyethylene in hip arthroplasty: comparison of two gamma sterilization techniques. *International Orthopaedics, 30*(1), 35-38. Epub 2005 Oct 2011.

Stein, A., Benayahu, D., Maltz, L., & Oron, U. (2005). Low-Level Laser Irradiation Promotes Proliferation and Differentiation of Human Osteoblasts in Vitro. *Photomedicine and Laser Surgery, 23*(2), 161-166.

Steinberg, B. M., Smith, K., Colozzo, M., & Pollack, R. (1980). Establishment and transformation diminish the ability of fibroblasts to contract a native collagen gel. *The Journal of Cell Biology, 87*(1), 304-308.

Sternberg, E., & Dolphin, D. (1998). Porphyrin-based Photosensitizers for Use in Photodynamic Therapy. *Tetrahedron, 54*, 4151-4202.

Stewart, S. F., & Lyman, D. J. (2004). Effects of an artery/vascular graft compliance mismatch on protein transport: a numerical study. *Annals of Biomedical Engineering, 32*(7), 991-1006.

Stoien, J. D., & Wang, R. J. (1974). Effect of near-ultraviolet and visible light on mammalian cells in culture II. Formation of toxic photoproducts in tissue culture medium by blacklight. *Proceedings of the National Acadamy of Sciences of the U S A., 71*(10), 3961-3965.

Strachan, C. J. L. (1993). Antibiotic prophylaxis in peripheral vascular and orthopaedic prosthetic surgery. *Journal of Antimicrobial Chemotherapy, 31*(suppl B), 65-78.

Strong, L. H., Berthiaume, F., & Yarmush, M. L. (1997). Control of fibroblast populated collagen lattice contraction by antibody targeted photolysis of fibroblasts. *Lasers in Surgery and Medicine, 21*(3), 235-247.

Suits, L. D., & Hsuan, Y. G. (2003). Assessing the photo-degradation of geosynthetics by outdoor exposure and laboratory weatherometer. *Geotextiles and Geomembranes, 21*(2), 111-122.

Tajali, S., Macdermid, J. C., Houghton, P., & Grewal, R. (2010). Effects of low power laser irradiation on bone healing in animals: a meta-analysis. *Journal of Orthopaedic Surgery and Research, 5*, 1 - 10.

Taoufik, K., Mavrogonatou, E., Eliades, T., Papagiannoulis, L., Eliades, G., & Kletsas, D. (2008). Effect of blue light on the proliferation of human gingival fibroblasts. *Dental materials : official publication of the Academy of Dental Materials, 24*(7), 895-900.

Taylor, G. J. S., Bannister, G. C., & Leeming, J. P. (1995). Wound disinfection with ultraviolet radiation. *Journal of Hospital Infection, 30*(2), 85-93.

Taylor, M. D., & Napolitano, L. M. (2004). Methicillin-resistant Staphylococcus aureus infections in vascular surgery: increasing prevalence. *Surgical Infections, 5*(2), 180-187.

Tenke, P., Riedl, C. R., Jones, G. L., Williams, G. J., Stickler, D., & Nagy, E. (2004). Bacterial biofilm formation on urologic devices and heparin coating as preventive strategy. *International Journal of Antimicrobial Agents, 23*(Suppl 1), S67-74.

Teplitz, C., Davis, D., Mason Jr, A. D., & Moncrief, J. A. (1964). Pseudomonas burn wound sepsis. I: Pathogenesis of experimental pseudomonas burn wound sepsis. *Journal of Surgical Research, 4*(5), 200-216.

Terman, M., & Terman, J. S. (2005). Light therapy for seasonal and nonseasonal depression: efficacy, protocol, safety, and side effects. *CNS Spectrums, 10*(8), 647-663; quiz 672.

Tess, B. H., Glenister, H. M., Rodrigues, L. C., & Wagner, M. B. (1993). Incidence of hospital-acquired infection and length of hospital stay. *European Journal of Clinical Microbiology & Infectious Diseases, 12*(2), 81-86.

Thomas, A. O., Michael, A., Victoria, S., Leesa, M. B., Laurens, W., Melissa, S. T., et al. (1990). Progressive development of the rat osteoblast phenotype in vitro: Reciprocal relationships in expression of genes associated with osteoblast proliferation and differentiation during formation of the bone extracellular matrix. *Journal of Cellular Physiology, 143*(3), 420-430.

Thomas, J. P., & Girotti, A. W. (1989). Role of Lipid Peroxidation in Hematoporphyrin Derivative-sensitized Photokilling of Tumor Cells: Protective Effects of Glutathione Peroxidase. *Cancer Research, 49*(7), 1682-1686.

Thomas, S. (1997). A structured approach to the selection of dressing [Electronic Version]. *World Wide Wounds*. Retrieved 9/11/11 from http://www.worldwidewounds.com/1997/july/Thomas-Guide/Dress-Select.html.

Todaro, G. J., & Green, H. (1963). Quantitative studies of the growth of mouse embryo cells in culture and their development into established lines. *The Journal of Cell Biology, 17*(2), 299.

Towner, K. J. (2009). Acinetobacter: an old friend, but a new enemy. *Journal of Hospital Infection, 73*(4), 355-363.

Tullberg-Reinert, H., & Jundt, G. (1999). In situ measurement of collagen synthesis by human bone cells with a Sirius Red-based colorimetric microassay: effects

of transforming growth factor β2 and ascorbic acid 2-phosphate. *Histochemistry and Cell Biology, 112*(4), 271-276.

Ueno, T., Yamada, M., Hori, N., Suzuki, T., & Ogawa, T. (2010). Effect of ultraviolet photoactivation of titanium on osseointegration in a rat model. *International Journal of Oral and Maxillofacial Implants, 25*(2), 287-294.

Upadya, M. H., & Kishen, A. (2009). Influence of bacterial growth modes on the susceptibility to light-activated disinfection. *International Endodontic Journal, 43*(11), 978-987.

Vaananen, H. K., Zhao, H., Mulari, M., & Halleen, J. M. (2000). The cell biology of osteoclast function. *Journal of Cell Science, 113*(3), 377-381.

Van Damme, H., Deprez, M., Creemers, E., & Limet, R. (2005). Intrinsic structural failure of polyester (Dacron) vascular grafts. A general review. *Acta Chirurgica Belgica, 105*(3), 249-255.

Vane, J. R. (1996). Introduction: Mechanism of Action of NSAIDs. *Rheumatology, 35*(suppl_1), 1-3.

Velnar, T., Bailey, T., & Smrkolj, V. (2009). The Wound Healing Process: an Overview of the Cellular and Molecular Mechanisms. *The Journal of International Medical Research, 37*(5), 1528-1542.

Verjee, L. S., Midwood, K., Davidson, D., Eastwood, M., & Nanchahal, J. Post-transcriptional regulation of α-smooth muscle actin determines the contractile phenotype of Dupuytren's nodular cells. *Journal of Cellular Physiology, 224*(3), 681-690.

Vidinsky, B., Gal, P., Toporcer, T., Balogacova, M., Hutnanova, Z., Kilik, R., et al. (2005). Effect of laser irradiation of diode laser on healing of surgical wounds in rats. *Rozhledy v Chirurgii- Mesicnik Ceskoslovenske Chirurgicke Spolecnosti, 84*(8), 417-421.

Vincent, J.-L., Bihari, D. J., Suter, P. M., Bruining, H. A., White, J., Nicolas-Chanoin, M.-H., et al. (1995). The Prevalence of Nosocomial Infection in Intensive Care Units in Europe. *JAMA: The Journal of the American Medical Association, 274*(8), 639-644.

Vinh, D. C., & Embil, J. M. (2005). Device-Related Infections: A Review. *Journal of Long-Term Effects of Medical Implants, 15*(5), 467-488.

Visentin, M., Stea, S., Squarzoni, S., Reggiani, M., Fagnano, C., Antonietti, B., et al. (2005). Isolation and characterization of wear debris generated in patients wearing polyethylene Hylamer inserts, gamma irradiated in air. *Journal of Biomaterials Applications, 20*(2), 103-121.

Vlad, C. S., Aron, P., Ha-Sheng, L.-K., Joseph, E. D., & Patricia, A. H. (2006). Prostaglandin E2 differentially modulates human fetal and adult dermal fibroblast migration and contraction: implication for wound healing. *Wound Repair and Regeneration, 14*(5), 633-643.

von Eiff, C., Jansen, B., Kohnen, W., & Becker, K. (2005). Infections associated with medical devices: pathogenesis, management and prophylaxis. *Drugs., 65*(2), 179-214.

Walsh, B. J., Thornton, S. C., Penny, R., & Breit, S. N. (1992). Microplate reader-based quantitation of collagens. *Analytical Biochemistry, 203*(2), 187-190.

Wang, H. P., Qian, S. Y., Schafer, F. Q., Domann, F. E., Oberley, L. W., & Buettner, G. R. (2001). Phospholipid hydroperoxide glutathione peroxidase protects

against singlet oxygen-induced cell damage of photodynamic therapy. *Free Radical Biology & Medicine, 30*(8), 825-835.

Wataha, J. C., Lewis, J. B., Lockwood, P. E., Hsu, S., Messer, R. L., Rueggeberg, F. A., et al. (2004). Blue Light Differentially Modulates Cell Survival and Growth. *Journal of Dental Research, 83*(2), 104-108.

Wenzel, R. P., & Edmond, M. B. (1998). Vancomycin-Resistant Staphylococcus aureus: Infection Control Considerations. *Clinical Infectious Diseases, 27*(2), 245-249.

Whelan, H. T., Smits, R. L., Jr., Buchman, E. V., Whelan, N. T., Turner, S. G., Margolis, D. A., et al. (2001). Effect of NASA light-emitting diode irradiation on wound healing. *Journal of Clinical Laser Medicine and Surgery, 19*(6), 305-314.

Whyte, W., Hodgson, R., & Tinkler, J. (1982). The importance of airborne bacterial contamination of wounds. *Journal of Hospital Infection, 3*(2), 123-135.

Wijesekera, T. P., & Dolphin, D. (1985). Some preparations and properties of porphyrins. *Advances in Experimental Medicine and Biology, 193*, 229-266.

Wilcox, M. H., Cunniffe, J. G., Trundle, C., & Redpath, C. (1996). Financial burden of hospital-acquired Clostridium difficile infection. *J Hosp Infect., 34*(1), 23-30.

Wilcox, M. H., & Dave, J. (2000). The cost of hospital-acquired infection and the value of infection control. *The Journal of Hospital Infection, 45*(2), 81-84.

Willert, H. G., & Buchhorn, G. H. (1999). Osseointegration of cemented and noncemented implants in artificial hip replacement: long-term findings in man. *Journal of Long-Term Effects of Medical Implants, 9*(1-2), 113-130.

Wilson, J., Charlett, A., Leong, G., McDougall, C., & Duckworth, G. (2008). Rates of surgical site infection after hip replacement as a hospital performance indicator: analysis of data from the English mandatory surveillance system. *Infection Control and Hospital Epidemiology, 29*(3), 219-226.

Wilson, M. (2004). Lethal photosensitisation of oral bacteria and its potential application in the photodynamic therapy of oral infections. *Photochemical & Photobiological Sciences, 3*(5), 412-418.

Winton, F., Corn, T., Huson, L. W., Franey, C., Arendt, J., & Checkley, S. A. (1989). Effects of light treatment upon mood and melatonin in patients with seasonal affective disorder. *Psychological Medicine, 19*(03), 585-590.

Wolberg, A. S. (2007). Thrombin generation and fibrin clot structure. *Blood Reviews, 21*(3), 131-142.

Wong, V. W., Sorkin, M., Glotzbach, J. P., Longaker, M. T., & Gurtner, G. C. (2011). Surgical Approaches to Create Murine Models of Human Wound Healing. *Journal of Biomedicine and Biotechnology, 2011*.

Wu, P., Xie, R., Imlay, J. A., & Shang, J. K. (2009). Visible-light-induced photocatalytic inactivation of bacteria by composite photocatalysts of palladium oxide and nitrogen-doped titanium oxide. *Applied Catalysis B: Environmental, 88*(3-4), 576-581.

Zetrenne, E., McIntosh, B., McRae, M., Gusberg, R., Evans, G., & Narayan, D. (2007). Prosthetic Vascular Graft Infection: A Multi-Center Review of Surgical Management. *Yale Journal of Biology and Medicine, 80*(3), 113-121.

Zolfaghari, P. S., Packer, S., Singer, M., Nair, S. P., Bennett, J., Street, C., et al. (2009). In vivo killing of Staphylococcus aureus using a light-activated antimicrobial agent. *BMC Microbiology, 9*, 27.

Zoutman, D., McDonald, S., & Vethanayagan, D. (1998). Total and attributable costs of surgical-wound infections at a Canadian tertiary-care center. *Infection Control and Hospital Epidemiology, 19*(4), 254-259.

Appendix A - SOLUTIONS

Bouin's solution:

75 ml picric acid (saturated)
25 ml 40% formaldehyde
5 ml glacial acetic acid

Glutaraldehye fixative:

2.5 ml 25% glutaraldehyde

12.5 ml 0.2M PO_4 buffer

10 ml dH_2O

Laemmli buffer:

4 ml dH_2O

1 ml 0.5M Tris pH 6.8

0.8 ml glycerol

1.6 ml 10% (w/v) SDS

0.4 ml β-mercaptoethanol

0.2 ml 0.05% (w/v) bromophenol blue

NaPi buffer 0.1M:

A – 0.2M Na_2HPO_4 (14.2g in 500ml dH_2O)

B – 0.2M NaH_2PO_4 (2.4g in 100ml dH_2O)

87ml A + 13ml B – dilute to 200ml with dH_2O

Adjusted to pH 7.4

Neutral Red de-stain:

50ml EtOH

1ml glacial acetic acid

49ml dH_20

Picric Sirius red solution:

Direct Red 80 (Sigma-Aldrich 365548) 0.2g

Saturated aqueous picric acid 200ml

Towbin's transfer buffer:

600ml dH_2O

3g Tris

14.4g glycine

200 ml methanol

Tris Buffered Saline

4g NaCl

0.05g Na_2HPO_4

0.5g glucose

1.5g Tris

0.19g KCl

1.5 ml of 0.5% (w/v) phenol red

Dissolve in 500ml dH_2O. Adjust to pH 7.7 with HCl

Tween Tris Buffered Saline

Tris Buffered Saline as above

0.5% (v/v) Tween 20 (Sigma P5927)